

AUTHOR QUERIES

AUTHOR PLEASE ANSWER ALL QUERIES

PLEASE NOTE: We cannot accept new source files as corrections for your article. If possible, please annotate the PDF proof we have sent you with your corrections and upload it via the Author Gateway. Alternatively, you may send us your corrections in list format. You may also upload revised graphics via the Author Gateway.

Carefully check the page proofs (and coordinate with all authors); additional changes or updates WILL NOT be accepted after the article is published online/print in its final form. Please check author names and affiliations, funding, as well as the overall article for any errors prior to sending in your author proof corrections. Your article has been peer reviewed, accepted as final, and sent in to IEEE. No text changes have been made to the main part of the article as dictated by the editorial level of service for your publication.

AQ:1 = Please confirm or add details for any funding or financial support for the research of this article.

AQ:2 = Please provide the expansion of the acronym CAREER for your funding agency. Providing the correct acknowledgment will ensure proper credit to the funder.

AQ:3 = Please provide the DOI of the earlier version of this paper.

AQ:4 = Please check the Associate Editor line in the first footnote for correctness.

AQ:5 = Please confirm the retention of the content in the acknowledgment section.

Answers to the Queries:

AQ1 & AQ2: The funding information is not correct in the initial footnote. It should be ``... supported in part by NSF under Grant CAREER DMS-2141865, Grant DMS...''; CAREER is the term that refers to the NSF Faculty Early Career Development Program and is not the acronym.

AQ3: The official citation of the earlier version at the AISTATS conference is: Hu, J. and Wang, M. (2022) ``Multiway Spherical Clustering via Degree-Corrected Tensor Block Models.'' Proceedings of The 25th International Conference on Artificial Intelligence and Statistic, PMLR 151:1078-1119, 2022.

(Official citation is the best identification information I could find for this conference publication.)

AQ4: The Associate Editor information is correct.

AQ5: The acknowledgment is correct.

Revised graph:

- Page 18, Fig.12. Missing subtitles ``a.'' and ``b.''

Text corrections: (Highlight in Yellow)

- Page 3, Table I. Move the sentences ``We list ...'' as the footnote 1; move the sentence ``The parameter ...'' as the footnote 2 and add a period after the sentence ``... dimension p'';
- Line 514. Capitalize the name of Theorem 2. ``Statistical critical value'' -> ``Statistical Critical Value'' ;
- Line 541. ``Appendix B, Section B-D and Section B-G'' -> ``Appendix B, Section D and Section G'';
- Line 619. ``Appendix B, Section B-E and Section B-G'' -> ``Appendix B, Section E and Section G'';
- Line 725. Seems no space between ``Error'' and ``for'';
- Line 840. Capitalize the name of Corollary 1. ``Exact recovery of dTBM with weighted higher-order initialization'' -> ``Exact Recovery of dTBM With Weighted Higher-Order Initialization'';
- Page 11, Algorithm 2. If possible, delete the term ``Algorithm 2'' and index the algorithm with bold ``Sub-algorithm 3:''; Otherwise, Delete the phrase ``Sub-algorithm 3:'' and the change all references correspondingly.
- Lines 1054 and 1056. No exclamation point before ``MLE''. ``! MLE ...'' -> ``MLE'';
- Line 1437. ``Appendix B, Section B-G'' -> ``Appendix B, Section G'';

Structure corrections: (Highlight in Green)

- Lines 1491 - 1504. Change the numbered list under ``1) Preliminaries'' to the bullet list;
- Lines 1608, 1948, 2129, 2345. Change the numbered texts ``Useful Lemmas....'', ``Useful Definitions and ...'', and ``Notation'' to unlisted bold text in a single line.
- Lines 1824, 1871, 2224, 2321. Change the numbered texts ``We firstly show the ...'', ``Next, we show ...'' ``Now, we show ...'', ``The initialization ...'' to unlisted plain texts.

Wording corrections based on IEEE Guidance: (Highlight in Pink)

- Delete the hyphen between the prefix words ``non'', ``sub'', ``multi'' and the modified word. E.g. ``non-degree'' -> ``nondegree'', ``sub-optimal'' -> ``suboptimal'', and ``multi-layer'' -> ``multilayer''.
- Use abbreviation ``Fig.'' to refer the figures. E.g. ``Figure 1'' -> ``Fig. 1''.

All mentioned annotations are highlighted in the following colored version! Yellow: text corrections; Green: structure corrections; Pink: wording corrections.

Multiway Spherical Clustering via Degree-Corrected Tensor Block Models

Jixin Hu¹ and Miaoyan Wang¹

Fig. 1

Abstract— We consider the problem of multiway clustering in the presence of unknown degree heterogeneity. Such data problems arise commonly in applications such as recommendation system, neuroimaging, community detection, and hypergraph partitions in social networks. The allowance of degree heterogeneity provides great flexibility in clustering models, but the extra complexity poses significant challenges in both statistics and computation. Here, we develop a degree-corrected tensor block model with estimation accuracy guarantees. We present the phase transition of clustering performance based on the notion of angle separability, and we characterize three signal-to-noise regimes corresponding to different statistical-computational behaviors. In particular, we demonstrate that an intrinsic statistical-to-computational gap emerges only for tensors of order three or greater. Further, we develop an efficient polynomial-time algorithm that provably achieves exact clustering under mild signal conditions. The efficacy of our procedure is demonstrated through two data applications, one on human brain connectome project, and another on Peru Legislation network dataset.

Index Terms— Tensor clustering, degree correction, statistical computational efficiency, human brain connectome networks.

I. INTRODUCTION

MULTIWAY arrays have been widely collected in various fields including social networks [1], neuroscience [2], and computer science [3]. Tensors effectively represent the multiway data and serve as the foundation in higher-order data analysis. One data example is from multi-tissue multi-individual gene expression study [4], [5], where the data tensor consists of expression measurements indexed by (gene, individual, tissue) triplets. Another example is *hypergraph* network [6], [7], [8], [9] in social science. A K -uniform hypergraph can be naturally represented as an order- K tensor, where each entry indicates the presence of K -way hyperedge among nodes (a.k.a. entities). In both examples, identifying the similarity among tensor entities is important for scientific discovery.

... by NSF under Grant CAREER DMS-214....

Manuscript received 18 January 2022; revised 23 December 2022; accepted 6 January 2023. The work of Miaoyan Wang was supported in part by NSF CAREER under Grant DMS-2141865, Grant DMS-1915978, Grant DMS-2023239, and Grant EF-2133740; and in part by the Wisconsin Alumni Research Foundation. An earlier version of this paper was presented in part at the 25th International Conference on Artificial Intelligence and Statistics (AISTATS). (Corresponding author: Miaoyan Wang.)

The authors are with the Department of Statistics, University of Wisconsin-Madison, Madison, WI 53706 USA (e-mail: jhu267@wisc.edu; miaoyan.wang@wisc.edu).

Communicated by R. Venkataraman, Associate Editor for Machine Learning.

Color versions of one or more figures in this article are available at <https://doi.org/10.1109/TIT.2023.3239521>.

Digital Object Identifier 10.1109/TIT.2023.3239521

We study the problem of multiway clustering based on a data tensor. The goal of multiway clustering is to identify a checkerboard structure from a noisy data tensor. Figure 1 illustrates the noisy tensor and the underlying checkerboard structures discovered by multiway clustering methods. In the hypergraph example, the multiway clustering aims to identify the underlying block partition of nodes based on their higher-order connectivities; therefore, we also refer to the clustering as *higher-order clustering*. The most common model for higher-order clustering is called *tensor block model* (TBM) [10], which extends the usual matrix stochastic block model [11] to tensors. The matrix analysis tools, however, are sub-optimal for higher-order clustering. Developing tensor tools for solving block models has received increased interest recently [10], [12], [13]. **suboptimal**

The classical tensor block model suffers from drawbacks to model real world data in spite of the popularity. The key underlying assumption of block model is that all nodes in the same community are exchangeable; i.e., the nodes have no individual-specific parameters apart from the community-specific parameters. However, the exchangeability assumption is often non-realistic. Each node may contribute to the data variation by its own multiplicative effect. We call the unequal node-specific effects the *degree heterogeneity*. Such degree heterogeneity appears commonly in social networks. Ignoring the degree heterogeneity may seriously mislead the clustering results. For example, the regular block model fails to model the member affiliation in the Karate Club network [14] without addressing degree heterogeneity.

The *degree-corrected tensor block model* (dTBM) has been proposed recently to account for the degree heterogeneity [9]. The dTBM combines a higher-order checkerboard structure with degree parameter $\theta = (\theta(1), \dots, \theta(p))^T$ to allow heterogeneity among p nodes. Figure 1 compares the underlying structures of TBM and dTBM with the same number of communities. The dTBM allows varying values within the same community, thereby allowing a richer structure. To solve dTBM, we project clustering objects to a unit sphere and perform iterative clustering based on angle similarity. We refer to the algorithm as the *spherical clustering*; detailed procedures are in Section IV. The spherical clustering avoids the estimation of nuisance degree heterogeneity. The usage of angle similarity brings new challenges to the theoretical results, and we develop new polar-coordinate based techniques in the proofs.

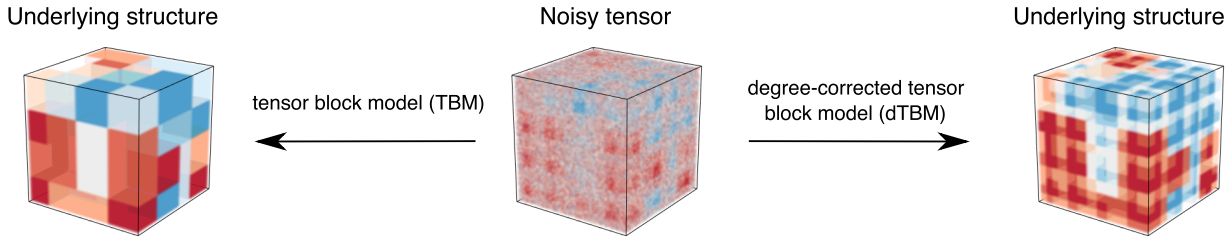


Fig. 1. Examples for order-3 tensor block model (TBM) with and without degree correction. Both TBM and dTBM have four communities on each mode, while dTBM allows a richer structure with degree heterogeneity.

83 A. Our Contributions

84 The primary goal of this paper is to provide both statistical
85 and computational guarantees for dTBM. Our main contributions
86 are summarized below.

- 87 • We develop a general dTBM and establish the identifiability
88 for the uniqueness of clustering using the notion of angle separability.
- 89 • We present the phase transition of clustering performance
90 with respect to three different statistical and computational behaviors. We characterize, for the first time,
91 the critical signal-to-noise (SNR) thresholds in dTBMs,
92 revealing the intrinsic distinctions among (vector) one-
93 dimensional clustering, (matrix) biclustering, and (tensor)
94 higher-order clustering. Specific SNR thresholds and
95 algorithm behaviors are depicted in Figure 2.
- 96 • We provide an angle-based algorithm that achieves exact
97 clustering *in polynomial time* under mild conditions. Sim-
98 ulation and data studies demonstrate that our algorithm
99 outperforms existing higher-order clustering algorithms.

100 The last two contributions, to our best knowledge, are new to
101 the literature of dTBMs.

104 B. Related Work

nonconvex
noncontinuous

105 Our work is closely related to but also distinct from several
106 lines of existing research. Table I summarizes the most relevant
107 models.

- 108 • *Block model for clustering.* The block model such as
109 stochastic block model (SBM) and degree-corrected SBM
110 has been widely used for matrix clustering problems.
111 The theoretical properties and algorithm performance for
112 matrix block models have been well-studied [15]; see the
113 review paper [11] and the references therein. However,
114 The tensor counterparts are relatively less understood.
115
- 116 • *Tensor block model.* The (non-degree) tensor block model
117 (TBM) is a higher-order extension of SBM, and its
118 statistical-computational properties are investigated in
119 recent literatures [7], [10], [13]. Some works [16] study
120 the TBM with sparse observations, while, others [10],
121 [13] and our work focus on the dense regime. Extending
122 results from non-degree to degree-corrected model
123 is highly challenging. Our dTBM parameter space is
124 equipped with angle-based similarity and nuisance degree
125 parameters. The extra complexity makes the Cartesian
126 coordinates based analysis [13] non-applicable to our
127 setting. Towards this goal, we have developed a new polar
128 nonapplicable

127 coordinates based analysis to control the model complex-
128 ity. We have also developed a new angle-based iteration
129 algorithm to achieve optimal clustering rates *without the*
130 *need of estimating nuisance degree parameters.*

- 131 • *Degree-corrected block model.* The hypergraph
132 degree-corrected block model (hDCBM) and its
133 variant have been proposed in the literature [9],
134 [17]. For this popular model, however, the optimal
135 statistical-computational rates remain an open problem.
136 Our main contribution is to provide a sharp statistical
137 and computational critical phase transition in dTBM
138 literature. In addition, our algorithm results in a faster
139 exponential error rate, in contrast to the polynomial
140 rate in [9]. The original hDCBM [9] is designed for
141 binary observations only, and we extend the model to
142 both continuous and binary observations. We believe
143 our results are novel and helpful to the community. See
144 Figure 2 for overview of our results.

- 145 • *Global-to-local algorithm strategy.* Our methods gen-
146 eralize the recent global-to-local strategy for matrix
147 learning [15], [18], [19] to tensors [13], [16], [20].
148 Despite the conceptual similarity, we address several
149 fundamental challenges associated with this non-convex,
150 non-continuous problem. We show the insufficiency of
151 the conventional tensor HOSVD [21], and we develop
152 a weighted higher-order initialization that relaxes the
153 singular-value gap separation condition. Furthermore,
154 our local iteration leverages the angle-based clustering
155 in order to avoid explicit estimation of degree heteroge-
156 neity. Our bounds reveal the interesting interplay between
157 the computational and statistical errors. We show that
158 our final estimate *provably* achieves the exact clustering
159 within only polynomial-time complexity.

160 C. Notation

161 We use lower-case letters (e.g., a, b) for scalars, lower-case
162 boldface letters (e.g., $\mathbf{a}, \boldsymbol{\theta}$) for vectors, upper-case boldface
163 letters (e.g., \mathbf{X}, \mathbf{Y}) for matrices, and calligraphy letters (e.g.,
164 \mathcal{X}, \mathcal{Y}) for tensors of order three or greater. We use $\mathbf{1}_p$ to denote
165 a vector of length p with all entries to be 1. We use $|\cdot|$ for
166 the cardinality of a set and $\mathbf{1}\{\cdot\}$ for the indicator function. For
167 an integer $p \in \mathbb{N}_+$, we use the shorthand $[p] = \{1, 2, \dots, p\}$.
168 For a length- p vector \mathbf{a} , we use $a(i) \in \mathbb{R}$ to denote the i -th
169 entry of \mathbf{a} , and use \mathbf{a}_I to denote the sub-vector by restricting
170 the indices in the set $I \subset [p]$. We use $\|\mathbf{a}\| = \sqrt{\sum_i a^2(i)}$ to
171 denote the ℓ_2 -norm, $\|\mathbf{a}\|_1 = \sum_i |a_i|$ to denote the ℓ_1 norm of
172 subvector

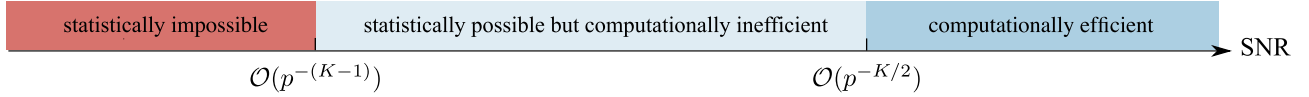


Fig. 2. SNR thresholds for statistical and computational limits in order- K dTBM with dimension (p, \dots, p) and $K \geq 2$. The SNR gap between statistical possibility and computational efficiency exists only for tensors with $K \geq 3$.

	TABLE I						Footnote 1	Footnote 2	Add period after "dimension p" when moving to the footnote
	COMPARISON BETWEEN PREVIOUS METHODS WITH OUR METHOD. *WE LIST THE RESULT FOR ORDER- K TENSORS WITH $K \geq 3$ AND GENERAL NUMBER OF COMMUNITIES $r = \mathcal{O}(1)$. **THE PARAMETER $\alpha = f(p) > 0$ DENOTES THE SPARSITY LEVEL WHICH IS SOME FUNCTION OF DIMENSION p								
Allow tensors of arbitrary order	Gao et al. (2018)[15]	Ahn et al. (2018)[16]	Han et al. (2022)[13]	Ghoshdastidar et al. (2019)[7]	Ke et al. (2019)[9]				Ours
Allow degree heterogeneity	✓	✗	✗	✓	✓				✓
Singular-value gap-free clustering	✓	✗	✗	✗	✗				✓
Misclustering rate (for order K^*)	-	$p^{-(K-1)\alpha^{-1}**}$	$\exp(-p^{K/2})$	p^{-1}	p^{-2}				$\exp(-p^{K/2})$
Consider sparse observation	✗	✓	✗	✗	✗				✗

- 172 a. For two vector \mathbf{a}, \mathbf{b} of the same dimension, we denote the
173 angle between \mathbf{a}, \mathbf{b} by

$$174 \cos(\mathbf{a}, \mathbf{b}) = \frac{\langle \mathbf{a}, \mathbf{b} \rangle}{\|\mathbf{a}\| \|\mathbf{b}\|},$$

175 where $\langle \mathbf{a}, \mathbf{b} \rangle$ is the inner product of two vectors and
176 $\cos(\mathbf{a}, \mathbf{b}) \in [-1, 1]$. We make the convention that $\cos(\mathbf{a}, \mathbf{b}) =$
177 $\cos(\mathbf{a}^T, \mathbf{b}^T)$.

178 Let $\mathcal{Y} \in \mathbb{R}^{p_1 \times \dots \times p_K}$ be an order- K (p_1, \dots, p_K) -
179 dimensional tensor. We use $\mathcal{Y}(i_1, \dots, i_K)$ to denote the
180 (i_1, \dots, i_K) -th entry of \mathcal{Y} . The multilinear multiplication of a
181 tensor $\mathcal{S} \in \mathbb{R}^{r_1 \times \dots \times r_K}$ by matrices $\mathbf{M}_k \in \mathbb{R}^{p_k \times r_k}$ results in
182 an order- K (p_1, \dots, p_K) -dimensional tensor \mathcal{X} , denoted

$$183 \mathcal{X} = \mathcal{S} \times_1 \mathbf{M}_1 \times \dots \times_K \mathbf{M}_K,$$

184 where the entries of \mathcal{X} are defined by

$$185 \mathcal{X}(i_1, \dots, i_K) \\ 186 = \sum_{(j_1, \dots, j_K)} \mathcal{S}(j_1, \dots, j_K) \mathbf{M}_1(i_1, j_1) \dots \mathbf{M}_K(i_K, j_K).$$

187 For a matrix \mathbf{Y} , we use $\mathbf{Y}_{i:}$ (respectively, $\mathbf{Y}_{:i}$) to denote the
188 i -th row (respectively, i -th column) of the matrix. Similarly,
189 for an order-3 tensor, we use $\mathcal{Y}_{::i}$ to denote the i -th matrix
190 slide of the tensor. We use $\text{Ave}(\cdot)$ to denote the operation of
191 taking averages across elements and $\text{Mat}_k(\cdot)$ to denote the
192 unfolding operation that reshapes the tensor along mode k
193 into a matrix. For a symmetric tensor $\mathcal{X} \in \mathbb{R}^{p \times \dots \times p}$, we omit
194 the subscript and use $\text{Mat}(\mathcal{X}) \in \mathbb{R}^{p \times p^{K-1}}$ to denote the
195 unfolding. For two sequences $\{a_p\}, \{b_p\}$, we denote $a_p \lesssim b_p$
196 or $a_p = \mathcal{O}(b_p)$ if $\lim_{p \rightarrow \infty} a_p/b_p \leq c$, $a_p \gtrsim b_p$ or $a_p = \Omega(b_p)$
197 if $\lim_{p \rightarrow \infty} a_p/b_p \geq c$, for some constant $c > 0$, $a_p = o(b_p)$
198 if $\lim_{p \rightarrow \infty} a_p/b_p = 0$, and $a_p \asymp b_p$ if both $b_p \lesssim a_p$ and
199 $a_p \lesssim b_p$. Throughout the paper, we use the terms “community”
200 and “clusters” exchangeably.

201 1) *Organization:* The rest of this paper is organized as
202 follows. Section II introduces the degree-corrected tensor
203 block model (dTBM) with three motivating examples and
204 presents the identifiability of dTBM under the angle gap
205 condition. We show the phase transition and the existence of
206 statistical-computational gaps for the higher-order dTBM in
207 Section III. In Section IV, we provide a polynomial-time two-
208 stage algorithm with misclustering rate guarantees. Extension

209 to Bernoulli models is also presented. In Section V, we compare
210 our work with non-degree tensor block models. Numerical
211 studies including the simulation, comparison with other
212 methods, and two real dataset analyses are in Sections VI-VII.
213 The main technical ideas we develop for addressing main
214 theorems are provided in Section VIII. Detailed proofs and
215 extra theoretical results are provided in Appendix.

II. MODEL FORMULATION AND MOTIVATIONS

A. Degree-Corrected Tensor Block Model

Suppose that we have an order- K data tensor $\mathcal{Y} \in \mathbb{R}^{p \times \dots \times p}$. Assume that there exist $r \geq 1$ disjoint communities among the p nodes. We represent the community assignment by a function $z: [p] \mapsto [r]$, where $z(i) = a$ for i -th node that belongs to the a -th community. Then, $z^{-1}(a) = \{i \in [p]: z(i) = a\}$ denotes the set of nodes that belong to the a -th community, and $|z^{-1}(a)|$ denotes the number of nodes in the a -th community. Let $\boldsymbol{\theta} = (\theta(1), \dots, \theta(p))^T$ denote the degree heterogeneity for p nodes. We consider the order- K dTBM [7], [9],

$$\mathcal{Y}(i_1, \dots, i_K) = \mathcal{S}(z(i_1), \dots, z(i_K)) \prod_{k=1}^K \theta_{i_k} + \mathcal{E}(i_1, \dots, i_K),$$

where $\mathcal{S} \in \mathbb{R}^{r \times \dots \times r}$ is an order- K tensor collecting the block means among communities, and $\mathcal{E} \in \mathbb{R}^{p \times \dots \times p}$ is a noise tensor consisting of independent zero-mean sub-Gaussian entries with variance bounded by σ^2 . The unknown parameters are z , \mathcal{S} , and $\boldsymbol{\theta}$. The dTBM can be equivalently written in a compact form of tensor-matrix product:

$$\mathbb{E}\mathcal{Y} = \mathcal{S} \times_1 \boldsymbol{\Theta} \mathbf{M} \times_2 \dots \times_K \boldsymbol{\Theta} \mathbf{M}, \quad (1)$$

where $\boldsymbol{\Theta} = \text{diag}(\theta(1), \dots, \theta(p)) \in \mathbb{R}^{p \times p}$ is a diagonal matrix, $\mathbf{M} \in \{0, 1\}^{p \times r}$ is the membership matrix associated with community assignment z such that $\mathbf{M}(i, j) = 1\{z(i) = j\}$. By definition, each row of \mathbf{M} has one copy of 1's and 0's elsewhere. Note that the discrete nature of \mathbf{M} renders our model (1) more challenging than Tucker decomposition. We call a tensor \mathcal{Y} an r -block tensor with degree $\boldsymbol{\theta}$ if \mathcal{Y} admits dTBM (1) and let $\mathcal{X} = \mathbb{E}\mathcal{Y}$ denote the mean tensor. The goal of clustering is to estimate z from a single noisy tensor \mathcal{Y} . We are particularly interested in the high-dimensional regime where p grows whereas $r = \mathcal{O}(1)$.

For ease of notation, we have focused on the case with symmetric mean tensor $\mathbb{E}\mathcal{Y}$. This assumption simplifies the notation because all modes have the same (Θ, M, z) ; the noise tensor \mathcal{E} and the data tensor \mathcal{Y} are still possibly asymmetric. In general, we allow asymmetric mean tensors with $\{(\Theta_k, M_k, z_k)\}_{k=1}^K$, one for each mode. The extension can be found in Appendix B.

B. Motivating Examples

Here, we provide four applications to illustrate the practical necessity of dTBM.

1) *Tensor Block Model*: Consider the model (1). Let $\theta(i) = 1$ for all $i \in [p]$. The model (1) reduces to the tensor block model, which is widely used in previous clustering algorithms [10], [12], [13]. The theoretical results in TBM serve as benchmarks for dTBM.

2) *Community Detection in Hypergraphs*: The hypergraph network is a powerful tool to represent the complex entity relations with higher-order interactions [9]. A typical undirected hypergraph is denoted as $H = (V, E)$, where $V = [p]$ is the set of nodes and E is the set of undirected hyperedges. Each hyperedge in E is a subset of V , and we call the hyperedge an order- K edge if the corresponding subset involves K nodes. We call H a K -uniform hypergraph if E only contains order- K edges.

It is natural to represent the K -uniform hypergraph using a binary order- K adjacency tensor. Let $\mathcal{Y} \in \{0, 1\}^{p \times \dots \times p}$ denote the adjacency tensor, where the entries encode the presence or absence of order- K edges among p nodes. Specifically, for all $(i_1, \dots, i_K) \in [p]^K$, we have

$$\mathcal{Y}(i_1, \dots, i_K) = \begin{cases} 1 & \text{if } (i_1, \dots, i_K) \in E, \\ 0 & \text{if } (i_1, \dots, i_K) \notin E. \end{cases}$$

Assume that there exist r disjoint communities among p nodes, and the connection probabilities depend on the community assignments and node-specific parameters. Then, the equation (1) models $\mathbb{E}\mathcal{Y}$ with unknown degree heterogeneity θ and sub-Gaussianity parameter $\sigma^2 = 1/4$.

3) *Multi-Layer Weighted Network*: Multi-layer weighted network data consists of multiple networks over the same set of nodes. One representative example is the brain connectome data [22]. The multi-layer weighted network \mathcal{Y} has dimension of $p \times p \times L$, where p denotes the number of brain regions of interest, and L denotes the number of layers (networks). Each of the L networks describes one aspect of the brain connectivity, such as functional connectivity or structural connectivity. The resulting tensor \mathcal{Y} consists of a mixture of slices with various data types.

Assume that there exist r disjoint communities among p nodes and r_l disjoint communities among the L layers. The multi-layer network community detection is modeled by the general asymmetric dTBM model (1)

$$\mathbb{E}\mathcal{Y} = \mathcal{S} \times_1 \Theta M \times_2 \Theta M \times_3 \Theta_l M_l,$$

where $(\Theta \in \mathbb{R}^p, M \in \{0, 1\}^{p \times r})$ and $(\Theta_l \in \mathbb{R}^L, M_l \in \{0, 1\}^{L \times r_l})$ are the degree heterogeneity and membership matrices corresponding to the community structure for p nodes and L layers, respectively.

4) *Gaussian Higher-Order Clustering*: Datasets in various fields such as medical image, genetics, and computer science are formulated as Gaussian tensors. One typical example is the multi-tissue gene expression dataset, which records different gene expressions in different individuals and different tissues. The dataset, denoted as $\mathcal{Y} \in \mathbb{R}^{p \times n \times t}$, consists of the expression data for p genes of n individuals in t tissues.

Assume that there exist r_1, r_2, r_3 disjoint clusters for p genes, n individuals, and t tissues, respectively. We apply the general asymmetric dTBM model (1)

$$\mathbb{E}\mathcal{Y} = \mathcal{S} \times_1 \Theta_1 M_1 \times_2 \Theta_2 M_2 \times_3 \Theta_3 M_3,$$

where $\{(\Theta_k, M_k)\}_{k=1}^3$ represents the degree heterogeneity and membership for genes, individuals, and tissues. **Nondegree**

Remark 1 (Comparison With Non-Degree Models): Our dTBM uses fewer block parameters than TBM. In particular, every non-degree r_1 -block tensor can be represented by a *degree-corrected* r_2 -block tensor with $r_2 \leq r_1$. In particular, there exist tensors with $r_1 = p$ but $r_2 = 1$, so the reduction in model complexity can be dramatic from p to 1. This fact highlights the benefits of introducing degree heterogeneity in higher-order clustering tasks.

C. Identifiability Under Angle Gap Condition

The goal of clustering is to estimate the partition function z from model (1). For ease of notation, we focus on symmetric tensors; the extension to non-symmetric tensors are similar. We use \mathcal{P} to denote the following parameter space for (z, \mathcal{S}, θ) ,

$$\begin{aligned} \mathcal{P} = & \left\{ (z, \mathcal{S}, \theta) : \theta \in \mathbb{R}_+^p, \frac{c_1 p}{r} \leq |z^{-1}(a)| \leq \frac{c_2 p}{r}, \right. \\ & \left. c_3 \leq \|\text{Mat}(\mathcal{S})_{:a}\| \leq c_4, \|\theta_{z^{-1}(a)}\|_1 = |z^{-1}(a)|, a \in [r] \right\} \end{aligned} \quad \begin{matrix} 321 \\ 322 \\ 323 \\ 324 \\ 325 \\ \text{Change to "asymmetric"} \end{matrix}$$

where $c_i > 0$'s are universal constants. We briefly describe the rationale of the constraints in (2). First, the entrywise positivity constraint on $\theta \in \mathbb{R}_+^p$ is imposed to avoid sign ambiguity between entries in $\theta_{z^{-1}(a)}$ and \mathcal{S} . This constraint allows the trigonometric cos to describe the angle similarity in the Assumption 1 below and Sub-algorithm 2 in Section IV. Note that the positivity constraint can be achieved without sacrificing model flexibility, by using a slightly larger dimension of \mathcal{S} in the factorization (1); see Example 1 below. Second, recall that the quantity $|z^{-1}(a)|$ denotes the number of nodes in the a -th community. The constants c_1, c_2 in the $|z^{-1}(a)|$ bounds assume the roughly balanced size across r communities. Third, the constant c_3 requires that all slides in \mathcal{S} have non-degenerate norm. Particularly, the lower bound c_3 excludes the purely zero slide to avoid trivial non-identifiability of model (1); see Example 2 below. The upper bound c_4 is a technical constraint to avoid the slides with diverging norm as dimension grows. Lastly, the ℓ_1 normalization $\|\theta_{z^{-1}(a)}\|_1 = |z^{-1}(a)|$ is imposed to avoid the scalar ambiguity between $\theta_{z^{-1}(a)}$ and \mathcal{S} . This constraint, again, incurs no restriction to model flexibility but makes our presentation cleaner. Our constraints in \mathcal{P} are mild compared with previous literature; see Table II for comparison.

nondegenerate; nonidentifiability

352 *Example 1 (Positivity of Degree Parameters):* Here we
 353 provide an example to show the positivity constraint
 354 on $\boldsymbol{\theta}$ incurs no loss on the model flexibility. Consider
 355 an order-3 dTBM with core tensor $\mathcal{S} = 1$ and degree
 356 $\boldsymbol{\theta} = (1, 1, -1, -1)^T$. We have the mean tensor

$$357 \quad \mathcal{X} = \mathcal{S} \times_1 \boldsymbol{\Theta} \mathbf{M} \times_2 \boldsymbol{\Theta} \mathbf{M} \times_3 \boldsymbol{\Theta} \mathbf{M},$$

358 where $\boldsymbol{\Theta} = \text{diag}(\boldsymbol{\theta})$ and $\mathbf{M} = (1, 1, 1, 1)^T$. Note that $\mathcal{X} \in$
 359 $\mathbb{R}^{4 \times 4 \times 4}$ is a 1-block tensor with *mixed-signed* degree $\boldsymbol{\theta}$, and
 360 the mode-3 slices of \mathcal{X} are

$$361 \quad \mathcal{X}_{::1} = \mathcal{X}_{::2} = -\mathcal{X}_{::3} = -\mathcal{X}_{::4} = \begin{bmatrix} 1 & 1 & -1 & -1 \\ 1 & 1 & -1 & -1 \\ -1 & -1 & 1 & 1 \\ -1 & -1 & 1 & 1 \end{bmatrix}.$$

362 Now, instead of original decomposition, we encode \mathcal{X} as
 363 a 2-block tensor with *positive-signed* degree. Specifically,
 364 we write

$$365 \quad \mathcal{X} = \mathcal{S}' \times_1 \boldsymbol{\Theta}' \mathbf{M}' \times_2 \boldsymbol{\Theta}' \mathbf{M}' \times_3 \boldsymbol{\Theta}' \mathbf{M}',$$

366 where $\boldsymbol{\Theta}' = \text{diag}(\boldsymbol{\theta}') = \text{diag}(1, 1, 1, 1)$, the core tensor $\mathcal{S}' \in$
 367 $\mathbb{R}^{2 \times 2 \times 2}$ has following mode-3 slices, and the membership
 368 matrix $\mathbf{M}' \in \{0, 1\}^{4 \times 2}$ defines the clustering $z' : [4] \rightarrow [2]$;
 369 i.e.,

$$370 \quad \mathcal{S}'_{::1} = -\mathcal{S}'_{::2} = \begin{bmatrix} 1 & -1 \\ -1 & 1 \end{bmatrix}, \quad \mathbf{M}' = \begin{bmatrix} 1 & 0 \\ 1 & 0 \\ 0 & 1 \\ 0 & 1 \end{bmatrix}.$$

371 The triplet $(z', \mathcal{S}', \boldsymbol{\theta}')$ lies in our parameter space (2). In general, we can always reparameterize an r -block tensor with mixed-signed degree using a $2r$ -block tensor with positive-signed degree. Since we assume $r = \mathcal{O}(1)$ throughout the paper, the splitting does not affect the error rates of our interest.

Nonidentifiability

377 *Example 2 (Non-Identifiability With Purely Zero Core Slice):*
 378 Consider an order-2 dTBM with core tensor $\mathcal{S} = \begin{pmatrix} 0 & 0 \\ 1 & -1 \end{pmatrix}$
 379 degree matrices $\boldsymbol{\Theta}_1 = \boldsymbol{\Theta}_2 = \text{diag}(1, 1, 1, 1)$, and mean tensor

$$380 \quad \mathcal{X} = \boldsymbol{\Theta}_1 \mathbf{M} \mathcal{S} \mathbf{M}^T \boldsymbol{\Theta}_2, \quad \text{with } \mathbf{M} = \begin{bmatrix} 1 & 0 \\ 1 & 0 \\ 0 & 1 \\ 0 & 1 \end{bmatrix}.$$

381 Replacing $\boldsymbol{\Theta}_1$ by $\boldsymbol{\Theta}'_1 = (3/2, 1/2, 1, 1)$ leads to the same
 382 mean tensor \mathcal{X} .

383 We now provide the identifiability conditions for our model
 384 before estimation procedures. When $r = 1$, the decomposition
 385 in (1) is always unique (up to cluster label permutation) in \mathcal{P} ,
 386 because dTBM is equivalent to the rank-1 tensor family under
 387 this case. When $r \geq 2$, the Tucker rank of signal tensor $\mathbb{E}\mathcal{Y}$
 388 in (1) is bounded by, but not necessarily equal to, the number
 389 of blocks r [10]. Therefore, one can not apply the classical
 390 identifiability conditions for low-rank tensors to dTBM. Here,
 391 we introduce a key separation condition on the core tensor.

392 *Assumption 1 (Angle Gap):* Let $\mathbf{S} = \text{Mat}(\mathcal{S})$. Assume that
 393 the minimal gap between normalized rows of \mathbf{S} is bounded

away from zero; i.e.,

$$394 \quad \Delta_{\min} := \min_{a \neq b \in [r]} \left\| \frac{\mathbf{S}_{a:}}{\|\mathbf{S}_{a:}\|} - \frac{\mathbf{S}_{b:}}{\|\mathbf{S}_{b:}\|} \right\| > 0, \quad \text{for } r \geq 2. \quad (3) \quad 395$$

We make the convention $\Delta_{\min} = 1$ for $r = 1$. Equivalently, (3) says that none of the two rows in \mathbf{S} are parallel; i.e., $\max_{a \neq b \in [r]} \cos(\mathbf{S}_{a:}, \mathbf{S}_{b:}) = 1 - \Delta_{\min}^2/2 < 1$. The quantity Δ_{\min} characterizes the *non-redundancy* among clusters measured by angle separation. The denominators involved in definition (3) are well posed because of the lower bound on $\|\mathbf{S}_{a:}\|$ in (2).

Our first main result is the following theorem showing the sufficiency and necessity of the angle gap separation condition for the parameter identifiability under dTBM.

Theorem 1 (Model Identifiability): Consider the dTBM with $r \geq 2$ and $K \geq 2$. The parameterization (1) is unique in \mathcal{P} up to cluster label permutations, if and only if Assumption 1 holds.

The identifiability guarantee for the dTBM is stronger than classical Tucker model. In the Tucker model, the factor matrix \mathbf{M} is identifiable only up to orthogonal rotations. In contrast, our model does not suffer from rotational invariance. As we will show in Section IV, each column of the membership matrix \mathbf{M} can be precisely recovered under our algorithm. This property benefits the interpretation of dTBM in practice.

III. STATISTICAL-COMPUTATIONAL CRITICAL VALUES FOR HIGHER-ORDER TENSORS

A. Assumptions

We propose the signal-to-noise ratio (SNR),

$$417 \quad \text{SNR} := \Delta_{\min}^2 / \sigma^2 = p^\gamma, \quad (4) \quad 421$$

422 with varying $\gamma \in \mathbb{R}$ that quantifies different regimes of
 423 interest. We call γ the *signal exponent*. Intuitively, a larger
 424 SNR, or equivalently a larger γ , benefits the clustering in the
 425 presence of noise. With quantification (4), we consider the
 426 following parameter space,

$$427 \quad \mathcal{P}(\gamma) = \mathcal{P} \cap \{\mathcal{S} \text{ satisfies SNR condition (4) with } \gamma\}. \quad (5) \quad 427$$

428 The 1-block dTBM does not belong to the space $\mathcal{P}(\gamma)$ when
 429 $\gamma < 0$, due to the convention in Assumption 1. Our goal is to
 430 characterize the clustering accuracy with respect to γ under
 431 the space $\mathcal{P}(\gamma)$.

432 In our algorithmic development, we often refer to the
 433 regime of balanced degree heterogeneity. We call the degree
 434 $\boldsymbol{\theta}$ *balanced* if

$$435 \quad \min_{a \in [r]} \|\boldsymbol{\theta}_{z^{-1}(a)}\| = (1 + o(1)) \max_{a \in [r]} \|\boldsymbol{\theta}_{z^{-1}(a)}\|. \quad (6) \quad 435$$

436 The following lemma provides the rationale of balanced degree
 437 assumption. We show the close relation between angle gaps
 438 in the mean tensor \mathcal{X} and the core tensor \mathcal{S} under balanced
 439 degree heterogeneity.

440 *Lemma 1 (Angle Gaps in \mathcal{X} and \mathcal{S}):* Consider the dTBM
 441 model (1) under the parameter space \mathcal{P} in (2) with $r \geq 2$.
 442 Suppose $\boldsymbol{\theta}$ is balanced satisfying (6) and $\min_{i \in [p]} \theta(i) \geq c$

TABLE II
PARAMETER SPACE COMPARISON BETWEEN PREVIOUS WORK WITH OUR ASSUMPTION

Assumptions in parameter space	Gao et al. (2018)[15]	Han et al. (2022)[13]	Ke et al. (2019)[9]	Ours
Balanced community sizes	✓	✓	✓	✓
Bounded core tensors	✓	✗	✓	✓
Balanced degrees	✓	-	✓	✓
Flexible in-group connections	✗	✓	✓	✓
Gaps among cluster centers	In-between cluster difference	Euclidean gap	Eigen gap	Angle gap

from some constant $c > 0$. Then, as $p \rightarrow \infty$, for all i, j such that $z(i) \neq z(j)$, we have

$$\cos(\mathbf{X}_{i:}, \mathbf{X}_{j:}) \asymp \cos(\mathbf{S}_{z(i):}, \mathbf{S}_{z(j):}),$$

where $\mathbf{X} = \text{Mat}(\mathcal{X})$ and $\mathbf{S} = \text{Mat}(\mathcal{S})$.

In practice, an estimation algorithm has access to a noisy version of \mathcal{X} but not \mathcal{S} . Our goal is to establish the algorithm performance with respect to the signal Δ_{\min}^2 in the core tensor. By Lemma 1, the mapping from the core tensor $\mathbf{S}_{z(i)}$ to the mean tensor $\mathbf{X}_{z(i)}$ preserves the angle information Δ_{\min}^2 under balanced degree heterogeneity (6). Therefore, the balanced degree assumption helps to exclude the cases in which the degree heterogeneity distorts the algorithm guarantees.

Here, we provide an example to illustrate the insufficiency of Δ_{\min}^2 in the absence of balanced degrees.

Example 3 (Insufficiency of Δ_{\min}^2 in the Absence of Balanced Degrees): Consider an order-2 (p, p) -dimensional dTBM with core matrix

$$\mathbf{S} = \begin{pmatrix} 1 & a \\ 1 & -a \end{pmatrix}, \quad (7)$$

and $\boldsymbol{\theta}$ such that $\|\boldsymbol{\theta}_{z^{-1}(1)}\|^2 = p^m \|\boldsymbol{\theta}_{z^{-1}(2)}\|^2$, where $m \in [-1, 1]$ is a scalar parameter controlling the skewness of degrees. Let $\Delta_{\mathbf{X}}^2$ denote the minimal angle gap of the mean tensor, defined by

$$\Delta_{\mathbf{X}}^2 := \min_{i,j \in [p], z(i) \neq z(j)} \left\| \frac{\mathbf{X}_{i:}}{\|\mathbf{X}_{i:}\|} - \frac{\mathbf{X}_{j:}}{\|\mathbf{X}_{j:}\|} \right\|, \quad (8)$$

where $\mathbf{X} = \text{Mat}(\mathcal{X})$. Take $a = p^{-1/4}$ in the model setup (7). We have

$$\begin{aligned} \Delta_{\min}^2 &= \frac{2a^2}{1+a^2} \asymp p^{-1/2}, \\ \Delta_{\mathbf{X}}^2 &= \frac{2\|\boldsymbol{\theta}_{z^{-1}(2)}\|^2 a^2}{\|\boldsymbol{\theta}_{z^{-1}(1)}\|^2 + \|\boldsymbol{\theta}_{z^{-1}(2)}\|^2 a^2} \asymp p^{-1/2-m}. \end{aligned}$$

Based on the Theorem 2 in Section III, the dTBM is impossible to solve when $\Delta_{\mathbf{X}}^2 \lesssim p^{-1}$ even though $\Delta_{\min}^2 \asymp p^{-1/2}$; that is, the dTBM estimation depends on the relative magnitude of m vs. $1/2$. In such a setting, the proposed signal notion Δ_{\min}^2 alone fails to fully characterize dTBM.

Remark 2 (Flexibility in Balanced Degree Assumption): One important note is that our balance assumption (6) does not preclude the mild degree heterogeneity. In fact, within each of the clusters, we allow the highest degree at the order $\mathcal{O}(p)$, whereas the lowest degree at the order $\Omega(1)$. This range is more relaxed than previous work [15] that restricts the highest degree in the sub-linear regime $o(p)$ and the lowest degree at the order $\Omega(1)$.

Remark 3 (Similar Assumptions in Literature): Similar degree regulations are not rare in literature. In higher-order tensor model [9], the degree assumption $\max_{a \in [r]} \|\boldsymbol{\theta}_{z^{-1}(a)}\| \leq C \min_{a \in [r]} \|\boldsymbol{\theta}_{z^{-1}(a)}\|$ is made to ensure degree balance across communities. In [15], the degree distribution is restricted to $\frac{1}{|z^{-1}(a)|} \sum_{i \in z^{-1}(a)} \theta_i = 1 + o(1)$ for all communities.

Last, let \hat{z} and z be the estimated and true clustering functions in the family (2). Define the misclustering error by

$$\ell(\hat{z}, z) = \frac{1}{p} \min_{\pi \in \Pi} \sum_{i \in [p]} \mathbb{1}\{\hat{z}(i) \neq \pi \circ z(i)\}, \quad (48)$$

where $\pi : [r] \mapsto [r]$ is a permutation of cluster labels, \circ denotes the composition operation, and Π denotes the collection of all possible permutations. The infimum over all permutations accounts for the ambiguity in cluster label permutation.

In Sections III-B and III-C, we provide the phase transition of $\ell(\hat{z}, z)$ for general Gaussian dTBMs (1) without symmetric assumptions. For general (asymmetric) Gaussian dTBMs, we assume Gaussian noise $\mathcal{E}(i_1, \dots, i_K) \stackrel{\text{i.i.d.}}{\sim} N(0, \sigma^2)$, and we extend the parameter space (2) to allow K clustering functions $\{z_k\}_{k \in [K]}$, one for each mode. For notational simplicity, we still use z and $\mathcal{P}(\gamma)$ for this general (asymmetric) model. All results should be interpreted as the worst-case results across K modes.

B. Statistical Critical Value

The statistical critical value means the SNR required for solving dTBMs with *unlimited computational cost*. Our following result shows the minimax lower bound for exact recovery and the matching upper bound for maximum likelihood estimator (MLE). We consider the Gaussian MLE, denoted as $(\hat{z}_{\text{MLE}}, \hat{\mathcal{S}}_{\text{MLE}}, \hat{\boldsymbol{\theta}}_{\text{MLE}})$, over the estimation space \mathcal{P} , where

$$(\hat{z}_{\text{MLE}}, \hat{\mathcal{S}}_{\text{MLE}}, \hat{\boldsymbol{\theta}}_{\text{MLE}}) = \arg \min_{(z, \mathcal{S}, \boldsymbol{\theta}) \in \mathcal{P}} \|\mathcal{Y} - \mathcal{X}(z, \mathcal{S}, \boldsymbol{\theta})\|_F^2. \quad (9)$$

Capitalize initial letters.

Statistical Critical Value

Theorem 2 (Statistical critical value): Consider general Gaussian dTBMs with parameter space $\mathcal{P}(\gamma)$ and $K \geq 2$. Then, we have the following statistical phase transition.

• Impossibility. Assume $p \rightarrow \infty$ and $2 \leq r \lesssim p^{1/3}$. Let $\mathcal{P}_{\mathcal{S}}(\gamma) := \{\mathcal{S} : c_3 \leq \|\text{Mat}(\mathcal{S})_a\| \leq c_4, a \in [r]\} \cap \{\mathcal{S} : \Delta_{\min}^2 = p^\gamma\}$ denote the space for valid \mathcal{S} satisfying SNR condition (4), and $\mathcal{P}_{z, \boldsymbol{\theta}} := \{\boldsymbol{\theta} \in \mathbb{R}_+^p, \frac{c_1 p}{r} \leq |z^{-1}(a)| \leq \frac{c_2 p}{r}, \|\boldsymbol{\theta}_{z^{-1}(a)}\|_1 = |z^{-1}(a)|, a \in [r]\}$ denote the space for valid $(z, \boldsymbol{\theta})$, where c_1, c_2, c_3, c_4 are the constants in parameter space (2). If the signal exponent satisfies $\gamma < -(K-1)$, then, for any true core tensor $\mathcal{S} \in \mathcal{P}_{\mathcal{S}}(\gamma)$, no estimator \hat{z}_{stat} achieves exact recovery in expectation;

526 that is, when $\gamma < -(K - 1)$, we have

$$\liminf_{p \rightarrow \infty} \inf_{\mathcal{S} \in \mathcal{P}_S(\gamma)} \inf_{\hat{z}_{\text{stat}}} \sup_{(z, \theta) \in \mathcal{P}_{z, \theta}} \mathbb{E} [p\ell(\hat{z}_{\text{stat}}, z)] \geq 1. \quad (10)$$

528 Further, we define the parameter space $\mathcal{P}'(\gamma') := \mathcal{P} \cap$
529 $\{\Delta_X^2 = p^{\gamma'}\}$, where Δ_X^2 is the mean tensor minimal gap
530 in (8). When $\gamma' < -(K - 1)$, we have

$$\liminf_{p \rightarrow \infty} \inf_{\hat{z}_{\text{stat}}} \sup_{(z, \mathcal{S}, \theta) \in \mathcal{P}'(\gamma')} \mathbb{E} [p\ell(\hat{z}_{\text{stat}}, z)] \geq 1.$$

- 532 • **MLE achievability.** Suppose that the signal exponent
533 satisfies $\gamma > -(K - 1) + c_0$ for an arbitrary constant
534 $c_0 > 0$. Furthermore, assume that θ is balanced and
535 $\min_{i \in [p]} \theta(i) \geq c$ from some constant $c > 0$. Then, when
536 $p \rightarrow \infty$, for fixed $r \geq 1$, the MLE in (9) achieves exact
537 recovery in high probability; that is,

$$\ell(\hat{z}_{\text{MLE}}, z) \lesssim \text{SNR}^{-1} \exp\left(-\frac{p^{K-1} \text{SNR}}{r^{K-1}}\right) \rightarrow 0,$$

539 with probability going to 1.

540 The proofs for the two parts in Theorem 2 are in the
541 Appendix B, Section B-D and Section B-G, respectively.
542 The first part of Theorem 2 demonstrates impossibility of
543 exact recovery whenever the core tensor \mathcal{S} satisfies SNR
544 condition (4) with exponent $\gamma < -(K - 1)$. The proof is
545 information-theoretical, and therefore the results apply to all
546 statistical estimators, including but not limited to MLE and
547 trace maximization [6]. The minimax bound (10) indicates the
548 worst case impossibility for a particular core tensor \mathcal{S} with
549 signal exponent $\gamma < -(K - 1)$; i.e., under the assumptions of
550 Theorem 2, when $\gamma < -(K - 1)$, we have

$$\liminf_{p \rightarrow \infty} \inf_{\hat{z}_{\text{stat}}} \sup_{(z, \mathcal{S}, \theta) \in \mathcal{P}(\gamma)} \mathbb{E} [p\ell(\hat{z}_{\text{stat}}, z)] \geq 1.$$

552 Such worst case impossibility is studied in related works [13],
553 [15] while our lower bound (10) provides a stronger impossibility
554 statement for arbitrary core tensors with weak signals.
555 The second part of Theorem 2 shows the exact recovery of
556 MLE when $\gamma > -(K - 1) + c_0$ for an arbitrary constant
557 $c_0 > 0$. Combining the impossibility and achievability results,
558 we conclude that the boundary $\gamma_{\text{stat}} := -(K - 1)$ is the critical
559 value for statistical performance of dTBM with respect to our
560 SNR.

561 C. Computational Critical Value

562 The computational critical value means the minimal SNR
563 required for exact recovery with *polynomial-time* computa-
564 tional cost. An important ingredient to establish the computa-
565 tional limits is the *hypergraphic planted clique (HPC) conjec-*
566 *ture* [23], [24]. The HPC conjecture indicates the impossibility
567 of fully recovering the planted cliques with polynomial-time
568 algorithm when the clique size is less than the number of ver-
569 tices in the hypergraph. The formal statement of HPC detection
570 conjecture is provided in Definition 1 and Conjecture 1 as
571 follows.

572 *Definition 1 (Hypergraphic Planted Clique (HPC) Detec-*
573 *tion):* Consider an order- K hypergraph $H = (V, E)$ where

574 $V = [p]$ collects vertices and E collects all the order- K
575 edges. Let $\mathcal{H}_k(p, 1/2)$ denote the Erdős-Rényi K -hypergraph
576 where the edge (i_1, \dots, i_K) belongs to E with probability
577 $1/2$. Further, we let $\mathcal{H}_K(p, 1/2, \kappa)$ denote the hyphpergraph
578 with planted cliques of size κ . Specifically, we generate a
579 hypergraph from $\mathcal{H}_k(p, 1/2)$, pick κ vertices uniformly from
580 $[p]$, denoted K , and then connect all the hyperedges with
581 vertices in K . Note that the clique size κ can be a function of
582 p , denoted κ_p . The order- K HPC detection aims to identify
583 whether there exists a planted clique hidden in an Erdős-
584 Rényi K -hypergraph. The HPC detection is formulated as the
585 following hypothesis testing problem

$$H_0 : H \sim \mathcal{H}_K(p, 1/2) \quad \text{versus} \quad H_1 : H \sim \mathcal{H}_K(p, 1/2, \kappa_p).$$

587 *Conjecture 1 (HPC Conjecture):* Consider the HPC detec-
588 tion problem in Definition 1 with $K \geq 2$. Suppose the
589 sequence $\{\kappa_p\}$ such that $\limsup_{p \rightarrow \infty} \log \kappa_p / \log \sqrt{p} \leq (1 - \tau)$
590 for any $\tau > 0$. Then, for every sequence of polynomial-time
591 test $\{\varphi_p\} : H \mapsto \{0, 1\}$ we have

$$\liminf_{p! \rightarrow \infty} \mathbb{P}_{H_0} (\varphi_p(H) = 1) + \mathbb{P}_{H_1} (\varphi_p(H) = 0) > \frac{1}{2}. \quad 592$$

593 Under the HPC conjecture, we establish the SNR lower
594 bound that is necessary for any *polynomial-time* estimator to
595 achieve exact clustering.

596 *Theorem 3 (Computational Critical Value):* Consider gen-
597 eral Gaussian dTBMs under the parameter space \mathcal{P} with
598 $K \geq 2$. Then, we have the following computational phase
599 transition.

- 600 • **Impossibility.** Assume HPC conjecture holds and $r \geq$
601 2. If the signal exponent satisfies $\gamma < -K/2$, then,
602 no *polynomial-time estimator* \hat{z}_{comp} achieves exact recov-
603 ery in expectation as $p \rightarrow \infty$; that is, when $\gamma < -K/2$,
604 we have

$$\liminf_{p \rightarrow \infty} \sup_{(z, \mathcal{S}, \theta) \in \mathcal{P}(\gamma)} \mathbb{E} [p\ell(\hat{z}_{\text{comp}}, z)] \geq 1. \quad 605$$

- 606 • **Polynomial-time algorithm achievability.** Suppose that
607 we have fixed $r \geq 1$, and the signal exponent satisfies
608 $\gamma > -K/2 + c_0$ for an arbitrary constant $c_0 > 0$.
609 Furthermore, assume that the degree θ is balanced, lower
610 bounded in that $\min_{i \in [p]} \theta_i \geq c$ for some constant $c > 0$,
611 and satisfies the locally linear stability in Definition 2 in
612 the neighborhood $\mathcal{N}(z, \varepsilon)$ for all $\varepsilon \leq E_0$ and some $E_0 \gtrsim$
613 $\log^{-1} p$. Then, as $p \rightarrow \infty$, there exists a polynomial-time
614 algorithm \hat{z}_{ploy} that achieves exact recovery in high prob-
615 ability; that is,

$$\ell(\hat{z}_{\text{poly}}, z) \lesssim \text{SNR}^{-1} \exp\left(-\frac{p^{K-1} \text{SNR}}{r^{K-1}}\right) \rightarrow 0, \quad 616$$

617 with probability going to 1. *Change to ``Section E and Section G''*

618 The proofs for the two parts in Theorem 3 are in the
619 Appendix B, Section B-E and Section B-G, respectively. The
620 first part of Theorem 3 indicates the impossibility of exact
621 recovery by polynomial-time algorithms when $\gamma < -K/2$,
622 and the second part shows the existence of such algorithm
623 when $\gamma > -K/2 + c_0$ for an arbitrary constant $c_0 > 0$ under
624 extra technical assumptions. In Section IV, we will present an

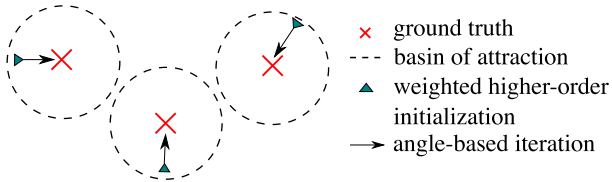


Fig. 3. Illustration of our global-to-local algorithm.

efficient polynomial-time algorithm in this setting. Therefore, we conclude that $\gamma_{\text{comp}} := -K/2$ is the critical value for computational performance of dTBM with respect to our SNR.

Remark 4 (Statistical-Computational Gaps): Now, we have established the phase transition of exact clustering under order- K dTBM by combining Theorems 2 and 3. Figure 2 summarizes our results of critical SNRs when $K \geq 2$. In the weak SNR region $\gamma < -(K-1)$, no statistical estimator succeeds in degree-corrected higher-order clustering. In the strong SNR region $\gamma > -K/2$, our proposed algorithm precisely recovers the clustering in polynomial time. In the moderate SNR regime, $-(K-1) \leq \gamma \leq -K/2$, the degree-corrected clustering problem is statistically easy but computationally hard. Particularly, dTBM reduces to matrix degree-corrected model when $K = 2$, and the statistical and computational bounds show the same critical value. When $K = 1$, dTBM reduces to the degree-corrected sub-Gaussian mixture model (GMM) with model

$$Y = \Theta M S + E,$$

where $Y \in \mathbb{R}^{p \times d}$ collects n data points in \mathbb{R}^d , $S \in \mathbb{R}^{r \times d}$ collects the d -dimensional centroids for r clusters, and $\Theta \in \mathbb{R}^{p \times p}$, $M \in \{0, 1\}^{p \times r}$, $E \in \mathbb{R}^{p \times d}$ have the same meaning as in dTBM. [25] implies that polynomial-time algorithms are able to achieve the statistical minimax lower bound in GMM. Therefore, we conclude that the statistical-computational gap emerges only for higher-order tensors with $K \geq 3$. The result reveals the intrinsic distinctions among (vector) one-dimensional clustering, (matrix) biclustering, and (tensor) higher-order clustering.

IV. POLYNOMIAL-TIME ALGORITHM UNDER MILD SNR

Fig. 3

In this section, we present an efficient polynomial-time clustering algorithm under mild SNR. The procedure takes a global-to-local approach. See Figure 3 for illustration. The global step finds the basin of attraction with polynomial misclustering error, whereas the local iterations improve the initial clustering to exact recovery. Both steps are critical to obtain a satisfactory algorithm output. In what follows, we first use the symmetric tensor as a working example to describe the algorithm procedures to gain insight. Our theoretical analysis focuses on dTBMs with symmetric mean tensor and independent sub-Gaussian noises such as Gaussian and uniform observations. The extensions for Bernoulli observations and other practical issues are in Sections IV-C and IV-D.

To construct algorithm guarantees, we introduce the misclustering loss between an estimator \hat{z} and the true z :

$$L(\hat{z}, z) = \frac{1}{p} \sum_{i \in [p]} \theta(i) \sum_{b \in [r]} \mathbb{1}\{\hat{z}(i) = b\} \cdot \|[\mathbf{S}_{z(i)}]_b^s - [\mathbf{S}_b]_b^s\|^2, \quad (11)$$

where the superscript \cdot^s denotes the normalized vector; i.e., $\mathbf{a}^s := \mathbf{a}/\|\mathbf{a}\|$ if $\mathbf{a} \neq 0$ and $\mathbf{a}^s = 0$ if $\mathbf{a} = 0$ for any vector \mathbf{a} . The following lemma indicates the close relationship between the loss $L(\hat{z}, z)$ and error $\ell(\hat{z}, z)$. The loss $L(\hat{z}, z)$ serves as an important intermediate quantity to control the misclustering error.

Lemma 2 (Relationship Between Misclustering Error and Loss): Consider the dTBM under the parameter space \mathcal{P} . Suppose $\min_{i \in [p]} \theta(i) > c$ for some constant $c > 0$. We have $\ell(\hat{z}, z) \Delta_{\min}^2 \leq L(\hat{z}, z)$.

A. Weighted Higher-Order Initialization

We start with weighted higher-order clustering algorithm as initialization. We take an order-3 tensor and the clustering on the first mode as illustration for insight. Consider noiseless case with $\mathcal{X} = \mathbb{E}\mathcal{Y}$ and $\mathbf{X} = \text{Mat}(\mathcal{X})$. By model (1), for all $i \in [p]$, we have

$$\theta(i)^{-1} \mathbf{X}_{i:} = [\text{Mat}(\mathcal{S} \times_2 \Theta \mathbf{M} \times_3 \Theta \mathbf{M})]_{z(i)} : . \quad (68)$$

This implies that, all node i belonging to the a -th community (i.e., $z(i) = a$) share the same normalized mean vector $\theta(i)^{-1} \mathbf{X}_{i:}$, and vice versa. Intuitively, one can apply k -means clustering to the vectors $\{\theta(i)^{-1} \mathbf{X}_{i:}\}_{i \in [p]}$, which leads to main idea of our Sub-algorithm 1.

Specifically, our initialization consists of the denoising step and the clustering step. The denoising step (lines 1-2 in Sub-algorithm 1) estimates \mathcal{X} from \mathcal{Y} by a double projection spectral method. The first projection performs HOSVD [21] via $\mathbf{U}_{\text{pre},k} = \text{SVD}_r(\text{Mat}_k(\mathcal{Y}))$, $k \in [3]$, where $\text{SVD}_r(\cdot)$ returns the top- r left singular vectors. The second projection performs HOSVD on the projected \mathcal{Y} onto the multilinear Kronecker space $\mathbf{U}_{\text{pre},k} \otimes \mathbf{U}_{\text{pre},k}$; i.e.,

$$\hat{\mathbf{U}}_1 = \text{SVD}_r(\text{Mat}_1(\mathcal{Y} \times_2 \mathbf{U}_{\text{pre},2} \mathbf{U}_{\text{pre},2}^T \times_3 \mathbf{U}_{\text{pre},3} \mathbf{U}_{\text{pre},3}^T)) . \quad (702)$$

and similar for $\hat{\mathbf{U}}_2, \hat{\mathbf{U}}_3$. The final denoised tensor $\hat{\mathcal{X}}$ is defined by

$$\hat{\mathcal{X}} = \mathcal{Y} \times_1 \hat{\mathbf{U}}_1 \hat{\mathbf{U}}_1^T \times_2 \hat{\mathbf{U}}_2 \hat{\mathbf{U}}_2^T \times_3 \hat{\mathbf{U}}_3 \hat{\mathbf{U}}_3^T . \quad (705)$$

The double projection improves usual matrix spectral methods in order to alleviate the noise effects for $K \geq 3$ [13].

The clustering step (lines 3-5 in Sub-algorithm 1) performs the weighted k -means clustering. We write $\hat{\mathbf{X}} = \text{Mat}_1(\hat{\mathcal{X}})$, and normalize the rows into $\hat{\mathbf{X}}_{i:}^s = \|\hat{\mathbf{X}}_{i:}\|^{-1} \hat{\mathbf{X}}_{i:}$ as a surrogate of $\theta(i)^{-1} \mathbf{X}_{i:}$. Then, a weighted k -means clustering is performed on the normalized rows with weights equal to $\|\hat{\mathbf{X}}_{i:}\|^2$. The choice of weights is to bound the k -means objective function by the Frobenius-norm accuracy of $\hat{\mathcal{X}}$. Unlike existing clustering algorithm [9], we apply the clustering on the unfolded tensor $\hat{\mathbf{X}}$ rather than on the factors $\hat{\mathbf{U}}_k$. This strategy relaxes the singular-value gap condition [13], [15]. We assign

718 degenerate rows with purely zero entries to an arbitrarily
 719 random cluster; these nodes are negligible in high-dimensions
 720 because of the lower bound on $\|\text{Mat}(\mathcal{S})_{a:}\|$ in (2). The final
 721 result gives the initial cluster assignment $z^{(0)}$. Full procedures
 722 for clustering are provided in Sub-algorithm 1.

723 We now establish the misclustering error rate of initialization.
 724 **Seems no space between ``Error'' and ``for''.**

725 **Theorem 4 (Error for Weighted Higher-Order Initialization):**
 726 Consider the general sub-Gaussian dTBM with fixed $r \geq 1$,
 727 $K \geq 2$, i.i.d. noise under the parameter space \mathcal{P} , and
 728 Assumption 1. Assume $\min_{i \in [p]} \theta(i) \geq c$ for some constant
 729 $c > 0$. Let Δ_X denote the minimal gap in mean tensor defined
 730 in (8), and let $z_k^{(0)}$ denote the output of Sub-algorithm 1.
 731 With probability going to 1, as $p \rightarrow \infty$, we have

$$\ell(z_k^{(0)}, z) \lesssim \frac{\sigma^2 r^K p^{-K/2}}{\Delta_X^2}.$$

732 Further, assume that θ is balanced as (6). We have

$$\ell(z_k^{(0)}, z) \lesssim \frac{r^K p^{-K/2}}{\text{SNR}} \quad \text{and} \quad L(z_k^{(0)}, z) \lesssim \sigma^2 r^K p^{-K/2}, \quad (12)$$

733 with probability going to 1 as $p \rightarrow \infty$.

734 **Remark 5 (Comparison to Previous Results):** For fixed
 735 SNR, our initialization error rate with $K = 2$ agrees with
 736 the initialization error rate $\mathcal{O}(p^{-1})$ in matrix models [15].
 737 Furthermore, in the special case of non-degree TBMs with
 738 $\theta = \mathbf{1}_p$, we achieve the same initial misclustering error
 739 $\mathcal{O}(p^{-K/2})$ as in non-degree models [13]. Theorem 4 implies
 740 the advantage of our algorithm in achieving both accuracy
 741 and model flexibility.

742 **Remark 6 (Failure of Conventional Tensor HOSVD):** If
 743 we use conventional HOSVD for tensor denoising; that is,
 744 we use $\mathbf{U}_{\text{pre},k}$ in place of $\hat{\mathbf{U}}_k$ in line 2, then the misclustering
 745 rate becomes $\mathcal{O}(p^{-1})$ for all $K \geq 2$. This rate is substantially
 746 worse than our current rate (12).

747 **Remark 7 (Singular-Value Gap-Free Clustering):** Note
 748 that our clustering directly applies to the estimated mean
 749 tensor $\hat{\mathcal{X}}$ rather than the leading tensor factors $\hat{\mathbf{U}}_k$.
 750 Applying clustering to the tensor factors suffers from the
 751 non-identifiability issue due to the infinitely many orthogonal
 752 rotations when the number of blocks $r \geq 3$ in the absence
 753 of singular-value gaps. Such ambiguity causes the trouble
 754 for effective clustering [26]. In contrast, our initialization
 755 algorithm applies the clustering to the overall mean tensor $\hat{\mathcal{X}}$.
 756 This strategy avoids the non-identifiability issue regardless of
 757 the number of blocks and singular-value gaps.

nonidentifiability

B. Angle-Based Iteration

760 Our Theorem 4 has shown the polynomially decaying error
 761 rate from our initialization. Now we improve the error rate
 762 to exponential decay using local iterations. We propose an
 763 angle-based local iteration to improve the outputs from Sub-
 764 algorithm 1. To gain the intuition, consider an one-dimensional
 765 degree-corrected clustering problem with data vectors $\mathbf{x}_i =$
 766 $\theta(i)\mathbf{s}_{z(i)} + \epsilon_i, i \in [p]$, where \mathbf{s}_i 's are known cluster centroids,
 767 $\theta(i)$'s are unknown positive degrees, and $z: [p] \mapsto [r]$ is
 768 the cluster assignment of interest. The angle-based k -means
 769

algorithm estimates the assignment z by minimizing the angle
 770 between data vectors and centroids; i.e.,
 771

$$z(i) = \arg \max_{a \in [r]} \cos(\mathbf{x}_i, \mathbf{s}_a), \quad \text{for all } i \in [p]. \quad (13)$$

772 The classical Euclidean-distance based clustering [13] fails
 773 to recover z in the presence of degree heterogeneity, even
 774 under noiseless case. In contrast, the proposed angle-based
 775 k -means algorithm achieves accurate recovery without the
 776 explicit estimation of θ .

777 Our Sub-algorithm 2 shares the same spirit as in the angle-
 778 based k -means. We still take the order-3 tensor for illustration.
 779 Specifically, Sub-algorithm 2 updates estimated core tensor
 780 and cluster assignment in each iteration. We use superscript
 781 (t) to denote the estimate from the t -th iteration, where $t =$
 782 $1, 2, \dots$. For core tensor, we consider the following update
 783 strategy

$$\mathcal{S}^{(t)}(a_1, a_2, a_3) = \text{Ave}\{\mathcal{Y}(i_1, i_2, i_3): z_k^{(t)}(i_k) = a_k, k \in [3]\}.$$

784 Intuitively, $\mathcal{S}^{(t)}$ becomes closer to the true core \mathcal{S} as $z_k^{(t)}$ is
 785 more precise. For cluster assignment, we first aggregate the
 786 slices of \mathcal{Y} and obtain the reduced tensor $\mathcal{Y}_1^d \in \mathbb{R}^{p \times r \times r}$ on
 787 the first mode with given $z_k^{(t)}$, where

$$\mathcal{Y}_1^d(i, a_2, a_3) = \text{Ave}\{\mathcal{Y}(i, i_2, i_3): z_k^{(t)}(i_k) = a_k, k \neq 1\}.$$

788 Similarly, we also obtain $\mathcal{Y}_2^d, \mathcal{Y}_3^d$. We use \mathbf{Y}_k^d and $\mathbf{S}_k^{(t)}$ to
 789 denote the $\text{Mat}_k(\mathcal{Y}^d)$ and $\text{Mat}_k(\mathcal{S}^{(t)})$. The rows $\mathbf{Y}_{k,i}^d$ and
 790 $\mathbf{S}_{k,a}^{(t)}$ correspond to the \mathbf{x}_i and \mathbf{s}_a in the one-dimensional
 791 clustering (13). Then, we obtain the updated assignment by

$$z_k(i)^{(t+1)} = \arg \max_{a \in [r]} \cos(\mathbf{Y}_{k,i}^d, \mathbf{S}_{k,a}^{(t)}), \quad \text{for all } i \in [p],$$

792 provided that $\mathbf{S}_{k,a}^{(t)}$ is a nonzero vector. Otherwise, if $\mathbf{S}_{k,a}^{(t)}$ is
 793 a zero vector, then we make the convention to assign $z_k^{(t+1)}(i)$
 794 randomly in $[r]$. Full procedures for our angle-based iteration
 795 are described in Sub-algorithm 2.

796 We now establish the misclustering error rate of iterations
 797 under the stability assumption.

798 **Definition 2 (Locally Linear Stability):** Define the ε -
 799 neighborhood of z by $\mathcal{N}(z, \varepsilon) = \{\bar{z}: \ell(\bar{z}, z) \leq \varepsilon\}$. Let
 800 $\bar{z}: [p] \rightarrow [r]$ be a clustering function. We define two vectors
 801 associated with \bar{z} ,

$$\begin{aligned} \mathbf{p}(\bar{z}) &= (|\bar{z}^{-1}(1)|, \dots, |\bar{z}^{-1}(r)|)^T, \\ \mathbf{p}_\theta(\bar{z}) &= (\|\theta_{\bar{z}^{-1}(1)}\|_1, \dots, \|\theta_{\bar{z}^{-1}(r)}\|_1)^T. \end{aligned}$$

802 We call the degree is ε -locally linearly stable if and only if

$$\sin(\mathbf{p}(\bar{z}), \mathbf{p}_\theta(\bar{z})) \lesssim \varepsilon \Delta_{\min}, \quad \text{for all } \bar{z} \in \mathcal{N}(z, \varepsilon). \quad (14)$$

810 Roughly speaking, the vector $\mathbf{p}(\bar{z})$ represents the raw cluster
 811 sizes, and $\mathbf{p}_\theta(\bar{z})$ represents the relative cluster sizes weighted
 812 by degrees. The local stability holds trivially for $\varepsilon = 0$ based
 813 on the construction of parameter space (2). The condition (14)
 814 controls the impact of node degree to the $\mathbf{p}_\theta(\cdot)$ with respect
 815 to the misclustering rate ε and angle gap. Intuitively, the
 816 condition (14) controls the skewness of degree so that the
 817 angle between raw cluster size and degree-weighted cluster

Algorithm 1 Multiway Spherical Clustering for Degree-Corrected Tensor Block Model**Sub-algorithm 1: Weighted higher-order initialization**

Input: Observation $\mathcal{Y} \in \mathbb{R}^{p \times \dots \times p}$, cluster number r , relaxation factor $\eta > 1$ in k -means clustering.

1: Compute factor matrices $\mathbf{U}_{\text{pre},k} = \text{SVD}_r(\text{Mat}_k(\mathcal{Y}))$, $k \in [K]$ and the $(K-1)$ -mode projections

$$\mathcal{X}_{\text{pre},k} = \mathcal{Y} \times_1 \mathbf{U}_{\text{pre},1} \mathbf{U}_{\text{pre},1}^T \times_2 \dots \times_{k-1} \mathbf{U}_{\text{pre},k-1} \mathbf{U}_{\text{pre},k-1}^T \times_{k+1} \mathbf{U}_{\text{pre},k+1} \mathbf{U}_{\text{pre},k+1}^T \times_{k+2} \dots \times_K \mathbf{U}_{\text{pre},K} \mathbf{U}_{\text{pre},K}^T.$$

2: Compute factor matrices $\hat{\mathbf{U}}_k = \text{SVD}_r(\text{Mat}_k(\mathcal{X}_{\text{pre},k}))$, $k \in [K]$ and the denoised tensor

$$\hat{\mathcal{X}} = \mathcal{Y} \times_1 \hat{\mathbf{U}}_1 \hat{\mathbf{U}}_1^T \times_2 \dots \times_K \hat{\mathbf{U}}_K \hat{\mathbf{U}}_K^T.$$

3: **for** $k \in [K]$ **do**

4: Let $\hat{\mathbf{X}} = \text{Mat}_k(\hat{\mathcal{X}})$ and $S_0 = \{i \in [p] : \|\hat{\mathbf{X}}_{i:\}\| = 0\}$. Set $\hat{z}(i)$ randomly in $[r]$ for $i \in S_0$.

5: For all $i \in S_0^c$, compute normalized rows $\hat{\mathbf{X}}_{i:\}^s := \|\hat{\mathbf{X}}_{i:\}\|^{-1} \hat{\mathbf{X}}_{i:\}$.

6: Solve the clustering $\hat{z}_k : [p] \rightarrow [r]$ and centroids $\{\hat{x}_j\}_{j \in [r]}$ using weighted k -means, such that

$$\sum_{i \in S_0^c} \|\hat{\mathbf{X}}_{i:\}\|^2 \|\hat{\mathbf{X}}_{i:\}^s - \hat{\mathbf{x}}_{\hat{z}_k(i)}\|^2 \leq \eta \min_{\bar{\mathbf{x}}_j, j \in [r], \bar{z}_k(i), i \in S_0^c} \sum_{i \in S_0^c} \|\hat{\mathbf{X}}_{i:\}\|^2 \|\hat{\mathbf{X}}_{i:\}^s - \bar{\mathbf{x}}_{\hat{z}_k(i)}\|^2.$$

7: **end for**

Output: Initial clustering $z_k^{(0)} \leftarrow \hat{z}_k$, $k \in [K]$.

Sub-algorithm 2: Angle-based iteration

Input: Observation $\mathcal{Y} \in \mathbb{R}^{p \times \dots \times p}$, initialization $z_k^{(0)} : [p] \rightarrow [r]$, $k \in [K]$ from Sub-algorithm 1, iteration number T .

8: **for** $t = 0$ to $T-1$ **do**

9: Update the block tensor $\mathcal{S}^{(t)}$ via $\mathcal{S}^{(t)}(a_1, \dots, a_K) = \text{Ave}\{\mathcal{Y}(i_1, \dots, i_K) : z_k^{(t)}(i_k) = a_k, k \in [K]\}$.

10: **for** $k \in [K]$ **do**

11: Calculate the reduced tensor $\mathcal{Y}_k^d \in \mathbb{R}^{r \times \dots \times r \times p \times r \times \dots \times r}$ via

$$\mathcal{Y}_k^d(a_1, \dots, a_{k-1}, i, a_{k+1}, \dots, a_K) = \text{Ave}\{\mathcal{Y}(i_1, \dots, i_{k-1}, i, i_{k+1}, \dots, i_K) : z^{(t)}(i_j) = a_j, j \neq k\}$$

12: Let $\mathbf{Y}_k^d = \text{Mat}_k(\mathcal{Y}_k^d)$ and $J_0 = \{i \in [p] : \|\mathbf{Y}_k^d_{i:\}\| = 0\}$. Set $z_k^{(t+1)}(i)$ randomly in $[r]$ for $i \in J_0$.

13: Let $\mathcal{S}_k^{(t)} = \text{Mat}_k(\mathcal{S}^{(t)})$. For all $i \in J_0^c$, update the cluster assignment by

$$z(i)_k^{(t+1)} = \arg \max_{a \in [r]} \cos \left(\mathbf{Y}_{k,i:\}, \mathcal{S}_{k,a:\}^{(t)} \right).$$

14: **end for**

15: **end for**

Output: Estimated clustering $z_k^{(T)} : [p] \mapsto [r]$, $k \in [K]$.

size is well controlled. The stability assumption is proposed for technical convenience, and we relax this condition in numerical studies; see Section VI.

Theorem 5 (Error for Angle-Based Iteration): Consider the general sub-Gaussian dTBM with fixed $r \geq 1$, $K \geq 2$, independent noise under the parameter space \mathcal{P} , and Assumption 1. Assume that the locally linear stability of degree holds in the neighborhood $\mathcal{N}(z, \varepsilon)$ for all $\varepsilon \leq E_0$ and some $E_0 \gtrsim \log^{-1} p$. Let $\{z_k^{(0)}\}_{k=1}^K$ be the initialization for Sub-algorithm 2 and $z_k^{(t)}$ be the t -th iteration output on the k -th mode. Suppose $\min_{i \in [p]} \theta(i) \geq c$ for some constant $c > 0$, the SNR $\geq \tilde{C} p^{-(K-1)} \log p$ for some sufficiently large positive constant \tilde{C} , and the initialization satisfies

Capitalize the initial letters in the name of Corollary 1.

$$L(z_k^{(0)}, z) \lesssim \frac{\Delta_{\min}^2}{r \log p}, \quad k \in [K].$$

With probability going to 1 as $p \rightarrow \infty$, there exists a contraction parameter $\rho \in (0, 1)$ such that

$$\ell(z, \hat{z}_k^{(t+1)}) \lesssim \underbrace{\text{SNR}^{-1} \exp \left(-\frac{p^{K-1} \text{SNR}}{r^{K-1}} \right)}_{\text{statistical error}} + \underbrace{\rho^t \ell(z, z_k^{(0)})}_{\text{computational error}}. \quad (15)$$

From the conclusion (15), we find that the iteration error is decomposed into two parts: statistical error and computational error. The statistical error is unavoidable with noisy data regardless t , whereas the computational error decays in an exponential rate as the number of iterations $t \rightarrow \infty$.

Corollary 1 (Exact recovery of dTBM with weighted higher-order initialization): Let the initialization $\{z_k^{(0)}\}_{k=1}^K$ be the output from Sub-algorithm 1. Assume $\text{SNR} \gtrsim p^{-K/2} \log p$. Combining all parameter assumptions and the results in Theorems 4 and 5, with probability going to 1 as $p \rightarrow \infty$, our estimate $z_k^{(T)}$ achieves exact recovery within polynomial

If possible, delete the term ``Algorithm 2'' and index the algorithm with bold ``Sub-algorithm 3''; Otherwise, Delete the phrase ``Sub-algorithm 3.'' and the change all references correspondingly.

iterations; more precisely,

$$z_k^{(T)} = \pi_k \circ z, \quad \text{for all } T \gtrsim \log_{1/\rho} p \text{ and } k \in [K].$$

for some permutation $\pi_k \in \Pi$.

Therefore, our combined algorithm is *computationally efficient* as long as $\text{SNR} \gtrsim p^{-K/2} \log p$. Note that, ignoring the logarithmic term, the minimal SNR requirement, $p^{-K/2}$, coincides with the computational critical value in Theorem 3. Therefore, our algorithm is optimal regarding the signal requirement and lies in the sharpest *computationally efficient* regime in Figure 2.

856 C. Extension to Bernoulli Observations

Bernoulli or network observations are common in multiple fields. Our iteration Theorem 5 holds for Bernoulli models, but our initialization Theorem 4 does not. Moreover, our current dTBM is insufficient to address sparsity with decaying mean tensor. Here, we provide extra discussions for Bernoulli initialization and strategies under sparse settings.

- *Extension to dense binary dTBMs.* The main difficulty to establish initialization guarantees for Bernoulli observations lies in the denoising step (lines 1-2 in Sub-algorithm 1). We now provide a high-level explanation for the technical difficulty when applying Theorem 4 to Bernoulli observations.

The derivation of Theorem 4 relies on the upper bound of the estimation error for the mean tensor in Lemma 7; i.e., with high probability

$$\|\hat{\mathcal{X}} - \mathcal{X}\|_F^2 \lesssim p^{K/2}, \quad (16)$$

where $\mathcal{X} = \mathbb{E}\mathcal{Y}$ and $\hat{\mathcal{X}}$ is defined in Step 2 of Sub-algorithm 1. Unfortunately, the inequality (16) holds only for i.i.d. sub-Gaussian observations, while Bernoulli observations are generally not identically distributed.

One possible remedy is to apply singular value decomposition to the *square unfolding* [27], $\text{Mat}_{sq}(\cdot)$, of Bernoulli tensor $\mathcal{Y} \in \{0, 1\}^{p_1 \times \dots \times p_K}$. Specifically, the square matricization $\text{Mat}_{sq}(\mathcal{Y}) \in \{0, 1\}^{p^{\lfloor K/2 \rfloor} \times p^{\lceil K/2 \rceil}}$ has entries $[\text{Mat}_{sq}(\mathcal{Y})](j_1, j_2) = \mathcal{Y}(i_1, \dots, i_K)$, where

$$\begin{aligned} j_1 &= i_1 + p_1(i_2 - 1) + \dots + p_{\lfloor K/2 \rfloor - 1}(i_{\lfloor K/2 \rfloor} - 1), \\ j_2 &= i_{\lceil K/2 \rceil} + p_{\lceil K/2 \rceil}(i_{\lceil K/2 \rceil + 1} - 1) + \dots \\ &\quad + p_{\lceil K/2 \rceil} \cdot p_{K-1}(i_K - 1). \end{aligned}$$

The matrix $\text{Mat}_{sq}(\mathcal{Y})$ is asymmetric. We interpret $\text{Mat}_{sq}(\mathcal{Y})$ as the adjacency matrix for a bipartite network with connections between two groups of nodes. The two groups of nodes in the bipartite network have $p_1 \cdots p_{\lfloor K/2 \rfloor}$ and $p_{\lceil K/2 \rceil} \cdots p_K$ nodes, respectively. The entry $[\text{Mat}_{sq}(\mathcal{Y})](j_1, j_2)$ refers to the presence of connection between the nodes indexed by combinations $(i_1, \dots, i_{\lfloor K/2 \rfloor})$ and $(i_{\lceil K/2 \rceil}, \dots, i_K)$. We summarize the procedure in Sub-algorithm 3.

Proposition 1 (Error for Bernoulli Initialization):

Consider the Bernoulli dTBM in the parameter space \mathcal{P} with fixed $r \geq 1, K \geq 2$. Assume that Assumption 1 holds, $\boldsymbol{\theta}$ is balanced, and $\min_{i \in [p]} \theta(i) \geq c$ for some

Algorithm 2 Sub-algorithm 3: Weighted Higher-Order Initialization for Bernoulli Observation

Input: Bernoulli tensor $\mathcal{Y} \in \{0, 1\}^{p \times \dots \times p}$, cluster number r , relaxation factor $\eta > 1$ in k -means clustering.

- 1: Let the matrix $\text{Mat}_{sq}(\mathcal{Y}) \in \{0, 1\}^{p^{\lfloor K/2 \rfloor} \times p^{\lceil K/2 \rceil}}$ denote the nearly square unfolded tensor. Compute the estimate \mathcal{X}' , where

$$\mathcal{X}' = \arg \min_{\text{rank}(\text{Mat}_{sq}(\mathcal{X})) \leq r^{\lceil K/2 \rceil}} \|\text{Mat}_{sq}(\mathcal{X}) - \text{Mat}_{sq}(\mathcal{Y})\|_F^2. \quad (17)$$

- 2: Implement lines 3-5 of Sub-algorithm 1 with $\hat{\mathcal{X}}$ replaced by $\hat{\mathcal{X}}'$ in (17).

Output: Initial clustering $z_k^{(0)} \leftarrow \hat{z}_k, k \in [K]$.

constant $c > 0$. Let $z_k^{(0)}$ denote the output of Sub-algorithm 3. With probability going to 1 as $p \rightarrow \infty$, we have

$$\ell(z_k^{(0)}, z_k) \lesssim \frac{r^K p^{-\lfloor K/2 \rfloor}}{\text{SNR}}, \text{ and } L(z_k^{(0)}, z_k) \lesssim \sigma^2 r^K p^{-\lfloor K/2 \rfloor}.$$

Remark 8 (Comparison with Gaussian model): The Bernoulli bound $\mathcal{O}(p^{-\lfloor K/2 \rfloor})$ in Proposition 1 is relatively looser than the Gaussian bound $\mathcal{O}(p^{-K/2})$ in Theorem 4. The gap between Bernoulli and Gaussian error decreases as the order K increases. Nevertheless, combining with angle iteration Sub-algorithm 2, Bernoulli clustering still achieves exponential error rate $\exp(-p^{(K-1)})$ at a price of a larger SNR. The investigation of the gap between upper bound $p^{-\lfloor K/2 \rfloor}$ and the lower bound $p^{-K/2}$ for Bernoulli tensors will be left as future work. In numerical experiments, we will use our original initialization, Sub-algorithm 1, to verify the robustness to Bernoulli observations.

Remark 9 (Comparison With Previous Methods):

Previous work [9] develops a spectral clustering method for Bernoulli dTBM. [9] adopts a different signal notion based on the singular gap in the core tensor, denoted as Δ_{singular} . By [9, Theorem 1], the spectral method achieves exact recovery with $\Delta_{\text{singular}} \gtrsim p^{-1/2}$. However, we are not able to infer the exact recovery of spectral method by our angle-base SNR condition. Consider an order-2 dTBM with $p > 2, \sigma^2 = 1, \boldsymbol{\theta} = \mathbf{1}_p$, equal size assignment $|z^{-1}(a)| = p/r$ for all $a \in [r]$, and core matrix equal to the 2-dimensional identity matrix $\mathbf{S} = \mathbf{I}_2$. The singular gap under this setting is $\Delta_{\text{singular}} = \min\{\lambda_1 - \lambda_2, \lambda_2\} = 0$, where $\lambda_1 \geq \lambda_2$ are singular values of \mathbf{S} . In contrast, our angle gap $\Delta_{\text{min}}^2 = 2$ satisfies the SNR condition in Theorem 5. Then, our algorithm achieves the exact recovery, but the spectral method in [9] fails.

Hence, for fair comparison, we compare the best performance of our algorithm and [9] under the strongest signal setting of each model. Since both methods contain an iteration procedure, we set the iteration number to infinity to avoid the computational error. Considering the largest angle-based SNR $\asymp 1$ in Theorem 5, our Bernoulli clustering achieves exponential error rate of order $\exp(-p^{(K-1)})$; considering the largest singular

gap $\Delta_{\text{singular}} \asymp 1$ in Theorem 1 of [9], the spectral clustering has a polynomial error rate of order p^{-2} . Our algorithm still shows a better theoretical accuracy than the competitive work for Bernoulli observations.

- *Extension to sparse binary dTBMs.* The sparsity is often a popular feature in hypergraphs [9], [16], [28]. Specifically, the sparse binary dTBM assumes that, the entries of \mathcal{Y} follow independent Bernoulli distributions with the mean

$$\mathbb{E}\mathcal{Y} = \alpha_p \mathcal{S} \times_1 \Theta M \times_2 \cdots \times_K \Theta M, \quad (18)$$

where the extra scalar parameter $\alpha_p \in (0, 1]$ is function of p that controls the sparsity. A smaller α_p indicates a higher level of sparsity. Our current work focuses on dense dTBM with $\alpha_p = 1$. While sparse dTBM is an interesting application, the algorithm and its analysis require different techniques. Below, we discuss possible modifications of the algorithm.

The sparsity affects our initialization guarantee in our Theorem 4. In our initialization, the spectral denoising step (lines 1-2 in Sub-algorithm 1) implements matrix SVD to unfolded tensors. However, SVD-based methods are believed to fail in extremely sparse SBM due to the localization phenomenon in the singular vectors [28]. Inspired by [28], we adopt the diagonal-deleted HOSVD (D-HOSVD) [9] as the initialization in our higher-order clustering.

The sparsity also affects the iteration guarantee in our Theorem 5. The decaying mean tensor leads to a worse statistical error of order $\mathcal{O}(-\alpha_p p^{K-1})$ on $\hat{\mathcal{X}}$. The theoretical analyses for sparse binary dTBM and algorithms are left as future directions. Instead, we add numerical experiments to evaluate the robustness of our algorithm and the improvement of D-HOSVD initialization in the sparse dTBM; see Appendix A.

D. Practical Issues

1) *Computational Complexity:* Our two-stage algorithm has a computational cost polynomial in tensor dimension p . Specifically, the complexity of Sub-algorithm 1 is $\mathcal{O}(Kp^{K+1} + Kp^K)$, where the first term is contributed by the double projection and the calculation of $\hat{\mathcal{X}}$, and the second term comes from normalization and the k -means. The cost of each update in Sub-algorithm 2 is $\mathcal{O}(p^K + pr^K)$, where p^K comes from the calculation of $\mathcal{S}^{(t)}$ and \mathcal{Y}_k^d , and pr^K comes from the normalization of \mathcal{Y}_k^d , the calculation of $\mathcal{S}^{(t)}$, and the cluster assignment update in Step 13.

2) *Hyper-Parameter Selection:* In our theoretical analysis, we have assumed the true cluster number r is given to our algorithm. In practice, the cluster number r is often unknown, and we now propose a method to choose r from data. We impose the Bayesian information criterion (BIC) and choose the cluster number that minimizes BIC; i.e., under the symmetric Gaussian dTBM (1),

$$\hat{r} = \arg \min_{r \in \mathbb{Z}_+} \left(p^K \log(\|\hat{\mathcal{X}} - \mathcal{Y}\|_F^2) + p_e(r)K \log p \right), \quad (19)$$

with $\hat{\mathcal{X}} = \hat{\mathcal{S}}(r) \times_1 \hat{\Theta}(r) \hat{M}(r) \times_2 \cdots \times_K \hat{\Theta}(r) \hat{M}(r)$, where the triplet $(\hat{z}(r), \hat{\mathcal{S}}(r), \hat{\Theta}(r))$ are estimated parameters with cluster number r , and $p_e(r) = r^K + p(\log r + 1) - r$ is the effective number of parameters. Note that we have added the argument (r) to related quantities as functions of r . In particular, the estimate $\hat{\Theta}(r)$ in (19) is obtained by first calculating the reduced tensor $\hat{\mathcal{Y}}^d$ with $\hat{z}(r)$, and then normalizing the row norms $\|\hat{\mathcal{Y}}_{i:}^d\|$ to 1 in each cluster; i.e.,

$$\hat{\theta}(r) = (\hat{\theta}(1, r), \dots, \hat{\theta}(p, r))^T, \quad 1001$$

with $\hat{\theta}(i, r) = \|\hat{\mathcal{Y}}^d(r)_{i:}\| / \sum_{j: \hat{z}(j, r) = \hat{z}(i, r)} \|\hat{\mathcal{Y}}^d(r)_{j:}\|$, $\hat{\mathcal{Y}}^d(r) = \text{Mat}(\hat{\mathcal{Y}}^d(r))$, $\hat{\mathcal{Y}}^d(r)(i, a_2, \dots, a_K) = \text{Ave}\{\mathcal{Y}(i, i_2, \dots, i_K) : \hat{z}(i_k, r) = a_k, k \neq 1\}$, and $\hat{z}(i, r)$ denotes the community label for the i -th node with given cluster number r . We evaluate the performance of the BIC criterion in Section VI-A.

V. COMPARISON WITH NON-DEGREE TENSOR BLOCK MODEL

We discuss the connections and differences between dTBM and TBM [13] from three aspects: signal notions, theoretical results, and algorithms. Without loss of generality, let $\sigma^2 = 1$.

- *Signal notion.* The signal levels in both TBM [13] and our dTBM are functions of the core tensor \mathcal{S} . We emphasize that the signal notions are different between the two models. In particular, the Euclidean-based signal notion in TBM [13] fails to accurately describe the phase transition in our dTBM due to the possible heterogeneity in degree θ . To compare, we denote our angle-based signal notion in (4) and the Euclidean-based SNR in [13] as Δ_{ang}^2 and Δ_{Euc}^2 , respectively:

$$\Delta_{\text{ang}}^2 = 2(1 - \max_{a \neq b \in [r]} \cos(\mathbf{S}_{a:}, \mathbf{S}_{b:})), \quad 1021$$

$$\Delta_{\text{Euc}}^2 = \min_{a \neq b \in [r]} \|\mathbf{S}_{a:} - \mathbf{S}_{b:}\|^2. \quad 1022$$

By Lemma 4 in the Appendix B, we have

$$\Delta_{\text{ang}}^2 \max_{a \in [r]} \|\mathbf{S}_{a:}\|^2 \leq \Delta_{\text{Euc}}^2. \quad 1024$$

The above inequality indicates that the condition $\Delta_{\text{Euc}}^2 \leq p^\gamma$ is sufficient but not necessary for $\Delta_{\text{ang}}^2 \leq p^\gamma$. In fact, if we were to use Δ_{Euc}^2 for both models, then the phase transition of dTBM can be arbitrarily worse than that for TBM.

Here, we provide an example to illustrate the dramatical difference between TBM and dTBM with the same core tensor.

Example 4 (Comparison With Euclidean-Based Signal Notion): Consider a biclustering model with $\theta = 1$ and an order-2 core matrix

$$\mathbf{S} = \begin{pmatrix} p^{(\gamma+1)/2} + 2 & 2 \\ 2 & 4 \end{pmatrix}, \quad \text{with } \gamma \leq -1. \quad 1036$$

The core matrix \mathbf{S} lies in the parameter spaces of TBM and our dTBM. Here, the constraint $\gamma \leq -1$ is added to ensure the bounded condition of \mathbf{S} in our parameter

space in (2). The angle-based and Euclidean-based signal levels of \mathcal{S} are

$$\Delta_{\text{ang}}^2(\mathcal{S}) = 0 \ (\leq p^\gamma), \quad \Delta_{\text{Euc}}^2(\mathcal{S}) = 5 p^{\gamma+1} \ (\geq p^\gamma).$$

We conclude that TBM with \mathcal{S} achieves exact recovery with a polynomial-time algorithm; see [13, Theorem 4]. By contrast, the dTBM with the same \mathcal{S} and input $r = 2$ violates the identifiability condition, and thus fails to be solved by all estimators; see our Theorem 1.

- *Theoretical results.* In both works, we study the phase transition of TBM and dTBM with respect to the Euclidean and angle-based SNRs. We briefly summarize the results in [13] and compare with ours.

Statistical critical value:

Ours: $\Delta_{\text{ang}}^2 \lesssim p^{-(K-1)} \Rightarrow$ statistically impossible;

$\Delta_{\text{ang}}^2 \gtrsim p^{-(K-1)} \Rightarrow$ MLE achieves exact recovery;

Han's: $\Delta_{\text{Euc}}^2 \lesssim p^{-(K-1)} \Rightarrow$ statistically impossible;

$\Delta_{\text{Euc}}^2 \gtrsim p^{-(K-1)} \Rightarrow$ MLE achieves exact recovery.

Computational critical value: ``!MLE'' -> ``MLE''

Ours: $\Delta_{\text{ang}}^2 \lesssim p^{-K/2} \Rightarrow$ computationally impossible;

$\Delta_{\text{ang}}^2 \gtrsim p^{-K/2} \Rightarrow$ computationally efficient;

Han's: $\Delta_{\text{Euc}}^2 \lesssim p^{-K/2} \Rightarrow$ computationally impossible;

$\Delta_{\text{Euc}}^2 \gtrsim p^{-K/2} \Rightarrow$ computationally efficient.

The above comparison reveals four major differences.

First, none of our results in Section III are corollaries of [13]. Both models show the similar conclusion but under different conditions. While the TBM impossibility [13] provides a necessary condition for our dTBM impossibility, we find that such a condition is often loose. There exists a regime of \mathcal{S} in which TBM problems are computationally efficient but dTBM problems are statistically impossible; see Example 4. This observation has motivated us to develop the new signal notion Δ_{ang}^2 for sharp dTBM phase transition conditions.

Second, to find the phase transition, we need to show both the impossibility and achievability when SNR is below and above the critical value, respectively. While the TBM impossibility can serve as a loose condition of our dTBM impossibility, more efforts are required to show the achievability. In particular, since TBM is a more restrictive model than dTBM, the achievability in [13] does not imply the achievability of dTBM in a larger parameter space. The latter requires us to develop new MLE and polynomial algorithms for dTBM achievability. Third, from the perspective of proofs, we develop new dTBM-specific techniques to handle the extra degree heterogeneity. In our Theorem 2, we construct a special non-trivial degree heterogeneity to establish the lower bound for arbitrary core tensor with small angle gap, while, TBM [13] considers the constructions without degree parameter. In our Theorem 3, we construct a rank-2 tensor to relate HPC conjecture to Δ_{ang}^2 , while TBM [13] constructs a rank-1 tensor to relate HPC

conjecture to Δ_{Euc}^2 . The asymptotic non-equivalence between Δ_{ang}^2 and Δ_{Euc}^2 renders our proof technically more involved.

Last, we discuss the statistical impossibility statements. Our Theorem 2 implies the statistical impossibility whenever the core tensor \mathcal{S} leads to an angle-based SNR below the critical value, while, Theorem 6 in [13] implies the worst case statistical impossibility for a particular core tensor \mathcal{S} with Euclidean-based SNR below the statistical limit. Hence, our Theorem 2 shows a stronger statistical impossibility for dTBM than that presented in TBM [13, Theorem 6]. However, inspecting the proof of [13], the proof of Theorem 6 indeed implies a stronger TBM impossibility statement for arbitrary core tensor; i.e., when $\gamma < -(K-1)$

$$\liminf_{p \rightarrow \infty} \inf_{\mathcal{S} \in \mathcal{P}_{\mathcal{S}, \text{TBM}} \cap \{\Delta_{\text{Euc}}^2 = p^\gamma\}} \inf_{\hat{z}_{\text{stats}}} \sup_{z \in \mathcal{P}_{z, \text{TBM}}} \mathbb{E}[\ell(\hat{z}_{\text{stats}}, z)] \geq 1,$$

where $\mathcal{P}_{\mathcal{S}, \text{TBM}}$ and $\mathcal{P}_{z, \text{TBM}}$ refer to the space for core tensor \mathcal{S} and assignment z under TBM, respectively. Again, in terms of the strong statistical impossibility, both models show the similar conclusion but under different conditions. Since two impossibilities consider different core tensor regimes with non-equivalent Δ_{ang}^2 and Δ_{Euc}^2 , we emphasize that different proof techniques are required to obtain these similar conclusions. See our proof sketch in Section VIII-A, Appendices B-D and B-E for detail technical differences.

- *Algorithms.* Both [13] and our work propose the two-step algorithm, which combines warm initialization and iterative refinement to achieve exact recovery. This local-to-global strategy is not new in clustering literature [29], [30]. The highlight of our algorithm is the angle-based update in lines 10-14, Sub-algorithm 2, which is specifically designed for dTBM to avoid the estimation of θ . This angle-based update brings new proof challenges. We develop polar-coordinate based techniques to establish the error rate for the proposed algorithm.

VI. NUMERICAL STUDIES

We evaluate the performance of the weighted higher-order initialization and angle-based iteration in this section. We report average errors and standard deviations across 30 replications in each experiment. Clustering accuracy is assessed by clustering error rate (CER, i.e., one minus rand index). The CER between (\hat{z}, z) is equivalent to misclustering error $\ell(\hat{z}, z)$ up to constant multiplications [31], and a lower CER indicates a better performance.

We generate order-3 tensors with *assortative* [15] core tensors to control SNR; i.e., we set $\mathcal{S}_{aaa} = s_1$ for $a \in [r]$ and others be s_2 , where $s_1 > s_2 > 0$. Let $\alpha = s_1/s_2$. We set α close to 1 such that $1 - \alpha = o(p)$. In particular, we have $\alpha = 1 + \Omega(p^{\gamma/2})$ with $\gamma < 0$ by Assumption 1 and definition (4). Hence, we easily adjust SNR via varying α . The assortative setting is proposed for simulations, and our algorithm is applicable for general tensors in practice. The cluster assignment z is randomly generated with equal

nontrivial

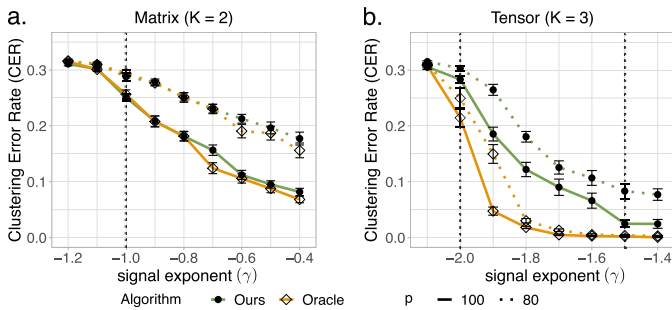


Fig. 4. SNR phase transitions for clustering in dTBM with $p = \{80, 100\}$, $r = 5$ under (a) matrix case with $\gamma \in [-1.2, -0.4]$ and (b) tensor case with $\gamma \in [-2.1, -1.4]$.

probability across r clusters for each mode. Without further explanation, we generate degree heterogeneity θ from absolute normal distribution by $\theta(i) = |X_i| + 1 - 1/\sqrt{2\pi}$ with $|X_i| \stackrel{\text{i.i.d.}}{\sim} N(0, 1)$, $i \in [p]$ and normalize θ to satisfy (2). Also, we set $\sigma^2 = 1$ for Gaussian data without further specification.

A. Verification of Theoretical Results Fig. 4

The first experiment verifies statistical-computational gap described in Section III. Consider the Gaussian model with $p = \{80, 100\}$, $r = 5$. We vary γ in $[-1.2, -0.4]$ and $[-2.1, -1.4]$ for matrix ($K = 2$) and tensor ($K = 3$) clustering, respectively. Note that finding MLE under dTBM is computationally intractable. We approximate MLE using an oracle estimator, i.e., the output of Sub-algorithm 2 initialized from true assignment. Figure 4a shows that both our algorithm and oracle estimator start to decrease around the critical value $\gamma_{\text{stat}} = \gamma_{\text{comp}} = -1$ in matrix case. In contrast, Figure 4b shows a significant gap in the phase transitions between the algorithm estimator and oracle estimator in tensor case. The oracle error rapidly decreases to 0 when $\gamma_{\text{stat}} = -2$, whereas the algorithm estimator tends to achieve exact clustering when $\gamma_{\text{comp}} = -1.5$. Figure 4 confirms the existence of the statistical-computational gap in our Theorems 2 and 3.

The second experiment verifies the performance guarantees of two algorithms: (i) weighted higher-order initialization; (ii) combined algorithm of weighted higher-order initialization and angle-based iteration. We consider both the Gaussian and Bernoulli models with $p = \{80, 100\}$, $r = 5$, $\gamma \in [-2.1, -1.4]$. Figure 5 shows the substantial improvement of combined algorithm over initialization, especially under weak and intermediate signals. This phenomenon agrees with the error rates in Theorems 4 and 5 and confirms the necessity of the local iterations.

The third experiment evaluates the empirical performance of the BIC criterion to select unknown cluster number. We generate the data from an order-3 Gaussian model with $p = \{50, 80\}$, $r = \{2, 4\}$, and noise level $\sigma^2 \in \{0.25, 1\}$. Table III shows that our BIC criterion well chooses the true r under most settings. Note that the BIC slightly underestimates the true cluster number ($r = 4$) with smaller dimension and higher noise ($p = 50, \sigma^2 = 1$), and the accuracy immediately increases with larger dimension $p = 80$. The improvement follows from the fact that a larger dimension p indicates

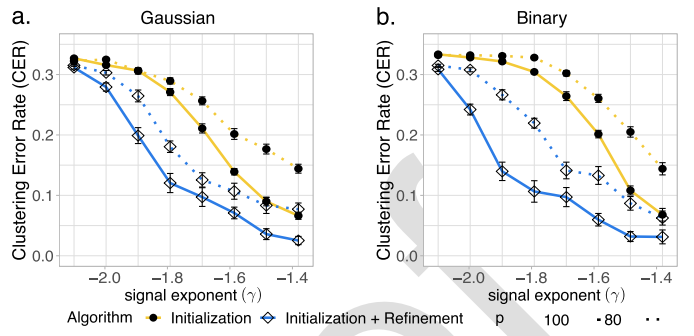


Fig. 5. CER versus signal exponent (γ) for initialization only and for combined algorithm. We set $p = \{80, 100\}$, $r = 5$, $\gamma \in [-2.1, -1.4]$ under (a) Gaussian models and (b) Bernoulli models.

a larger sample size in the tensor block model. Therefore, we conclude that BIC criterion is a reasonable way to tune the cluster number.

B. Comparison With Other Methods

We compare our algorithm with following higher-order clustering methods:

- **HOSVD**: HOSVD on data tensor and k -means on the rows of the factor matrix;
- **HOSVD+**: HOSVD on data tensor and k -means on the ℓ_2 -normalized rows of the factor matrix;
- **HLloyd** [13]: High-order clustering algorithm developed for non-degree tensor block models; **nondegree**
- **SCORE** [9]: Tensor-SCORE for clustering developed for sparse binary tensors.

Among the four alternative algorithms, the **SCORE** is the closest method to ours. We set the tuning parameters of **SCORE** as in previous literature [9]. The methods **SCORE** and **HOSVD+** are designed for degree models, whereas **HOSVD** and **HLloyd** are designed for non-degree models. We conduct two experiments to assess the impacts of (i) signal strength and (ii) degree heterogeneity, based on Gaussian and Bernoulli models with $p = 100, r = 5$. We refer to our algorithm as **dTBM** in the comparison.

We investigate the effects of signal to clustering performance by varying $\gamma \in [-1.5, -1.1]$. Figure 6 shows that our method **dTBM** outperforms all other algorithms. The sub-optimality of **SCORE** and **HOSVD+** indicates the necessity of local iterations on the clustering. Furthermore, Figure 6 shows the inadequacy of non-degree algorithms in the presence of mild degree heterogeneity. The experiment demonstrates the benefits of addressing heterogeneity in higher-order clustering tasks.

The only exception in Figure 6 is the slightly better performance of **HLloyd** over **HOSVD+** under Gaussian model. However, we find the advantage of **HLloyd** disappears with higher degree heterogeneity. We perform extra simulations to verify the impact of degree effects. We use the same setting as in the first experiment in the Section VI-B, except that we now generate the degree heterogeneity θ from Pareto distribution prior to normalization. The density function of Pareto distribution is $f(x|a, b) = ab^a x^{-(a+1)} \mathbb{1}\{x \geq b\}$, where

TABLE III

ESTIMATED CLUSTER NUMBER GIVEN BY BIC CRITERION UNDER THE LOW NOISE LEVEL ($\sigma^2 = 0.25$) AND HIGH NOISE LEVEL ($\sigma^2 = 0.5$) SETTINGS. NUMBERS IN PARENTHESES ARE STANDARD DEVIATIONS OF \hat{r} OVER 30 REPLICATIONS

Settings	$p = 50, \sigma^2 = 0.25$		$p = 50, \sigma^2 = 1$		$p = 80, \sigma^2 = 0.25$		$p = 80, \sigma^2 = 1$	
	2	4	2	4	2	4	2	4
True cluster number r								
Estimated cluster number \hat{r}	2(0)	3.9(0.25)	2(0)	3.1(0.52)	2(0)	4(0)	2(0)	3.9(0.31)

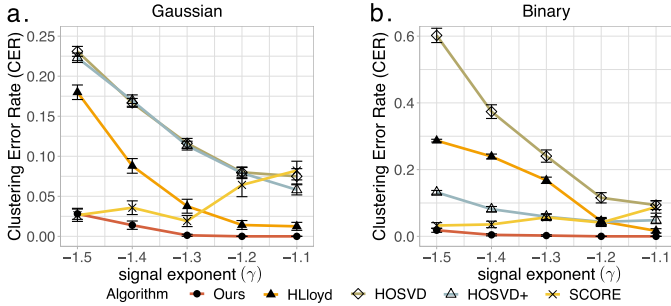


Fig. 6. CER versus signal exponent (denoted γ) for different methods. We set $p = 100, r = 5, \gamma \in [-1.5, -1.1]$ under (a) Gaussian and (b) Bernoulli models.

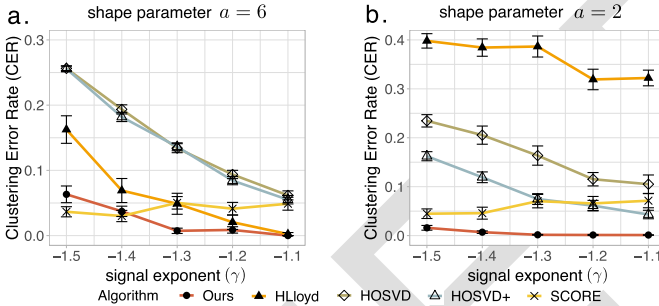


Fig. 7. CER comparison versus signal exponent (denoted γ) under (a) low (shape parameter $a = 6$) (b) high (shape parameter $a = 2$) degree heterogeneity. We set $p = 100, r = 5, \gamma \in [-1.5, -1.1]$ under Gaussian model.

1229 a is called *shape parameter*. We vary $a \in \{2, 6\}$ and choose b
1230 such that $\mathbb{E}X = a(a-1)^{-1}b = 1$ for X following $\text{Pareto}(a, b)$.
1231 Note that a smaller a leads to a larger variance in θ and hence a
1232 larger degree heterogeneity. We consider the Gaussian model
1233 under low ($a = 6$) and high ($a = 2$) degree heterogeneity.
1234 Figure 7 shows that the errors for non-degree algorithms
1235 (**HLlloyd**, **HOSVD**) increase with degree heterogeneity. In addition,
1236 the advantage of **HLlloyd** over **HOSVD+** disappears with
1237 higher degree heterogeneity. **nondegree**

1238 The last experiment investigates the effects of degree hetero-
1239 geneity to clustering performance. We fix the signal exponent
1240 $\gamma = -1.2$ and vary the extent of degree heterogeneity.
1241 In this experiment, we generate θ from Pareto distribution
1242 prior to normalization. We vary the shape parameter $a \in$
1243 $[3, 6]$ in the Pareto distribution to investigate a range of
1244 degree heterogeneities. Figure 8 demonstrates the stability
1245 of degree-corrected algorithms (**dTBM**, **SCORE**, **HOSVD+**)
1246 over the entire range of degree heterogeneity under consid-
1247 eration. In contrast, non-degree algorithms (**HLlloyd**, **HOSVD**)
1248 show poor performance with large heterogeneity, especially in
1249 Bernoulli cases. This experiment, again, highlights the benefit
1250 of addressing degree heterogeneity in higher-order clustering.

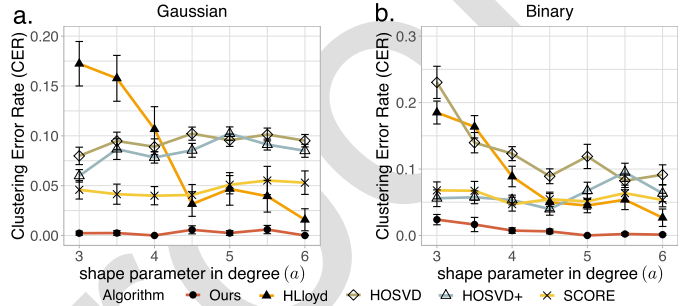


Fig. 8. CER versus shape parameter in degree ($a \in [3, 6]$) for different methods. We set $p = 100, r = 5, \gamma = -1.2$ under (a) Gaussian and (b) Bernoulli models.

VII. REAL DATA APPLICATIONS

A. Human Brain Connectome Data Analysis

The Human Connectome Project (HCP) aims to construct the structural and functional neural connections in human brains [32]. We preprocess the original dataset following [33] and partition the brain into 68 regions. The cleaned dataset includes brain networks for 136 individuals. Each brain network is represented by a 68-by-68 binary symmetric matrix, where the entry with value 1 indicates the presence of connection between node pairs, while the value 0 indicates the absence. We use $\mathcal{Y} \in \{0, 1\}^{68 \times 68 \times 136}$ to denote the binary tensor. Individual attributes such as gender and sex are recorded.

We apply our general asymmetric algorithm to the HCP data with the numbers of clusters on three modes $r_1 = r_2 = 4$ and $r_3 = 3$. The selection of r_1 and r_2 follows the human brain anatomy and the symmetry in the brain network, and the r_3 is specified following previous analysis [34]. Because of the symmetry in the data, the estimated brain node clustering results are the same on the first and second modes. Figure 9 shows that brain connection exhibits a strong spatial separation structure. Specifically, the first cluster, named *L.Hemis*, involves all the nodes in the left hemisphere. The nodes in the right hemisphere are further separated into three clusters led by the middle-part tissues in Temporal and Parietal lobes (*R.Temporal*), the back-part tissues in Occipital lobe (*R.Occipital*), and the front-part tissues in Frontal and Parietal lobes (*R.Supra*). This clustering result is reasonable since the left and right hemispheres often play different roles in human brains.

Figure 10 illustrates the estimated core tensor $\hat{\mathcal{S}}$ with estimated clustering, and Figure 11 visualizes the average brain connections and the connection enrichment in contrast to average networks in each group. In general, we find

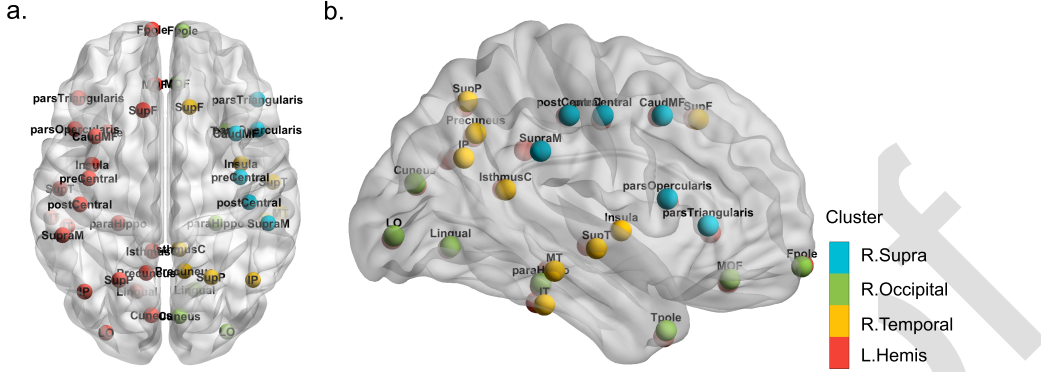


Fig. 9. Illustration of brain node clustering results for HCP data with (a) top and (b) side views.

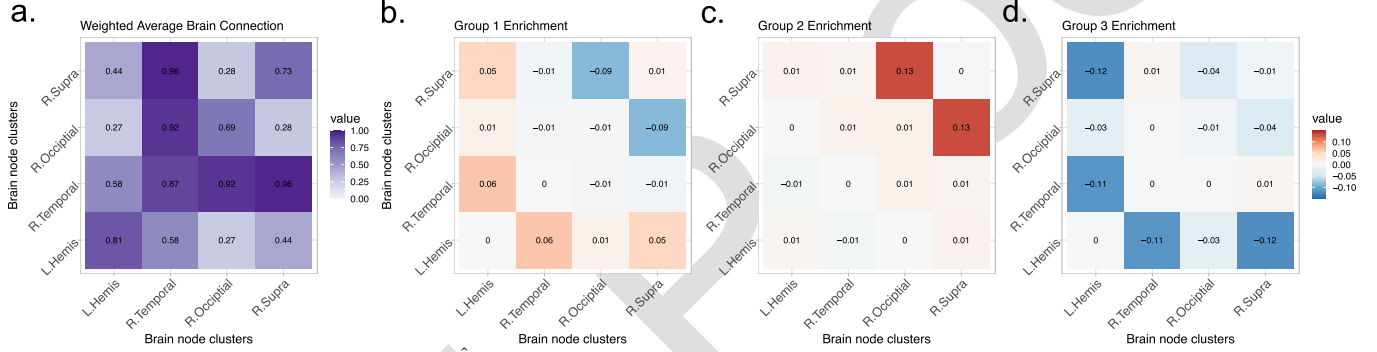


Fig. 10. Mode 3 slices of estimated core tensor \hat{S} . (a) Average estimated slice weighted by the group size; (b)-(d) Group-specified enrichment, i.e., the difference between each slice of \hat{S} and the averaged slice.

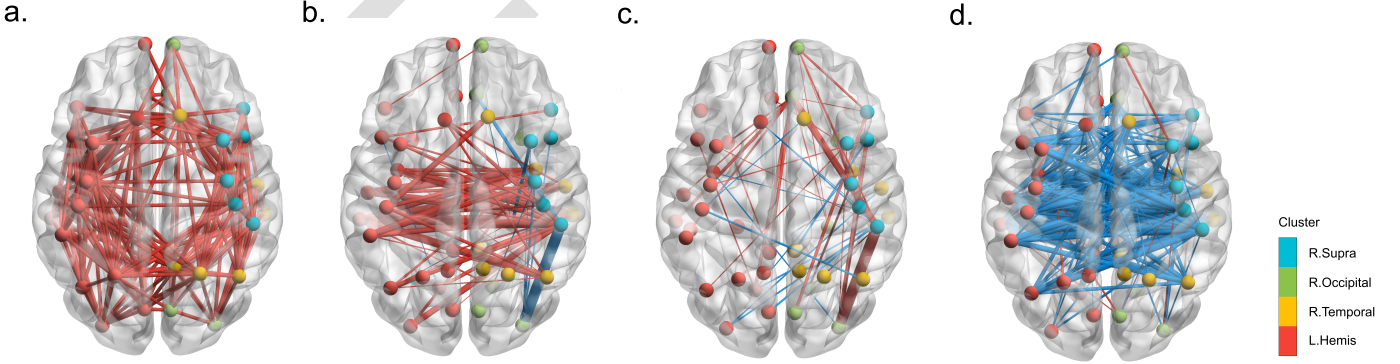


Fig. 11. Observed brain connections in the population and each group of individuals. (a) Average brain network; (b)-(d) Group-specified brain network enrichments in Groups 1-3. Red edges represent the positive enrichment and blue edges represent the negative enrichment.

Fig. 10a

that the inner-hemisphere connection has stronger connection compared to inter-hemisphere connections (Figure 10a). Also, the back and front parts (*R.Occipital*, *R.Supra*) are shown to have more interactions with temporal tissues than inner-cluster connections. In addition, the group 1 with 54% females shows an enrichment on the inter-hemisphere connections (Figure 10b), while group 4 with only 36% females exhibits a reduction (Figure 10d). This result agrees with previous findings in [34]. The enrichment on the back-front connection is also recognized in group 3 (Figure 10c). The interpretive patterns in our results demonstrate the usefulness of our clustering methods in the human brain connectome data application.

B. Peru Legislation Data Analysis

We also apply our method to the legislation networks in the Congress of the Republic of Peru [35]. Because of the frequent political power shifts in the Peruvian Congress during 2006-2011, we choose to focus on the data for the first half of 2006-2007 year. The dataset records the co-sponsorship of 116 legislators from top 5 parties and 802 bill proposals. We reconstruct legislation network as an order-3 binary tensor $\mathcal{Y} \in \{0, 1\}^{116 \times 116 \times 116}$, where $\mathcal{Y}_{ijk} = 1$ if the legislators (i, j, k) have sponsored the same bill, and $\mathcal{Y}_{ijk} = 0$ otherwise. The true party affiliations of legislators are provided and serve as the ground truth. We apply various higher-order

TABLE IV
CLUSTERING ERRORS (MEASURED BY CER) FOR VARIOUS METHODS IN
THE ANALYSIS OF PERU LEGISLATION DATASET

Method	dTBM	HOSVD	HOSVD+	HLloyd	SCORE
CER	0.116	0.22	0.213	0.149	0.199

clustering methods to \mathcal{Y} with $r = 5$. Table IV shows that our **dTBM** achieves the best performance compared to others. The second best method is the two-stage algorithm **HLloyd**, followed by the spectral methods **SCORE** and **HOSVD+**. This result is consistent with our simulations under strong signal and moderate degree heterogeneity. The comparison suggests that our method **dTBM** is more appealing in real-world applications.

VIII. PROOF SKETCHES

In this section, we provide the proof sketches for the main Theorem 2 (Impossibility), Theorem 3 (Impossibility), and Theorems 4-5. Detail proofs and extra theoretical results are provided in Appendix B.

A. Proof Sketch of Theorem 2 (Impossibility) and Theorem 3 (Impossibility)

The proofs of impossibility in Theorems 2 and 3 share the same proof idea with [13, Theorems 6 and 7] and [15, Theorem 2]. In both proofs of statistical and computational impossibilities, the key idea is to construct a particular set of parameters to lower bound the minimax rate. Specifically, for statistical impossibility in Theorem 2, we construct a particular $(z_{\text{stats}}^*, \theta_{\text{stats}}^*) \in \mathcal{P}_{z,\theta}$ such that for all $\mathcal{S}^* \in \mathcal{P}_S(\gamma)$

$$\begin{aligned} & \inf_{\hat{z}_{\text{stats}}} \sup_{(z,\theta) \in \mathcal{P}_{z,\theta}} \mathbb{E}[p\ell(\hat{z}_{\text{stats}}, z)] \\ & \geq \inf_{\hat{z}_{\text{stats}}} \mathbb{E}[p\ell(\hat{z}_{\text{stats}}, z_{\text{stats}}^*) | (z_{\text{stats}}^*, \mathcal{S}^*, \theta_{\text{stats}}^*)] \geq 1; \end{aligned} \quad (20)$$

for computational impossibility in Theorem 3, we construct a particular $(z_{\text{comp}}^*, \mathcal{S}_{\text{comp}}^*, \theta_{\text{comp}}^*) \in \mathcal{P}(\gamma)$ such that

$$\begin{aligned} & \inf_{\hat{z}_{\text{comp}}} \sup_{(z,\mathcal{S},\theta) \in \mathcal{P}(\gamma)} \mathbb{E}[p\ell(\hat{z}_{\text{comp}}, z)] \\ & \geq \inf_{\hat{z}_{\text{comp}}} \mathbb{E}[p\ell(\hat{z}_{\text{comp}}, z_{\text{comp}}^*) | (z_{\text{comp}}^*, \mathcal{S}_{\text{comp}}^*, \theta_{\text{comp}}^*)] \geq 1. \end{aligned}$$

The constructions of $(z_{\text{stats}}^*, \theta_{\text{stats}}^*)$ and $(z_{\text{comp}}^*, \mathcal{S}_{\text{comp}}^*, \theta_{\text{comp}}^*)$ are the most critical steps. With good constructions, the lower bound “ ≥ 1 ” can be verified by classical statistical conclusions (e.g. Neyman-Pearson Lemma) or prior work (e.g. HPC Conjecture).

A notable detail in the proof of statistical impossibility is the arbitrariness of \mathcal{S}^* . The first infimum over $\mathcal{P}_S(\gamma)$ in the minimax rate (10) requires that the lower bound (20) holds for any $\mathcal{S}^* \in \mathcal{P}_S(\gamma)$. The arbitrary choice of \mathcal{S}^* brings extra difficulties in the parameter construction, and consequently a non-trivial $\theta_{\text{stats}}^* \neq 1$ is chosen to address the arbitrariness. Previous TBM construction in the proof of [13, Theorem 6] with $\theta_{\text{stats}}^* = 1$ is no longer applicable in our case. Meanwhile, our construction $(z_{\text{comp}}^*, \mathcal{S}_{\text{comp}}^*, \theta_{\text{comp}}^*)$ leads to a rank-2 mean tensor to relate the HPC Conjecture while TBM [13, Theorem

7] constructs a rank-1 mean tensor. Hence, we emphasize that dTBM-specific techniques are required to obtain our impossibility results, though the proof idea is common for minimax lower bound analysis.

B. Proof Sketch of Theorem 4

The proof of Theorem 4 is inspired by the proof idea of [15, Lemma 1]. The extra difficulties are the angle gap characterization and multilinear algebra property in tensors; we address both challenges in our proof. Specifically, we control the misclustering error by the estimation error of $\hat{\mathcal{X}}$ calculated in Step 2 of Sub-algorithm 1. We prove the following inequality

$$\begin{aligned} \ell(z^{(0)}, z) & \lesssim \frac{1}{p} \min_{\pi \in \Pi} \sum_{i: z^{(0)}(i) \neq \pi(z(i))} \theta(i)^2 \\ & \lesssim \frac{\sigma^2 r^{K-1}}{\Delta_{\min}^2 p^K} \|\hat{\mathcal{X}} - \mathcal{X}\|_F^2 \\ & \lesssim \frac{r^K p^{-K/2}}{\text{SNR}}, \end{aligned} \quad (21)$$

where $\mathcal{X} = \mathbb{E}\mathcal{Y}$ is the true mean. The first inequality in (21) holds with the assumption $\min_{i \in [p]} \theta(i) \geq c > 0$ in Theorem 4. The second inequality relies on the key Lemma 1, which indicates

$$\min_{z(i) \neq z(j)} \|[\mathbf{X}_{i:}]^s - [\mathbf{X}_{j:}]^s\| \gtrsim \Delta_{\min}, \quad (22)$$

where $\mathbf{X} = \text{Mat}(\mathcal{X})$. The most challenging part in the proof of Theorem 4 lies in the derivation of inequality (22) (or the proof of Lemma 1), in which the proof of [15] is no longer applicable due to different angle gap assumption in our dTBM. To address the angle gap notion, we develop the extra padding technique in Lemma 5 and balance assumption (6). Last, we finish the proof of Theorem 4 by showing the third inequality of (21) using [13, Proposition 1].

C. Proof Sketch of Theorem 5

The proof of Theorem 5 is inspired by the proof idea of [13, Theorem 2]. We develop extra polar-coordinate based techniques with angle gap characterization to address the nuisance degree heterogeneity. Recall the intermediate quantity, misclustering loss, defined in (11)

$$\begin{aligned} L^{(t)} & := L(z, z^{(t)}) \\ & = \frac{1}{p} \sum_{i \in [p]} \theta(i) \sum_{b \in [r]} \mathbb{1}\left\{z^{(t)}(i) = b\right\} \|[\mathbf{S}_{z(i)}]_b^s - [\mathbf{S}_b]_i^s\|^2. \end{aligned}$$

We show that $L^{(t)}$ provides an upper bound for the misclustering error of interest via the inequality $\ell^{(t)} \leq \frac{L^{(t)}}{\Delta_{\min}^2}$ in Lemma 2. Therefore, it suffices to control $L^{(t)}$. Further, we introduce the oracle estimators for core tensor under the true cluster assignment via

$$\tilde{\mathcal{S}} = \mathcal{Y} \times_1 \mathbf{W}^T \times_2 \cdots \times_K \mathbf{W}^T,$$

where $\mathbf{W} = \mathbf{M} (\text{diag}(\mathbf{1}_p^T \mathbf{M}))^{-1}$ is the weighted true membership matrix. Let $\mathbf{V} = \mathbf{W}^{\otimes(K-1)}$ denote the Kronecker product of $(K-1)$ copies of \mathbf{W} matrices, and we define the

Missing subtitles ``a.'' and ``b.'' here.

1397 t -th iteration quantities $\mathbf{W}^{(t)}, \mathbf{V}^{(t)}$ corresponding to $\mathbf{M}^{(t)}$ (or
 1398 equivalently $z^{(t)}$). To evaluate $L^{(t+1)}$, we prove the bound

$$\begin{aligned} & \mathbb{1} \left\{ z^{(t+1)}(i) = b \right\} \\ &= \mathbb{1} \left\{ \|[\mathbf{Y}_{i:} \mathbf{V}^{(t)}]_s - [\mathbf{S}_{b:}^{(t)}]_s\|^2 \leq \|[\mathbf{Y}_{i:} \mathbf{V}^{(t)}]_s - [\mathbf{S}_{z(i):}^{(t)}]_s\|^2 \right\} \\ &\leq A_{ib} + B_{ib}, \end{aligned} \quad (23)$$

1402 where $\mathbf{Y} = \text{Mat}(\mathcal{Y}), \mathbf{S} = \text{Mat}(\mathcal{S}), \mathbf{S}^{(t)} = \text{Mat}(\mathcal{S}^{(t)})$ and

$$\begin{aligned} 1403 \quad A_{ib} &= \mathbb{1} \left\{ \langle \mathbf{E}_{i:} \mathbf{V}, [\tilde{\mathbf{S}}_{z(i):}]^s - [\tilde{\mathbf{S}}_{b:}]^s \rangle \lesssim -\|[\mathbf{S}_{z(i):}]^s - [\mathbf{S}_{b:}]^s\|^2 \right\}, \\ 1404 \quad B_{ib} &= \mathbb{1} \left\{ \|[\mathbf{S}_{z(i):}]^s - [\mathbf{S}_{b:}]^s\|^2 \lesssim F_{ib}^{(t)} + G_{ib}^{(t)} + H_{ib}^{(t)} \right\}. \end{aligned}$$

1405 The terms $F_{ib}^{(t)}, G_{ib}^{(t)}, H_{ib}^{(t)}$ are controlled by $z^{(t)}, \mathcal{S}^{(t)}$; see the
 1406 detailed definitions in (68), (69), (70). Note that the event A_{ib}
 1407 only involves the oracle estimator independent of t , while all
 1408 the terms related to the t -th iteration are in B_{ib} . Thus, the
 1409 inequality (23) decomposes the misclustering loss in the $(t+1)$ -th iteration
 1410 into the oracle loss and the loss in t -th iteration.
 1411 This decomposition leads to the separation of statistical error
 1412 and computational error in the final upper bound of Theorem 5.
 1413 Specifically, we prove the contraction inequality

$$\begin{aligned} 1414 \quad L^{(t+1)} &\leq M\xi + \rho L^{(t)}, \\ 1415 \quad \text{with } \xi &= \frac{1}{p} \sum_{i \in [p]} \theta(i) \sum_{b \in [r]} A_{ib} \|[\mathbf{S}_{z(i):}]^s - [\mathbf{S}_{b:}]^s\|^2, \end{aligned} \quad (24)$$

1416 where M is a positive constant, $\rho \in (0, 1)$ is the contraction
 1417 parameter, and we call ξ the oracle loss. Controlling the
 1418 probability of event B_{ib} and obtaining the $\rho L^{(t)}$ term in the
 1419 right hand side of (24) are the most challenging parts in
 1420 the proof of Theorem 5. Note that the true and estimated
 1421 core tensors are involved via their normalized rows such
 1422 as $\mathbf{S}_{a:}^s, \tilde{\mathbf{S}}_{a:}^s, [\mathbf{S}_{a:}^{(t)}]^s$. The Cartesian coordinate based analysis
 1423 in [13] is no longer applicable in our case. Instead, we use
 1424 the polar-coordinate based analysis and the geometry property
 1425 of trigonometric functions to derive the high probability upper
 1426 bounds for $F_{ib}^{(t)}, G_{ib}^{(t)}, H_{ib}^{(t)}$.

1427 Further, by sub-Gaussian concentration, we prove the high
 1428 probability upper bound for oracle loss

$$\xi \lesssim \text{SNR}^{-1} \exp \left(-\frac{p^{K-1} \text{SNR}}{r^{K-1}} \right). \quad (25)$$

1430 Combining the decomposition (24) and the oracle bound (25),
 1431 we finish the proof of Theorem 5.

1432 The proof of MLE error shares the similar idea as Theorems 4-5. We first show a weaker polynomial rate for MLE
 1433 and then improve the rate from polynomial to exponential
 1434 through the iterations. The only difference is that the MLE
 1435 remains the same over iterations due to its global optimality.
 1436 See Appendix B, Section B-G for the detailed proof.

Section G

APPENDIX A

ADDITIONAL NUMERICAL EXPERIMENTS

A. Bernoulli Phase Transition

1441 The first additional experiment verifies the
 1442 statistical-computational gap in Section III under the Bernoulli
 1443 model. Consider the Bernoulli model with $p = \{80, 100\}$,

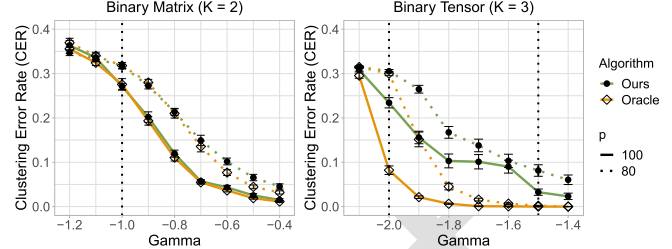


Fig. 12. SNR phase transitions for Bernoulli dTBM with $p = \{80, 100\}, r = 5$ under (a) matrix case with $\gamma \in [-1.2, -0.4]$ and (b) tensor case with $\gamma \in [-2.0, -1.4]$.

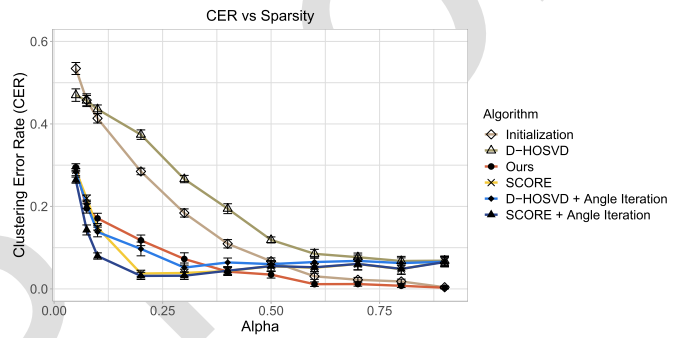


Fig. 13. CER comparison versus sparsity parameter α_p in $[0.05, 0.9]$. We set $p = 100, r = 5$ and $\gamma = -1.2$ under sparse binary dTBM.

Fig. 12

1444 $r = 5$. We vary γ in $[-1.2, -0.4]$ and $[-2.1, -1.4]$ for
 1445 matrix ($K = 2$) and tensor ($K = 3$) clustering, respectively.
 1446 We approximate MLE using an oracle estimator, i.e., the
 1447 output of Sub-algorithm 2 initialized from the true assignment.
 1448 Figure 12 shows a similar pattern as Figure 4. The algorithm
 1449 and oracle estimators have no gap in the matrix case, while an
 1450 error gap emerges between the critical values $\gamma_{\text{stat}} = -2$ and
 1451 $\gamma_{\text{comp}} = -1.5$ in the tensor case. Figure 4 suggests the
 1452 statistical-computational gap in Bernoulli models.
 1453

B. Sparsity

1454 The second additional experiment evaluates the algorithm
 1455 performances under the sparse binary dTBM (18). We fix the
 1456 signal exponent $\gamma = -1.2$ and vary the sparsity parameter
 1457 $\alpha_p \in [0.05, 0.9]$. A smaller α_p leads to a higher probability
 1458 of zero entries in the observation. In addition to the three
 1459 algorithms mentioned in Section VI-B (denoted **Initialization**,
 1460 **dTBM**, and **SCORE**), we consider other three algorithms based
 1461 on the discussion in Section IV-C:

- **D-HOSVD**, the diagonal-deleted HOSVD in [9];
- **D-HOSVD + Angle**, the combined algorithm of our
 1462 angle-based iteration with initialization from **D-HOSVD**;
- **SCORE + Angle**, the combined algorithms of our
 1463 angle-based iteration with initialization from **SCORE**.

1464 Figure 13 shows a slightly larger error in **dTBM** than that in
 1465 **SCORE**, **D-HOSVD + Angle**, and **SCORE + Angle** under the
 1466 sparse setting with $\alpha_p < 0.3$. The small gap between **dTBM**
 1467 and other sparse-specific methods implies the robustness of our
 1468 algorithm. In addition, comparing **SCORE** versus **SCORE + Angle**
 1469 (or **D-HOSVD** versus **D-HOSVD + Angle**) indicates the
 1470 benefit of our angle iterations under the sparse dTBM. In the
 1471

intermediate and dense cases with $\alpha_p \geq 0.3$, our proposed **dTBM** has a clear improvement over others, which again verifies the success of our algorithm in dense settings.

APPENDIX B PROOFS

subsection

We provide the proofs for all the theorems in our main paper. In each **sub-section**, we first show the proof of main theorem and then collect the useful lemmas in the end. We combine the proofs of MLE achievement in Theorem 2 and polynomial-time achievement in Theorem 5 in the last section due to the similar idea.

A. Notation

Before the proofs, we first introduce the notation used throughout the appendix and the general dTBM without symmetric assumptions. The parameter space and minimal gap assumption are also extended for the general asymmetric dTBM.

Numbered list -> bulleted list

1) *Preliminaries:* 1) For mode $k \in [K]$, denote mode- k tensor matricizations by

$$\begin{aligned} \mathbf{Y}_k &= \text{Mat}_k(\mathcal{Y}), \quad \mathbf{S}_k = \text{Mat}_k(\mathcal{S}), \\ \mathbf{E}_k &= \text{Mat}_k(\mathcal{E}), \quad \mathbf{X}_k = \text{Mat}_k(\mathcal{X}). \end{aligned}$$

2) For a vector \mathbf{a} , let $\mathbf{a}^s := \mathbf{a}/\|\mathbf{a}\|$ denote the normalized vector. We make the convention that $\mathbf{a}^s = \mathbf{0}$ if $\mathbf{a} = \mathbf{0}$.

3) For a matrix $\mathbf{A} \in \mathbb{R}^{n \times m}$, let $\mathbf{A}^{\otimes K} := \mathbf{A} \otimes \cdots \otimes \mathbf{A} \in \mathbb{R}^{n^K \times m^K}$ denote the Kronecker product of K copies of matrices \mathbf{A} .

4) For a matrix \mathbf{A} , let $\|\mathbf{A}\|_\sigma$ denote the spectral norm of matrix \mathbf{A} , which is equal to the maximal singular value of \mathbf{A} ; let $\lambda_k(\mathbf{A})$ denote the k -th largest singular value of \mathbf{A} ; let $\|\mathbf{A}\|_F$ denote the Frobenius norm of matrix \mathbf{A} .

2) *Extension to General Asymmetric dTBM.:* The general order- K (p_1, \dots, p_K)-dimensional dTBM with r_k communities and degree heterogeneity $\boldsymbol{\theta}_k = [\theta_k(i)] \in \mathbb{R}_+^{p_k}$ is represented by

$$\mathcal{Y} = \mathcal{X} + \mathcal{E}, \quad \text{where } \mathcal{X} = \mathcal{S} \times_1 \boldsymbol{\Theta}_1 \mathbf{M}_1 \times_2 \cdots \times_K \boldsymbol{\Theta}_K \mathbf{M}_K, \quad (26)$$

where $\mathcal{Y} \in \mathbb{R}^{p_1 \times \cdots \times p_K}$ is the data tensor, $\mathcal{X} \in \mathbb{R}^{p_1 \times \cdots \times p_K}$ is the mean tensor, $\mathcal{S} \in \mathbb{R}^{r_1 \times \cdots \times r_K}$ is the core tensor, $\mathcal{E} \in \mathbb{R}^{p_1 \times \cdots \times p_K}$ is the noise tensor consisting of independent zero-mean sub-Gaussian entries with variance bounded by σ^2 , $\boldsymbol{\Theta}_k = \text{diag}(\boldsymbol{\theta}_k)$, and $\mathbf{M}_k \in \{0, 1\}^{p_k \times r_k}$ is the membership matrix corresponding to the assignment $z_k : [p_k] \mapsto [r_k]$, for all $k \in [K]$.

For ease of notation, we use $\{z_k\}$ to denote the collection $\{z_k\}_{k=1}^K$, and $\{\boldsymbol{\theta}_k\}$ to denote the collection $\{\boldsymbol{\theta}_k\}_{k=1}^K$. Correspondingly, we consider the parameter space for the triplet $(\{z_k\}, \mathcal{S}, \{\boldsymbol{\theta}_k\})$,

$$\begin{aligned} \mathcal{P}(\{r_k\}) &= \left\{ (\{z_k\}, \mathcal{S}, \{\boldsymbol{\theta}_k\}) : \boldsymbol{\theta}_k \in \mathbb{R}_+^p, \frac{c_1 p_k}{r_k} |z_k^{-1}(a)| \leq \frac{c_2 p_k}{r_k}, \right. \\ &\quad c_3 \leq \|\mathbf{S}_{k,a,:}\| \leq c_4, \|\boldsymbol{\theta}_{k,z_k^{-1}(a)}\|_1 = |z_k^{-1}(a)|, \\ &\quad \left. \text{for all } a \in [r_k], k \in [K] \right\}. \end{aligned} \quad (27)$$

We call the degree heterogeneity $\{\boldsymbol{\theta}_k\}$ is balanced if for all $k \in [K]$,

$$\min_{a \in [r]} \|\boldsymbol{\theta}_{k,z_k^{-1}(a)}\| = (1 + o(1)) \max_{a \in [r]} \|\boldsymbol{\theta}_{k,z_k^{-1}(a)}\|. \quad (1526)$$

We also consider the generalized Assumption 1 on angle gap.

Assumption 2 (Generalized Angle Gap): Recall $\mathbf{S}_k = \text{Mat}_k(\mathcal{S})$. We assume the minimal gap between normalized rows of \mathbf{S}_k is bounded away from zero for all $k \in [K]$; i.e.,

$$\Delta_{\min} := \min_{k \in [K]} \min_{a \neq b \in [r_k]} \|\mathbf{S}_{k,a,:}^s - \mathbf{S}_{k,b,:}^s\| > 0. \quad (1533)$$

Similarly, let $\text{SNR} = \Delta_{\min}^2/\sigma^2$ with the generalized minimal gap Δ_{\min}^2 defined in Assumption 2. We define the regime

$$\mathcal{P}(\gamma) = \mathcal{P}(\{r_k\}) \cap \{\mathcal{S} \text{ satisfies } \text{SNR} = p^\gamma \text{ and } p_k \asymp p, k \in [K]\}. \quad (1536)$$

B. Proof of Theorem 1

Proof of Theorem 1: To study the identifiability, we consider the noiseless model with $\mathcal{E} = 0$. Assume that there exist two parameterizations satisfying

$$\begin{aligned} \mathcal{X} &= \mathcal{S} \times_1 \boldsymbol{\Theta}_1 \mathbf{M}_1 \times_2 \cdots \times_K \boldsymbol{\Theta}_K \mathbf{M}'_K \\ &= \mathcal{S}' \times_1 \boldsymbol{\Theta}'_1 \mathbf{M}'_1 \times_2 \cdots \times_K \boldsymbol{\Theta}'_K \mathbf{M}'_K, \end{aligned} \quad (28)$$

where $(\{z_k\}, \mathcal{S}, \{\boldsymbol{\theta}_k\}) \in \mathcal{P}(\{r_k\})$ and $(\{z'_k\}, \mathcal{S}', \{\boldsymbol{\theta}'_k\}) \in \mathcal{P}(\{r'_k\})$ are two sets of parameters. We prove the sufficient and necessary conditions separately.

(\Leftarrow) For the necessity, it suffices to construct two distinct parameters up to cluster label permutation, if the model (26) violates Assumption 2. Note that $\Delta_{\min}^2 = 1$ when there exists $k \in [K]$ such that $r_k = 1$. Hence, we consider the case that $r_k \geq 2$ for all $k \in [K]$. Without loss of generality, we assume $\|\mathbf{S}_{1,1,:}^s - \mathbf{S}_{1,2,:}^s\| = 0$.

By constraints in parameter space (27), neither $\mathbf{S}_{1,1,:}$ nor $\mathbf{S}_{1,2,:}$ is a zero vector. There exists a positive constant c such that $\mathbf{S}_{1,1,:} = c \mathbf{S}_{1,2,:}$. Thus, there exists a core tensor $\mathcal{S}_0 \in \mathbb{R}^{r_1-1 \times \cdots \times r_K}$ such that

$$\mathcal{S} = \mathcal{S}_0 \times_1 \mathbf{C} \mathbf{R}, \quad (1556)$$

where $\mathbf{C} = \text{diag}(1, c, 1, \dots, 1) \in \mathbb{R}^{r_1 \times r_1}$ and

$$\mathbf{R} = \begin{pmatrix} 1 & 0 \\ 1 & 0 \\ 0 & \mathbf{1}_{r_1-2} \end{pmatrix} \in \mathbb{R}^{r_1 \times (r_1-1)}. \quad (1558)$$

Let $\mathbf{D} = \text{diag}(1 + c, 1, \dots, 1) \in \mathbb{R}^{r_1-1 \times r_1-1}$. Consider the parameterization $\mathbf{M}'_1 = \mathbf{M}_1 \mathbf{R}$, $\mathcal{S}' = \mathcal{S}_0 \times_1 \mathbf{D}$, and

$$\theta'_1(i) = \begin{cases} \frac{1}{1+c} \theta_1(i) & i \in z_1^{-1}(1), \\ \frac{c}{1+c} \theta_1(i) & i \in z_1^{-1}(2), \\ \theta_1(i) & \text{otherwise,} \end{cases} \quad (1561)$$

and $\mathbf{M}'_k = \mathbf{M}_k$, $\boldsymbol{\theta}'_k = \boldsymbol{\theta}_k$ for all $k = 2, \dots, K$. Then we have constructed a triplet $(\{z'_k\}, \mathcal{S}', \{\boldsymbol{\theta}'_k\})$ that is distinct from $(\{z_k\}, \mathcal{S}, \{\boldsymbol{\theta}_k\})$ up to label permutation.

(\Rightarrow) For the sufficiency, it suffices to show that all possible triplets $(\{z'_k\}, \mathcal{S}', \{\boldsymbol{\theta}'_k\})$ are identical to $(\{z_k\}, \mathcal{S}, \{\boldsymbol{\theta}_k\})$ up

to label permutation if the model (26) satisfies Assumption (2). We show the uniqueness of the three parameters, $\{\mathbf{M}_k\}, \{\mathcal{S}\}, \{\boldsymbol{\theta}_k\}$ separately.

First, we show the uniqueness of \mathbf{M}_k for all $k \in [K]$. When $r_k = 1$, all possible \mathbf{M}_k 's are equal to the vector $\mathbf{1}_{p_k}$, and the uniqueness holds trivially. Hence, we consider the case that $r_k \geq 2$. Without loss of generality, we consider $k = 1$ with $r_1 \geq 2$ and show the uniqueness of the first mode membership matrix; i.e., $\mathbf{M}'_1 = \mathbf{M}_1 \mathbf{P}_1$ where \mathbf{P}_1 is a permutation matrix. The conclusion for $k \geq 2$ can be showed similarly and thus omitted.

Consider an arbitrary node pair (i, j) . If $z_1(i) = z_1(j)$, then we have $\|\mathbf{X}_{1,z_1(i)}^s - \mathbf{X}_{1,z_1(j)}^s\| = 0$ and thus $\|(\mathbf{S}')_{1,z_1(i)}^s - (\mathbf{S}')_{1,z_1(j)}^s\| = 0$ by Lemma 3. Then, by Assumption (2), we have $z'_1(i) = z'_1(j)$. Conversely, if $z_1(i) \neq z_1(j)$, then we have $\|\mathbf{X}_{1,i}^s - \mathbf{X}_{1,j}^s\| \neq 0$ and thus $\|(\mathbf{S}')_{1,z_1(i)}^s - (\mathbf{S}')_{1,z_1(j)}^s\| \neq 0$ by Lemma 3. Hence, we have $z'_1(i) \neq z'_1(j)$. Therefore, we have proven that z'_1 is identical z_i up to label permutation.

Next, we show the uniqueness of $\boldsymbol{\theta}_k$ for all $k \in [K]$ provided that $z_k = z'_k$. Similarly, consider $k = 1$ only, and omit the procedure for $k \geq 2$.

Consider an arbitrary $j \in [p_1]$ such that $z_1(j) = a$. Then for all the nodes $i \in z_1^{-1}(a)$ in the same cluster of j , we have

$$\frac{\mathbf{X}_{1,z_1(i)}^s}{\mathbf{X}_{1,z_1(j)}^s} = \frac{\mathbf{X}'_{1,z_1(i)}^s}{\mathbf{X}'_{1,z_1(j)}^s}, \text{ which implies } \frac{\theta_1(j)}{\theta_1(i)} = \frac{\theta'_1(j)}{\theta'_1(i)}. \quad (29)$$

Let $\theta'_1(j) = c\theta_1(j)$ for some positive constant c . By equation (29), we have $\theta'_1(i) = c\theta_1(i)$ for all $i \in z_1^{-1}(a)$. By the constraint $(\{z_k\}, \mathcal{S}', \{\boldsymbol{\theta}'_k\}) \in \mathcal{P}(\{r_k\})$, we have

$$\sum_{j \in z_1^{-1}(a)} \theta'_1(j) = c \sum_{j \in z_1^{-1}(a)} \theta_1(j) = 1,$$

which implies $c = 1$. Hence, we have proven $\boldsymbol{\theta}_1 = \boldsymbol{\theta}'_1$ provided that $z_1 = z'_1$.

Last, we show the uniqueness of \mathcal{S} ; i.e., $\mathcal{S}' = \mathcal{S} \times_1 \mathbf{P}_1^{-1} \times_2 \cdots \times_K \mathbf{P}_K^{-1}$, where \mathbf{P}_k 's are permutation matrices for all $k \in [K]$. Provided $z'_k = z_k, \boldsymbol{\theta}'_k = \boldsymbol{\theta}_k$, we have $\mathbf{M}'_k = \mathbf{M}_k \mathbf{P}_k$ and $\boldsymbol{\Theta}'_k = \boldsymbol{\Theta}_k$ for all $k \in [K]$.

Let $\mathbf{D}_k = [(\boldsymbol{\Theta}'_k \mathbf{M}'_k)^T (\boldsymbol{\Theta}'_k \mathbf{M}'_k)]^{-1} (\boldsymbol{\Theta}'_k \mathbf{M}'_k)^T, k \in [K]$. By the parameterization (28), we have

$$\begin{aligned} \mathcal{S}' &= \mathcal{X} \times_1 \mathbf{D}_1 \times_2 \cdots \times_K \mathbf{D}_K \\ &= \mathcal{S} \times_1 \mathbf{D}_1 \boldsymbol{\Theta}_1 \mathbf{M}_1 \times_1 \cdots \times_K \mathbf{D}_K \boldsymbol{\Theta}_K \mathbf{M}_K \\ &= \mathcal{S} \times_1 \mathbf{P}_1^{-1} \times_2 \cdots \times_K \mathbf{P}_K^{-1}. \end{aligned}$$

Therefore, we finish the proof of Theorem 1. \square

1) Useful Lemma for the Proof of Theorem 1: Change to unlisted bold text in a single line.

Lemma 3 (Motivation of Angle-Based Clustering):

Consider the signal tensor \mathcal{X} in the general asymmetric dTBM (26) with $(\{z_k\}, \mathcal{S}, \{\boldsymbol{\theta}_k\}) \in \mathcal{P}(\{r_k\})$ and $r_k \geq 2, k \in [K]$. Then, for any $k \in [K]$ and index pair $(i, j) \in [p_k]^2$, we have

$$\begin{aligned} \left\| \mathbf{S}_{k,z_k(i)}^s - \mathbf{S}_{k,z_k(j)}^s \right\| &= 0 \quad \text{if and only if} \\ \left\| \mathbf{X}_{k,z_k(i)}^s - \mathbf{X}_{k,z_k(j)}^s \right\| &= 0. \end{aligned}$$

Proof of Lemma 3: Without loss of generality, we prove $k = 1$ only and drop the subscript k in $\mathbf{X}_k, \mathbf{S}_k$ for notational convenience. By tensor matricization, we have

$$\mathbf{X}_{j:} = \theta_1(j) \mathbf{S}_{z_1(j):} [\boldsymbol{\Theta}_2 \mathbf{M}_2 \otimes \cdots \otimes \boldsymbol{\Theta}_K \mathbf{M}_K]^T. \quad (1619)$$

Let $\tilde{\mathbf{M}} = \boldsymbol{\Theta}_2 \mathbf{M}_2 \otimes \cdots \otimes \boldsymbol{\Theta}_K \mathbf{M}_K$. Notice that for two vectors \mathbf{a}, \mathbf{b} and two positive constants $c_1, c_2 > 0$, we have

$$\|\mathbf{a}^s - \mathbf{b}^s\| = \|(c_1 \mathbf{a})^s - (c_2 \mathbf{b})^s\|. \quad (1622)$$

Thus it suffices to show the following statement holds for any index pair $(i, j) \in [p_1]^2$,

$$\left\| \mathbf{S}_{z_1(i):}^s - \mathbf{S}_{z_1(j):}^s \right\| = 0 \quad \text{if and only if} \quad (1625)$$

$$\left\| [\mathbf{S}_{z_1(i):} \tilde{\mathbf{M}}^T]^s - [\mathbf{S}_{z_1(j):} \tilde{\mathbf{M}}^T]^s \right\| = 0. \quad (1626)$$

$$(\Leftarrow) \text{ Suppose } \left\| [\mathbf{S}_{z_1(i):} \tilde{\mathbf{M}}^T]^s - [\mathbf{S}_{z_1(j):} \tilde{\mathbf{M}}^T]^s \right\| = 0. \quad (1627)$$

There exists a positive constant c such that $\mathbf{S}_{z_1(i):} \tilde{\mathbf{M}}^T = c \mathbf{S}_{z_1(j):} \tilde{\mathbf{M}}^T$. Note that

$$\mathbf{S}_{z_1(i):} = \mathbf{S}_{z_1(i):} \tilde{\mathbf{M}}^T \left[\tilde{\mathbf{M}} \left(\tilde{\mathbf{M}}^T \tilde{\mathbf{M}} \right)^{-1} \right], \quad (1630)$$

where $\tilde{\mathbf{M}}^T \tilde{\mathbf{M}}$ is an invertible diagonal matrix with positive diagonal elements. Thus, we have $\mathbf{S}_{z_1(i):} = c \mathbf{S}_{z_1(j):}$, which implies $\left\| \mathbf{S}_{z_1(i):}^s - \mathbf{S}_{z_1(j):}^s \right\| = 0$.

(\Rightarrow) Suppose $\left\| \mathbf{S}_{z_1(i):}^s - \mathbf{S}_{z_1(j):}^s \right\| = 0$. There exists a positive constant c such that $\mathbf{S}_{z_1(i):} = c \mathbf{S}_{z_1(j):}$, and thus $\mathbf{S}_{z_1(i):} \tilde{\mathbf{M}}^T = c \mathbf{S}_{z_1(j):} \tilde{\mathbf{M}}^T$, which implies $\left\| [\mathbf{S}_{z_1(i):} \tilde{\mathbf{M}}^T]^s - [\mathbf{S}_{z_1(j):} \tilde{\mathbf{M}}^T]^s \right\| = 0$.

Therefore, we finish the proof of Lemma 3. \square

C. Proof of Lemma 1 and Lemma 2

Proof of Lemma 1: Note that the vector $\mathbf{S}_{z(i):}$ can be folded to a tensor $\mathcal{S}' = [\mathcal{S}'_{a_2, \dots, a_K}] \in \mathbb{R}^{r^{K-1}}$; i.e., $\text{vec}(\mathcal{S}') = \mathbf{S}_{z(i):}$. Define weight vectors $\mathbf{w}_{a_2, \dots, a_K}$ corresponding to the elements in $\mathcal{S}'_{a_2, \dots, a_K}$ by

$$\begin{aligned} \mathbf{w}_{a_2 \dots a_K} &= [\theta_{z^{-1}(a_2)}^T \otimes \cdots \otimes \theta_{z^{-1}(a_K)}^T] \in \mathbb{R}^{|z^{-1}(a_2)| \times \cdots \times |z^{-1}(a_K)|}, \end{aligned} \quad (1645)$$

for all $a_k \in [r], k = 2, \dots, K$, where \otimes denotes the Kronecker product. Therefore, we have $\mathbf{X}_{i:} = \theta(i) \text{Pad}_{\mathbf{w}}(\mathbf{S}_{z(i)})$ where $\mathbf{w} = \{\mathbf{w}_{a_2, \dots, a_K}\}_{a_k \in [r], k \in [K] \setminus \{1\}}$. Specifically, we have $\|\mathbf{w}_{a_2, \dots, a_K}\|^2 = \prod_{k=2}^K \|\theta_{z^{-1}(a_k)}\|^2$, and by the balanced assumption (6) we have

$$\max_{(a_2, \dots, a_K)} \|\mathbf{w}_{a_2, \dots, a_K}\|^2 = (1 + o(1)) \min_{(a_2, \dots, a_K)} \|\mathbf{w}_{a_2, \dots, a_K}\|^2. \quad (30)$$

Consider the inner product of $\mathbf{X}_{i:}$ and $\mathbf{X}_{j:}$ for $z(i) \neq z(j)$. By the definition of weighted padding operator (56) and the balanced assumption (30), we have

$$\begin{aligned} &\langle \mathbf{X}_{i:}, \mathbf{X}_{j:} \rangle \\ &= \theta(i)\theta(j) \langle \text{Pad}_{\mathbf{w}}(\mathbf{S}_{z(i)}), \text{Pad}_{\mathbf{w}}(\mathbf{S}_{z(j)}) \rangle \\ &= \theta(i)\theta(j) \min_{(a_2, \dots, a_K)} \|\mathbf{w}_{a_2, \dots, a_K}\|^2 \langle \mathbf{S}_{z(i)}, \mathbf{S}_{z(j)} \rangle (1 + o(1)). \end{aligned} \quad (1657)$$

Therefore, when p large enough, the inner product $\langle \mathbf{X}_{i:}, \mathbf{X}_{j:} \rangle$ has the same sign as $\langle \mathbf{S}_{z(i):}, \mathbf{S}_{z(j):} \rangle$.

Then, we have

$$\begin{aligned} \cos(\mathbf{S}_{z_1(i):}, \mathbf{S}_{z_1(j):}) &= \frac{\langle \mathbf{S}_{z_1(i):}, \mathbf{S}_{z_1(j):} \rangle}{\|\mathbf{S}_{z_1(i):}\| \|\mathbf{S}_{z_1(j):}\|} \\ &= (1 + o(1)) \frac{\langle \mathbf{X}_{i:}, \mathbf{X}_{j:} \rangle}{\|\mathbf{X}_{i:}\| \|\mathbf{X}_{j:}\|} \\ &= (1 + o(1)) \cos(\mathbf{X}_{i:}, \mathbf{X}_{j:}), \end{aligned}$$

where the second inequality follows by the balance assumption on θ .

Further, notice that $\|\mathbf{v}_1^s - \mathbf{v}_2^s\|^2 = 2(1 - \cos(\mathbf{v}_1, \mathbf{v}_2))$. For all i, j such that $z(i) \neq z(j)$, when $p \rightarrow \infty$, we have

$$\|\mathbf{X}_{i:}^s - \mathbf{X}_{j:}^s\| \asymp \|\mathbf{S}_{z_1(i):}^s - \mathbf{S}_{z_1(j):}^s\| \gtrsim \Delta_{\min}.$$

Combining the inequalities (12) and (12) in the proof of Theorem 2 in [15], we have

$$\begin{aligned} \inf_{\hat{z}_1} \mathbb{E} [\ell(\hat{z}_1, z_1^*) | (z_k^*, \mathcal{S}^*, \theta_k^*)] &\geq \\ \frac{C}{r^3 |T_1^c|} \sum_{i \in T_1^c} \inf_{\hat{z}_1(i)} \{ &\mathbb{P}[\hat{z}_1(i) = 1 | z_1^*(i) = 2, z_k^*, \mathcal{S}^*, \theta_k^*] \\ &+ \mathbb{P}[\hat{z}_1(i) = 2 | z_1^*(i) = 1, z_k^*, \mathcal{S}^*, \theta_k^*]\}, \end{aligned} \quad (31)$$

where C is some positive constant, \hat{z}_1 on the left hand side denote the generic assignment functions in $\mathcal{P}(\gamma)$, and the infimum on the right hand side is taken over the generic assignment function family of $\hat{z}_1(i)$ for all nodes $i \in T_1^c$. Here, the factor $r^3 = r \cdot r^2$ in (31) comes from two sources: $r^2 \asymp \binom{r}{2}$ comes from the multiple testing burden for all pairwise comparisons among r clusters; and another r comes from the number of elements $|T_k^c| \asymp p/r$ to be clustered.

Proof of Lemma 2: By the definition of minimal gap in Assumption 1, we have

$$\begin{aligned} L^{(t)} &= \frac{1}{p} \sum_{i \in [p]} \theta(i) \sum_{b \in [r]} \mathbb{1} \{z^{(t)}(i) = b\} \|[\mathbf{S}_{z(i):}]^s - [\mathbf{S}_b:]^s\|^2 \\ &\geq \frac{1}{p} \sum_{i \in [p]} \theta(i) \sum_{b \in [r]} \mathbb{1} \{z^{(t)}(i) = b\} \Delta_{\min}^2 \\ &\geq c \ell^{(t)} \Delta_{\min}^2, \end{aligned}$$

where the last inequality follows from the assumption $\min_{i \in [p]} \theta(i) \geq c > 0$. \square

D. Proof of Theorem 2 (Impossibility)

Proof of Theorem 2 (Impossibility): Consider the general asymmetric dTBM (26) in the special case that $p_k = p$ and $r_k = r$ for all $k \in [K]$ with $K \geq 2$, $2 \leq r \lesssim p^{1/3}$ as $p \rightarrow \infty$. For simplicity, we show the minimax rate for the estimation on the first mode \hat{z}_1 ; the proof for other modes are essentially the same.

To prove the minimax rate (10), it suffices to take an arbitrary $\mathcal{S}^* \in \mathcal{P}_S(\gamma)$ with $\gamma < -(K-1)$ and construct (z_k^*, θ_k^*) such that

$$\inf_{\hat{z}_1} \mathbb{E} [p \ell(\hat{z}_1, z_1^*) | (z_k^*, \mathcal{S}^*, \theta_k^*)] \geq 1.$$

We first define a subset of indices $T_k \subset [p_k]$, $k \in [K]$ in order to avoid the complication of label permutation. Based on [13, Proof of Theorem 6], we consider the restricted family of \hat{z}_k 's for which the following three conditions are satisfied:

- (a) $\hat{z}_k(i) = z_k(i)$ for all $i \in T_k$; (b) $|T_k^c| \asymp \frac{p}{r}$;
- (c) $\min_{\pi \in \Pi} \sum_{i \in [p]} \mathbb{1}\{\hat{z}_k(i) \neq \pi \circ z_k(i)\} = \sum_{i \in [p]} \mathbb{1}\{\hat{z}_k(i) \neq z_k(i)\}$,

for all $k \in [K]$. Now, we consider the construction:

- (i) $\{z_k^*\}$ satisfies properties (a)-(c) with misclassification sets T_k^c for all $k \in [K]$;
- (ii) $\{\theta_k^*\}$ such that $\theta_k^*(i) \leq \sigma r^{(K-1)/2} p^{-(K-1)/2}$ for all $i \in T_k^c$, $k \in [K]$ and $\max_{k \in [K], a \in [r]} \|\theta_{k,z_k^{*, -1}(a)}\|_2^2 \asymp p/r$.

Next, we need to find the lower bound of the rightmost side in (31). We consider the hypothesis test based on model (26). First, we reparameterize the model under the construction (i)-(ii).

$$\mathbf{x}_a^* = [\text{Mat}_1(\mathcal{S}^* \times_2 \Theta_2^* \mathbf{M}_2^* \times_3 \cdots \times_K \Theta_K^* \mathbf{M}_K^*)]_{a:}, \quad (32)$$

for all $a \in [r]$, where \mathbf{x}_a^* 's are centroids in $\mathbb{R}^{p^{K-1}}$. Without loss of generality, we consider the lower bound for the summand in (31) for $i = 1$. The analysis for other $i \in T_1^c$ are similar. For notational simplicity, we suppress the subscript i and write \mathbf{y}, θ^*, z in place of $\mathbf{y}_1, \theta_1^*(1)$ and $z_1(1)$, respectively. The equivalent vector problem for assessing the summand in (31) is

$$\mathbf{y} = \theta^* \mathbf{x}_z^* + \mathbf{e}, \quad (32)$$

where $z \in \{1, 2\}$ is an unknown parameter, $\theta^* \in \mathbb{R}_+$ is the given heterogeneity degree, $\mathbf{x}_1^*, \mathbf{x}_2^* \in \mathbb{R}^{p^{K-1}}$ are given centroids, and $\mathbf{e} \in \mathbb{R}^{p^{K-1}}$ consists of i.i.d. $N(0, \sigma^2)$ entries. Then, we consider the hypothesis testing under the model (32):

$$H_0 : z = 1, \mathbf{y} = \theta^* \mathbf{x}_1^* + \mathbf{e} \leftrightarrow H_1 : z = 2, \mathbf{y} = \theta^* \mathbf{x}_2^* + \mathbf{e}, \quad (33)$$

The hypothesis testing (33) is a simple versus simple testing, since the assignment z is the only unknown parameter in the test. By Neyman-Pearson lemma, the likelihood ratio test is optimal with minimal Type I + II error. Under Gaussian model, the likelihood ratio test of (33) is equivalent to the least square estimator $\hat{z}_{LS} = \arg \min_{a=\{1,2\}} \|\mathbf{y} - \theta^* \mathbf{x}_a^*\|_F^2$.

Let $\mathbf{S} = \text{Mat}_1(\mathcal{S})$. Note that

$$\begin{aligned} &\|\theta^* \mathbf{x}_1^* - \theta^* \mathbf{x}_2^*\|_F \\ &\leq \theta^* \|\mathbf{S}_{1:}^* - \mathbf{S}_{2:}^*\|_F \prod_{k=2}^K \lambda_{\max}(\Theta_k^* \mathbf{M}_k^*) \\ &\leq \theta^* \|\mathbf{S}_{1:}^* - \mathbf{S}_{2:}^*\|_F \max_{k \in [K]/\{1\}, a \in [r]} \|\theta_{k,z_k^{*, -1}(a)}\|_2^{K-1} \\ &\leq \sigma r^{(K-1)/2} p^{-(K-1)/2} 2 c_4 p^{(K-1)/2} r^{-(K-1)/2} \\ &\leq 2 c_4 \sigma, \end{aligned}$$

where $\lambda_{\max}(\cdot)$ denotes the maximal singular value, the second inequality follows from Lemma 6, and the third inequality

nondegree

- 1744 follows from property (ii) and the boundedness constraint in
1745 $\mathcal{P}_S(\gamma)$ such that $\|\mathbf{S}_{1:}^* - \mathbf{S}_{2:}^*\|_F \leq \|\mathbf{S}_{1:}^*\|_F + \|\mathbf{S}_{2:}^*\|_F \leq 2c_4$.
1746 Hence, we have
- 1747
$$\inf_{\hat{z}_1(1)} \{\mathbb{P}[\hat{z}_1(1) = 1 | z_1^*(1) = 2, z_k^*, \mathcal{S}^*, \boldsymbol{\theta}_k^*]$$

$$+ \mathbb{P}[\hat{z}_1(1) = 2 | z_1^*(1) = 1, z_k^*, \mathcal{S}^*, \boldsymbol{\theta}_k^*]\}$$

$$= 2\mathbb{P}[\hat{z}_{LS} = 1 | z_1^*(1) = 2, z_k^*, \mathcal{S}^*, \boldsymbol{\theta}_k^*]$$

$$= 2\mathbb{P}[\|\mathbf{y} - \boldsymbol{\theta}^* \mathbf{x}_1^*\|_F^2 \leq \|\mathbf{y} - \boldsymbol{\theta}^* \mathbf{x}_2^*\|_F^2 | z_1^*(1) = 2, z_k^*, \mathcal{S}^*, \boldsymbol{\theta}_k^*]$$

$$= 2\mathbb{P}[2\langle \mathbf{e}, \boldsymbol{\theta}^* \mathbf{x}_1^* - \boldsymbol{\theta}^* \mathbf{x}_2^* \rangle \geq \|\boldsymbol{\theta}^* \mathbf{x}_1^* - \boldsymbol{\theta}^* \mathbf{x}_2^*\|_F^2]$$

$$= 2\mathbb{P}[N(0, 1) \geq \boldsymbol{\theta}^* \|\mathbf{x}_1^* - \mathbf{x}_2^*\|_F / (2\sigma)]$$

$$\geq 2\mathbb{P}[N(0, 1) \geq c_4] \geq c,$$
 (34)

The verification of the above two properties is provided in the end
1793 of this proof.

Now, following the proof of [13, Theorem 7], when $\gamma < -K/2$,
1795 every polynomial-time algorithm estimator $(\hat{\mathbf{M}}_k)_{k \in [K]}$ obeys
1796

$$\liminf_{p \rightarrow \infty} \sup_{\mathcal{X} \in \mathcal{P}_{\text{non-degree}}(\gamma)} \mathbb{P}(\exists k \in [K], \hat{\mathbf{M}}_k \neq \mathbf{M}_k) \geq 1/2, \quad (36)$$

under the HPC Conjecture 1. The inequality (36) implies

$$\liminf_{p \rightarrow \infty} \sup_{\mathcal{X} \in \mathcal{P}_{\text{non-degree}}(\gamma)} \max_{k \in [K]} \mathbb{E}[p\ell(z_k, \hat{z}_k)] \geq 1.$$

Based on properties (i)-(ii), we conclude that

$$\liminf_{p \rightarrow \infty} \sup_{\mathcal{X} \in \mathcal{P}(\gamma)} \max_{k \in [K]} \mathbb{E}[p\ell(z_k, \hat{z}_k)] \geq 1.$$

We complete the proof by verifying the properties (i)-(ii). For (i),
1802 we verify that the angle gap for the core tensor \mathcal{S} in (35) is on the
1803 order of $\sigma p^{-\gamma/2}$. Specifically, write $\mathbf{1} = (1, 1, 1)$ and $\mathbf{e} = (1, -1, 0)$.
1804 We have
1805

$$\text{Mat}(\mathcal{S}) = \begin{bmatrix} \text{Vec}(\mathbf{1}^{\otimes K-1}) + \sigma p^{-\gamma/2} \text{Vec}\left(\mathbf{e}^{\otimes(K-1)}\right) \\ \text{Vec}(\mathbf{1}^{\otimes K-1}) - \sigma p^{-\gamma/2} \text{Vec}\left(\mathbf{e}^{\otimes(K-1)}\right) \\ \text{Vec}(\mathbf{1}^{\otimes K-1}) \end{bmatrix}. \quad (35)$$

Based on the orthogonality $\langle \mathbf{1}, \mathbf{e} \rangle = 0$, the minimal angle gap among
1807 rows of $\text{Mat}(\mathcal{S})$ is
1808

$$\begin{aligned} \Delta_{\min}^2(\mathcal{S}) &\asymp \tan^2(\text{Mat}(\mathcal{S})_{1:}, \text{Mat}(\mathcal{S})_{3:}) \\ &= \left(\frac{\|\mathbf{e}\|_2}{\|\mathbf{1}\|_2}\right)^{2(K-1)} \sigma^2 d^{-\gamma} \\ &\asymp \sigma^2 d^{-\gamma}. \end{aligned}$$

Therefore, we have shown that $\mathcal{P}_{\text{shifted}}(\gamma) = \mathcal{P}(\gamma)$. Finally, the
1812 property (ii) follows directly by comparing the definition of \mathcal{S} in (35)
1813 with that in the proof of [13, Theorem 7]. \square
1814

E. Proof of Theorem 3 (Impossibility)

Proof of Theorem 3 (Impossibility): The idea of proving computational hardness is to show the computational lower bound for a special class of degree-corrected tensor clustering model with $K \geq 2$ and $r \geq 2$. We construct the following special class of higher-order degree-corrected tensor clustering model. For a given signal level $\gamma \in \mathbb{R}$ and noise variance σ , define a rank-2 symmetric tensor $\mathcal{S} \in \mathbb{R}^{3 \times \dots \times 3}$ subject to

$$\mathcal{S} = \mathcal{S}(\gamma) = \begin{bmatrix} 1 \\ 1 \\ 1 \end{bmatrix}^{\otimes K} + \sigma p^{-\gamma/2} \begin{bmatrix} 1 \\ -1 \\ 0 \end{bmatrix}^{\otimes K}. \quad (35)$$

F. Proof of Theorem 4 and Proposition 1

Proof of Theorem 4: We prove Theorem 4 under the dTBM (1) with symmetric mean tensor, parameters $(z, \mathcal{S}, \boldsymbol{\theta})$, fixed $r \geq 1, K \geq 2$, and i.i.d. noise. For the case $r = 1$, we have $L(z^{(0)}, z) = 0, \ell(z^{(0)}, z) = 0$ trivially. Hence, we focus on the proof of the first mode clustering $z_1^{(0)}$ with $r \geq 2$; the proofs for the other modes can be extended similarly. We drop the subscript k in the matricizations $\mathbf{M}_k, \mathbf{X}_k, \mathbf{S}_k$ and in the estimate $z_1^{(0)}$. We firstly show the proof with balanced $\boldsymbol{\theta}$.

Change to unlisted plain text.

1) We Firstly Show the Upper Bound for Misclustering Error $\ell(z^{(0)}, z)$: First, by Lemma 1, there exists a positive constant such that $\min_{z(i) \neq z(j)} \|\mathbf{X}_i^s - \mathbf{X}_j^s\| \geq c_0 \Delta_{\min}$. By the balance assumption on $\boldsymbol{\theta}$ and Lemma 8, we have

$$\min_{\pi \in \Pi} \sum_{i: z^{(0)}(i) \neq \pi(z(i))} \theta(i)^2 \leq \sum_{i \in S_I} \theta(i)^2 + 4 \sum_{i \in S} \theta(i)^2, \quad (37)$$

where

$$S_0 = \{i : \|\hat{\mathbf{X}}_i\| = 0\}, S = \{i \in S_0^c : \|\hat{\mathbf{x}}_{z^{(0)}(i)} - \mathbf{X}_i^s\| \geq c_0 \Delta_{\min}/2\}.$$

1831 On one hand, note that for any set $P \in [p]$,

$$\begin{aligned} 1832 \quad \sum_{i \in P} \|\mathbf{X}_{i:}\|^2 &= \sum_{i \in P} \|\theta(i) \mathbf{S}_{z(i)} : (\Theta \mathbf{M})^{T, \otimes(K-1)}\|^2 \\ 1833 \quad &\geq \sum_{i \in P} \theta(i)^2 \min_{a \in [r]} \|\mathbf{S}_{a:}\|^2 \lambda_r^{2(K-1)}(\Theta \mathbf{M}) \\ 1834 \quad &\gtrsim \sum_{i \in P} \theta(i)^2 p^{K-1} r^{-(K-1)}, \end{aligned}$$

1835 where the last inequality follows Lemma 6, the assumption that
1836 $\min_{i \in [p]} \theta(i) \geq c$, and the constraint $\min_{a \in [r]} \|\mathbf{S}_{a:}\| \geq c_3$ in
1837 the parameter space (2). Thus, we have

$$1838 \quad \sum_{i \in P} \theta(i)^2 \lesssim \sum_{i \in P} \|\mathbf{X}_{i:}\|^2 p^{-(K-1)} r^{K-1}. \quad (38)$$

1839 On the other hand, note that

$$\begin{aligned} 1840 \quad &\sum_{i \in S} \|\mathbf{X}_{i:}\|^2 \\ 1841 \quad &\leq 2 \sum_{i \in S} \|\hat{\mathbf{X}}_{i:}\|^2 + 2 \sum_{i \in S} \|\hat{\mathbf{X}}_{i:} - \mathbf{X}_{i:}\|^2 \\ 1842 \quad &\leq \frac{8}{c_0^2 \Delta_{\min}^2} \sum_{i \in S} \|\hat{\mathbf{X}}_{i:}\|^2 \|\hat{\mathbf{x}}_{z^{(0)}(i)} - \mathbf{X}_{i:}^s\|^2 + 2 \|\hat{\mathcal{X}} - \mathcal{X}\|_F^2 \\ 1843 \quad &\quad (40) \end{aligned}$$

$$\begin{aligned} 1844 \quad &\leq \frac{16}{c_0^2 \Delta_{\min}^2} \sum_{i \in S} \|\hat{\mathbf{X}}_{i:}\|^2 \left[\|\hat{\mathbf{x}}_{z^{(0)}(i)} - \hat{\mathbf{X}}_{i:}^s\|^2 + \|\hat{\mathbf{X}}_{i:}^s - \mathbf{X}_{i:}^s\|^2 \right] \\ 1845 \quad &\quad + 2 \|\hat{\mathcal{X}} - \mathcal{X}\|_F^2 \\ 1846 \quad &\leq \frac{16(1+\eta)}{c_0^2 \Delta_{\min}^2} \sum_{i \in S} \|\hat{\mathbf{X}}_{i:}\|^2 \|\hat{\mathbf{X}}_{i:}^s - \mathbf{X}_{i:}^s\|^2 + 2 \|\hat{\mathcal{X}} - \mathcal{X}\|_F^2 \quad (42) \end{aligned}$$

$$1847 \quad \leq \left(\frac{16(1+\eta)}{c_0^2 \Delta_{\min}^2} + 2 \right) \|\hat{\mathcal{X}} - \mathcal{X}\|_F^2 \quad (43)$$

$$1848 \quad \lesssim \left(\frac{16(1+\eta)}{c_0^2 \Delta_{\min}^2} + 2 \right) (p^{K/2} r + pr^2 + r^K) \sigma^2, \quad (44)$$

1849 where inequalities (39) and (41) follow from the triangle
1850 inequality, (40) follows from the definition of S , (42) follows
1851 from the update rule of k -means in Step 6 of Sub-algorithm 1,
1852 (43) follows from Lemma 4, and the last inequality (44)
1853 follows from Lemma 7. Also, note that

$$\begin{aligned} 1854 \quad \sum_{i \in S_0} \|\mathbf{X}_{i:}\|^2 &= \sum_{i \in S_0} \|\hat{\mathbf{X}}_{i:} - \mathbf{X}_{i:}\|^2 \\ 1855 \quad &\leq \|\hat{\mathcal{X}} - \mathcal{X}\|_F^2 \\ 1856 \quad &\lesssim (p^{K/2} r + pr^2 + r^K) \sigma^2, \quad (45) \end{aligned}$$

1857 where the equation follows from the definition of S_0 . Therefore,
1858 combining the inequalities (37), (38), (44), and (45),
1859 we have

$$\begin{aligned} 1860 \quad &\min_{\pi \in \Pi} \sum_{i: z^{(0)}(i) \neq \pi(z(i))} \theta(i)^2 \\ 1861 \quad &\lesssim \left(\sum_{i \in S} \|\mathbf{X}_{i:}\|^2 + \sum_{i \in S_0} \|\mathbf{X}_{i:}\|^2 \right) p^{-(K-1)} r^{K-1} \\ 1862 \quad &\lesssim \frac{\sigma^2 r^{K-1}}{\Delta_{\min}^2 p^{K-1}} (p^{K/2} r + pr^2 + r^K). \quad (46) \end{aligned}$$

With the assumption that $\min_{i \in [p]} \theta(i) \geq c$, we finally obtain
1863 the result

$$\ell(z^{(0)}, z) \lesssim \frac{1}{p} \min_{\pi \in \Pi} \sum_{i: z^{(0)}(i) \neq \pi(z(i))} \theta(i)^2 \lesssim \frac{r^K p^{-K/2}}{\text{SNR}}, \quad (47)$$

where the last inequality follows from the definition $\text{SNR} = \Delta_{\min}^2 / \sigma^2$.

Without the balanced θ , we have $\min_{z(i) \neq z(j)} \|\mathbf{X}_{i:}^s - \mathbf{X}_{j:}^s\| \geq c_0 \Delta_{\mathbf{X}}$. Replacing the definition of S with $\Delta_{\mathbf{X}}$, we obtain the desired result.

2) Next, we Show the Bound for $L(z^{(0)}, z)$: Note that $\mathbf{X}_{i:}^s$ have only r different values. We let $\mathbf{X}_a^s = \mathbf{X}_{i:}^s$ for all i such that $z(i) = a$, $a \in [r]$.

Change to unlisted plain text.

Notice that

$$\|\mathbf{X}_{i:}\|^2 \gtrsim p^{K-1} r^{-(K-1)} \quad (48)$$

and

$$\|\mathbf{X}_{i:} - \hat{\mathbf{X}}_{i:}\|^2 \leq \|\hat{\mathcal{X}} - \mathcal{X}\|_F^2 \lesssim p^{K/2} r + pr^2 + r^K. \quad (49)$$

Therefore, when p is large enough, we have

$$\begin{aligned} 1870 \quad &\sum_{i \in [p]} \|\mathbf{X}_{i:}\|^2 \|\hat{\mathbf{X}}_{i:}^s - \hat{\mathbf{x}}_{z^{(0)}(i)}\|^2 \\ 1871 \quad &\lesssim \sum_{i \in [p]} \left(\|\mathbf{X}_{i:}\|^2 - \|\mathbf{X}_{i:} - \hat{\mathbf{X}}_{i:}\|^2 \right) \|\hat{\mathbf{X}}_{i:}^s - \hat{\mathbf{x}}_{z^{(0)}(i)}\|^2 \\ 1872 \quad &\lesssim \sum_{i \in [p]} \|\hat{\mathbf{X}}_{i:}\|^2 \|\hat{\mathbf{X}}_{i:}^s - \hat{\mathbf{x}}_{z^{(0)}(i)}\|^2 \\ 1873 \quad &\lesssim \eta \sum_{i \in [p]} \|\hat{\mathbf{X}}_{i:}\|^2 \|\hat{\mathbf{X}}_{i:}^s - \mathbf{X}_{i:}^s\|^2 \\ 1874 \quad &\lesssim \|\hat{\mathcal{X}} - \mathcal{X}\|_F^2 \\ 1875 \quad &\lesssim p^{K/2} r + pr^2 + r^K. \quad (47) \end{aligned}$$

Hence, we have

$$\begin{aligned} 1876 \quad \sum_{i \in [p]} \|\hat{\mathbf{X}}_{i:}^s - \hat{\mathbf{x}}_{z^{(0)}(i)}\|^2 &\lesssim \sum_{i \in [p]} \theta(i)^2 \|\hat{\mathbf{X}}_{i:}^s - \hat{\mathbf{x}}_{z^{(0)}(i)}\|^2 \\ 1877 \quad &\lesssim \frac{r^{K-1}}{p^{K-1}} \sum_{i \in [p]} \|\mathbf{X}_{i:}\|^2 \|\hat{\mathbf{X}}_{i:}^s - \hat{\mathbf{x}}_{z^{(0)}(i)}\|^2 \\ 1878 \quad &\lesssim \frac{r^{K-1}}{p^{K-1}} (p^{K/2} r + pr^2 + r^K), \quad (48) \end{aligned}$$

where the first inequality follows from the assumption $\min_{i \in [p]} \theta(i) \geq c > 0$, the second inequality follows from the inequality (38), and the last inequality comes from the inequality (47).

Next, we consider the following quantity,

$$\begin{aligned} 1885 \quad &\sum_{i \in [p]} \theta(i) \|\mathbf{X}_{i:}^s - \hat{\mathbf{x}}_{z^{(0)}(i)}\|^2 \\ 1886 \quad &\lesssim \sum_{i \in [p]} \theta(i)^2 \|\mathbf{X}_{i:}^s - \hat{\mathbf{X}}_{i:}^s\|^2 + \sum_{i \in [p]} \theta(i)^2 \|\hat{\mathbf{X}}_{i:}^s - \hat{\mathbf{x}}_{z^{(0)}(i)}\|^2 \\ 1887 \quad &\lesssim \sum_{i \in [p]} \frac{\theta(i)^2}{\|\mathbf{X}_{i:}\|^2} \|\mathbf{X}_{i:} - \hat{\mathbf{X}}_{i:}\|^2 + \sum_{i \in [p]} \theta(i)^2 \|\hat{\mathbf{X}}_{i:}^s - \hat{\mathbf{x}}_{z^{(0)}(i)}\|^2 \\ 1888 \quad &\lesssim \frac{r^{K-1}}{p^{K-1}} (p^{K/2} r + pr^2 + r^K), \quad (49) \end{aligned}$$

where the first inequality follows from the assumption of $\theta(i)$ and triangle inequality, the second inequality follows from Lemma 4, and the last inequality follows from (48). In addition, with Theorem 4 and the condition $\text{SNR} \gtrsim p^{-K/2} \log p$, for all $a \in [r]$, we have

$$|z^{-1}(a) \cap (z^{(0)})^{-1}(a)| \geq |z^{-1}(a)| - p\ell(z^{(0)}, z) \gtrsim \frac{p}{r} - \frac{p}{\log p} \gtrsim \frac{p}{r},$$

when p is large enough. Therefore, for all $a \in [r]$, we have

$$\begin{aligned} \|\hat{\mathbf{x}}_a - \mathbf{X}_a^s\|^2 &= \frac{\sum_{i \in z^{-1}(a) \cap (z^{(0)})^{-1}(a)} \left\| \mathbf{X}_{i:}^s - \hat{\mathbf{x}}_{z^{(0)}(i)} \right\|^2}{|z^{-1}(a) \cap (z^{(0)})^{-1}(a)|} \\ &\lesssim \frac{r}{p} \left(\sum_{i \in [p]} \|\mathbf{X}_{i:}^s - \hat{\mathbf{X}}_{i:}^s\|^2 + \sum_{i \in [p]} \|\hat{\mathbf{X}}_{i:}^s - \hat{\mathbf{x}}_{z^{(0)}(i)}\|^2 \right) \\ &\lesssim \frac{r^K}{p^K} \left(p^{K/2} r + pr^2 + r^K \right), \end{aligned} \quad (50)$$

where the last inequality follows from the inequality (48).

Finally, we obtain

$$\begin{aligned} L^{(0)} &= \frac{1}{p} \sum_{i \in [p]} \theta(i) \sum_{b \in [r]} \mathbb{1} \left\{ z^{(0)}(i) = b \right\} \|[\mathbf{S}_{z(i):}]^s - [\mathbf{S}_{b:}]^s\|^2 \\ &\lesssim \frac{1}{p} \sum_{i \in [p], z^{(0)}(i) \neq z(i)} \theta(i) \|\mathbf{X}_{i:}^s - \mathbf{X}_{z^{(0)}(i)}^s\|^2 \\ &\lesssim \frac{1}{p} \sum_{i \in [p], z^{(0)}(i) \neq z(i)} \theta(i) \left(\|\mathbf{X}_{i:}^s - \hat{\mathbf{x}}_{z^{(0)}(i)}\|^2 \right. \\ &\quad \left. + \|\hat{\mathbf{x}}_{z^{(0)}(i)} - \mathbf{X}_{z^{(0)}(i)}^s\|^2 \right) \\ &\leq \bar{C} \frac{r^K}{p^K} \left(p^{K/2} r + pr^2 + r^K \right), \\ &\leq \bar{C} \Delta_{\min}^2 \bar{C} r \log p \end{aligned}$$

where the first inequality follows from Lemma 1, the third inequality follows from inequalities (49) and (50), and the last inequality follows from the assumption that $\text{SNR} \geq \tilde{C} p^{-K/2} \log p$. \square

Proof of Proposition 1: Sub-algorithm 3 shares the same algorithm strategy as Sub-algorithm 1 but with a different estimation of the mean tensor, $\hat{\mathcal{X}}'$. Hence, the proof of Proposition 1 follows the same proof idea with the proof of Theorem 4. Replacing the estimation $\hat{\mathcal{X}}$ by $\hat{\mathcal{X}}'$ in the proof of Theorem 4, we have

$$\begin{aligned} \min_{\pi \in \Pi} \sum_{i: z^{(0)}(i) \neq \pi(z(i))} \theta(i)^2 \\ \lesssim \left(\sum_{i \in S} \|\mathbf{X}_{i:}\|^2 + \sum_{i \in S_0} \|\mathbf{X}_{i:}\|^2 \right) p^{-(K-1)} r^{K-1}. \end{aligned} \quad (51)$$

By inequalities (43) and (45), we have

$$\sum_{i \in S} \|\mathbf{X}_{i:}\|^2 \leq \left(\frac{16(1+\eta)}{c_0^2 \Delta_{\min}^2} + 2 \right) \|\hat{\mathcal{X}}' - \mathcal{X}\|_F^2, \quad (52)$$

$$\sum_{i \in S_0} \|\mathbf{X}_{i:}\|^2 \leq \|\hat{\mathcal{X}}' - \mathcal{X}\|_F^2. \quad (53)$$

Hence, it suffices to find the upper bound of the estimation error $\|\hat{\mathcal{X}}' - \mathcal{X}\|_F^2$ to complete our proof. Note that the matricization $\text{Mat}_{sq}(\mathcal{X}) \in \mathbb{R}^{p^{\lceil K/2 \rceil} \times p^{\lceil K/2 \rceil}}$ has $\text{rank}(\text{Mat}_{sq}(\mathcal{X})) \leq r^{\lceil K/2 \rceil}$, and Bernoulli random variables follow the sub-Gaussian distribution with bounded variance $\sigma^2 = 1/4$. Apply Lemma 9 to $\mathbf{Y} = \text{Mat}_{sq}(\mathcal{Y})$, $\mathbf{X} = \text{Mat}_{sq}(\mathcal{X})$, and $\hat{\mathbf{X}} = \text{Mat}_{sq}(\hat{\mathcal{X}}')$. Then, with probability tending to 1 as $p \rightarrow \infty$, we have

$$\|\hat{\mathcal{X}}' - \mathcal{X}\|_F^2 = \|\text{Mat}_{sq}(\hat{\mathcal{X}}') - \text{Mat}_{sq}(\mathcal{X})\|_F^2 \lesssim p^{\lceil K/2 \rceil}. \quad (54)$$

Combining the estimation error (54) with inequalities (52), (53), and (51), we obtain

$$\min_{\pi \in \Pi} \sum_{i: z^{(0)}(i) \neq \pi(z(i))} \theta(i)^2 \lesssim \frac{\sigma^2 r^{K-1}}{\Delta_{\min}^2 p^{K-1}} p^{\lceil K/2 \rceil}. \quad (55)$$

Replace the inequality (46) in the proof of Theorem 4 by inequality (55). With the the same procedures to obtain $\ell(\hat{z}^{(0)}, z)$ and $L(\hat{z}^{(0)}, z)$ for Theorem 4, we finish the proof of Proposition 1. \square

3) Useful Definitions and Lemmas for the Proof of Theorem 4: Change to unlisted bold text in a single line.

Lemma 4 (Basic Inequality): For any two nonzero vectors $\mathbf{v}_1, \mathbf{v}_2$ of same dimension, we have

$$\sin(\mathbf{v}_1, \mathbf{v}_2) \leq \|\mathbf{v}_1^s - \mathbf{v}_2^s\| \leq \frac{2 \|\mathbf{v}_1 - \mathbf{v}_2\|}{\max(\|\mathbf{v}_1\|, \|\mathbf{v}_2\|)}. \quad (56)$$

Proof of Lemma 4: For the first inequality, let $\alpha \in [0, \pi]$ denote the angle between \mathbf{v}_1 and \mathbf{v}_2 . We have

$$\|\mathbf{v}_1^s - \mathbf{v}_2^s\| = \sqrt{2(1 - \cos \alpha)} = 2 \sin \frac{\alpha}{2} \geq \sin \alpha, \quad (57)$$

where the equations follow from the properties of trigonometric function and the inequality follows from the fact the $\cos \frac{\alpha}{2} \leq 1$ and $\sin \alpha = 2 \sin \frac{\alpha}{2} \cos \frac{\alpha}{2} > 0$ for $\alpha \in [0, \pi]$.

For the second inequality, without loss of generality, we assume $\|\mathbf{v}_1\| \geq \|\mathbf{v}_2\|$. Then

$$\begin{aligned} \|\mathbf{v}_1^s - \mathbf{v}_2^s\| &= \left\| \frac{\mathbf{v}_1}{\|\mathbf{v}_1\|} - \frac{\mathbf{v}_2}{\|\mathbf{v}_1\|} + \frac{\mathbf{v}_2}{\|\mathbf{v}_1\|} - \frac{\mathbf{v}_2}{\|\mathbf{v}_2\|} \right\| \\ &\leq \frac{\|\mathbf{v}_1 - \mathbf{v}_2\|}{\|\mathbf{v}_1\|} + \frac{\|\mathbf{v}_2\| \|\mathbf{v}_1\| - \|\mathbf{v}_2\|}{\|\mathbf{v}_1\| \|\mathbf{v}_2\|} \\ &\leq \frac{2 \|\mathbf{v}_1 - \mathbf{v}_2\|}{\|\mathbf{v}_2\|}. \end{aligned} \quad (58)$$

Therefore, Lemma 4 is proved. \square

Definition 3 (Weighted Padding Vectors): For a vector $\mathbf{a} = [\mathbf{a}_i] \in \mathbb{R}^d$, we define the padding vector of \mathbf{a} with the weight collection $\mathbf{w} = \{\mathbf{w}_i : \mathbf{w}_i = [\mathbf{w}_{ik}] \in \mathbb{R}^{p_i}\}_{i=1}^d$ as

$$\text{Pad}_{\mathbf{w}}(\mathbf{a}) = [a_1 \circ \mathbf{w}_1, \dots, a_d \circ \mathbf{w}_d]^T, \quad (59)$$

where $a_i \circ \mathbf{w}_i = [a_i w_{i1}, \dots, a_i w_{ip_i}]^T$, for all $i \in [d]$. Here we also view $\text{Pad}_{\mathbf{w}}(\cdot) : \mathbb{R}^d \mapsto \mathbb{R}^{\sum_{i \in [d]} p_i}$ as an operator. We have the bounds of the weighted padding vector

$$\min_{i \in [d]} \|\mathbf{w}_i\|^2 \|\mathbf{a}\|^2 \leq \|\text{Pad}_{\mathbf{w}}(\mathbf{a})\|^2 \leq \max_{i \in [d]} \|\mathbf{w}_i\|^2 \|\mathbf{a}\|^2. \quad (60)$$

Further, we define the inverse weighted padding operator $\text{Pad}_{\mathbf{w}}^{-1} : \mathbb{R}^{\sum_{i \in [d]} p_i} \mapsto \mathbb{R}^d$ which satisfies

$$\text{Pad}_{\mathbf{w}}^{-1}(\text{Pad}_{\mathbf{w}}(\mathbf{a})) = \mathbf{a}. \quad (61)$$

Lemma 5 (Angle for Weighted Padding Vectors): Suppose that we have two non-zero vectors $\mathbf{a}, \mathbf{b} \in \mathbb{R}^d$. Given the weight collection \mathbf{w} , we have nonzero

$$\begin{aligned} \frac{\min_{i \in [d]} \|\mathbf{w}_i\|}{\max_{i \in [d]} \|\mathbf{w}_i\|} \sin(\mathbf{a}, \mathbf{b}) &\stackrel{*}{\leq} \sin(\text{Pad}_{\mathbf{w}}(\mathbf{a}), \text{Pad}_{\mathbf{w}}(\mathbf{b})) \\ &\stackrel{**}{\leq} \frac{\max_{i \in [d]} \|\mathbf{w}_i\|}{\min_{i \in [d]} \|\mathbf{w}_i\|} \sin(\mathbf{a}, \mathbf{b}). \quad (58) \end{aligned}$$

Proof of Lemma 5: We prove the two inequalities separately with similar ideas.

First, we prove the inequality $**$ in (58). Decomposing \mathbf{b} yields

$$\mathbf{b} = \cos(\mathbf{a}, \mathbf{b}) \frac{\|\mathbf{b}\|}{\|\mathbf{a}\|} \mathbf{a} + \sin(\mathbf{a}, \mathbf{b}) \frac{\|\mathbf{b}\|}{\|\mathbf{a}^\perp\|} \mathbf{a}^\perp,$$

where $\mathbf{a}^\perp \in \mathbb{R}^d$ is in the orthogonal complement space of \mathbf{a} . By the Definition 3, we have

$$\text{Pad}_{\mathbf{w}}(\mathbf{b}) = \cos(\mathbf{a}, \mathbf{b}) \frac{\|\mathbf{b}\|}{\|\mathbf{a}\|} \text{Pad}_{\mathbf{w}}(\mathbf{a}) + \sin(\mathbf{a}, \mathbf{b}) \frac{\|\mathbf{b}\|}{\|\mathbf{a}^\perp\|} \text{Pad}_{\mathbf{w}}(\mathbf{a}^\perp).$$

Note that $\text{Pad}_{\mathbf{w}}(\mathbf{a}^\perp)$ is not necessary equal to the orthogonal vector of $\text{Pad}_{\mathbf{w}}(\mathbf{a})$; i.e., $\text{Pad}_{\mathbf{w}}(\mathbf{a}^\perp) \neq (\text{Pad}_{\mathbf{w}}(\mathbf{a}))^\perp$. By the geometry property of trigonometric functions, we obtain

$$\begin{aligned} \sin(\text{Pad}_{\mathbf{w}}(\mathbf{a}), \text{Pad}_{\mathbf{w}}(\mathbf{b})) &\leq \frac{\|\mathbf{b}\| \|\text{Pad}_{\mathbf{w}}(\mathbf{a}^\perp)\|}{\|\mathbf{a}^\perp\| \|\text{Pad}_{\mathbf{w}}(\mathbf{b})\|} \sin(\mathbf{a}, \mathbf{b}) \\ &\leq \frac{\max_{i \in [d]} \|\mathbf{w}_i\|}{\min_{i \in [d]} \|\mathbf{w}_i\|} \sin(\mathbf{a}, \mathbf{b}), \end{aligned}$$

where the second inequality follows by applying the property (57) to vectors \mathbf{b} and \mathbf{a}^\perp .

Next, we prove inequality $*$ in (58). With the decomposition of $\text{Pad}_{\mathbf{w}}(\mathbf{b})$ and the inverse weighted padding operator, we have

$$\begin{aligned} \mathbf{b} &= \cos(\text{Pad}_{\mathbf{w}}(\mathbf{a}), \text{Pad}_{\mathbf{w}}(\mathbf{b})) \frac{\|\text{Pad}_{\mathbf{w}}(\mathbf{b})\|}{\|\text{Pad}_{\mathbf{w}}(\mathbf{a})\|} \mathbf{a} \\ &\quad + \sin(\text{Pad}_{\mathbf{w}}(\mathbf{a}), \text{Pad}_{\mathbf{w}}(\mathbf{b})) \frac{\|\text{Pad}_{\mathbf{w}}(\mathbf{b})\|}{\|(\text{Pad}_{\mathbf{w}}(\mathbf{a}))^\perp\|} \text{Pad}_{\mathbf{w}}^{-1}((\text{Pad}_{\mathbf{w}}(\mathbf{a}))^\perp). \end{aligned}$$

Therefore, we obtain

$$\begin{aligned} \sin(\mathbf{a}, \mathbf{b}) &\leq \frac{\|\text{Pad}_{\mathbf{w}}(\mathbf{b})\| \|\text{Pad}_{\mathbf{w}}^{-1}((\text{Pad}_{\mathbf{w}}(\mathbf{a}))^\perp)\|}{\|(\text{Pad}_{\mathbf{w}}(\mathbf{a}))^\perp\| \|\mathbf{b}\|} \sin(\text{Pad}_{\mathbf{w}}(\mathbf{a}), \text{Pad}_{\mathbf{w}}(\mathbf{b})) \\ &\leq \frac{\max_{i \in [d]} \|\mathbf{w}_i\|}{\min_{i \in [d]} \|\mathbf{w}_i\|} \sin(\text{Pad}_{\mathbf{w}}(\mathbf{a}), \text{Pad}_{\mathbf{w}}(\mathbf{b})), \end{aligned}$$

where the second inequality follows by applying the property (57) to vectors \mathbf{b} and $\text{Pad}_{\mathbf{w}}^{-1}((\text{Pad}_{\mathbf{w}}(\mathbf{a}))^\perp)$. \square

Lemma 6 (Singular Value of Weighted Membership Matrix): Under the parameter space (2) and assumption that $\min_{i \in [p]} \theta(i) \geq c$ for some constant $c > 0$, the singular values of ΘM are bounded as

$$\begin{aligned} \sqrt{p/r} &\lesssim \sqrt{\min_{a \in [r]} \|\theta_{z^{-1}(a)}\|^2} \leq \lambda_r(\Theta M) \\ &\leq \|\Theta M\|_\sigma \leq \sqrt{\max_{a \in [r]} \|\theta_{z^{-1}(a)}\|^2} \lesssim p/r. \end{aligned}$$

Proof of Lemma 6: Note that

$$(\Theta M)^T \Theta M = D,$$

with $D = \text{diag}(D_1, \dots, D_r)$ where $D_a = \|\theta_{z^{-1}(a)}\|^2, a \in [r]$. By the definition of singular values, we have

$$\sqrt{\min_{a \in [r]} \|\theta_{z^{-1}(a)}\|^2} \leq \lambda_r(\Theta M) \leq \|\Theta M\|_\sigma \leq \sqrt{\max_{a \in [r]} \|\theta_{z^{-1}(a)}\|^2}.$$

Since that $\min_{i \in [p]} \theta(i) \geq c$ by the constraints in parameter space, we have

$$\min_{a \in [r]} \|\theta_{z^{-1}(a)}\|^2 \geq c^2 \min_{a \in [r]} |z^{-1}(a)| \gtrsim \frac{p}{r},$$

where the last inequality follows from the constraint in parameter space (2). Finally, notice that

$$\sqrt{\max_{a \in [r]} \|\theta_{z^{-1}(a)}\|^2} \leq \max_{a \in [r]} \sqrt{\|\theta_{z^{-1}(a)}\|_1^2} \lesssim \frac{p}{r}.$$

Therefore, we complete the proof of Lemma 6. \square

Lemma 7 (Singular-Value Gap-Free Tensor Estimation Error Bound): Consider an order- K tensor $\mathcal{A} = \mathcal{X} + \mathcal{Z} \in \mathbb{R}^{p \times \dots \times p}$, where \mathcal{X} has Tucker rank (r, \dots, r) and \mathcal{Z} has independent sub-Gaussian entries with parameter σ^2 . Let $\hat{\mathcal{X}}$ denote the double projection estimated tensor in Step 2 of Sub-algorithm 1 in the main paper. Then with probability at least $1 - C \exp(-cp)$, we have

$$\|\hat{\mathcal{X}} - \mathcal{X}\|_F^2 \leq C \sigma^2 (p^{K/2} r + pr^2 + r^K),$$

where C, c are some positive constants.

Proof of Lemma 7: See [13, Proposition 1]. \square

Lemma 8 (Upper Bound of Misclustering Error): Let $z : [p] \mapsto [r]$ be a cluster assignment such that $|z^{-1}(a)| \asymp p/r$ for all $a \in [r]$ with $r \geq 2$. Let node i correspond to a vector $\mathbf{x}_i = \theta(i) \mathbf{v}_{z(i)} \in \mathbb{R}^d$, where $\{\mathbf{v}_a\}_{a=1}^r$ are the cluster centers and $\boldsymbol{\theta} = [\theta(i)] \in \mathbb{R}_+^p$ is the positive degree heterogeneity. Assume that $\boldsymbol{\theta}$ satisfies the balanced assumption (6) such that $\frac{\max_{a \in [r]} \|\theta_{z^{-1}(a)}\|^2}{\min_{a \in [r]} \|\theta_{z^{-1}(a)}\|^2} = 1 + o(1)$. Consider an arbitrary estimate \hat{z} with $\hat{\mathbf{x}}_i = \hat{\mathbf{v}}_{\hat{z}(i)}$ for all $i \in S$. Then, if

$$\min_{a \neq b \in [r]} \|\mathbf{v}_a - \mathbf{v}_b\| \geq 2c, \quad (59)$$

for some constant $c > 0$, we have

$$\min_{\pi \in \Pi} \sum_{i: \hat{z}(i) \neq \pi(z(i))} \theta(i)^2 \leq \sum_{i \in S_0} \theta(i)^2 + 4 \sum_{i \in S} \theta(i)^2,$$

where S_0 is defined in Step 4 of Sub-algorithm 1 and

$$S = \{i \in S_0^c : \|\hat{\mathbf{x}}_i - \mathbf{v}_{z(i)}\| \geq c\}.$$

Proof of Lemma 8: For each cluster $u \in [r]$, we use C_u to collect the subset of points for which the estimated and true positions $\hat{\mathbf{x}}_i, \mathbf{x}_i$ are within distance c . Specifically, define

$$C_u = \{i \in z^{-1}(u) \cap S_0^c : \|\hat{\mathbf{x}}_i - \mathbf{v}_{z(i)}\| < c\},$$

and divide $[r]$ into three groups based on C_u as

$$R_1 = \{u \in [r] : C_u = \emptyset\},$$

$$R_2 = \{u \in [r] : C_u \neq \emptyset, \text{ for all } i, j \in C_u, \hat{z}(i) = \hat{z}(j)\},$$

$$R_3 = \{u \in [r] : C_u \neq \emptyset, \text{ there exist } i, j \in C_u, \hat{z}(i) \neq \hat{z}(j)\}.$$

2056 Note that $\cup_{u \in [r]} C_u = S_0^c / S^c$ and $C_u \cap C_v = \emptyset$ for any $u \neq v$.
 2057 Suppose there exist $i \in C_u$ and $j \in C_v$ with $u \neq v \in [r]$ and
 2058 $\hat{z}(i) = \hat{z}(j)$. Then we have

2059 $\|\mathbf{v}_{z(i)} - \mathbf{v}_{z(j)}\| \leq \|\mathbf{v}_{z(i)} - \hat{\mathbf{x}}_i\| + \|\mathbf{v}_{z(j)} - \hat{\mathbf{x}}_j\| < 2c,$

2060 which contradicts to the assumption (59). Hence, the estimates
 2061 $\hat{z}(i) \neq \hat{z}(j)$ for the nodes $i \in C_u$ and $j \in C_v$ with $u \neq v$.
 2062 By the definition of R_2 , the nodes in $\cup_{u \in R_2} C_u$ have the same
 2063 assignment with z and \hat{z} . Then, we have

2064 $\min_{\pi \in \Pi} \sum_{i: \hat{z}(i) \neq \pi(z(i))} \theta(i)^2 \leq \sum_{i \in S_0} \theta(i)^2 + \sum_{i \in S} \theta(i)^2 + \sum_{i \in \cup_{u \in R_2} C_u} \theta(i)^2.$

2065 We only need to bound $\sum_{i \in \cup_{u \in R_3} C_u} \theta(i)^2$ to finish the proof.
 2066 Note that every C_u with $u \in R_3$ contains at least two
 2067 nodes assigned to different clusters by \hat{z} . Then, we have
 2068 $|R_2| + 2|R_3| \leq r$. Since $|R_1| + |R_2| + |R_3| = r$, we have
 2069 $|R_3| \leq |R_1|$. Hence, we obtain

2070
$$\begin{aligned} \sum_{i \in \cup_{u \in R_3} C_u} \theta(i)^2 &\leq |R_3| \max_{a \in [r]} \|\boldsymbol{\theta}_{z^{-1}(a)}\|^2 \\ 2071 &\leq |R_1| \max_{a \in [r]} \|\boldsymbol{\theta}_{z^{-1}(a)}\|^2 \\ 2072 &\leq \frac{\max_{a \in [r]} \|\boldsymbol{\theta}_{z^{-1}(a)}\|^2}{\min_{a \in [r]} \|\boldsymbol{\theta}_{z^{-1}(a)}\|^2} \sum_{i \in \cup_{u \in R_1} z^{-1}(u)} \theta(i)^2 \\ 2073 &\leq 2 \sum_{i \in S} \theta(i)^2, \end{aligned}$$

2074 where the last inequality holds by the balanced assumption on
 2075 $\boldsymbol{\theta}$ when p is large enough, and the fact that $\cup_{u \in R_1} z^{-1}(u) \subset S$.

2076 \square

2077 *Lemma 9 (Low-Rank Matrix Estimation):* Let $\mathbf{Y} = \mathbf{X} +$
 2078 $\mathbf{E} \in \mathbb{R}^{m \times n}$, where $n > m$ and \mathbf{E} contains independent mean-
 2079 zero sub-Gaussian entries with bounded variance σ^2 . Suppose
 2080 $\text{rank}(\mathbf{X}) = r$. Consider the least square estimator

2081
$$\hat{\mathbf{X}} = \arg \min_{\mathbf{X}' \in \mathbb{R}^{m \times n}, \text{rank}(\mathbf{X}') \leq r} \|\mathbf{X}' - \mathbf{Y}\|_F^2.$$

Change to unlisted bold text in a single line

2082 There exist positive constants C_1, C_2 such that

2083
$$\|\hat{\mathbf{X}} - \mathbf{X}\|_F^2 \leq C_1 \sigma^2 nr,$$

2084 with probability at least $1 - \exp(-C_2 nr)$.

2085 *Proof of Lemma 9:* Note that $\|\hat{\mathbf{X}} - \mathbf{Y}\|_F^2 \leq \|\mathbf{X} - \mathbf{Y}\|_F^2$ by
 2086 the definition of least square estimator.

2087 We have

2088
$$\begin{aligned} \|\hat{\mathbf{X}} - \mathbf{X}\|_F^2 \\ 2089 &\leq 2 \langle \hat{\mathbf{X}} - \mathbf{X}, \mathbf{Y} - \mathbf{X} \rangle \\ 2090 &\leq 2 \|\hat{\mathbf{X}} - \mathbf{X}\|_F \sup_{\mathbf{T} \in \mathbb{R}^{m \times n}, \text{rank}(\mathbf{T}) \leq 2r, \|\mathbf{T}\|_F=1} \langle \mathbf{T}, \mathbf{Y} - \mathbf{X} \rangle \end{aligned} \quad (60)$$

2091 with probability at least $1 - \exp(-C_2 nr)$, where the second
 2092 inequality follows by re-arrangement.

2093 Consider the SVD for matrix $\mathbf{T} = \mathbf{U} \Sigma \mathbf{V}^T$ with orthogonal
 2094 matrices $\mathbf{U} \in \mathbb{R}^{m \times 2r}, \mathbf{V} \in \mathbb{R}^{n \times 2r}$ and diagonal matrix $\Sigma \in$

$\mathbb{R}^{2r \times 2r}$. We have

2095
$$\begin{aligned} &\sup_{\mathbf{T} \in \mathbb{R}^{m \times n}, \text{rank}(\mathbf{T}) \leq 2r, \|\mathbf{T}\|_F=1} \langle \mathbf{T}, \mathbf{Y} - \mathbf{X} \rangle \\ 2096 &= \sup_{\mathbf{T} \in \mathbb{R}^{m \times n}, \text{rank}(\mathbf{T}) \leq 2r, \|\mathbf{T}\|_F=1} \langle \mathbf{U} \Sigma, \mathbf{EV} \rangle \\ 2097 &= \sup_{\mathbf{v} \in \mathbb{R}^{2nr}} \mathbf{v}^T \mathbf{e} \leq C \sigma \sqrt{nr}, \end{aligned} \quad (61)$$

2098 with probability $1 - \exp(-C_2 nr)$, where C, C_2 are two
 2099 positive constants, the vectorization $\mathbf{e} = \text{Vec}(\mathbf{EV}) \in \mathbb{R}^{2nr}$
 2100 has independent mean-zero sub-Gaussian entries with bounded
 2101 variance σ^2 due to the orthogonality of \mathbf{V} , and the last
 2102 inequality follows from [36, Theorem 1.19].

2103 Combining inequalities (60) and (61), we obtain the desired
 2104 conclusion. \square

G. Proofs of Theorem 2 (Achievability) and Theorem 5

2105 *Proof of Theorem 2 (Achievability) and Theorem 5:* The
 2106 proofs of Theorem 2 (Achievability) and Theorem 5 share the
 2107 same idea. We prove the contraction step by step. In each
 2108 step, we show the specific procedures for the algorithm loss
 2109 and address the MLE loss by stating the difference.

2110 We consider dTBM (1) with symmetric mean tensor, param-
 2111 eters $(z, \mathcal{S}, \boldsymbol{\theta})$, fixed $r \geq 1, K \geq 2$, and i.i.d. noise. Let
 2112 $(\hat{z}, \hat{\mathcal{S}}, \hat{\boldsymbol{\theta}})$ denote the MLE in (9), and $(z_k^{(0)}, \mathcal{S}^{(0)}, \boldsymbol{\theta}_k^{(0)})$ denote
 2113 parameters related to the initialization. For the case $r = 1$,
 2114 $\ell(z_k^{(t)}, z) = 0$ trivially for all $t \geq 0, k \in [k]$. Hence, we focus
 2115 on the proof of the first mode clustering $z_1^{(t+1)}$ with $r \geq 2$; the
 2116 extension for other modes can be obtained similarly. We drop
 2117 the subscript k in the matricizations $\boldsymbol{\Theta}, \mathbf{M}_k, \mathbf{S}_k, \mathbf{X}_k$ and in
 2118 estimates $z_k^{(0)}, z_k^{(t+1)}, z_k^{(t)}$ for ease of the notation. Without
 2119 loss of generality, we assume that the variance $\sigma = 1$, and that
 2120 the identity permutation minimizes the initial misclustering
 2121 error; i.e., $\pi^{(0)} = \arg \min_{\pi \in \Pi} \sum_{i \in [p]} \mathbb{1} \{z^{(0)}(i) \neq \pi \circ z(i)\}$
 2122 and $\pi^{(0)}(a) = a$ for all $a \in [r]$, and so for \hat{z} .

2123 *Step 1 (Notation and Conditions):* We first introduce addi-
 2124 tional notations and the necessary conditions used in the proof.
 2125 We will verify that the conditions hold in our context under
 2126 high probability in the last step of the proof.

2127 *1) Notation:* 1) Projection. We use \mathbf{I}_d to denote the identity
 2128 matrix of dimension d . For a vector $\mathbf{v} \in \mathbb{R}^d$, let $\text{Proj}(\mathbf{v}) \in$
 2129 $\mathbb{R}^{d \times d}$ denote the projection matrix to \mathbf{v} . Then, $\mathbf{I}_d - \text{Proj}(\mathbf{v})$
 2130 is the projection matrix to the orthogonal complement \mathbf{v}^\perp .

2131 2) We define normalized membership matrices

2132
$$\mathbf{W} = \mathbf{M} \left(\text{diag}(\mathbf{1}_p^T \mathbf{M}) \right)^{-1}, \mathbf{W}^{(t)} = \mathbf{M}^{(t)} \left(\text{diag}(\mathbf{1}_p^T \mathbf{M}^{(t)}) \right)^{-1},$$

2133 weighted normalized membership matrices

2134
$$\mathbf{P} = \boldsymbol{\Theta} \mathbf{M} (\text{diag}(\|\boldsymbol{\theta}_{z^{-1}(1)}\|^2, \dots, \|\boldsymbol{\theta}_{z^{-1}(r)}\|^2))^{-1},$$

2135
$$\hat{\mathbf{P}} = \hat{\boldsymbol{\Theta}} \hat{\mathbf{M}} (\text{diag}(\|\hat{\boldsymbol{\theta}}_{z^{-1}(1)}\|^2, \dots, \|\hat{\boldsymbol{\theta}}_{z^{-1}(r)}\|^2))^{-1},$$

2136 and the dual normalized and dual weighted normalized mem-
 2137 bership matrices

2138
$$\mathbf{V} = \mathbf{W}^{\otimes(K-1)}, \quad \mathbf{V}^{(t)} = \left(\mathbf{W}^{(t)} \right)^{\otimes(K-1)},$$

2139
$$\mathbf{Q} = \mathbf{P}^{\otimes K-1}, \quad \hat{\mathbf{Q}} = \hat{\mathbf{P}}^{\otimes K-1}.$$

2140 Also, let $\mathbf{B} = (\boldsymbol{\Theta} \mathbf{M})^{\otimes(K-1)}, \hat{\mathbf{B}} = (\hat{\boldsymbol{\Theta}} \hat{\mathbf{M}})^{\otimes(K-1)}$. By the
 2141 definition, we have $\mathbf{B}^T \mathbf{Q} = \hat{\mathbf{B}}^T \hat{\mathbf{Q}} = \mathbf{I}_{r^{K-1}}$.

3) We use $\mathcal{S}^{(t)}$ to denote the estimator of \mathcal{S} in the t -th iteration, $\hat{\mathcal{S}}$ for MLE, $\tilde{\mathcal{S}}$ to denote the oracle estimator of \mathcal{S} given true assignment z , and $\bar{\mathcal{S}}$ for weighted oracle estimator; i.e.,

$$\begin{aligned}\mathcal{S}^{(t)} &= \mathcal{Y} \times_1 (\mathbf{W}^{(t)})^T \times_2 \cdots \times_K (\mathbf{W}^{(t)})^T, \\ \tilde{\mathcal{S}} &= \mathcal{Y} \times_1 \mathbf{W}^T \times_2 \cdots \times_K \mathbf{W}^T, \\ \hat{\mathcal{S}} &= \mathcal{Y} \times_1 \hat{\mathbf{P}}^T \times_2 \cdots \times_K \hat{\mathbf{P}}^T, \\ \bar{\mathcal{S}} &= \mathcal{Y} \times_1 \mathbf{P}^T \times_2 \cdots \times_K \mathbf{P}^T.\end{aligned}$$

4) We define the matricizations of tensors

$$\begin{aligned}\mathbf{S} &= \text{Mat}(\mathcal{S}), \quad \mathbf{Y} = \text{Mat}(\mathcal{Y}), \quad \mathbf{X} = \text{Mat}(\mathcal{X}), \quad \mathbf{E} = \text{Mat}(\mathcal{E}), \\ \mathbf{S}^{(t)} &= \text{Mat}(\mathcal{S}^{(t)}), \quad \hat{\mathcal{S}} = \text{Mat}(\hat{\mathcal{S}}), \quad \tilde{\mathcal{S}} = \text{Mat}(\tilde{\mathcal{S}}), \quad \bar{\mathcal{S}} = \text{Mat}(\bar{\mathcal{S}}).\end{aligned}$$

5) We define the extended core tensor on $K - 1$ modes

$$\mathbf{A} = \mathbf{S}\mathbf{B}^T, \quad \bar{\mathbf{A}} = \bar{\mathbf{S}}\mathbf{B}^T, \quad \hat{\mathbf{A}} = \hat{\mathbf{S}}\hat{\mathbf{B}}^T.$$

By the assumption in parameter space (2), we have $\mathbf{A} = \mathbf{P}\mathbf{X} = \mathbf{W}\mathbf{X}$, $\hat{\mathbf{A}} = \hat{\mathbf{P}}\hat{\mathbf{X}} = \hat{\mathbf{W}}\hat{\mathbf{X}}$.

6) We define the angle-based misclustering loss in the t -th iteration and loss for MLE

$$\begin{aligned}L^{(t)} &= \frac{1}{p} \sum_{i \in [p]} \theta(i) \sum_{b \in [r]} \mathbb{1}\{z^{(t)}(i) = b\} \|[\mathbf{S}_{z(i)}]_s - [\mathbf{S}_b]_s\|^2, \\ L(\hat{z}) &= \frac{1}{p} \sum_{i \in [p]} \theta(i)^2 \sum_{b \in [r]} \mathbb{1}\{\hat{z}(i) = b\} \|[\mathbf{A}_{z(i)}]_s - [\mathbf{A}_b]_s\|^2.\end{aligned}$$

We also define the loss for oracle and weighted oracle estimators

$$\begin{aligned}\xi &= \frac{1}{p} \sum_{i \in [p]} \theta(i) \sum_{b \in [r]} \mathbb{1}\left\{ \langle \mathbf{E}_{i:} \mathbf{V}, [\tilde{\mathcal{S}}_{z(i)}]_s - [\tilde{\mathcal{S}}_b]_s \rangle \right. \\ &\quad \left. \leq -\frac{\theta(i)m}{4} \|[\mathbf{S}_{z(i)}]_s - [\mathbf{S}_b]_s\|^2 \right\} \\ &\quad \cdot \|[\mathbf{S}_{z(i)}]_s - [\mathbf{S}_b]_s\|^2, \\ \xi' &= \frac{1}{p} \sum_{i \in [p]} \theta(i)^2 \sum_{b \in [r]} \mathbb{1}\left\{ \langle \mathbf{E}_{i:} [\bar{\mathbf{A}}_{z(i)}]_s - [\bar{\mathbf{A}}_b]_s \rangle \right. \\ &\quad \left. \leq -\frac{m'}{4} \sqrt{\frac{p^{K-1}}{r^{K-1}}} \|[\mathbf{A}_{z(i)}]_s - [\mathbf{A}_b]_s\|_F^2 \right\} \\ &\quad \cdot \|[\mathbf{A}_{z(i)}]_s - [\mathbf{A}_b]_s\|^2.\end{aligned}$$

where m and m' are some positive universal constants.

Then we introduce the necessary conditions in Condition 1.

Step 2 (Misclustering Loss Decomposition): Next, we derive the upper bound of $L^{(t+1)}$ for $t = 0, 1, \dots, T - 1$. By Sub-algorithm 2, we update the assignment in t -th iteration via

$$z^{(t+1)}(i) = \arg \min_{a \in [r]} \|[\mathbf{Y}_{i:} \mathbf{V}^{(t)}]_s - [\mathbf{S}_a]_s\|^2,$$

following the facts that $\|\mathbf{a}^s - \mathbf{b}^s\|^2 = 1 - \cos(\mathbf{a}, \mathbf{b})$ for vectors \mathbf{a}, \mathbf{b} of same dimension and $\text{Mat}(\mathcal{Y}^d) = \mathbf{Y}\mathbf{V}^{(t)}$ where \mathcal{Y}^d is the reduced tensor defined in Step 8 of Sub-algorithm 2. Then the event $z^{(t+1)}(i) = b$ implies

$$\|[\mathbf{Y}_{i:} \mathbf{V}^{(t)}]_s - [\mathbf{S}_b]_s\|^2 \leq \|[\mathbf{Y}_{i:} \mathbf{V}^{(t)}]_s - [\mathbf{S}_{z(i)}]_s\|^2. \quad (67)$$

Note that the event (67) also holds for the degenerate entity i with $\|\mathbf{Y}_{i:} \mathbf{V}^{(t)}\| = 0$ due to the convention that $\mathbf{a}^s = \mathbf{0}$ if $\mathbf{a} = \mathbf{0}$. Arranging the terms in (67) yields the decomposition

$$\begin{aligned}2 \langle \mathbf{E}_{i:} \mathbf{V}, [\tilde{\mathcal{S}}_{z(i)}]_s - [\tilde{\mathcal{S}}_b]_s \rangle \\ \leq \|\mathbf{X}_{i:} \mathbf{V}^{(t)}\| \left(-\|[\mathbf{S}_{z(i)}]_s - [\mathbf{S}_b]_s\|^2 + G_{ib}^{(t)} + H_{ib}^{(t)} \right) + F_{ib}^{(t)},\end{aligned}$$

where

$$\begin{aligned}F_{ib}^{(t)} &= 2 \langle \mathbf{E}_{i:} \mathbf{V}^{(t)}, ([\tilde{\mathcal{S}}_{z(i)}]_s - [\mathbf{S}_{z(i)}]_s) - ([\tilde{\mathcal{S}}_b]_s - [\mathbf{S}_b]_s) \rangle \\ &\quad + 2 \langle \mathbf{E}_{i:} (\mathbf{V} - \mathbf{V}^{(t)}), [\tilde{\mathcal{S}}_{z(i)}]_s - [\tilde{\mathcal{S}}_b]_s \rangle,\end{aligned}$$

$$\begin{aligned}G_{ib}^{(t)} &= \left(\|[\mathbf{X}_{i:} \mathbf{V}^{(t)}]_s - [\mathbf{S}_{z(i)}]_s\|^2 \right. \\ &\quad \left. - \|[\mathbf{X}_{i:} \mathbf{V}^{(t)}]_s - [\mathbf{W}_{:z(i)}^T \mathbf{Y} \mathbf{V}^{(t)}]_s\|^2 \right)\end{aligned}$$

$$\begin{aligned}- \left(\|[\mathbf{X}_{i:} \mathbf{V}^{(t)}]_s - [\mathbf{S}_b]_s\|^2 \right. \\ &\quad \left. - \|[\mathbf{X}_{i:} \mathbf{V}^{(t)}]_s - [\mathbf{W}_{:b}^T \mathbf{Y} \mathbf{V}^{(t)}]_s\|^2 \right),\end{aligned}$$

$$\begin{aligned}H_{ib}^{(t)} &= \|[\mathbf{X}_{i:} \mathbf{V}^{(t)}]_s - [\mathbf{W}_{:z(i)}^T \mathbf{Y} \mathbf{V}^{(t)}]_s\|^2 - \|[\mathbf{X}_{i:} \mathbf{V}^{(t)}]_s \\ &\quad - [\mathbf{W}_{:b}^T \mathbf{Y} \mathbf{V}^{(t)}]_s\|^2 + \|[\mathbf{S}_{z(i)}]_s - [\mathbf{S}_b]_s\|^2.\end{aligned}$$

Therefore, the event $\mathbb{1}\{z^{(t+1)}(i) = b\}$ can be upper bounded as

$$\begin{aligned}\mathbb{1}\{z^{(t+1)}(i) = b\} \\ \leq \mathbb{1}\left\{ z^{(t+1)}(i) = b, \langle \mathbf{E}_{j:} \mathbf{V}, [\tilde{\mathcal{S}}_{z(i)}]_s - [\tilde{\mathcal{S}}_b]_s \rangle \right\}\end{aligned}$$

$$\begin{aligned}\leq -\frac{1}{4} \|\mathbf{X}_{i:} \mathbf{V}^{(t)}\| \|[\mathbf{S}_{z(i)}]_s - [\mathbf{S}_b]_s\|^2\end{aligned}$$

$$\begin{aligned}+ \mathbb{1}\left\{ z^{(t+1)}(i) = b, \frac{1}{2} \|[\mathbf{S}_{z(i)}]_s - [\mathbf{S}_b]_s\|^2 \right. \\ \left. \leq \|\mathbf{X}_{i:} \mathbf{V}^{(t)}\|^{-1} F_{ib}^{(t)} + G_{ib}^{(t)} + H_{ib}^{(t)} \right\}.\end{aligned}$$

Note that

$$\begin{aligned}\|\mathbf{X}_{i:} \mathbf{V}^{(t)}\| &= \theta(i) \|\mathbf{S}_{i:} (\Theta \mathbf{M})^{\otimes(K-1), T} \mathbf{W}^{(t), \otimes K-1}\| \\ &\geq \theta(i) \|\mathbf{S}_{z(i)}\| \lambda_r^{K-1} (\Theta \mathbf{M}) \lambda_r^{K-1} (\mathbf{W}^{(t)}) \\ &\geq \theta(i)m,\end{aligned}$$

where the first inequality follows from the property of eigenvalues; the last inequality follows from Lemma 6, Lemma 10, and assumption that $\min_{a \in [r]} \|\mathbf{S}_{z(a)}\| \geq c_3 > 0$; and $m > 0$ is a positive constant related to c_3 . Plugging the lower bound of $\|\mathbf{X}_{i:} \mathbf{V}^{(t)}\|$ (72) into the inequality (71) gives

$$\mathbb{1}\{z^{(t+1)}(i) = b\} \leq A_{ib} + B_{ib},$$

where

$$\begin{aligned} A_{ib} &= \mathbb{1} \left\{ z^{(t+1)}(i) = b, \langle \mathbf{E}_{i:} \mathbf{V}, [\tilde{\mathbf{S}}_{z(i):}]^s - [\tilde{\mathbf{S}}_{b:}]^s \rangle \right. \\ &\quad \left. \leq -\frac{\theta(i)m}{4} \|[\mathbf{S}_{z(i):}]^s - [\mathbf{S}_{b:}]^s\|^2 \right\}, \end{aligned}$$

$$\begin{aligned} B_{ib} &= \mathbb{1} \left\{ z^{(t+1)}(i) = b, \frac{1}{2} \|[\mathbf{S}_{z(i):}]^s - [\mathbf{S}_{b:}]^s\|^2 \right. \\ &\quad \left. \leq (\theta(i)m)^{-1} F_{ib}^{(t)} + G_{ib}^{(t)} + H_{ib}^{(t)} \right\}. \end{aligned}$$

Taking the weighted summation of (73) over $i \in [p]$ yields

$$L^{(t+1)} \leq \xi + \frac{1}{p} \sum_{i \in [p]} \sum_{b \in [r]/z(i)} \zeta_{ib}^{(t)},$$

where ξ is the oracle loss such that

$$\xi = \frac{1}{p} \sum_{i \in [p]} \theta(i) \sum_{b \in [r]/z(i)} A_{ib} \|[\mathbf{S}_{z(i):}]^s - [\mathbf{S}_{b:}]^s\|^2. \quad (74)$$

Similarly to ξ in (74), we define

$$\zeta_{ib}^{(t)} = \theta(i) B_{ib} \|[\mathbf{S}_{z(i):}]^s - [\mathbf{S}_{b:}]^s\|^2.$$

Change to unlisted plain text.

2) Now, we Show the Decomposition for MLE Loss: By the definition of Gaussian MLE, the estimator $\hat{\theta}$ satisfies $\hat{\theta}(i) = \langle \mathbf{Y}_{i:}, \hat{\mathbf{A}}_{z(i):} \rangle / \|\hat{\mathbf{A}}_{z(i):}\|_F^2$ for all $i \in [p]$. Hence, we have

$$\hat{z}(i) = \arg \min_{a \in [r_1]} \|[\mathbf{Y}_{i:}]^s - [\hat{\mathbf{A}}_{a:}]^s\|_F^2,$$

and the decomposition

$$L(\hat{z}) \leq \xi' + \frac{1}{p} \sum_{i \in [p]} \sum_{b \in [r]/z(i)} \zeta'_{ib},$$

Condition 1: (Intermediate Results) Let $\mathbb{O}_{p,r}$ denote the collection of all the p -by- r matrices with orthonormal columns. We have

$$\|\mathbf{EV}\|_\sigma \lesssim \sqrt{\frac{r^{K-1}}{p^{K-1}}} \left(p^{1/2} + r^{(K-1)/2} \right), \quad \|\mathbf{EV}\|_F \lesssim \sqrt{\frac{r^{2(K-1)}}{p^{K-2}}}, \quad \|\mathbf{W}_a^T \mathbf{EV}\| \lesssim \frac{r^K}{p^{K/2}}, \text{ for all } a \in [r], \quad (62)$$

$$\sup_{\mathbf{U}_k \in \mathbb{O}_{p,r}, k=2,\dots,K} \|\mathbf{E}(\mathbf{U}_2 \otimes \cdots \otimes \mathbf{U}_K)\|_\sigma \lesssim \left(\sqrt{r^{K-1}} + K\sqrt{pr} \right), \quad (63)$$

$$\sup_{\mathbf{U}_k \in \mathbb{O}_{p,r}, k=2,\dots,K} \|\mathbf{E}(\mathbf{U}_2 \otimes \cdots \otimes \mathbf{U}_K)\|_F \lesssim \left(\sqrt{pr^{K-1}} + K\sqrt{pr} \right), \quad (64)$$

$$\xi \leq \exp \left(-M \frac{\Delta_{\min}^2 p^{K-1}}{r^{K-1}} \right), \quad \xi' \lesssim \exp \left(-\frac{\Delta_{\min}^2 p^{K-1}}{r^{K-1}} \right), \quad (65)$$

$$L^{(t)} \leq \frac{\bar{C}}{\tilde{C}} \frac{\Delta_{\min}^2}{r \log p}, \quad \text{for } t = 0, 1, \dots, T, \quad L(\hat{z}) \leq \frac{\bar{C}}{\tilde{C}} \frac{\Delta_{\min}^2}{r \log p}, \quad (66)$$

where M is a positive universal constant in inequality (84), \bar{C}, \tilde{C} are positive universal constants in the proof of Theorem 4 and assumption $\text{SNR} \geq \tilde{C} p^{-K/2} \log p$, respectively. Further, inequality (62) holds by replacing \mathbf{V} to $\mathbf{V}^{(t)}, \mathbf{Q}, \hat{\mathbf{Q}}$ and $\mathbf{W}_{:a}$ to $\mathbf{W}_{:a}^{(t)}, \mathbf{P}_{:a}^T, \hat{\mathbf{P}}_{:a}^T$ when initialization condition (66) holds.

where $\zeta'_{ib} = \theta(i)^2 B'_{ib} \|[\mathbf{A}_{z(i):}]^s - [\mathbf{A}_{b:}]^s\|^2$ and

$$A'_{ib} = \mathbb{1} \left\{ \hat{z}(i) = b, \langle \mathbf{E}_{i:}, [\tilde{\mathbf{A}}_{z(i):}]^s - [\tilde{\mathbf{A}}_{b:}]^s \rangle \right. \quad (223) \\ \left. \leq -\frac{m'}{4} \sqrt{\frac{p^{K-1}}{r^{K-1}}} \|[\mathbf{A}_{z(i):}]^s - [\mathbf{A}_{b:}]^s\|_F^2 \right\}, \quad (222)$$

$$\begin{aligned} B'_{ib} &= \mathbb{1} \left\{ \hat{z}(i) = b, -\frac{1}{2} \|[\mathbf{A}_{z(i):}]^s - [\mathbf{A}_{b:}]^s\|_F^2 \right. \quad (223) \\ &\quad \left. \leq \sqrt{\frac{r^{K-1}}{(m')^2 p^{K-1}}} \hat{F}_{ib} + \hat{G}_{ib} + \hat{H}_{ib} \right\} \quad (224) \end{aligned}$$

with terms

$$\hat{F}_{ib} = 2 \left\langle \mathbf{E}_{i:}, ([\tilde{\mathbf{A}}_{z(i):}]^s - [\hat{\mathbf{A}}_{a:}]^s) - ([\tilde{\mathbf{A}}_{b:}]^s - [\hat{\mathbf{A}}_{b:}]^s) \right\rangle, \quad (223)$$

$$\hat{G}_{ib} = \left(\|\mathbf{X}_{i:}^s - [\hat{\mathbf{A}}_{z(i):}]^s\|_F^2 - \|\mathbf{X}_{i:}^s - [\mathbf{P}_{:z(i)}^T \mathbf{Y} \hat{\mathbf{Q}} \hat{\mathbf{B}}^T]^s\|_F^2 \right) \quad (223) \\ - \left(\|\mathbf{X}_{i:}^s - [\hat{\mathbf{A}}_{b:}]^s\|_F^2 - \|\mathbf{X}_{i:}^s - [\mathbf{P}_{:b}^T \mathbf{Y} \hat{\mathbf{Q}} \hat{\mathbf{B}}^T]^s\|_F^2 \right), \quad (223)$$

$$\begin{aligned} \hat{H}_{ib} &= \|\mathbf{X}_{i:}^s - [\mathbf{P}_{:z(i)}^T \mathbf{Y} \hat{\mathbf{Q}} \hat{\mathbf{B}}^T]^s\|_F^2 - \|\mathbf{X}_{i:}^s - [\mathbf{P}_{:b}^T \mathbf{Y} \hat{\mathbf{Q}} \hat{\mathbf{B}}^T]^s\|_F^2 \quad (223) \\ &\quad + \|\mathbf{A}_{z(i):}^s - \mathbf{A}_{b:}^s\|_F^2. \quad (224) \end{aligned}$$

Step 3 (Derivation of Contraction Inequality): In this step we derive the upper bound of ζ_{ib} and obtain the contraction inequality (24). We show the analysis in the following one-column box for a better presentation.

Step 4 (Verification of Condition 1): Last, we verify the Condition 1 under high probability to finish the proof. Note that the inequalities (62), (63), and (64) describe the property of the sub-Gaussian noise tensor \mathcal{E} , and the readers can find the proof directly in [13, Step 5, Proof of Theorem 2]. The initial condition (66) for MLE is satisfied by Lemma 13. Here, we include only the verification of inequalities (65) and (66) for algorithm estimators.

Now, we verify the oracle loss condition (65). Recall the definition of ξ ,

$$\xi = \frac{1}{p} \sum_{i \in [p]} \theta(i) \sum_{b \in [r]} \mathbb{1} \left\{ \langle \mathbf{E}_{i:} \mathbf{V}, [\tilde{\mathbf{S}}_{z(i):}]^s - [\tilde{\mathbf{S}}_{b:}]^s \rangle \right. \quad (225) \\ \left. \leq -\frac{m'}{4} \sqrt{\frac{p^{K-1}}{r^{K-1}}} \|[\mathbf{A}_{z(i):}]^s - [\mathbf{A}_{b:}]^s\|_F^2 \right\}$$

$$\begin{aligned} &\leq -\frac{\theta(i)m}{4} \left\| [\mathbf{S}_{z(i)}]_s^s - [\mathbf{S}_b]_s^s \right\|^2 \\ &\cdot \left\| [\mathbf{S}_{z(i)}]_s^s - [\mathbf{S}_b]_s^s \right\|^2. \end{aligned} \quad \leq P_1 + P_2 + P_3, \quad 2265$$

2258 Let $e_i = \mathbf{E}_i \mathbf{V}$ denote the aggregated noise vector for all $i \in [p]$, and e_i 's are independent zero-mean sub-Gaussian vector in $\mathbb{R}^{r^{K-1}}$. The entries in e_i are independent zero-mean sub-Gaussian variables with sub-Gaussian norm upper bounded by $m_1 \sqrt{r^{K-1}/p^{K-1}}$ with some positive constant m_1 . We have the probability inequality

$$\mathbb{P} \left(\left\langle e_i, [\tilde{\mathbf{S}}_{z(i)}]_s^s - [\tilde{\mathbf{S}}_b]_s^s \right\rangle \leq -\frac{\theta(i)m}{4} \left\| [\mathbf{S}_{z(i)}]_s^s - [\mathbf{S}_b]_s^s \right\|^2 \right)$$

where

$$P_1 = \mathbb{P} \left(\left\langle e_i, [\mathbf{S}_{z(i)}]_s^s - [\mathbf{S}_b]_s^s \right\rangle \leq -\frac{\theta(i)m}{8} \left\| [\mathbf{S}_{z(i)}]_s^s - [\mathbf{S}_b]_s^s \right\|^2 \right), \quad 2266$$

$$P_2 = \mathbb{P} \left(\left\langle e_i, [\tilde{\mathbf{S}}_{z(i)}]_s^s - [\mathbf{S}_{z(i)}]_s^s \right\rangle \leq -\frac{\theta(i)m}{16} \left\| [\mathbf{S}_{z(i)}]_s^s - [\mathbf{S}_b]_s^s \right\|^2 \right), \quad 2267$$

$$P_3 = \mathbb{P} \left(\left\langle e_i, [\mathbf{S}_b]_s^s - [\tilde{\mathbf{S}}_b]_s^s \right\rangle \leq -\frac{\theta(i)m}{16} \left\| [\mathbf{S}_{z(i)}]_s^s - [\mathbf{S}_b]_s^s \right\|^2 \right). \quad 2268$$

For P_1 , notice that the inner product $\left\langle e_j, \mathbf{S}_{z(j)}^s - \mathbf{S}_b^s \right\rangle$ is a sub-Gaussian variable with sub-Gaussian norm bounded by

Step 3: Choose the constant \tilde{C} in the condition $\text{SNR} \geq \tilde{C} p^{-K/2} \log p$ that satisfies the condition of Lemma 11, inequalities (98), and (102). Note that

$$\begin{aligned} \zeta_{ib}^{(t)} &= \theta(i) \left\| [\mathbf{S}_{z(i)}]_s^s - [\mathbf{S}_b]_s^s \right\|^2 \mathbb{1} \left\{ z^{(t+1)}(i) = b, \frac{1}{2} \left\| [\mathbf{S}_{z(i)}]_s^s - [\mathbf{S}_b]_s^s \right\|^2 \leq (\theta(i)m)^{-1} F_{ib}^{(t)} + G_{ib}^{(t)} + H_{ib}^{(t)} \right\} \\ &\leq \theta(i) \left\| [\mathbf{S}_{z(i)}]_s^s - [\mathbf{S}_b]_s^s \right\|^2 \mathbb{1} \left\{ z^{(t+1)}(i) = b, \frac{1}{4} \left\| [\mathbf{S}_{z(i)}]_s^s - [\mathbf{S}_b]_s^s \right\|^2 \leq (\theta(i)m)^{-1} F_{ib}^{(t)} + G_{ib}^{(t)} \right\} \\ &\leq 64 \mathbb{1} \left\{ z^{(t+1)}(i) = b \right\} \left(\frac{(F_{ib}^{(t)})^2}{cm^2 \left\| [\mathbf{S}_{z(i)}]_s^s - [\mathbf{S}_b]_s^s \right\|^2} + \frac{\theta(i)(G_{ib}^{(t)})^2}{\left\| [\mathbf{S}_{z(i)}]_s^s - [\mathbf{S}_b]_s^s \right\|^2} \right) \end{aligned} \quad 2270$$

where the first inequality follows from the inequality (89) in Lemma 11, and the last inequality follows from the assumption that $\min_{i \in [p]} \theta(i) \geq c > 0$. Following [13, Step 4, Proof of Theorem 2] and Lemma 11, we have

$$\frac{1}{p} \sum_{i \in [p]} \sum_{b \in [r]/z(i)} \mathbb{1} \left\{ z^{(t+1)}(i) = b \right\} \frac{(F_{ib}^{(t)})^2}{cm^2 \left\| [\mathbf{S}_{z(i)}]_s^s - [\mathbf{S}_b]_s^s \right\|^2} \leq \frac{C_0 \bar{C}}{cm^2 \tilde{C}^2} L^{(t)},$$

for a positive universal constant C and

$$\begin{aligned} \frac{1}{p} \sum_{i \in [p]} \sum_{b \in [r]/z(i)} \mathbb{1} \left\{ z^{(t+1)}(i) = b \right\} \frac{\theta(i)(G_{ib}^{(t)})^2}{\left\| [\mathbf{S}_{z(i)}]_s^s - [\mathbf{S}_b]_s^s \right\|^2} &\leq \frac{1}{512} \frac{1}{p} \sum_{i \in [p]} \theta(i) \sum_{b \in [r]/z(i)} \mathbb{1} \left\{ z^{(t+1)}(i) = b \right\} (\Delta_{\min}^2 + L^{(t)}) \\ &\leq \frac{1}{512} (L^{(t+1)} + L^{(t)}), \end{aligned}$$

where the last inequality follows from the definition of $L^{(t)}$ and the constraint of θ in parameter space (2). For \tilde{C} also satisfies

$$\frac{C_0 \bar{C}}{cm^2 \tilde{C}^2} \leq \frac{1}{512}, \quad 75$$

we have

$$\frac{1}{p} \sum_{i \in [p]} \sum_{b \in [r]/z(i)} \zeta_{ib}^{(t)} \leq \frac{1}{8} L^{(t+1)} + \frac{1}{4} L^{(t)}. \quad 76$$

Plugging the inequality (76) into the decomposition (74), we obtain the contraction inequality

$$L^{(t+1)} \leq \frac{3}{2} \xi + \frac{1}{2} L^{(t)}, \quad 77$$

where $\frac{1}{2}$ is the contraction parameter.

Therefore, with \tilde{C} satisfying inequalities (75), (98) and (102), we obtain the conclusion in Theorem 5 via inequality (77) combining the inequality (65) in Condition 1 and Lemma 2.

We also have the contraction inequality for MLE. Change to unlisted plain text.

Following the same derivation of (77) with the upper bound of $\hat{F}_{ib}, \hat{G}_{ib}, \hat{H}_{ib}$ in Lemma 12, we also have

$$L(\hat{z}) \leq \frac{3}{2} \xi' + \frac{1}{2} L(\hat{z}),$$

which indicates the conclusion $\ell(\hat{z}, z) \lesssim \Delta_{\min}^2 \exp \left(-\frac{p^{K-1}}{r^{K-1}} \Delta_{\min}^2 \right)$.

2272 $m_2 \sqrt{r^{K-1}/p^{K-1}} \|S_{z(i)}^s - S_{b:}^s\|$ with some positive constant
2273 m_2 . Then, by Chernoff bound, we have

$$2274 P_1 \lesssim \exp \left(-\frac{p^{K-1}}{r^{K-1}} \|S_{z(j)}^s - [S_{b:}]^s\|^2 \right). \quad (78)$$

2275 For P_2 and P_3 , we only need to derive the upper bound
2276 of P_2 due to the symmetry. By the law of total probability,
2277 we have

$$2278 P_2 \leq P_{21} + P_{22}, \quad (79)$$

2279 where with some positive constant $t > 0$,

$$\begin{aligned} 2280 P_{21} &= \mathbb{P} \left(t \leq \|[\tilde{S}_{z(i)}]^s - [S_{z(i)}]^s\| \right), \\ 2281 P_{22} &= \mathbb{P} \left(\left\langle e_i, [\tilde{S}_{z(i)}]^s - [S_{z(i)}]^s \right\rangle \leq -\frac{\theta(i)m}{16} \right. \\ 2282 &\quad \cdot \|S_{z(i)}^s - [S_{b:}]^s\|^2 \left| \|[\tilde{S}_{z(i)}]^s - [S_{z(i)}]^s\| < t \right. \right). \end{aligned}$$

2283 For P_{21} , note that the term $\mathbf{W}_{:z(i)}^T \mathbf{EV} =$
2284 $\frac{\sum_{j \neq i, j \in [p]} \mathbf{1}\{z(j)=z(i)\} e_j}{\sum_{j \in [p]} \mathbf{1}\{z(j)=z(i)\}}$ is a sub-Gaussian vector with
2285 sub-Gaussian norm bounded by $m_3 \sqrt{r^K/p^K}$ with some
2286 positive constant m_3 . This implies

$$\begin{aligned} 2287 P_{21} &\leq \mathbb{P} \left(t \|S_{z(i)}\| \leq \|\tilde{S}_{z(i)} - S_{z(i)}\| \right) \\ 2288 &\leq \mathbb{P} \left(c_3 t \leq \|\mathbf{W}_{:z(i)}^T \mathbf{EV}\| \right) \\ 2289 &\lesssim \exp \left(-\frac{p^K t^2}{r^K} \right), \end{aligned} \quad (80)$$

2290 where the first inequality follows from the basic inequality in
2291 Lemma 4, the second inequality follows from the assumption
2292 that $\min_{a \in [r]} \|S_{z(i)}\| \geq c_3 > 0$ in (2), and the last inequality
2293 follows from the Bernstein inequality.

2294 For P_{22} , the inner product $\left\langle e_i, [\tilde{S}_{z(i)}]^s - [S_{z(i)}]^s \right\rangle$ is
2295 also a sub-Gaussian variable with sub-Gaussian norm
2296 $m_4 \sqrt{r^{K-1}/p^{K-1}} t$, conditioned on $\|[\tilde{S}_{z(i)}]^s - [S_{z(i)}]^s\| < t$
2297 with some positive constant m_4 . Then, by Chernoff bound,
2298 we have

$$2299 P_{22} \lesssim \exp \left(-\frac{p^{K-1}}{r^{K-1} t^2} \|S_{z(j)}^s - [S_{b:}]^s\|^4 \right). \quad (81)$$

2300 We take $t = \|S_{z(i)}^s - [S_{b:}]^s\|$ in P_{21} and P_{22} , and plug
2301 the inequalities (80) and (81) into to the upper bound for
2302 P_2 in (79). We obtain that

$$2303 P_2 \lesssim \exp \left(-\frac{p^{K-1}}{r^{K-1}} \|S_{z(i)}^s - [S_{b:}]^s\|^2 \right). \quad (82)$$

2304 Combining the upper bounds (78) and (82) gives

$$\begin{aligned} 2305 \mathbb{P} \left(\left\langle e_i, [\tilde{S}_{z(i)}]^s - [S_{b:}]^s \right\rangle \leq -\frac{\theta(i)m}{4} \|S_{z(i)}^s - [S_{b:}]^s\|^2 \right) \\ 2306 \lesssim \exp \left(-\frac{p^{K-1}}{r^{K-1}} \|S_{z(i)}^s - [S_{b:}]^s\|^2 \right). \end{aligned} \quad (83)$$

Hence, we have

$$\begin{aligned} 2308 \mathbb{E} \xi &= \frac{1}{p} \sum_{i \in [p]} \theta(i) \sum_{b \in [r]} \mathbb{P} \left\{ \left\langle \mathbf{E}_i \mathbf{V}, [\tilde{S}_{z(i)}]^s - [S_{b:}]^s \right\rangle \right. \\ 2309 &\quad \left. \leq -\frac{\theta(i)m}{4} \|S_{z(i)}^s - [S_{b:}]^s\|^2 \right\} \|S_{z(i)}^s - [S_{b:}]^s\|^2 \\ 2310 &\lesssim \frac{1}{p} \sum_{i \in [p]} \theta(i) \max_{i \in [p], b \in [r]} \|S_{z(i)}^s - [S_{b:}]^s\|^2 \\ 2311 &\quad \cdot \exp \left(-\frac{p^{K-1}}{r^{K-1}} \|S_{z(i)}^s - [S_{b:}]^s\|^2 \right) \\ 2312 &\leq \exp \left(-M \frac{p^{K-1}}{r^{K-1}} \Delta_{\min}^2 \right), \end{aligned} \quad (84)$$

2313 where M is a positive constant, the first inequality follows
2314 from the constraint that $\sum_{i \in [p]} \theta(i) = p$, and the last inequality
2315 follows from (83).

2316 By Markov's inequality, we have

$$\begin{aligned} 2317 \mathbb{P} \left(\xi \lesssim \mathbb{E} \xi + \exp \left(-\frac{Mp^{K-1}}{2r^{K-1}} \Delta_{\min}^2 \right) \right) \\ 2318 \geq 1 - C \exp \left(-\frac{Mp^{K-1}}{2r^{K-1}} \Delta_{\min}^2 \right), \end{aligned}$$

2319 and thus the condition (65) holds with probability at least $1 - C \exp \left(-\frac{Mp^{K-1}}{2r^{K-1}} \Delta_{\min}^2 \right)$ for some constant $C > 0$.
2320

2321 3) **The Initialization Condition for MLE Also Holds:** For
2322 ξ' , notice that $\langle \mathbf{E}_i, \mathbf{A}_{a:}^s - \mathbf{A}_{b:}^s \rangle$ is a sub-Gaussian vector with
2323 variance bounded by $\|\mathbf{A}_{a:}^s - \mathbf{A}_{b:}^s\|^2$ and

$$\begin{aligned} 2324 \mathbb{P} \left(t \leq \|[\bar{\mathbf{A}}_{a:}]^s - \mathbf{A}_{a:}^s\| \right) &\leq (t \leq \|[\mathbf{P}_{:a}^T \mathbf{YQ}]^s - [\mathbf{P}_{:a}^T \mathbf{XQ}]^s\|) \\ 2325 &\leq \mathbb{P} \left(t \min_{a \in [r]} \|\mathbf{S}_{a:}\| \leq \|\mathbf{P}_{:a}^T \mathbf{EQ}\| \right) \\ 2326 &\lesssim \exp \left(-\frac{p^K t^2}{r^K} \right), \end{aligned}$$

2327 where the first inequality follows from the property in later
2328 inequality (105). We also have

$$2329 \xi' \lesssim \left(-\frac{p^{K-1}}{r^{K-1}} \Delta_{\min}^2 \right).$$

2330 Finally, we verify the bounded loss condition (66) for algorithm
2331 estimator by induction. With output $z^{(0)}$ from Sub-
2332 algorithm 2 and the assumption $\text{SNR} \geq \tilde{C} p^{-K/2} \log p$, by Theorem 4, we have
2333

$$2334 L^{(0)} \leq \frac{\tilde{C} \Delta_{\min}^2}{\tilde{C} r \log p}, \quad \text{when } p \text{ is large enough.}$$

2335 Therefore, the condition (66) holds for $t = 0$. Assume that
2336 the condition (66) also holds for all $t \leq t_0$. Then, by the
2337 decomposition (77), we have

$$\begin{aligned} 2338 L^{(t_0+1)} &\leq \frac{3}{2} \xi + \frac{1}{2} L^{(t_0)} \\ 2339 &\leq \exp \left(-M \frac{p^{K-1}}{r^{K-1}} \Delta_{\min}^2 \right) + \frac{\Delta_{\min}^2}{r \log p} \\ 2340 &\leq \frac{\tilde{C}}{\tilde{C} r \log p} \Delta_{\min}^2, \end{aligned}$$

where the second inequality follows from the condition (65) and the last inequality follows from the assumption that $\Delta_{\min}^2 \gtrsim p^{-K/2} \log p$. Thus, the condition (66) holds for t_0+1 , and the condition (66) is proved by induction. \square

4) Useful Lemmas for the Proof of Theorem 5: Change to unlisted bold text in a single line.

Lemma 10 (Singular-Value Property of Membership Matrices): Under the setup of Theorem 5, suppose that the condition (66) holds. Then, for all $a \in [r]$, we have $|(\mathbf{z}^{(t)})^{-1}(a)| \asymp p/r$. Moreover, we have

$$\lambda_r(\mathbf{M}) \asymp \|\mathbf{M}\|_\sigma \asymp \sqrt{p/r}, \quad \lambda_r(\mathbf{W}) \asymp \|\mathbf{W}\|_\sigma \asymp \sqrt{r/p}, \\ \lambda_r(\mathbf{P}) \asymp \|\mathbf{P}\|_\sigma \asymp \min_{a \in [r]} \|\boldsymbol{\theta}_{\mathbf{z}^{-1}(a)}\|^{-1} \lesssim \sqrt{r/p}. \quad (85)$$

The inequalities (85) also hold by replacing \mathbf{M} and \mathbf{W} to $\mathbf{M}^{(t)}$ and $\mathbf{W}^{(t)}$ respectively. Further, we have

$$\lambda_r(\mathbf{W}\mathbf{W}^T) \asymp \|\mathbf{W}\mathbf{W}^T\|_\sigma \asymp r/p, \quad (86)$$

which is also true for $\mathbf{W}^{(t)}\mathbf{W}^{(t),T}$.

Proof of Lemma 10: The proof for the inequality (85) for \mathbf{M}, \mathbf{W} can be found in [13, Proof of Lemma 4]. The inequalities for \mathbf{P} follows the same derivation with balance assumption on $\boldsymbol{\theta}$ and $\min_{i \in [p]} \theta(i) \geq c$.

For inequality (86), note that for all $k \in [r]$,

$$\begin{aligned} \lambda_k(\mathbf{W}\mathbf{W}^T) &= \sqrt{\text{eigen}_k(\mathbf{W}\mathbf{W}^T\mathbf{W}\mathbf{W}^T)} \\ &\asymp \sqrt{\frac{r}{p} \text{eigen}_k(\mathbf{W}\mathbf{W}^T)} \\ &= \sqrt{\frac{r}{p} \lambda_k^2(\mathbf{W})} \asymp \frac{r}{p}, \end{aligned}$$

where $\text{eigen}_k(\mathbf{A})$ denotes the k -th largest eigenvalue of the square matrix \mathbf{A} , the first inequality follows the fact that $\mathbf{W}^T\mathbf{W}$ is a diagonal matrix with elements of order r/p , and the second equation follows from the definition of singular value. \square

Lemma 11 (Upper Bound for $F_{ib}^{(t)}, G_{ib}^{(t)}$ and $H_{ib}^{(t)}$): Under the Condition 1 and the setup of Theorem 5 with fixed $r \geq 2$, assume the constant \tilde{C} in the condition $\text{SNR} \geq \tilde{C}p^{-K/2} \log p$ is large enough to satisfy the inequalities (98) and (102). As $p \rightarrow \infty$, we have

$$\begin{aligned} \max_{i \in [p]} \max_{b \neq z(i)} \frac{(F_{ib}^{(t)})^2}{\|[\mathbf{S}_{z(i)}]_s - [\mathbf{S}_{b:}]_s\|^2} \\ \lesssim \frac{rL^{(t)}}{\Delta_{\min}^2} \|\mathbf{E}_{i:}\mathbf{V}\|^2 + \left(1 + \frac{rL^{(t)}}{\Delta_{\min}^2}\right) \|\mathbf{E}_{i:}(\mathbf{V} - \mathbf{V}^{(t)})\|^2, \quad (87) \end{aligned}$$

$$\max_{i \in [p]} \max_{b \neq z(i)} \frac{(G_{ib}^{(t)})^2}{\|[\mathbf{S}_{z(i)}]_s - [\mathbf{S}_{b:}]_s\|^2} \leq \frac{1}{512} (\Delta_{\min}^2 + L^{(t)}), \quad (88)$$

$$\max_{i \in [p]} \max_{b \neq z(i)} \frac{|H_{ib}^{(t)}|}{\|[\mathbf{S}_{z(i)}]_s - [\mathbf{S}_{b:}]_s\|^2} \leq \frac{1}{4}. \quad (89)$$

Similarly, when the $\text{SNR} \geq \tilde{C}p^{-(K-1)} \log p$ with a large constant \tilde{C} , we have

$$\max_{i \in [p]} \max_{b \neq z(i)} \frac{(\hat{F}_{ib})^2}{\|[\mathbf{A}_{z(i)}]_s - [\mathbf{A}_{b:}]_s\|^2} \lesssim p^{K-1} \frac{rL(\hat{z})}{\Delta_{\min}^2} \quad (2380)$$

$$\max_{i \in [p]} \max_{b \neq z(i)} \frac{(\hat{G}_{ib})^2}{\|[\mathbf{A}_{z(i)}]_s - [\mathbf{A}_{b:}]_s\|^2} \leq \frac{1}{512} (\Delta_{\min}^2 + L(\hat{z})), \quad (2381)$$

$$\max_{i \in [p]} \max_{b \neq z(i)} \frac{|\hat{H}_{ib}|}{\|[\mathbf{A}_{z(i)}]_s - [\mathbf{A}_{b:}]_s\|^2} \leq \frac{1}{4}. \quad (2382)$$

Proof of Lemma 11: We prove the the first three inequalities in Lemma 11 separately.

1) Upper bound for $F_{ib}^{(t)}$, i.e., inequality (87). Recall the definition of $F_{ib}^{(t)}$,

$$\begin{aligned} F_{ib}^{(t)} &= 2 \left\langle \mathbf{E}_{i:}\mathbf{V}^{(t)}, \left([\tilde{\mathbf{S}}_{z(i)}]_s - [\mathbf{S}_{z(i)}]_s^{(t)}\right) - \left([\tilde{\mathbf{S}}_{b:}]_s - [\mathbf{S}_{b:}]_s^{(t)}\right) \right\rangle \\ &\quad + 2 \left\langle \mathbf{E}_{i:}(\mathbf{V} - \mathbf{V}^{(t)}), [\tilde{\mathbf{S}}_{z(i)}]_s - [\tilde{\mathbf{S}}_{b:}]_s \right\rangle. \end{aligned} \quad (2387)$$

By Cauchy-Schwartz inequality, we have

$$\begin{aligned} &\left(F_{ib}^{(t)}\right)^2 \\ &\leq 8 \left(\left\langle \mathbf{E}_{i:}\mathbf{V}^{(t)}, \left([\tilde{\mathbf{S}}_{z(i)}]_s - [\mathbf{S}_{z(i)}]_s^{(t)}\right) - \left([\tilde{\mathbf{S}}_{b:}]_s - [\mathbf{S}_{b:}]_s^{(t)}\right) \right\rangle \right)^2 \\ &\quad + 8 \left(\left\langle \mathbf{E}_{i:}(\mathbf{V} - \mathbf{V}^{(t)}), [\tilde{\mathbf{S}}_{z(i)}]_s - [\tilde{\mathbf{S}}_{b:}]_s \right\rangle \right)^2 \\ &\leq 8 \left(\|\mathbf{E}_{i:}\mathbf{V}\|^2 + \|\mathbf{E}_{i:}(\mathbf{V} - \mathbf{V}^{(t)})\|^2 \right) \max_{a \in [r]} \|[\tilde{\mathbf{S}}_{a:}]_s - [\mathbf{S}_{a:}]_s^{(t)}\| \\ &\quad + \|\mathbf{E}_{i:}(\mathbf{V} - \mathbf{V}^{(t)})\|^2 \|[\tilde{\mathbf{S}}_{z(i)}]_s - [\tilde{\mathbf{S}}_{b:}]_s\|. \end{aligned} \quad (90)$$

Note that for all $a \in [r]$,

$$\begin{aligned} \|[\tilde{\mathbf{S}}_{a:}]_s - [\mathbf{S}_{a:}]_s^{(t)}\|^2 &= \|[\mathbf{W}_{:a}^T \mathbf{Y} \mathbf{V}]_s - [\mathbf{W}_{:a}^{(t),T} \mathbf{Y} \mathbf{V}^{(t)}]_s\|^2 \\ &\leq 2 \|[\mathbf{W}_{:a}^T \mathbf{Y} \mathbf{V}]_s - [\mathbf{W}_{:a}^{(t),T} \mathbf{Y} \mathbf{V}]_s\|^2 \\ &\quad + 2 \|[\mathbf{W}_{:a}^{(t),T} \mathbf{Y} \mathbf{V}]_s - [\mathbf{W}_{:a}^{(t),T} \mathbf{Y} \mathbf{V}^{(t)}]_s\|^2 \\ &\lesssim \frac{r^2(L^{(t)})^2}{\Delta_{\min}^2} + \frac{rr^{2K} + pr^{K+2}}{p^K} \frac{L^{(t)}}{\Delta_{\min}^2} \\ &\lesssim rL^{(t)} + \frac{rr^{2K} + pr^{K+2}}{p^K} \frac{L^{(t)}}{\Delta_{\min}^2} \\ &\lesssim rL^{(t)}, \end{aligned} \quad (91)$$

where the second inequality follows from the inequalities (108) and (109) in Lemma 12, the third inequality follows from the condition (66) in Condition 1, and the last inequality follows from the assumption that $\Delta_{\min}^2 \geq \tilde{C}p^{-K/2} \log p$.

Note that

$$\begin{aligned} &\|[\tilde{\mathbf{S}}_{z(i)}]_s - [\tilde{\mathbf{S}}_{b:}]_s\|^2 \\ &= \|[\tilde{\mathbf{S}}_{z(i)}]_s - [\mathbf{S}_{z(i)}]_s + [\mathbf{S}_{z(i)}]_s - [\mathbf{S}_{b:}]_s + [\mathbf{S}_{b:}]_s - [\tilde{\mathbf{S}}_{b:}]_s\|^2 \\ &\lesssim \|[\mathbf{S}_{z(i)}]_s - [\mathbf{S}_{b:}]_s\|^2 + \max_{a \in [r]} \|[\mathbf{S}_{a:}]_s - [\tilde{\mathbf{S}}_{a:}]_s\|^2 \\ &\lesssim \|[\mathbf{S}_{z(i)}]_s - [\mathbf{S}_{b:}]_s\|^2 + \max_{a \in [r]} \frac{1}{\|\mathbf{S}_{a:}\|^2} \|\mathbf{W}_{:a}^T \mathbf{E} \mathbf{V}\|^2 \\ &\lesssim \|[\mathbf{S}_{z(i)}]_s - [\mathbf{S}_{b:}]_s\|^2, \end{aligned} \quad (92)$$

where the second inequality follows from Lemma 4, and the last inequality follows from the assumptions on $\|S_{a:}\|$ in the parameter space (2), the inequality (62) in Condition 1 and the assumption $\Delta_{\min}^2 \gtrsim p^{-K/2} \log p$.

Therefore, we finish the proof of inequality (87) by plugging the inequalities (91) and (92) into the upper bound (90).

2) Upper bound for $G_{ib}^{(t)}$, i.e., inequality (88). By definition of $G_{ib}^{(t)}$, we rearrange terms and obtain

$$\begin{aligned} G_{ib}^{(t)} &= \left(\|[\mathbf{X}_{i:} \mathbf{V}^{(t)}]^s - [\mathbf{S}_{z(i):}^{(t)}]^s\|^2 \right. \\ &\quad \left. - \|[\mathbf{X}_{i:} \mathbf{V}^{(t)}]^s - [\mathbf{W}_{:z(i)}^T \mathbf{Y} \mathbf{V}^{(t)}]^s\|^2 \right) \\ &\quad - \left(\|[\mathbf{X}_{i:} \mathbf{V}^{(t)}]^s - [\mathbf{S}_{b:}^{(t)}]^s\|^2 \right. \\ &\quad \left. - \|[\mathbf{X}_{i:} \mathbf{V}^{(t)}]^s - [\mathbf{W}_{:b}^T \mathbf{Y} \mathbf{V}^{(t)}]^s\|^2 \right) \\ &= 2 \left\langle [\mathbf{X}_{i:} \mathbf{V}^{(t)}]^s, \left([\mathbf{W}_{:z(i)}^T \mathbf{Y} \mathbf{V}^{(t)}]^s - [\mathbf{S}_{z(i):}^{(t)}]^s \right) \right. \\ &\quad \left. - \left([\mathbf{W}_{:b}^T \mathbf{Y} \mathbf{V}^{(t)}]^s - [\mathbf{S}_{b:}^{(t)}]^s \right) \right\rangle \\ &= G_1 + G_2 - G_3, \end{aligned} \tag{93}$$

where

$$\begin{aligned} G_1 &= \|[\mathbf{W}_{:z(i)}^T \mathbf{Y} \mathbf{V}^{(t)}]^s - [\mathbf{S}_{z(i):}^{(t)}]^s\|^2 - \|[\mathbf{W}_{:b}^T \mathbf{Y} \mathbf{V}^{(t)}]^s - [\mathbf{S}_{b:}^{(t)}]^s\|^2, \\ G_2 &= 2 \left\langle [\mathbf{X}_{i:} \mathbf{V}^{(t)}]^s - [\mathbf{W}_{:z(i)}^T \mathbf{Y} \mathbf{V}^{(t)}]^s, [\mathbf{W}_{:z(i)}^T \mathbf{Y} \mathbf{V}^{(t)}]^s - [\mathbf{S}_{z(i):}^{(t)}]^s \right\rangle, \\ G_3 &= 2 \left\langle [\mathbf{X}_{i:} \mathbf{V}^{(t)}]^s - [\mathbf{W}_{:b}^T \mathbf{Y} \mathbf{V}^{(t)}]^s, [\mathbf{W}_{:b}^T \mathbf{Y} \mathbf{V}^{(t)}]^s - [\mathbf{S}_{b:}^{(t)}]^s \right\rangle. \end{aligned}$$

For G_1 , we have

$$\begin{aligned} |G_1|^2 &\leq \left| \|[\mathbf{W}_{:z(i)}^T \mathbf{Y} \mathbf{V}^{(t)}]^s - [\mathbf{S}_{z(i):}^{(t)}]^s\|^2 \right. \\ &\quad \left. - \|[\mathbf{W}_{:b}^T \mathbf{Y} \mathbf{V}^{(t)}]^s - [\mathbf{S}_{b:}^{(t)}]^s\|^2 \right|^2 \\ &\leq \max_{a \in [r]} \|[\mathbf{W}_{:a}^T \mathbf{Y} \mathbf{V}^{(t)}]^s - [\mathbf{W}_{:a}^{(t),T} \mathbf{Y} \mathbf{V}^{(t)}]^s\|^4 \\ &\leq C^4 \frac{r^4}{\Delta_{\min}^4} (L^{(t)})^4 + \frac{r^2 r^{4K} + p^2 r^{2K+4}}{p^{2K}} \frac{(L^{(t)})^2}{\Delta_{\min}^4} \\ &\leq C^4 \frac{\bar{C}}{\tilde{C}^3} \left(\Delta_{\min}^4 + \Delta_{\min}^2 L^{(t)} \right), \end{aligned} \tag{94}$$

where the third inequality follows from the inequality (110) in Lemma 12 and the last inequality follows from the assumption that $\Delta_{\min}^2 \geq \tilde{C} p^{-K/2} \log p$ and inequality (66) in Condition 1.

For G_2 , noticing that $[\mathbf{X}_{i:} \mathbf{V}^{(t)}]^s = [\mathbf{W}_{:z(i)}^T \mathbf{X} \mathbf{V}^{(t)}]^s$, we have

$$\begin{aligned} |G_2|^2 &\leq 2 \|[\mathbf{X}_{i:} \mathbf{V}^{(t)}]^s - [\mathbf{W}_{:z(i)}^T \mathbf{Y} \mathbf{V}^{(t)}]^s\|^2 \\ &\quad \cdot \|[\mathbf{W}_{:z(i)}^T \mathbf{Y} \mathbf{V}^{(t)}]^s - [\mathbf{S}_{z(i):}^{(t)}]^s\|^2 \\ &\leq \frac{2}{\|\mathbf{W}_{:z(i)}^T \mathbf{X} \mathbf{V}^{(t)}\|^2} \max_{a \in [r]} \|\mathbf{W}_{:a}^T \mathbf{E} \mathbf{V}^{(t)}\|^2 \\ &\quad \cdot \max_{a \in [r]} \|[\mathbf{W}_{:a}^T \mathbf{Y} \mathbf{V}^{(t)}]^s - [\mathbf{W}_{:a}^{(t),T} \mathbf{Y} \mathbf{V}^{(t)}]^s\|^2 \end{aligned}$$

$$\begin{aligned} &\leq C' \frac{r^{2K-1} + K p r^{K+1}}{p^K} \\ &\quad \cdot \left(\frac{r^2}{\Delta_{\min}^2} (L^{(t)})^2 + \frac{r r^{2K} + p r^{K+2}}{p^K} \frac{L^{(t)}}{\Delta_{\min}^2} \right) \\ &\leq \frac{C'}{\tilde{C}^2} \Delta_{\min}^2 L^{(t)}, \end{aligned} \tag{95}$$

where C' is a positive universal constant, the second inequality follows from Lemma 4, the third inequality follows from the inequality (63) in Condition 1, the inequalities (110) and (129) in the proof of Lemma 12, and the last inequality follows from the assumption $\Delta_{\min}^2 \geq \tilde{C} p^{-K/2} \log p$ and inequality (66) in Condition 1.

For G_3 , note that by triangle inequality

$$\begin{aligned} &\|[\mathbf{X}_{i:} \mathbf{V}^{(t)}]^s - [\mathbf{W}_{:b}^T \mathbf{X} \mathbf{V}^{(t)}]^s\|^2 \\ &\leq \|[\mathbf{S}_{z(i):}^s - \mathbf{S}_{b:}^s\|^2 + 2 \max_{a \in [r]} \|[\mathbf{W}_{:a}^T \mathbf{X} \mathbf{V}^{(t)}]^s - [\mathbf{W}_{:a}^T \mathbf{X} \mathbf{V}^{(t)}]^s\|^2 \\ &\leq \|[\mathbf{S}_{z(i):}^s - \mathbf{S}_{b:}^s\|^2 + C \frac{r^2 (L^{(t)})^2}{\Delta_{\min}^2}], \end{aligned} \tag{96}$$

where the last inequality follows from the inequality (128) in the proof of Lemma 12 and C is a positive constant. Then we have

$$\begin{aligned} |G_3|^2 &\leq 2 \|[\mathbf{X}_{i:} \mathbf{V}^{(t)}]^s - [\mathbf{W}_{:b}^T \mathbf{Y} \mathbf{V}^{(t)}]^s\|^2 \\ &\quad \cdot \max_{a \in [r]} \|[\mathbf{W}_{:a}^T \mathbf{Y} \mathbf{V}^{(t)}]^s - [\mathbf{W}_{:a}^{(t),T} \mathbf{Y} \mathbf{V}^{(t)}]^s\|^2 \\ &\leq 2 \left(\|[\mathbf{X}_{i:} \mathbf{V}^{(t)}]^s - [\mathbf{W}_{:b}^T \mathbf{X} \mathbf{V}^{(t)}]^s\|^2 \right. \\ &\quad \left. + \|[\mathbf{W}_{:b}^T \mathbf{Y} \mathbf{V}^{(t)}]^s - [\mathbf{W}_{:b}^T \mathbf{X} \mathbf{V}^{(t)}]^s\|^2 \right) \\ &\quad \cdot \max_{a \in [r]} \|[\mathbf{W}_{:a}^T \mathbf{Y} \mathbf{V}^{(t)}]^s - [\mathbf{W}_{:a}^{(t),T} \mathbf{Y} \mathbf{V}^{(t)}]^s\|^2 \\ &\leq C^2 \left(\|[\mathbf{S}_{z(i):}^s - \mathbf{S}_{b:}^s\|^2 + C \frac{r^2 (L^{(t)})^2}{\Delta_{\min}^2}] \right) \\ &\quad \cdot \left(\frac{r^2 (L^{(t)})^2}{\Delta_{\min}^2} + \frac{r r^{2K} + p r^{K+2}}{p^K} \frac{L^{(t)}}{\Delta_{\min}^2} \right) + \frac{C'}{\tilde{C}^2} \Delta_{\min}^2 L^{(t)} \\ &\leq \frac{C^2 \bar{C}^2}{\tilde{C}} \|[\mathbf{S}_{z(i):}^s - \mathbf{S}_{b:}^s\|^2 (\Delta_{\min}^2 + L^{(t)}) \\ &\quad + \frac{C^3 C' \bar{C}^2}{\tilde{C}^2} (\Delta_{\min}^4 + \Delta_{\min}^2 L^{(t)})], \end{aligned} \tag{97}$$

where the third inequality follows from the same procedure to derive (94) and (95), and the last inequality follows from the assumption $\Delta_{\min}^2 \geq \tilde{C} p^{-K/2} \log p$ and inequality (66) in Condition 1.

Choose the \tilde{C} such that

$$3 \left(C^4 \frac{\bar{C}}{\tilde{C}^3} + \frac{C'}{\tilde{C}^2} + \frac{C^2 \bar{C}^2}{\tilde{C}} + \frac{C^3 C' \bar{C}^2}{\tilde{C}^2} \right) \leq \frac{1}{512}. \tag{98}$$

Then, we finish the proof of inequality (88) by plugging the inequalities (94), (95), and (97) into the upper bound (93).

3) Upper bound for $H_{ib}^{(t)}$, i.e., the inequality (89). By definition of H_{ib} , we rearrange terms and obtain

$$\begin{aligned} H_{ib} &= \|[\mathbf{X}_{i:}\mathbf{V}^{(t)}]^s - [\mathbf{W}_{:z(i)}^T \mathbf{Y} \mathbf{V}^{(t)}]^s\|^2 \\ &\quad - \|[\mathbf{X}_{i:}\mathbf{V}^{(t)}]^s - [\mathbf{W}_{:b}^T \mathbf{Y} \mathbf{V}^{(t)}]^s\|^2 + \|[\mathbf{S}_{z(i):}]^s - [\mathbf{S}_{b:}]^s\|^2 \\ &= \|[\mathbf{X}_{i:}\mathbf{V}^{(t)}]^s - [\mathbf{W}_{:z(i)}^T \mathbf{Y} \mathbf{V}^{(t)}]^s\|^2 \\ &\quad + \left(\|[\mathbf{S}_{z(i):}]^s - [\mathbf{S}_{b:}]^s\|^2 - \|[\mathbf{X}_{i:}\mathbf{V}^{(t)}]^s - [\mathbf{W}_{:b}^T \mathbf{Y} \mathbf{V}^{(t)}]^s\|^2 \right) \\ &\quad - \left(\|[\mathbf{X}_{i:}\mathbf{V}^{(t)}]^s - [\mathbf{W}_{:b}^T \mathbf{Y} \mathbf{V}^{(t)}]^s\| \right. \\ &\quad \quad \left. - \|[\mathbf{X}_{i:}\mathbf{V}^{(t)}]^s - [\mathbf{W}_{:b}^T \mathbf{X} \mathbf{V}^{(t)}]^s\| \right) \\ &= H_1 + H_2 + H_3, \end{aligned}$$

where

$$\begin{aligned} H_1 &= \|[\mathbf{X}_{i:}\mathbf{V}^{(t)}]^s - [\mathbf{W}_{:z(i)}^T \mathbf{Y} \mathbf{V}^{(t)}]^s\|^2 \\ &\quad - \|[\mathbf{W}_{:b}^T \mathbf{X} \mathbf{V}^{(t)}]^s - [\mathbf{W}_{:b}^T \mathbf{Y} \mathbf{V}^{(t)}]^s\|^2, \\ H_2 &= \|[\mathbf{S}_{z(i):}]^s - [\mathbf{S}_{b:}]^s\|^2 - \|[\mathbf{X}_{i:}\mathbf{V}^{(t)}]^s - [\mathbf{W}_{:b}^T \mathbf{X} \mathbf{V}^{(t)}]^s\|^2, \\ H_3 &= 2 \left\langle [\mathbf{X}_{i:}\mathbf{V}^{(t)}]^s - [\mathbf{W}_{:b}^T \mathbf{X} \mathbf{V}^{(t)}]^s, \right. \\ &\quad \quad \left. [\mathbf{W}_{:b}^T \mathbf{Y} \mathbf{V}^{(t)}]^s - [\mathbf{W}_{:b}^T \mathbf{X} \mathbf{V}^{(t)}]^s \right\rangle. \end{aligned}$$

For H_1 , we have

$$\begin{aligned} |H_1| &\leq \frac{4 \max_{a \in [r]} \|\mathbf{W}_{:a}^T \mathbf{E} \mathbf{V}^{(t)}\|^2}{\|\mathbf{W}_{:z(i)}^T \mathbf{X} \mathbf{V}^{(t)}\|^2} \\ &\leq \frac{r^{2K-1} + K p r^{K+1}}{p^K} \\ &\leq \tilde{C}^{-2} \|[\mathbf{S}_{z(i):}]^s - [\mathbf{S}_{b:}]^s\|^2, \end{aligned} \quad (99)$$

following the derivation of G_2 in inequality (95) and the assumption that $\Delta_{\min}^2 \geq \tilde{C} p^{-K/2} \log p$.

For H_2 , by the inequality (96), we have

$$\begin{aligned} |H_2| &\lesssim 2 \max_{a \in [r]} \|[\mathbf{W}_{:a}^T \mathbf{X} \mathbf{V}^{(t)}]^s - [\mathbf{W}_{:a}^T \mathbf{X} \mathbf{V}^{(t)}]^s\|^2 \\ &\lesssim \frac{r^2 (L^{(t)})^2}{\Delta_{\min}^2} \\ &\leq C \frac{\bar{C}^2}{\tilde{C}^2} \|[\mathbf{S}_{z(i):}]^s - [\mathbf{S}_{a:}]^s\|^2, \end{aligned} \quad (100)$$

where the last inequality follows from the condition (66) in Condition 1.

For H_3 , by Cauchy-Schwartz inequality, we have

$$\begin{aligned} |H_3| &\lesssim \|[\mathbf{X}_{i:}\mathbf{V}^{(t)}]^s - [\mathbf{W}_{:b}^T \mathbf{X} \mathbf{V}^{(t)}]^s\| |H_1|^{1/2} \\ &\leq 2 \tilde{C}^{-1} \|[\mathbf{S}_{z(i):}]^s - [\mathbf{S}_{a:}]^s\|^2, \end{aligned} \quad (101)$$

following the inequalities (96) and (99).

Choose \tilde{C} such that

$$\tilde{C}^{-2} + C \frac{\bar{C}^2}{\tilde{C}^2} + \tilde{C}^{-1} \leq \frac{1}{4}. \quad (102)$$

Therefore, we finish the proof of inequality (89) combining inequalities (99), (100), and (101).

5) Next, we Show the Upper Bounds for \hat{F}_{ib} , \hat{G}_{ib} and \hat{H}_{ib} :
By Lemma 1, we have

$$\|\mathbf{S}_{a:}^s - \mathbf{S}_{b:}^s\| = (1 + o(1)) \|\mathbf{A}_{a:}^s - \mathbf{A}_{b:}^s\|. \quad (2516)$$

Also, notice that the matrix product of \mathbf{B}^T corresponds to the padding operation in Lemma 5, and the padding weights are balanced such that $\|\mathbf{v} \mathbf{B}\| = (1 + o(1)) \max_a \|\theta_{z^{-1}(a)}\|^{(K-1)/2} \|\mathbf{v}\|$ for all $\mathbf{v} \in \mathbb{R}^{r(K-1)}$. For two vectors $\mathbf{v}_1, \mathbf{v}_2 \in \mathbb{R}^{r(K-1)}$, we have

$$\|\mathbf{v}_1^s - \mathbf{v}_2^s\| = (1 + o(1)) \|[\mathbf{v}_1 \mathbf{B}^T]^s - [\mathbf{v}_2 \mathbf{B}^T]^s\|. \quad (103) \quad (2522)$$

The equation (103) also holds for $\hat{\mathbf{B}}^T$.

Note that for all $i \in [p]$ we have

$$\begin{aligned} \|\mathbf{A}_{i:} \hat{\mathbf{Q}}\| &= \|\mathbf{S}_{z(i):} \mathbf{B}^T \hat{\mathbf{Q}}\| \\ &= \|\mathbf{S}_{z(i):} \hat{\mathbf{D}}^{\otimes(K-1)}\| \\ &= (1 + o(1)) \|\mathbf{S}_{z(i):}\| \\ &= (1 + o(1)) \max_a \|\theta_{z^{-1}(a)}\|^{-(K-1)/2} \|\mathbf{A}_{i:}\|, \end{aligned} \quad (104) \quad (2525-2528)$$

where the third inequality follows from the singular property of MLE confusion matrix (135) and the last inequality follows from the fact that $\mathbf{A}_{i:} = \mathbf{S}_{z(i):} \mathbf{B}^T$ and Lemma 10. Above equation indicates that $\mathbf{A}_{i:}$ is the span space of the singular values as $p \rightarrow \infty$. Also, notice that the row space of $\mathbf{P}_{:a}^T \mathbf{Y} \hat{\mathbf{Q}} \hat{\mathbf{B}}^T$ is equal to the column space of $\hat{\mathbf{Q}}$, and $\mathbf{A}_{i:} \neq \mathbf{P}_{:a}^T \mathbf{Y} \hat{\mathbf{Q}} \hat{\mathbf{B}}^T$ in noisy case.

Hence, for all $a \in [r]$, we have

$$\begin{aligned} &\|[\mathbf{X}_i \hat{\mathbf{Q}}]^s - [\mathbf{P}_{:a}^T \mathbf{Y} \hat{\mathbf{Q}}]^s\| \\ &= \left\| \frac{\mathbf{A}_{z(i):} \hat{\mathbf{Q}}}{\|\mathbf{A}_{z(i):} \hat{\mathbf{Q}}\|} - \frac{\mathbf{P}_{:a}^T \mathbf{Y} \hat{\mathbf{Q}}}{\|\mathbf{P}_{:a}^T \mathbf{Y} \hat{\mathbf{Q}}\|} \right\| \\ &= (1 + o(1)) \left\| \frac{\mathbf{A}_{z(i):}}{\|\mathbf{A}_{z(i):}\|} - \frac{\mathbf{P}_{:a}^T \mathbf{Y} \hat{\mathbf{Q}} \hat{\mathbf{B}}^T}{\|\mathbf{P}_{:a}^T \mathbf{Y} \hat{\mathbf{Q}} \hat{\mathbf{B}}^T\|} \right\| \\ &= (1 + o(1)) \|[\mathbf{X}_i]^s - [\mathbf{P}_{:a}^T \mathbf{Y} \hat{\mathbf{Q}} \hat{\mathbf{B}}^T]^s\| \end{aligned} \quad (105) \quad (2537-2540)$$

where the second equation follows from (104), $\|\mathbf{P}_{:a}^T \mathbf{Y} \hat{\mathbf{Q}} \hat{\mathbf{B}}^T\| = (1 + o(1)) \max_a \|\theta_{z^{-1}(a)}\|^{(K-1)/2} \|\mathbf{P}_{:a}^T \mathbf{Y} \hat{\mathbf{Q}}\|$, and singular property of $\hat{\mathbf{B}}^T$. Similar result holds after replacing $\mathbf{P}_{:a}^T \mathbf{Y} \hat{\mathbf{Q}}$ by $\mathbf{P}_{:a}^T \mathbf{Y} \mathbf{Q}$ or $\mathbf{P}_{:a}^T \mathbf{Y} \hat{\mathbf{Q}}$.

We are now ready to show the upper bounds for \hat{F}_{ib} , \hat{G}_{ib} and \hat{H}_{ib} .

For \hat{F}_{ib} , we have

$$\begin{aligned} (\hat{F}_{ib})^2 &\leq \|\mathbf{E}_{i:}\|^2 \|[\bar{\mathbf{A}}_{a:}]^s - [\hat{\mathbf{A}}_{a:}]^s\|^2 \\ &\leq \|\mathbf{E}_{i:}\|^2 \left[\|[\bar{\mathbf{S}}_{a:} \mathbf{B}^T]^s - [\bar{\mathbf{S}}_{a:} \hat{\mathbf{B}}^T]^s\| \right. \\ &\quad \quad \left. + \|[\bar{\mathbf{S}}_{a:} \hat{\mathbf{B}}^T]^s - [\hat{\mathbf{S}}_{a:} \hat{\mathbf{B}}^T]^s\| \right]^2 \\ &\lesssim \|\mathbf{E}_{i:}\|^2 \left[\|[\bar{\mathbf{S}}_{a:} \mathbf{B}^T \hat{\mathbf{Q}}]^s - [\bar{\mathbf{S}}_{a:}]^s\| + \|[\bar{\mathbf{S}}_{a:}]^s - [\hat{\mathbf{S}}_{a:}]^s\| \right]^2. \end{aligned} \quad (2549-2552)$$

Following similar derivations in inequalities (91), (92), and the upper bound for J_1 in the proof of Lemma 12, respectively,

we have

$$\|[\bar{S}_{a:}]^s - [\hat{S}_{a:}]^s\| \lesssim rL(\hat{z}), \quad \|[\bar{S}_{a:}]^s - [\bar{S}_{b:}]^s\| \lesssim \|S_{a:}^s - S_{b:}^s\|^2,$$

and

$$\|[\bar{S}_{a:}\mathbf{B}^T\hat{\mathbf{Q}}]^s - [\bar{S}_{a:}]^s\| \lesssim L(\hat{z}).$$

We then obtain the upper bound for \hat{F}_{ib} by noticing that $\|\mathbf{E}_i\|^2 \lesssim p^{K-1}$.

For \hat{G}_{ib} and \hat{H}_{ib} , by the property (105), we have

$$(1 + o(1))\hat{G}_{ib}$$

$$\begin{aligned} &= \left(\|[\mathbf{X}_{i:}\hat{\mathbf{Q}}]^s - [\hat{S}_{a:}]^s\|_F^2 - \|[\mathbf{X}_{i:}\hat{\mathbf{Q}}]^s - [\mathbf{P}_{:a}^T\mathbf{Y}\hat{\mathbf{Q}}]^s\|_F^2 \right) \\ &\quad - \left(\|[\mathbf{X}_{i:}\hat{\mathbf{Q}}]^s - [\hat{S}_{b:}]^s\|_F^2 - \|[\mathbf{X}_{i:}\hat{\mathbf{Q}}]^s - [\mathbf{P}_{:b}^T\mathbf{Y}\hat{\mathbf{Q}}]^s\|_F^2 \right), \\ &(1 + o(1))\hat{H}_{ib} \\ &= \|[\mathbf{X}_{i:}\hat{\mathbf{Q}}]^s - [\mathbf{P}_{:a}^T\mathbf{Y}\hat{\mathbf{Q}}]^s\|_F^2 - \|[\mathbf{X}_{i:}\hat{\mathbf{Q}}]^s - [\mathbf{P}_{:b}^T\mathbf{Y}\hat{\mathbf{Q}}]^s\|_F^2 \\ &\quad + \|\mathbf{A}_{a:}^s - \mathbf{A}_{b:}^s\|_F^2. \end{aligned}$$

We obtain the upper bounds following the proof for inequalities (88) and (89). \square

Lemma 12 (Relationship Between Misclustering Loss and Intermediate Parameters): Under the Condition 1 and the setup of Theorem 5 with fixed $r \geq 2$, as $p \rightarrow \infty$, we have

$$\|\mathbf{V} - \mathbf{V}^{(t)}\|_\sigma \lesssim \sqrt{\frac{r^{K-1}}{p^{K-1}} \frac{r}{\Delta_{\min}^2} L^{(t)}}, \quad (106)$$

$$\|\mathbf{E}(\mathbf{V} - \mathbf{V}^{(t)})\|_\sigma \lesssim \sqrt{\frac{r^{K-1}(pr^{K-1} + pr)}{p^{K-1}} \frac{r}{\Delta_{\min}^2} L^{(t)}}, \quad (107)$$

$$\begin{aligned} &\max_{b \in [r]} \|[\mathbf{W}_{:b}^T\mathbf{Y}\mathbf{V}]^s - [\mathbf{W}_{:b}^{(t),T}\mathbf{Y}\mathbf{V}]^s\| \\ &\leq C \left(\frac{rL^{(t)}}{\Delta_{\min}} + \sqrt{\frac{r^{2K} + pr^{K+1}}{p^K} \frac{\sqrt{L^{(t)}}}{\Delta_{\min}}} \right), \quad (108) \end{aligned}$$

$$\begin{aligned} &\max_{b \in [r]} \|[\mathbf{W}_{:b}^{(t),T}\mathbf{Y}\mathbf{V}]^s - [\mathbf{W}_{:b}^{(t),T}\mathbf{Y}\mathbf{V}^{(t)}]^s\| \\ &\leq C \left(\sqrt{\frac{rr^{2K} + pr^{K+2}}{p^K} \frac{\sqrt{L^{(t)}}}{\Delta_{\min}}} + \frac{rL^{(t)}}{\Delta_{\min}} \right), \quad (109) \end{aligned}$$

$$\begin{aligned} &\max_{b \in [r]} \|[\mathbf{W}_{:b}^T\mathbf{Y}\mathbf{V}^{(t)}]^s - [\mathbf{W}_{:b}^{(t),T}\mathbf{Y}\mathbf{V}^{(t)}]^s\| \\ &\leq C \left(\frac{rL^{(t)}}{\Delta_{\min}} + \sqrt{\frac{rr^{2K} + pr^{K+2}}{p^K} \frac{\sqrt{L^{(t)}}}{\Delta_{\min}}} \right), \quad (110) \end{aligned}$$

for some positive universal constant C . In addition, the inequality (109) also holds by replacing $\mathbf{W}_{:b}^{(t)}$ to $\mathbf{W}_{:b}$. Further, the above inequalities holds after replacing \mathbf{W} to \mathbf{P} , \mathbf{V} to \mathbf{Q} , and $L^{(t)}$ to $L(\hat{z})$.

Proof of Lemma 12: We follow and use several intermediate conclusions in [13, Proof of Lemma 5]. We prove each inequality separately.

1) Inequality (106). By [13, Proof of Lemma 5], we have

$$\|\mathbf{V} - \mathbf{V}^{(t)}\|_\sigma \lesssim \sqrt{\frac{r^{K-1}}{p^{K-1}} r\ell^{(t)}}.$$

Then, we complete the proof of inequality (106) by applying Lemma 2 to the above inequality.

2) Inequality (107). By [13, Proof of Lemma 5], we have

$$\|\mathbf{E}(\mathbf{V} - \mathbf{V}^{(t)})\|_\sigma \lesssim \sqrt{\frac{r^{K-1}(pr^{K-1} + pr)}{p^{K-1}} r\ell^{(t)}}. \quad (2594)$$

Also, we complete the proof of inequality (106) by applying Lemma 2 to the above inequality.

3) Inequality (108). We upper bound the desired quantity by triangle inequality,

$$\|[\mathbf{W}_{:b}^T\mathbf{Y}\mathbf{V}]^s - [\mathbf{W}_{:b}^{(t),T}\mathbf{Y}\mathbf{V}]^s\| \leq I_1 + I_2 + I_3, \quad (2599)$$

where

$$I_1 = \left\| \frac{\mathbf{W}_{:b}^T\mathbf{Y}\mathbf{V}}{\|\mathbf{W}_{:b}^T\mathbf{X}\mathbf{V}\|} - \frac{\mathbf{W}_{:b}^{(t),T}\mathbf{Y}\mathbf{V}}{\|\mathbf{W}_{:b}^{(t),T}\mathbf{X}\mathbf{V}\|} \right\|, \quad (2601)$$

$$I_2 = \left\| \left(\frac{1}{\|\mathbf{W}_{:b}^T\mathbf{Y}\mathbf{V}\|} - \frac{1}{\|\mathbf{W}_{:b}^{(t),T}\mathbf{X}\mathbf{V}\|} \right) \mathbf{W}_{:b}^T\mathbf{Y}\mathbf{V} \right\|, \quad (2602)$$

$$I_3 = \left\| \left(\frac{1}{\|\mathbf{W}_{:b}^{(t),T}\mathbf{Y}\mathbf{V}\|} - \frac{1}{\|\mathbf{W}_{:b}^{(t),T}\mathbf{X}\mathbf{V}\|} \right) \mathbf{W}_{:b}^{(t),T}\mathbf{Y}\mathbf{V} \right\|. \quad (2603)$$

Next, we upper bound the quantities I_1, I_2, I_3 separately.

For I_1 , we further bound I_1 by triangle inequality,

$$I_1 \leq I_{11} + I_{12}, \quad (2606)$$

where

$$I_{11} = \left\| \frac{\mathbf{W}_{:b}^T\mathbf{X}\mathbf{V}}{\|\mathbf{W}_{:b}^T\mathbf{X}\mathbf{V}\|} - \frac{\mathbf{W}_{:b}^{(t),T}\mathbf{X}\mathbf{V}}{\|\mathbf{W}_{:b}^{(t),T}\mathbf{X}\mathbf{V}\|} \right\|, \quad (2608)$$

and

$$I_{12} = \left\| \frac{\mathbf{W}_{:b}^T\mathbf{E}\mathbf{V}}{\|\mathbf{W}_{:b}^T\mathbf{X}\mathbf{V}\|} - \frac{\mathbf{W}_{:b}^{(t),T}\mathbf{E}\mathbf{V}}{\|\mathbf{W}_{:b}^{(t),T}\mathbf{X}\mathbf{V}\|} \right\|. \quad (2610)$$

We first consider I_{11} . Define the confusion matrix $\mathbf{D} = \mathbf{M}^T \Theta^T \mathbf{W}^{(t)} = [D_{ab}] \in \mathbb{R}^{r \times r}$ where

$$D_{ab} = \frac{\sum_{i \in [p]} \theta(i) \mathbb{1}\{z(i) = a, z^{(t)}(i) = b\}}{\sum_{i \in [p]} \mathbb{1}\{z^{(t)}(i) = b\}}, \text{ for all } a, b \in [r]. \quad (2613)$$

By Lemma 10, we have $\sum_{i \in [p]} \mathbb{1}\{z^{(t)}(i) = b\} \gtrsim p/r$. Then, we have

$$\sum_{a \neq b, a, b \in [r]} D_{ab} \lesssim \frac{r}{p} \sum_{i: z^{(t)}(i) \neq z(i)} \theta(i) \lesssim \frac{L^{(t)}}{\Delta_{\min}^2} \lesssim \frac{1}{\log p}, \quad (2616)$$

and for all $b \in [r]$,

$$\begin{aligned} D_{bb} &= \frac{\sum_{i \in [p]} \theta(i) \mathbb{1}\{z(i) = z^{(t)}(i) = b\}}{\sum_{i \in [p]} \mathbb{1}\{z^{(t)}(i) = b\}} \\ &\geq \frac{c(\sum_{i \in [p]} \mathbb{1}\{z^{(t)}(i) = b\} - p\ell^{(t)})}{\sum_{i \in [p]} \mathbb{1}\{z^{(t)}(i) = b\}} \\ &\gtrsim 1 - \frac{1}{\log p}, \end{aligned} \quad (112) \quad (2620)$$

under the inequality (66) in Condition 1. By the definition of $\mathbf{W}, \mathbf{W}^{(t)}, \mathbf{V}$, we have

$$\frac{\mathbf{W}_{:b}^T \mathbf{X} \mathbf{V}}{\|\mathbf{W}_{:b}^T \mathbf{X} \mathbf{V}\|} = [\mathbf{S}_{b:}]^s,$$

and

$$\frac{\mathbf{W}_{:b}^{(t),T} \mathbf{X} \mathbf{V}}{\|\mathbf{W}_{:b}^{(t),T} \mathbf{X} \mathbf{V}\|} = [D_{bb} \mathbf{S}_{b:} + \sum_{a \neq b, a \in [r]} D_{ab} \mathbf{S}_{a:}]^s.$$

Let α denote the angle between $\mathbf{S}_{b:}$ and $D_{bb} \mathbf{S}_{b:} + \sum_{a \neq b, a \in [r]} D_{ab} \mathbf{S}_{a:}$. To roughly estimate the range of α , we consider the inner product

$$\begin{aligned} & \left\langle \mathbf{S}_{b:}, D_{bb} \mathbf{S}_{b:} + \sum_{a \neq b, a \in [r]} D_{ab} \mathbf{S}_{a:} \right\rangle \\ &= D_{bb} \|\mathbf{S}_{b:}\|^2 + \sum_{a \neq b} D_{ab} \langle \mathbf{S}_{b:}, \mathbf{S}_{a:} \rangle \\ &\geq D_{bb} \|\mathbf{S}_{b:}\|^2 - \sum_{a \neq b, a \in [r]} D_{ab} \|\mathbf{S}_{b:}\| \max_{a \in [r]} \|\mathbf{S}_{a:}\| \\ &\geq C, \end{aligned}$$

where C is a positive constant, and the last inequality holds when p is large enough following the constraint of $\|\mathbf{S}_{b:}\|$ in parameter space (2) and the bounds of \mathbf{D} in (111) and (112).

The positive inner product between $\mathbf{S}_{b:}$ and $D_{bb} \mathbf{S}_{b:} + \sum_{a \neq b, a \in [r]} D_{ab} \mathbf{S}_{a:}$ indicates $\alpha \in [0, \pi/2]$, and thus $2 \sin \frac{\alpha}{2} \leq \sqrt{2} \sin \alpha$. Then, by the geometry property of trigonometric function, we have

$$\begin{aligned} & \| [D_{bb} \mathbf{S}_{b:} + \sum_{a \neq b, a \in [r]} D_{ab} \mathbf{S}_{a:}] \sin \alpha \| \\ &= \| (\mathbf{I}_d - \text{Proj}(\mathbf{S}_{b:})) \sum_{a \neq b, a \in [r]} D_{ab} \mathbf{S}_{a:} \| \\ &\leq \sum_{a \neq b, a \in [r]} D_{ab} \| (\mathbf{I}_d - \text{Proj}(\mathbf{S}_{b:})) \mathbf{S}_{a:} \| \\ &= \sum_{a \neq b, a \in [r]} D_{ab} \| \mathbf{S}_{a:} \sin(\mathbf{S}_{b:}, \mathbf{S}_{a:}) \| \\ &\leq \sum_{a \neq b, a \in [r]} D_{ab} \|\mathbf{S}_{a:}\| \|\mathbf{S}_{b:}^s - \mathbf{S}_{a:}^s\|, \end{aligned} \quad (113)$$

where the first inequality follows from the triangle inequality, and the last inequality follows from Lemma 4. Note that with bounds (111) and (112), when p is large enough, we have

$$\begin{aligned} \|\mathbf{W}_{:b}^{(t),T} \mathbf{X} \mathbf{V}\| &= \|D_{bb} \mathbf{S}_{b:} + \sum_{a \neq b, a \in [r]} D_{ab} \mathbf{S}_{a:}\| \\ &\geq D_{bb} \|\mathbf{S}_{b:}\| - \sum_{a \neq b, a \in [r]} D_{ab} \|\mathbf{S}_{a:}\| \\ &\geq C_1, \end{aligned} \quad (114)$$

for some positive constant C_1 . Notice that $I_{11} = \sqrt{1 - \cos \alpha} = 2 \sin \frac{\alpha}{2}$. Therefore, we obtain

$$\begin{aligned} I_{11} &\leq \sqrt{2} \sin \alpha \\ &= \frac{\| [D_{bb} \mathbf{S}_{b:} + \sum_{a \neq b, a \in [r]} D_{ab} \mathbf{S}_{a:}] \sin \alpha \|}{\| D_{bb} \mathbf{S}_{b:} + \sum_{a \neq b, a \in [r]} D_{ab} \mathbf{S}_{a:} \|} \\ &\leq \frac{1}{C_1} \sum_{a \neq b, a \in [r]} D_{ab} \|\mathbf{S}_{a:}\| \|\mathbf{S}_{b:}^s - \mathbf{S}_{a:}^s\| \\ &\lesssim \frac{r}{p} \sum_{i \in [p]} \theta(i) \sum_{b \in [r]} \mathbb{1} \{ z^{(t)}(i) = b \} \|\mathbf{S}_{b:}^s - \mathbf{S}_{a:}^s\| \\ &\leq \frac{r L^{(t)}}{\Delta_{\min}}, \end{aligned} \quad (115)$$

where the second inequality follows from (113) and (114), and the last two inequalities follow by the definition of D_a and $L^{(t)}$, and the constraint of $\|\mathbf{S}_{b:}\|$ in parameter space (2).

We now consider I_{12} . By triangle inequality, we have

$$\begin{aligned} I_{12} &\leq \frac{1}{\|\mathbf{W}_{:b}^T \mathbf{X} \mathbf{V}\|} \| (\mathbf{W}_{:b}^T - \mathbf{W}_{:b}^{(t),T}) \mathbf{E} \mathbf{V} \| \\ &\quad + \frac{\| (\mathbf{W}_{:b}^T - \mathbf{W}_{:b}^{(t),T}) \mathbf{X} \mathbf{V} \|}{\|\mathbf{W}_{:b}^T \mathbf{X} \mathbf{V}\| \|\mathbf{W}_{:b}^{(t),T} \mathbf{X} \mathbf{V}\|} \|\mathbf{W}_{:b}^{(t),T} \mathbf{E} \mathbf{V}\|. \end{aligned} \quad (116)$$

By [13, Proof of Lemma 5], we have

$$\begin{aligned} \| (\mathbf{W}_{:b}^T - \mathbf{W}_{:b}^{(t),T}) \mathbf{E} \mathbf{V} \| &\lesssim \sqrt{\frac{r^{2K} + pr^{K+1}}{p^K} \frac{\sqrt{L^{(t)}}}{\Delta_{\min}}}. \quad (116) \\ \text{Notice that} \quad & \\ \| (\mathbf{W}_{:b}^T - \mathbf{W}_{:b}^{(t),T}) \mathbf{X} \mathbf{V} \| &\leq \|\mathbf{W}_{:b}^T - \mathbf{W}_{:b}^{(t),T}\| \|\mathbf{X} \mathbf{V}\|_F \quad (117) \\ &\lesssim \frac{r^{3/2} L^{(t)}}{\sqrt{p} \Delta_{\min}^2} \|\mathbf{S}\| \|\Theta \mathbf{M}\|_\sigma \\ &\lesssim \frac{\sqrt{r L^{(t)}}}{\Delta_{\min}}, \end{aligned}$$

where the second inequality follows from [13, Inequality (121), Proof of Lemma 5] and the last inequality follows from Lemma 6 and (66) in Condition 1. Note that $\|\mathbf{W}_{:b}^T \mathbf{X} \mathbf{V}\| = \|\mathbf{S}_{b:}\| \geq c_3$ and $\|\mathbf{W}_{:b}^{(t),T} \mathbf{X} \mathbf{V}\| \geq C_1$ by inequality (114). Therefore, we have

$$\begin{aligned} I_{12} &\lesssim \| (\mathbf{W}_{:b}^T - \mathbf{W}_{:b}^{(t),T}) \mathbf{E} \mathbf{V} \| \\ &\quad + \| (\mathbf{W}_{:b}^T - \mathbf{W}_{:b}^{(t),T}) \mathbf{X} \mathbf{V} \| \|\mathbf{W}_{:b}^{(t),T} \mathbf{E} \mathbf{V}\| \\ &\lesssim \sqrt{\frac{r^{2K} + pr^{K+1}}{p^K} \frac{\sqrt{L^{(t)}}}{\Delta_{\min}}} + \frac{\sqrt{r L^{(t)}}}{\Delta_{\min}} \sqrt{\frac{r^{2K}}{p^K}} \\ &\lesssim \sqrt{\frac{r^{2K} + pr^{K+1}}{p^K} \frac{\sqrt{L^{(t)}}}{\Delta_{\min}}}, \end{aligned} \quad (118)$$

where second inequality follows from the inequalities (116), (117), and (62) in Condition 1.

Hence, combining inequalities (115) and (118) yields

$$I_1 \lesssim \frac{r L^{(t)}}{\Delta_{\min}} + \sqrt{\frac{r^{2K} + pr^{K+1}}{p^K} \frac{\sqrt{L^{(t)}}}{\Delta_{\min}}}. \quad (119)$$

For I_2 and I_3 , recall that $\|\mathbf{W}_{:b}^T \mathbf{X} \mathbf{V}\| = \|\mathbf{S}_{b:}\| \geq c_3$ and $\|\mathbf{W}_{:b}^{(t),T} \mathbf{X} \mathbf{V}\| \geq C_1$ by inequality (114). By triangle inequality and (62) in Condition 1, we have

$$I_2 \leq \frac{\|\mathbf{W}_{:b}^T \mathbf{E} \mathbf{V}\|}{\|\mathbf{W}_{:b}^T \mathbf{X} \mathbf{V}\|} \lesssim \|\mathbf{W}_{:b}^T \mathbf{E} \mathbf{V}\| \lesssim \frac{r^K}{p^{K/2}}, \quad (120)$$

and

$$I_3 \leq \frac{\|\mathbf{W}_{:b}^{(t),T} \mathbf{E} \mathbf{V}\|}{\|\mathbf{W}_{:b}^{(t),T} \mathbf{X} \mathbf{V}\|} \lesssim \|\mathbf{W}_{:b}^{(t),T} \mathbf{E} \mathbf{V}\| \lesssim \frac{r^K}{p^{K/2}}. \quad (121)$$

Therefore, combining the inequalities (119), (120), and (121), we finish the proof of inequality (108).

4) Inequality (109). Here we only show the proof of inequality (109) with $\mathbf{W}_{:b}^{(t)}$. The proof also holds by replacing $\mathbf{W}_{:b}^{(t)}$ to $\mathbf{W}_{:b}$, and we omit the repeated procedures.

We upper bound the desired quantity by triangle inequality

$$\|[\mathbf{W}_{:b}^{(t),T} \mathbf{Y} \mathbf{V}]^s - [\mathbf{W}_{:b}^{(t),T} \mathbf{Y} \mathbf{V}^{(t)}]^s\| \leq J_1 + J_2 + J_3,$$

where

$$J_1 = \left\| \frac{\mathbf{W}_{:b}^{(t),T} \mathbf{Y} \mathbf{V}}{\|\mathbf{W}_{:b}^{(t),T} \mathbf{X} \mathbf{V}\|} - \frac{\mathbf{W}_{:b}^{(t),T} \mathbf{Y} \mathbf{V}^{(t)}}{\|\mathbf{W}_{:b}^{(t),T} \mathbf{X} \mathbf{V}^{(t)}\|} \right\|,$$

$$J_2 = \left\| \left(\frac{1}{\|\mathbf{W}_{:b}^{(t),T} \mathbf{Y} \mathbf{V}\|} - \frac{1}{\|\mathbf{W}_{:b}^{(t),T} \mathbf{X} \mathbf{V}\|} \right) \mathbf{W}_{:b}^{(t),T} \mathbf{Y} \mathbf{V} \right\|,$$

$$J_3 = \left\| \left(\frac{1}{\|\mathbf{W}_{:b}^{(t),T} \mathbf{Y} \mathbf{V}^{(t)}\|} - \frac{1}{\|\mathbf{W}_{:b}^{(t),T} \mathbf{X} \mathbf{V}^{(t)}\|} \right) \mathbf{W}_{:b}^{(t),T} \mathbf{Y} \mathbf{V}^{(t)} \right\|.$$

Next, we upper bound the quantities J_1, J_2, J_3 separately.

For J_1 , by triangle inequality, we have

$$J_1 \leq J_{11} + J_{12},$$

where

$$J_{11} = \left\| \frac{\mathbf{W}_{:b}^{(t),T} \mathbf{X} \mathbf{V}}{\|\mathbf{W}_{:b}^{(t),T} \mathbf{X} \mathbf{V}\|} - \frac{\mathbf{W}_{:b}^{(t),T} \mathbf{X} \mathbf{V}^{(t)}}{\|\mathbf{W}_{:b}^{(t),T} \mathbf{X} \mathbf{V}^{(t)}\|} \right\|$$

and

$$J_{12} = \left\| \frac{\mathbf{W}_{:b}^{(t),T} \mathbf{E} \mathbf{V}}{\|\mathbf{W}_{:b}^{(t),T} \mathbf{X} \mathbf{V}\|} - \frac{\mathbf{W}_{:b}^{(t),T} \mathbf{E} \mathbf{V}^{(t)}}{\|\mathbf{W}_{:b}^{(t),T} \mathbf{X} \mathbf{V}^{(t)}\|} \right\|.$$

We first consider J_{11} . Define the matrix $\mathbf{V}^k := \mathbf{W}^{\otimes(k-1)} \otimes \mathbf{W}^{(t),\otimes(K-k)}$ for $k = 2, \dots, K-1$, and denote $\mathbf{V}^1 = \mathbf{V}^{(t)}, \mathbf{V}^K = \mathbf{V}$. Also, define the quantity

$$J_{11}^k = \|[\mathbf{W}_{:b}^{(t),T} \mathbf{X} \mathbf{V}^k]^s - [\mathbf{W}_{:b}^{(t),T} \mathbf{X} \mathbf{V}^{k+1}]^s\|,$$

for $k = 1, \dots, K-1$. Let β_k denote the angle between $\mathbf{W}_{:b}^{(t),T} \mathbf{X} \mathbf{V}^k$ and $\mathbf{W}_{:b}^{(t),T} \mathbf{X} \mathbf{V}^{k+1}$. With the same idea to prove I_{11} in inequality (115), we bound J_{11}^k by the trigonometric function of β_k .

To roughly estimate the range of β_k , we consider the inner product between $\mathbf{W}_{:b}^{(t),T} \mathbf{X} \mathbf{V}^k$ and $\mathbf{W}_{:b}^{(t),T} \mathbf{X} \mathbf{V}^{k+1}$. Before the specific derivation of the inner product, note that

$$\mathbf{W}_{:b}^{(t),T} \mathbf{X} \mathbf{V}^k = \text{Mat}_1(\mathcal{T}_k), \quad \mathbf{W}_{:b}^{(t),T} \mathbf{X} \mathbf{V}^{k+1} = \text{Mat}_1(\mathcal{T}_{k+1}),$$

where

$$\mathcal{T}_k = \mathcal{X} \times_1 \mathbf{W}_{:b}^{(t),T} \times_2 \mathbf{W}^T \times_3 \cdots \times_k \mathbf{W}^T$$

$$\times_{k+1} \mathbf{W}^{(t),T} \times_{k+2} \cdots \times_K \mathbf{W}^{(t),T}$$

$$\mathcal{T}_{k+1} = \mathcal{X} \times_1 \mathbf{W}_{:b}^{(t),T} \times_2 \mathbf{W}^T \times_3 \cdots \times_k \mathbf{W}^T$$

$$\times_{k+1} \mathbf{W}^T \times_{k+2} \cdots \times_K \mathbf{W}^{(t),T}.$$

Recall the definition of confusion matrix $\mathbf{D} = \mathbf{M}^T \Theta^T \mathbf{W}^{(t)} = [\mathbf{D}_{ab}] \in \mathbb{R}^{r \times r}$. We have

$$\langle \mathbf{W}_{:b}^{(t),T} \mathbf{X} \mathbf{V}^k, \mathbf{W}_{:b}^{(t),T} \mathbf{X} \mathbf{V}^{k+1} \rangle$$

$$= \langle \text{Mat}_{k+1}(\mathcal{T}_k), \text{Mat}_{k+1}(\mathcal{T}_{k+1}) \rangle$$

$$= \langle \mathbf{D}^T \mathbf{S} \mathbf{Z}^k, \mathbf{S} \mathbf{Z}^k \rangle$$

$$= \sum_{b \in [r]} \left(D_{bb} \|\mathbf{S}_{b:} \mathbf{Z}^k\|^2 + \sum_{a \neq b, a \in [r]} D_{ab} \langle \mathbf{S}_{a:} \mathbf{Z}^k, \mathbf{S}_{b:} \mathbf{Z}^k \rangle \right)$$

$$\gtrsim (1 - \log p^{-1}) \min_{a \in [r]} \|\mathbf{S}_{a:} \mathbf{Z}^k\|^2 - \log p^{-1} \max_{a \in [r]} \|\mathbf{S}_{a:} \mathbf{Z}^k\|^2, \quad (122)$$

where $\mathbf{Z}^k = \mathbf{D}_{:b} \otimes \mathbf{I}_r^{\otimes(k-1)} \otimes \mathbf{D}^{\otimes(K-k-1)}$, the equations follow by the tensor algebra and definitions, and the last inequality follows from the bounds of \mathbf{D} in (111) and (112).

Note that

$$\|\mathbf{D}\|_\sigma \leq \|\mathbf{D}\|_F$$

$$\leq \sqrt{\sum_{b \in [r]} D_{bb}^2 + (\sum_{a \neq b, a \in [r]} D_{ab})^2}$$

$$\lesssim \sqrt{r + \log^2 p^{-1}} \lesssim 1, \quad (123)$$

where the second inequality follows from inequality (111), and the fact that for all $b \in [r]$,

$$D_{bb} \lesssim \frac{r}{p} \sum_{i: z(i)=b} \theta(i) \lesssim 1.$$

Also, we have

$$\lambda_r(\mathbf{D}) \geq \lambda_r(\mathbf{W}^{(t)}) \lambda_r(\Theta \mathbf{M}) \gtrsim 1, \quad (124)$$

following the Lemma 6 and Lemma 10. Then, for all $k \in [K]$, we have

$$1 \lesssim \|\mathbf{D}_{:b}\| \lambda_r(\mathbf{D})^{K-k-1} \leq \lambda_{r^{K-2}}(\mathbf{Z}^k)$$

$$\leq \|\mathbf{Z}^k\|_\sigma \leq \|\mathbf{D}_{:b}\| \|\mathbf{D}\|_\sigma^{K-k-1} \lesssim 1. \quad (125)$$

Thus, we have bounds

$$\max_{a \in [r]} \|\mathbf{S}_{a:} \mathbf{Z}^k\| \leq \max_{a \in [r]} \|\mathbf{S}_{a:}\| \|\mathbf{Z}^k\|_\sigma \lesssim 1,$$

$$\min_{a \in [r]} \|\mathbf{S}_{a:} \mathbf{Z}^k\| \geq \min_{a \in [r]} \|\mathbf{S}_{a:}\| \lambda_{r^{K-2}}(\mathbf{Z}^k) \gtrsim 1.$$

Hence, when p is large enough, the inner product (122) is positive, which implies $\beta_k \in [0, \pi/2]$ and thus $2 \sin \frac{\beta_k}{2} \leq \sqrt{2} \sin \beta_k$.

2755 Next, we upper bound the trigonometric function $\sin \beta_k$.
 2756 Note that

$$\begin{aligned} 2757 \sin \beta_k &= \sin(\mathbf{D}_{:b}^T \mathbf{S} \mathbf{I}_r^{\otimes k-1} \otimes \mathbf{D}^{\otimes K-k}, \mathbf{D}_{:b}^T \mathbf{S} \mathbf{I}_r^{\otimes k} \otimes \mathbf{D}^{\otimes K-k-1}) \\ 2758 &\leq \sin \beta_{k1} + \sin \beta_{k2}, \end{aligned}$$

2759 where

$$\begin{aligned} 2760 \sin \beta_{k1} &= \sin(\mathbf{D}_{:b}^T \mathbf{S} \mathbf{I}_r^{\otimes k-1} \otimes \mathbf{D}^{\otimes K-k}, \\ 2761 &\quad \mathbf{D}_{:b}^T \mathbf{S} \mathbf{I}_r^{\otimes k-1} \otimes \tilde{\mathbf{D}} \otimes \mathbf{D}^{\otimes K-k-1}), \\ 2762 \sin \beta_{k2} &= \sin(\mathbf{D}_{:b}^T \mathbf{S} \mathbf{I}_r^{\otimes k-1} \otimes \tilde{\mathbf{D}} \otimes \mathbf{D}^{\otimes K-k-1}, \\ 2763 &\quad \mathbf{D}_{:b}^T \mathbf{S} \mathbf{I}_r^{\otimes k} \otimes \mathbf{D}^{\otimes K-k-1}), \end{aligned}$$

2764 and $\tilde{\mathbf{D}}$ is the normalized confusion matrix with entries $\tilde{\mathbf{D}}_{ab} = \frac{\sum_{i \in [p]} \theta(i) \mathbf{1}\{z^{(t)}=b, z(i)=a\}}{\sum_{i \in [p]} \theta(i) \mathbf{1}\{z^{(t)}=b\}}$.

2765 To bound $\sin \beta_{k1}$, recall Definition 2 that for any cluster
 2766 assignment \bar{z} in the ε -neighborhood of true z ,

$$\begin{aligned} 2768 \mathbf{p}(\bar{z}) &= (|\bar{z}^{-1}(1)|, \dots, |\bar{z}^{-1}(r)|)^T, \\ 2769 \mathbf{p}_{\theta}(\bar{z}) &= (\|\theta_{\bar{z}^{-1}(1)}\|_1, \dots, \|\theta_{\bar{z}^{-1}(r)}\|_1)^T. \end{aligned}$$

2770 Note that we have $\ell^{(t)} \leq \frac{L^{(t)}}{\Delta_{\min}^2} \leq \frac{\bar{C}}{C} r \log^{-1}(p)$ by Condition 1 and Lemma 2. Then, with the locally linear stability
 2771 assumption, the θ is $\ell^{(t)}$ -locally linearly stable; i.e.,

$$2773 \sin(\mathbf{p}(z^{(t)}), \mathbf{p}_{\theta}(z^{(t)})) \lesssim \frac{L^{(t)}}{\Delta_{\min}}.$$

2774 Note that $\text{diag}(\mathbf{p}(z^{(t)}))\mathbf{D} = \text{diag}(\mathbf{p}_{\theta}(z^{(t)}))\tilde{\mathbf{D}}$, and
 2775 $\sin(\mathbf{a}, \mathbf{b}) = \min_{c \in \mathbb{R}} \frac{\|\mathbf{a}-c\mathbf{b}\|}{\|\mathbf{a}\|}$ for vectors \mathbf{a}, \mathbf{b} of same
 2776 dimension. Let $c_0 = \arg \min_{c \in \mathbb{R}} \frac{\|\mathbf{p}(z^{(t)}) - c\mathbf{p}_{\theta}(z^{(t)})\|}{\|\mathbf{p}(z^{(t)})\|}$. Then,
 2777 we have

$$\begin{aligned} 2778 \min_{c \in \mathbb{R}} \|\mathbf{D} - c\tilde{\mathbf{D}}\|_F \\ 2779 &\leq \|\mathbf{I}_r - c_0 \text{diag}(\mathbf{p}(z^{(t)})) \text{diag}^{-1}(\mathbf{p}_{\theta}(z^{(t)}))\|_F \|\mathbf{D}\|_F \\ 2780 &\lesssim \frac{\|\mathbf{p}(z^{(t)}) - c_0 \mathbf{p}_{\theta}(z^{(t)})\|}{\min_{a \in [r]} \|\theta_{z^{(t)}, -1(a)}\|_1} \\ 2781 &= \frac{\|\mathbf{p}(z^{(t)})\|}{\min_{a \in [r]} \|\theta_{z^{(t)}, -1(a)}\|_1} \sin(\mathbf{p}(z^{(t)}), \mathbf{p}_{\theta}(z^{(t)})) \\ 2782 &\lesssim \frac{L^{(t)}}{\Delta_{\min}}, \end{aligned}$$

2783 where the last inequality follows from Lemma 10, the
 2784 constraint $\min_{i \in [p]} \theta(i) \geq c > 0$, $\|\mathbf{p}(z^{(t)})\| \lesssim p$ and
 2785 $\min_{a \in [r]} \|\theta_{z^{(t)}, -1(a)}\|_1 \gtrsim p$.

2786 By the geometry property of trigonometric function,
 2787 we have

$$\begin{aligned} 2788 \sin \beta_{k1} &= \min_{c \in \mathbb{R}} \frac{\|\mathbf{D}_{:b}^T \mathbf{S} \mathbf{I}_r^{\otimes k-1} \otimes (\mathbf{D} - c\tilde{\mathbf{D}}) \otimes \mathbf{D}^{\otimes K-k-1}\|}{\|\mathbf{D}_{:b}^T \mathbf{S} \mathbf{I}_r^{\otimes k-1} \otimes \mathbf{D}^{\otimes K-k}\|} \\ 2789 &\leq \frac{\|\mathbf{D}_{:b}^T \mathbf{S}\| \|\mathbf{D} - c_0 \tilde{\mathbf{D}}\|_{\sigma} \|\mathbf{D}\|_{\sigma}^{K-k-1}}{\|\mathbf{D}_{:b}^T \mathbf{S}\| \lambda_r^{K-k}(\mathbf{D})} \\ 2790 &\lesssim \|\mathbf{D} - c_0 \tilde{\mathbf{D}}\|_F \\ 2791 &\lesssim \frac{L^{(t)}}{\Delta_{\min}}, \end{aligned} \tag{126}$$

2792 where the second inequality follows from the singular property
 2793 of \mathbf{D} in (123), (124) and the constraint of \mathbf{S} in (2).

2794 To bound $\sin \beta_{k2}$, let $\mathbf{C} = \text{diag}(\{\|\mathbf{S}_{a:}\|\}_{a \in [r]})$. We have

$$\begin{aligned} 2795 \sin \beta_{k2} &\lesssim \frac{\|\mathbf{D}_{:b}^T \mathbf{S} \mathbf{I}_r^{\otimes k-1} \otimes (\mathbf{I}_r - \tilde{\mathbf{D}}) \otimes \mathbf{D}^{\otimes K-k-1}\|}{\|\mathbf{D}_{:b}^T \mathbf{S} \mathbf{I}_r^{\otimes k} \otimes \mathbf{D}^{\otimes K-k-1}\|} \\ 2796 &\lesssim \frac{\|(\mathbf{I}_r - \tilde{\mathbf{D}}^T) \mathbf{S} \mathbf{Z}^k\|_F}{\|\mathbf{D}_{:b}^T \mathbf{S}\| \lambda_r^{K-k-1}(\mathbf{D})} \\ 2797 &\lesssim \|(\mathbf{I}_r - \tilde{\mathbf{D}}^T) \mathbf{S} \mathbf{C}^{-1}\|_F \|\mathbf{C} \mathbf{Z}^k\|_{\sigma} \\ 2798 &\lesssim \frac{r}{p} \sum_{i \in [p]} \theta(i) \sum_{b \in [r]} \mathbf{1}\{z^{(t)}(i) = b\} \|\mathbf{S}_{b:}^s - \mathbf{S}_{z(i)}^s\| \\ 2799 &\lesssim \frac{L^{(t)}}{\Delta_{\min}}, \end{aligned} \tag{127}$$

2800 where the third inequality follows from the singular property
 2801 of \mathbf{D} and the boundedness of \mathbf{S} , and the fourth inequality
 2802 follows from the definition of $\tilde{\mathbf{D}}$, boundedness of \mathbf{S} , the
 2803 lower bound of θ , and the singular property of \mathbf{Z}^k in inequality
 2804 (125), and the last line follows from the definition of $L^{(t)}$.

2805 Combining (126) and (127) yields

$$\sin \beta_k \leq \sin \beta_{k1} + \sin \beta_{k2} \lesssim \frac{L^{(t)}}{\Delta_{\min}}.$$

2806 Finally, by triangle inequality, we obtain

$$2807 J_{11} \leq \sum_{k=1}^{K-1} J_{11}^k \lesssim \sum_{k=1}^{K-1} \sin \beta_k \lesssim (K-1) \frac{r L^{(t)}}{\Delta_{\min}}. \tag{128}$$

2808 We now consider J_{12} . By triangle inequality, we have

$$\begin{aligned} 2809 J_{12} &\leq \frac{1}{\|\mathbf{W}_{:b}^{(t),T} \mathbf{X} \mathbf{V}\|} \|\mathbf{W}_{:b}^{(t),T} \mathbf{E}(\mathbf{V} - \mathbf{V}^{(t)})\| \\ 2810 &\quad + \frac{\|\mathbf{W}_{:b}^{(t),T} \mathbf{X}(\mathbf{V} - \mathbf{V}^{(t)})\|}{\|\mathbf{W}_{:b}^{(t),T} \mathbf{X} \mathbf{V}\| \|\mathbf{W}_{:b}^{(t),T} \mathbf{X} \mathbf{V}^{(t)}\|} \|\mathbf{W}_{:b}^{(t),T} \mathbf{E} \mathbf{V}^{(t)}\|. \end{aligned} \tag{129}$$

2812 Note that

$$\begin{aligned} 2813 \|\mathbf{W}_{:b}^{(t),T} \mathbf{X} \mathbf{V}^{(t)}\| &= \|\mathbf{D}^T \mathbf{S} \mathbf{Z}^1\| \\ 2814 &\geq \lambda_r(\mathbf{D}) \|\mathbf{S}\| \lambda_{r^{K-2}}(\mathbf{Z}^1) \gtrsim 1, \\ 2815 \end{aligned} \tag{129}$$

2816 where the inequality follows from the bounds (124) and (125).

2817 By [13, Proof of Lemma 5], we have

$$\begin{aligned} 2818 \|\mathbf{W}_{:b}^{(t),T} \mathbf{E}(\mathbf{V} - \mathbf{V}^{(t)})\| \\ 2819 &\lesssim \sqrt{\frac{r^{2K+1} + pr^{2+K}}{p^K}} \frac{(K-1)\sqrt{L^{(t)}}}{\Delta_{\min}}. \end{aligned} \tag{130}$$

2820 Notice that

$$\begin{aligned} 2821 \|\mathbf{X}(\mathbf{V}^k - \mathbf{V}^{k+1})\|_F \\ 2822 &\leq \|(\mathbf{I} - \mathbf{D}^T) \mathbf{S}(\mathbf{I}_r^{\otimes(k-1)} \otimes \mathbf{D}^{\otimes(K-k-1)})\|_F \\ 2823 &\leq \|(\mathbf{W}^T - \mathbf{W}^{(t),T}) \Theta \mathbf{M}\|_F \|\mathbf{S}\|_F \|\mathbf{D}\|_{\sigma}^{K-k-1} \\ 2824 &\lesssim \|\mathbf{W}^T - \mathbf{W}^{(t),T}\| \|\Theta \mathbf{M}\|_{\sigma} \\ 2825 &\lesssim \frac{\sqrt{r L^{(t)}}}{\Delta_{\min}}, \end{aligned} \tag{131}$$

where the first inequality follows from the tensor algebra in inequality (122), the second inequality follows from the fact that $\mathbf{I} = \mathbf{W}^T \Theta \mathbf{M}$, and the last inequality follows from [13, Proof of Lemma 5]. It follows from (131) and Lemma 10 that

$$\begin{aligned} \|\mathbf{W}_{:b}^{(t),T} \mathbf{X}(\mathbf{V} - \mathbf{V}^{(t)})\| &\leq \|\mathbf{W}_{:b}^{(t),T}\| \sum_{k=1}^{K-1} \|\mathbf{X}(\mathbf{V}^k - \mathbf{V}^{k+1})\|_F \\ &\lesssim \frac{\sqrt{rL^{(t)}}}{\sqrt{p}\Delta_{\min}}. \end{aligned} \quad (132)$$

Note that $\|\mathbf{W}_{:b}^{(t),T} \mathbf{X} \mathbf{V}\|$ and $\|\mathbf{W}_{:b}^{(t),T} \mathbf{X} \mathbf{V}^{(t)}\|$ are lower bounded by inequalities (114) and (129), respectively. We have

$$\begin{aligned} J_{12} &\lesssim \|\mathbf{W}_{:b}^{(t),T} \mathbf{E}(\mathbf{V} - \mathbf{V}^{(t)})\| \\ &\quad + \|\mathbf{W}_{:b}^{(t),T} \mathbf{X}(\mathbf{V} - \mathbf{V}^{(t)})\| \|\mathbf{W}_{:b}^{(t),T} \mathbf{E} \mathbf{V}^{(t)}\| \\ &\lesssim \sqrt{\frac{r^{2K+1} + pr^{2+K}}{p^K} \frac{\sqrt{L^{(t)}}}{\Delta_{\min}}} + \frac{\sqrt{rL^{(t)}}}{\sqrt{p}\Delta_{\min}} \sqrt{\frac{r^{2K}}{p^K}} \\ &\lesssim \sqrt{\frac{r^{2K+1} + pr^{2+K}}{p^K} \frac{\sqrt{L^{(t)}}}{\Delta_{\min}}}, \end{aligned}$$

where the second inequality follows from inequalities (130), (132), and the inequality (62) in Condition 1.

For J_2 and J_3 , recall that $\|\mathbf{W}_{:b}^{(t),T} \mathbf{X} \mathbf{V}\|$ and $\|\mathbf{W}_{:b}^{(t),T} \mathbf{X} \mathbf{V}^{(t)}\|$ are lower bounded by inequalities (114) and (129), respectively. By triangle inequality and inequality (62) in Condition 1, we have

$$J_2 \leq \frac{\|\mathbf{W}_{:b}^{(t),T} \mathbf{E} \mathbf{V}\|}{\|\mathbf{W}_{:b}^{(t),T} \mathbf{X} \mathbf{V}\|} \lesssim \|\mathbf{W}_{:b}^{(t),T} \mathbf{E} \mathbf{V}\| \lesssim \frac{r^K}{p^{K/2}}, \quad (133)$$

and

$$J_3 \leq \frac{\|\mathbf{W}_{:b}^{(t),T} \mathbf{E} \mathbf{V}^{(t)}\|}{\|\mathbf{W}_{:b}^{(t),T} \mathbf{X} \mathbf{V}^{(t)}\|} \lesssim \|\mathbf{W}_{:b}^{(t),T} \mathbf{E} \mathbf{V}\| \lesssim \frac{r^K}{p^{K/2}}. \quad (134)$$

Therefore, combining the inequalities (128), (133), and (134), we finish the proof of inequality (109).

5) Inequality (110). By triangle inequality, we upper bound the desired quantity

$$\begin{aligned} &\|[\mathbf{W}_{:b}^T \mathbf{Y} \mathbf{V}^{(t)}]^s - [\mathbf{W}_{:b}^{(t),T} \mathbf{Y} \mathbf{V}^{(t)}]^s\| \\ &\leq \|[\mathbf{W}_{:b}^T \mathbf{Y} \mathbf{V}^{(t)}]^s - [\mathbf{W}_{:b}^T \mathbf{Y} \mathbf{V}]^s\| \\ &\quad + \|[\mathbf{W}_{:b}^T \mathbf{Y} \mathbf{V}]^s - [\mathbf{W}_{:b}^{(t),T} \mathbf{Y} \mathbf{V}]^s\| \\ &\quad + \|[\mathbf{W}_{:b}^{(t),T} \mathbf{Y} \mathbf{V}]^s - [\mathbf{W}_{:b}^{(t),T} \mathbf{Y} \mathbf{V}^{(t)}]^s\| \\ &\lesssim \frac{rL^{(t)}}{\Delta_{\min}} + \sqrt{\frac{r^{2K} + pr^{K+2}}{p^K} \frac{\sqrt{L^{(t)}}}{\Delta_{\min}}}, \end{aligned}$$

following the inequalities (108) and (109). Therefore, we finish the proof of inequality (110).

6) Next, we Show the Intermediate Inequalities Holds With \mathbf{P}, \mathbf{Q} and $L(\hat{z})$: Consider the MLE confusion matrix $\hat{\mathbf{D}} = \mathbf{M}^T \Theta^T \hat{\mathbf{P}} = \llbracket \hat{D}_{ab} \rrbracket \in \mathbb{R}^{r \times r}$ with entries

$$\begin{aligned} \hat{D}_{ab} &= \frac{\sum_{i \in [p]} \theta(i)\hat{\theta}(i)\mathbf{1}\{z(i) = a, \hat{z}(i) = b\}}{\|\hat{\theta}_{\hat{z}^{-1}(b)}\|^2} \\ &= \frac{\sum_{i \in [p]} (1 + o(p^{K-2}))(\hat{\theta}(i))^2 \mathbf{1}\{z(i) = a, \hat{z}(i) = b\}}{\|\hat{\theta}_{\hat{z}^{-1}(b)}\|^2}, \end{aligned} \quad (135)$$

where the second equation follows from Lemma 13, and thus $\sum_{a \in [r]} \hat{D}_{ab} = 1 + o(1)$. By the derivation of (111), (112), (124), and (123), we have

$$\begin{aligned} \sum_{a \neq b \in [r]} \hat{D}_{ab} &\lesssim \frac{1}{p} \sum_{i \in [p]} \mathbf{1}\{\hat{z}(i) \neq z(i)\}(\hat{\theta}(i))^2 \lesssim \frac{1}{\log p}, \\ \hat{D}_{bb} &\gtrsim 1 - \frac{1}{\log p}, \quad \lambda_{\min}(\hat{\mathbf{D}}) \asymp \|\hat{\mathbf{D}}\|_\sigma = (1 + o(1)). \end{aligned}$$

for all $a \neq b \in [r]$.

Now, we are ready to show the intermediate inequalities. First, by Lemma 1 and $\min_{i \in [p]} \theta(i) \geq c$, we have

$$\|\mathbf{S}_{a:}^s - \mathbf{S}_{b:}^s\| \asymp \|\mathbf{A}_{a:}^s - \mathbf{A}_{b:}^s\|. \quad (2872)$$

Then we can replace the $L^{(t)}$ by $L(\hat{z})$ in the proof of Lemma 12. The analogies of inequalities (106), (107), (108), (109), and (110) hold by using the MLE confusion matrix and the definition of $L(\hat{z})$.

Particularly, for the analogy of (109), the usage of MLE confusion matrix avoids the stability condition on θ . Let $\bar{\mathbf{D}}$ be the normalized version of $\hat{\mathbf{D}}$. The angle in inequality (126) decays to 0 at speed $p^{-(K-2)} \lesssim \Delta_{\min}$ when $K \geq 3$, and the inequality (127) holds by the fact that

$$\begin{aligned} \|(\mathbf{I}_r - \bar{\mathbf{D}})\mathbf{S}\mathbf{C}^{-1}\|_F &\lesssim \frac{r}{p} \sum_{i \in [p]} (\theta(i))^2 \sum_{b \in [r]} \|\mathbf{S}_{b:}^s - \mathbf{S}_{z(i):}^s\| \\ &\lesssim \frac{r}{p} \sum_{i \in [p]} (\theta(i))^2 \sum_{b \in [r]} \|\mathbf{A}_{b:}^s - \mathbf{A}_{z(i):}^s\|. \end{aligned} \quad (2882)$$

□

Lemma 13 (Polynomial Estimation Error of MLE): Let $(\hat{z}, \hat{\mathcal{S}}, \hat{\theta})$ denote the MLE in (9) with fixed $K \geq 2$ and symmetric mean tensor, and $\hat{\mathcal{X}}$ denote the mean tensor consisting of parameter $(\hat{z}, \hat{\mathcal{S}}, \hat{\theta})$. With high probability going to 1 as $p \rightarrow \infty$, we have

$$\|\mathcal{X} - \hat{\mathcal{X}}\|_F^2 \lesssim \sigma^2 (r^K + Kpr), \quad (2890)$$

with probability going to 1. When SNR $\gtrsim p^{-(K-1)} \log p$, θ is balanced, and $\min_{i \in [p]} \theta(i) \geq c$ for some positive constant c , the MLE satisfies

$$\frac{1}{p} \sum_{i \in [p]} \mathbf{1}\{\hat{z}(i) \neq z(i)\}(\theta(i))^2 \lesssim \frac{1}{r \log p}, \quad (2894)$$

$$\frac{1}{p} \sum_{i \in [p]} \mathbf{1}\{\hat{z}(i) \neq z(i)\}(\hat{\theta}(i))^2 \lesssim \frac{1}{r \log p}, \quad (2895)$$

$$\text{and } L(\hat{z}) \lesssim \frac{\Delta_{\min}^2}{r \log p}, \quad (2896)$$

Further, we have

$$\theta(i)^2 = (1 + o(p^{-(K-2)}))\hat{\theta}(i)^2. \quad (2898)$$

Proof of Lemma 13: Without loss of generality, we assume $\sigma^2 = 1$ and identity mapping minimizes the misclustering error for MLE. For arbitrary two sets of parameters $(z, \mathcal{S}, \boldsymbol{\theta}), (z', \mathcal{S}', \boldsymbol{\theta}') \in \mathcal{P}(\gamma)$ and corresponding mean tensors $\mathcal{X}, \mathcal{X}'$, we have

$$\begin{aligned} & \text{rank}(\text{Mat}_k(\mathcal{X}) - \text{Mat}_k(\mathcal{X}')) \\ & \leq \text{rank}(\text{Mat}_k(\mathcal{X})) + \text{rank}(\text{Mat}_k(\mathcal{X}')) \\ & \leq 2r, \quad k \in [K]. \end{aligned}$$

Hence, we have

$$\mathcal{X} - \mathcal{X}' \in \mathcal{Q}(2r, \dots, 2r), \quad (136)$$

where $\mathcal{Q}(r, \dots, r) := \{\text{Tucker tensor with rank } (r, \dots, r)\}$. Then, we obtain that

$$\begin{aligned} & \mathbb{P}(\|\mathcal{X} - \hat{\mathcal{X}}_{ML}\|_F \geq t) \\ & \leq 2\mathbb{P}\left(\sup_{\mathcal{X}, \mathcal{X}' \in \mathcal{Q}(r, \dots, r)} \left\langle \frac{\mathcal{X} - \mathcal{X}'}{\|\mathcal{X} - \mathcal{X}'\|_F}, \mathcal{E} \right\rangle \geq t\right) \\ & \leq 2\mathbb{P}\left(\sup_{\mathcal{T} \in \mathcal{Q}(2r, \dots, 2r) \cap \{\|\mathcal{T}\|_F=1\}} \langle \mathcal{T}, \mathcal{E} \rangle \geq t\right) \\ & \lesssim \exp(-Kpr), \end{aligned}$$

with the choice $t \asymp \sigma\sqrt{(Kpr + r^K)}$. Here the first inequality follows from [10, Lemma 1], the second inequality follows from (136), and the last inequality follows from [37, Lemma E5].

When $\Delta_{\min}^2 \gtrsim p^{-(K-1)} \log p$, we replace the vector $\hat{x}_{\hat{z}(i)}$ and $\hat{\mathbf{X}}$ by our MLE estimator in the proof of Theorem 4. With estimation error $\|\mathcal{X} - \hat{\mathcal{X}}\|_F^2 \lesssim (r^K + Kpr)$ and $\Delta_{\min}^2 \gtrsim p^{-(K-1)} \log p$, we have

$$\begin{aligned} \frac{1}{p} \sum_{i \in [p]} \mathbb{1}\{\hat{z}(i) \neq z(i)\} (\theta(i))^2 & \lesssim \frac{r^{K-1}}{\Delta_{\min}^2 p^K} \|\mathcal{X} - \hat{\mathcal{X}}\|_F^2 \\ & \lesssim \frac{r^{K-2}}{p^{K-1} \Delta_{\min}^2} \\ & \lesssim \frac{1}{r \log p}, \end{aligned}$$

and

$$L(\hat{z}) \lesssim \frac{\Delta_{\min}^2}{r \log p}.$$

Above result holds for $\hat{\theta}(i)$ after switching the parameters \mathbf{X} with $\hat{\mathbf{X}}$ and switch $\boldsymbol{\theta}$ with $\hat{\boldsymbol{\theta}}$ in the proof.

Last, notice that for all $a \in [r]$

$$\begin{aligned} & (1 - O(1)) \frac{p^2}{r^2} \|\mathbf{W}_{:a}^T \mathbf{X} - \hat{\mathbf{W}}_{:a}^T \hat{\mathbf{X}}\|_F^2 \\ & \leq \sum_{\hat{z}(i)=z(i)=a} (\theta(i) \mathbf{W}_{:a}^T \mathbf{X} - \hat{\theta}(i) \hat{\mathbf{W}}_{:a}^T \hat{\mathbf{X}})^2 \\ & \leq \|\mathcal{X} - \hat{\mathcal{X}}\|_F^2 \leq pr, \end{aligned}$$

where the first inequality follows from the facts that $\ell(\hat{z}, z) \lesssim \frac{1}{\log p}, |z^{-1}(a)| \asymp p/r$,

$$\begin{aligned} |z^{-1}(a)| - C \frac{p}{r} \ell(\hat{z}, z) & \leq |\hat{z}^{-1}(a)| \leq |z^{-1}(a)| + C \frac{p}{r} \ell(\hat{z}, z), \\ |z^{-1}(a)| - C \frac{p}{r} \ell(\hat{z}, z) & \leq \sum_{z(i)=\hat{z}(i)=a} \theta(i) \leq |z^{-1}(a)|, \end{aligned}$$

and

$$|\hat{z}^{-1}(a)| - C \frac{p}{r} \ell(\hat{z}, z) \leq \sum_{\hat{z}(i)=z(i)=a} \hat{\theta}(i) \leq |\hat{z}^{-1}(a)|.$$

Hence, for all $i \in [p]$

$$\begin{aligned} & (\theta(i) - \hat{\theta}(i))^2 \|\mathbf{W}_{:a}^T \mathbf{X}\|_F^2 - O(p) \\ & \leq \|(\theta(i) - \hat{\theta}(i)) \mathbf{W}_{:a}^T \mathbf{X}\|_F^2 - \|\hat{\theta}(i)(\mathbf{W}_{:a}^T \mathbf{X} - \hat{\mathbf{W}}_{:a}^T \hat{\mathbf{X}})\|_F^2 \\ & \leq \|\mathcal{X} - \hat{\mathcal{X}}\|_F^2 \leq pr, \end{aligned}$$

where the first inequality follows from $\|\mathbf{W}_{:a}^T \mathbf{X} - \hat{\mathbf{W}}_{:a}^T \hat{\mathbf{X}}\|_F^2 \lesssim 1/p$ and $\hat{\theta}(i) \lesssim \frac{p}{r}$. Notice that for all $a \in [r]$

$$\|\mathbf{W}_{:a}^T \mathbf{X}\|_F^2 \geq \|\mathbf{S}_a\|_F^2 \lambda_{\min}^{2(K-1)} (\Theta \mathbf{M}) \gtrsim p^{K-1}.$$

The inequality indicates that $\theta(i)^2 = (1 + o(p^{-(K-2)}))\hat{\theta}(i)^2$. \square

ACKNOWLEDGMENT

The authors would like to thank Zheng Tracy Ke, Anru Zhang, Rungang Han, and Yuetian Luo for helpful discussions and for sharing software packages.

REFERENCES

- [1] A. Anandkumar, R. Ge, D. J. Hsu, S. M. Kakade, and M. Telgarsky, “Tensor decompositions for learning latent variable models,” *J. Mach. Learn. Res.*, vol. 15, pp. 2773–2832, Aug. 2014.
- [2] L. Wang, D. Durante, R. E. Jung, and D. B. Dunson, “Bayesian network-response regression,” *Bioinformatics*, vol. 33, no. 12, pp. 1859–1866, 2017.
- [3] P. Koniusz and A. Cherian, “Sparse coding for third-order supersymmetric tensor descriptors with application to texture recognition,” in *Proc. IEEE Conf. Comput. Vis. Pattern Recognit. (CVPR)*, Jun. 2016, pp. 5395–5403.
- [4] M. Wang, J. Fischer, and Y. S. Song, “Three-way clustering of multi-tissue multi-individual gene expression data using semi-nonnegative tensor decomposition,” *Ann. Appl. Statist.*, vol. 13, no. 2, pp. 1103–1127, Jun. 2019.
- [5] V. Hore et al., “Tensor decomposition for multiple-tissue gene expression experiments,” *Nature Genet.*, vol. 48, no. 9, p. 1094, 2016.
- [6] D. Ghoshdastidar and A. Dukkipati, “Uniform hypergraph partitioning: Provable tensor methods and sampling techniques,” *J. Mach. Learn. Res.*, vol. 18, no. 50, pp. 1–41, 2017.
- [7] D. Ghoshdastidar and A. Dukkipati, “Consistency of spectral hypergraph partitioning under planted partition model,” *Ann. Statist.*, vol. 45, no. 1, pp. 289–315, 2017.
- [8] K. Ahn, K. Lee, and C. Suh, “Community recovery in hypergraphs,” *IEEE Trans. Inf. Theory*, vol. 65, no. 10, pp. 6561–6579, Oct. 2019.
- [9] Z. T. Ke, F. Shi, and D. Xia, “Community detection for hypergraph networks via regularized tensor power iteration,” 2019, *arXiv:1909.06503*.
- [10] M. Wang and Y. Zeng, “Multiway clustering via tensor block models,” in *Proc. Adv. Neural Inf. Process. Syst.*, vol. 32, 2019, pp. 715–725.
- [11] E. Abbe, “Community detection and stochastic block models: Recent developments,” *J. Mach. Learn. Res.*, vol. 18, pp. 1–86, Jan. 2018.
- [12] E. C. Chi, B. J. Gaines, W. W. Sun, H. Zhou, and J. Yang, “Provable convex co-clustering of tensors,” *J. Mach. Learn. Res.*, vol. 21, no. 214, pp. 1–58, 2020.
- [13] R. Han, Y. Luo, M. Wang, and A. R. Zhang, “Exact clustering in tensor block model: Statistical optimality and computational limit,” *J. Roy. Stat. Soc., Ser. B, Stat. Methodol.*, vol. 84, no. 5, pp. 1666–1698, Nov. 2022.

- | | | |
|------|---|------|
| 2990 | [14] P. J. Bickel and A. Chen, "A nonparametric view of network models and | 3035 |
| 2991 | Newman–Girvan and other modularities," <i>Proc. Nat. Acad. Sci. USA</i> , | 3036 |
| 2992 | vol. 106, no. 50, pp. 21068–21073, 2009. | 3037 |
| 2993 | [15] C. Gao, Z. Ma, A. Y. Zhang, and H. H. Zhou, "Community detection in degree-corrected block models," <i>Ann. Statist.</i> , vol. 46, no. 5, | 3038 |
| 2994 | pp. 2153–2185, Oct. 2018. | 3039 |
| 2995 | [16] K. Ahn, K. Lee, and C. Suh, "Hypergraph spectral clustering in the | 3040 |
| 2996 | weighted stochastic block model," <i>IEEE J. Sel. Topics Signal Process.</i> , | 3041 |
| 2997 | vol. 12, no. 5, pp. 959–974, Oct. 2018. | 3042 |
| 2998 | [17] M. Yuan, R. Liu, Y. Feng, and Z. Shang, "Testing community structure | 3043 |
| 2999 | for hypergraphs," <i>Ann. Statist.</i> , vol. 50, no. 1, pp. 147–169, Feb. 2022. | 3044 |
| 3000 | [18] Y. Chi, Y. M. Lu, and Y. Chen, "Nonconvex optimization meets low- | 3045 |
| 3001 | rank matrix factorization: An overview," <i>IEEE Trans. Signal Process.</i> , | 3046 |
| 3002 | vol. 67, no. 20, pp. 5239–5269, Oct. 2019. | 3047 |
| 3003 | [19] S.-Y. Yun and A. Proutiere, "Optimal cluster recovery in the labeled | 3048 |
| 3004 | stochastic block model," in <i>Proc. Adv. Neural Inf. Process. Syst.</i> , vol. 29, | 3049 |
| 3005 | 2016, pp. 973–981. | 3050 |
| 3006 | [20] C. Kim, A. S. Bandeira, and M. X. Goemans, "Stochastic block | 3051 |
| 3007 | model for hypergraphs: Statistical limits and a semidefinite programming | 3052 |
| 3008 | approach," 2018, <i>arXiv:1807.02884</i> . | 3053 |
| 3009 | [21] L. De Lathauwer, B. De Moor, and J. Vandewalle, "A multilinear | 3054 |
| 3010 | singular value decomposition," <i>SIAM J. Matrix Anal. Appl.</i> , vol. 21, | 3055 |
| 3011 | no. 14, pp. 1253–1278, 2006. | 3056 |
| 3012 | [22] Z. Zhang, G. I. Allen, H. Zhu, and D. Dunson, "Tensor network | 3057 |
| 3013 | factorizations: Relationships between brain structural connectomes and | |
| 3014 | traits," <i>NeuroImage</i> , vol. 197, pp. 330–343, Aug. 2019. | |
| 3015 | [23] A. Zhang and D. Xia, "Tensor SVD: Statistical and computational | |
| 3016 | limits," <i>IEEE Trans. Inf. Theory</i> , vol. 64, no. 11, pp. 7311–7338, | |
| 3017 | Nov. 2018. | |
| 3018 | [24] M. Brennan and G. Bresler, "Reducibility and statistical-computational | |
| 3019 | gaps from secret leakage," in <i>Proc. 33rd Conf. Learn. Theory</i> , vol. 125, | |
| 3020 | 2020, pp. 648–847. | |
| 3021 | [25] Y. Lu and H. H. Zhou, "Statistical and computational guarantees of | |
| 3022 | Lloyd's algorithm and its variants," 2016, <i>arXiv:1612.02099</i> . | |
| 3023 | [26] E. Abbe, J. Fan, K. Wang, and Y. Zhong, "Entrywise eigenvector analysis | |
| 3024 | of random matrices with low expected rank," <i>Ann. Statist.</i> , vol. 48, no. 3, | |
| 3025 | pp. 1452–1474, Jun. 2020. | |
| 3026 | [27] C. Mu, B. Huang, J. Wright, and D. Goldfarb, "Square deal: Lower | |
| 3027 | bounds and improved relaxations for tensor recovery," in <i>Proc. 31th Int.</i> | |
| 3028 | <i>Conf. Mach. Learn. (ICML)</i> , vol. 32, 2014, pp. 73–81. | |
| 3029 | [28] L. Florescu and W. Perkins, "Spectral thresholds in the bipartite stochastic | |
| 3030 | block model," in <i>Proc. 29th Conf. Learn. Theory</i> , vol. 49, 2016, | |
| 3031 | pp. 943–959. | |
| 3032 | [29] C. Gao and A. Y. Zhang, "Iterative algorithm for discrete structure | |
| 3033 | recovery," <i>Ann. Statist.</i> , vol. 50, no. 2, pp. 1066–1094, Apr. 2022. | |
| 3034 | | |
| | [30] I. E. Chien, C.-Y. Lin, and I.-H. Wang, "On the minimax misclassification | |
| | ratio of hypergraph community detection," <i>IEEE Trans. Inf. Theory</i> , | |
| | vol. 65, no. 12, pp. 8095–8118, Dec. 2019. | |
| | [31] M. Meilă, "Local equivalences of distances between clusterings—A | |
| | geometric perspective," <i>Mach. Learn.</i> , vol. 86, no. 3, pp. 369–389, | |
| | Mar. 2012. | |
| | [32] D. C. Van Essen et al., "The WU-minn human connectome project: | |
| | An overview," <i>NeuroImage</i> , vol. 80, pp. 62–79, Oct. 2013. | |
| | [33] R. S. Desikan et al., "An automated labeling system for subdividing | |
| | the human cerebral cortex on MRI scans into gyral based regions of | |
| | interest," <i>NeuroImage</i> , vol. 31, no. 3, pp. 968–980, Jul. 2006. | |
| | [34] J. Hu, C. Lee, and M. Wang, "Generalized tensor decomposition with | |
| | features on multiple modes," <i>J. Comput. Graph. Statist.</i> , vol. 31, no. 1, | |
| | pp. 204–218, Jan. 2022. | |
| | [35] S. H. Lee, J. M. Magallanes, and M. A. Porter, "Time-dependent com- | |
| | munity structure in legislation cosponsorship networks in the congress | |
| | of the republic of Peru," <i>J. Complex Netw.</i> , vol. 5, no. 1, pp. 127–144, | |
| | 2017. | |
| | [36] P. Rigollet and J.-C. Hütter, "High dimensional statistics," <i>Lect. Notes</i> | |
| | <i>Course 18S997</i> , vol. 813, no. 814, p. 46, 2015. | |
| | [37] R. Han, R. Willett, and A. R. Zhang, "An optimal statistical and com- | |
| | putational framework for generalized tensor estimation," <i>Ann. Statist.</i> , | |
| | vol. 50, no. 1, pp. 1–29, Feb. 2022. | |

Jiaxin Hu received the B.S. degree from Wuhan University in 2019 and the master's degree in statistics from the University of Wisconsin–Madison in 2020, where she is currently pursuing the Ph.D. degree with the Department of Statistics. Her research interests include tensor methods, network analysis, and applications in genetics and social science.

Miaoyan Wang received the B.S. degree in mathematics from Fudan University in 2010 and the Ph.D. degree in statistics from the University of Chicago in 2015. She is currently an Assistant Professor of statistics at the University of Wisconsin–Madison. She is also a Faculty Affiliate with the Mathematical Foundations of Machine Learning and the Institute for Foundations of Data Science. Her research interests include the intersection of statistics, machine learning, and genetics. She was a recipient of NSF CAREER Award in 2022, Best Student Paper Awards (with her as an Advisor) from American Statistical Association (three times in 2021, 2022, and 2023), and New England Statistical Society in 2022.

AUTHOR QUERIES

AUTHOR PLEASE ANSWER ALL QUERIES

PLEASE NOTE: We cannot accept new source files as corrections for your article. If possible, please annotate the PDF proof we have sent you with your corrections and upload it via the Author Gateway. Alternatively, you may send us your corrections in list format. You may also upload revised graphics via the Author Gateway.

Carefully check the page proofs (and coordinate with all authors); additional changes or updates WILL NOT be accepted after the article is published online/print in its final form. Please check author names and affiliations, funding, as well as the overall article for any errors prior to sending in your author proof corrections. Your article has been peer reviewed, accepted as final, and sent in to IEEE. No text changes have been made to the main part of the article as dictated by the editorial level of service for your publication.

AQ:1 = Please confirm or add details for any funding or financial support for the research of this article.

AQ:2 = Please provide the expansion of the acronym CAREER for your funding agency. Providing the correct acknowledgment will ensure proper credit to the funder.

AQ:3 = Please provide the DOI of the earlier version of this paper.

AQ:4 = Please check the Associate Editor line in the first footnote for correctness.

AQ:5 = Please confirm the retention of the content in the acknowledgment section.

Multiway Spherical Clustering via Degree-Corrected Tensor Block Models

Jiaxin Hu[✉] and Miaoyan Wang[✉]

Abstract— We consider the problem of multiway clustering in the presence of unknown degree heterogeneity. Such data problems arise commonly in applications such as recommendation system, neuroimaging, community detection, and hypergraph partitions in social networks. The allowance of degree heterogeneity provides great flexibility in clustering models, but the extra complexity poses significant challenges in both statistics and computation. Here, we develop a degree-corrected tensor block model with estimation accuracy guarantees. We present the phase transition of clustering performance based on the notion of angle separability, and we characterize three signal-to-noise regimes corresponding to different statistical-computational behaviors. In particular, we demonstrate that an intrinsic statistical-to-computational gap emerges only for tensors of order three or greater. Further, we develop an efficient polynomial-time algorithm that provably achieves exact clustering under mild signal conditions. The efficacy of our procedure is demonstrated through two data applications, one on human brain connectome project, and another on Peru Legislation network dataset.

Index Terms— Tensor clustering, degree correction, statistical computational efficiency, human brain connectome networks.

I. INTRODUCTION

MULTIWAY arrays have been widely collected in various fields including social networks [1], neuroscience [2], and computer science [3]. Tensors effectively represent the multiway data and serve as the foundation in higher-order data analysis. One data example is from multi-tissue multi-individual gene expression study [4], [5], where the data tensor consists of expression measurements indexed by (gene, individual, tissue) triplets. Another example is *hypergraph* network [6], [7], [8], [9] in social science. A K -uniform hypergraph can be naturally represented as an order- K tensor, where each entry indicates the presence of K -way hyperedge among nodes (a.k.a. entities). In both examples, identifying the similarity among tensor entities is important for scientific discovery.

AQ:1
AQ:2
AQ:3
AQ:4
AQ:5
AQ:6
AQ:7
AQ:8
AQ:9
AQ:10
AQ:11
AQ:12
AQ:13
AQ:14
AQ:15
AQ:16
AQ:17
AQ:18
AQ:19
AQ:20
AQ:21
AQ:22
AQ:23
AQ:24
AQ:25
AQ:26
AQ:27
AQ:28
AQ:29
AQ:30
AQ:31
AQ:32
AQ:33
AQ:34
AQ:35
AQ:36
AQ:37
AQ:38
AQ:39
AQ:40
AQ:41
AQ:42
AQ:43
AQ:44
AQ:45
AQ:46
AQ:47
AQ:48
AQ:49
AQ:50
AQ:51
AQ:52
AQ:53
AQ:54
AQ:55
AQ:56
AQ:57
AQ:58
AQ:59
AQ:60
AQ:61
AQ:62
AQ:63
AQ:64
AQ:65
AQ:66
AQ:67
AQ:68
AQ:69
AQ:70
AQ:71
AQ:72
AQ:73
AQ:74
AQ:75
AQ:76
AQ:77
AQ:78
AQ:79
AQ:80
AQ:81
AQ:82

Manuscript received 18 January 2022; revised 23 December 2022; accepted 6 January 2023. The work of Miaoyan Wang was supported in part by NSF CAREER under Grant DMS-2141865, Grant DMS-1915978, Grant DMS-2023239, and Grant EF-2133740; and in part by the Wisconsin Alumni Research Foundation. An earlier version of this paper was presented in part at the 25th International Conference on Artificial Intelligence and Statistics (AISTATS). (Corresponding author: Miaoyan Wang.)

The authors are with the Department of Statistics, University of Wisconsin-Madison, Madison, WI 53706 USA (e-mail: jhu267@wisc.edu; miaoyan.wang@wisc.edu).

Communicated by R. Venkataraman, Associate Editor for Machine Learning.

Color versions of one or more figures in this article are available at <https://doi.org/10.1109/TIT.2023.3239521>.

Digital Object Identifier 10.1109/TIT.2023.3239521

We study the problem of multiway clustering based on a data tensor. The goal of multiway clustering is to identify a checkerboard structure from a noisy data tensor. Figure 1 illustrates the noisy tensor and the underlying checkerboard structures discovered by multiway clustering methods. In the hypergraph example, the multiway clustering aims to identify the underlying block partition of nodes based on their higher-order connectivities; therefore, we also refer to the clustering as *higher-order clustering*. The most common model for higher-order clustering is called *tensor block model* (TBM) [10], which extends the usual matrix stochastic block model [11] to tensors. The matrix analysis tools, however, are sub-optimal for higher-order clustering. Developing tensor tools for solving block models has received increased interest recently [10], [12], [13].

The classical tensor block model suffers from drawbacks to model real world data in spite of the popularity. The key underlying assumption of block model is that all nodes in the same community are exchangeable; i.e., the nodes have no individual-specific parameters apart from the community-specific parameters. However, the exchangeability assumption is often non-realistic. Each node may contribute to the data variation by its own multiplicative effect. We call the unequal node-specific effects the *degree heterogeneity*. Such degree heterogeneity appears commonly in social networks. Ignoring the degree heterogeneity may seriously mislead the clustering results. For example, the regular block model fails to model the member affiliation in the Karate Club network [14] without addressing degree heterogeneity.

The *degree-corrected tensor block model* (dTBM) has been proposed recently to account for the degree heterogeneity [9]. The dTBM combines a higher-order checkerboard structure with degree parameter $\theta = (\theta(1), \dots, \theta(p))^T$ to allow heterogeneity among p nodes. Figure 1 compares the underlying structures of TBM and dTBM with the same number of communities. The dTBM allows varying values within the same community, thereby allowing a richer structure. To solve dTBM, we project clustering objects to a unit sphere and perform iterative clustering based on angle similarity. We refer to the algorithm as the *spherical clustering*; detailed procedures are in Section IV. The spherical clustering avoids the estimation of nuisance degree heterogeneity. The usage of angle similarity brings new challenges to the theoretical results, and we develop new polar-coordinate based techniques in the proofs.

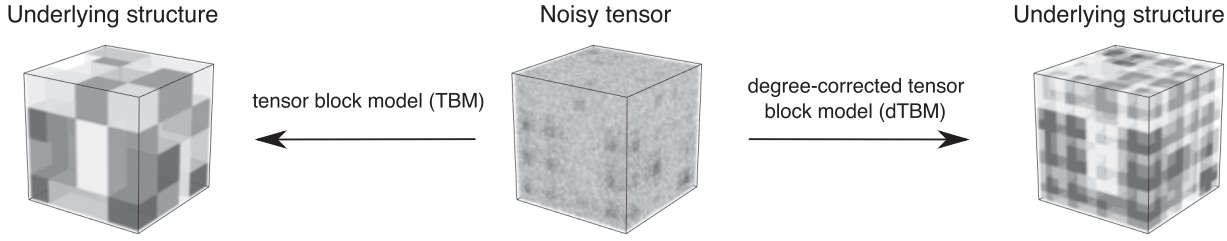


Fig. 1. Examples for order-3 tensor block model (TBM) with and without degree correction. Both TBM and dTBM have four communities on each mode, while dTBM allows a richer structure with degree heterogeneity.

83 A. Our Contributions

84 The primary goal of this paper is to provide both statistical
85 and computational guarantees for dTBM. Our main contributions
86 are summarized below.

- 87 • We develop a general dTBM and establish the identifiability
88 for the uniqueness of clustering using the notion of angle separability.
- 89 • We present the phase transition of clustering performance
90 with respect to three different statistical and computational behaviors. We characterize, for the first time,
91 the critical signal-to-noise (SNR) thresholds in dTBMs,
92 revealing the intrinsic distinctions among (vector) one-
93 dimensional clustering, (matrix) biclustering, and (ten-
94 sor) higher-order clustering. Specific SNR thresholds and
95 algorithm behaviors are depicted in Figure 2.
- 96 • We provide an angle-based algorithm that achieves exact
97 clustering *in polynomial time* under mild conditions. Sim-
98 ulation and data studies demonstrate that our algorithm
99 outperforms existing higher-order clustering algorithms.

100 The last two contributions, to our best knowledge, are new to
101 the literature of dTBMs.

104 B. Related Work

105 Our work is closely related to but also distinct from several
106 lines of existing research. Table I summarizes the most relevant
107 models.

- 108 • *Block model for clustering.* The block model such as
109 stochastic block model (SBM) and degree-corrected SBM
110 has been widely used for matrix clustering problems.
111 The theoretical properties and algorithm performance for
112 matrix block models have been well-studied [15]; see the
113 review paper [11] and the references therein. However,
114 The tensor counterparts are relatively less understood.
- 115 • *Tensor block model.* The (non-degree) tensor block model
116 (TBM) is a higher-order extension of SBM, and its
117 statistical-computational properties are investigated in
118 recent literatures [7], [10], [13]. Some works [16] study
119 the TBM with sparse observations, while, others [10],
120 [13] and our work focus on the dense regime. Extending
121 results from non-degree to degree-corrected model
122 is highly challenging. Our dTBM parameter space is
123 equipped with angle-based similarity and nuisance degree
124 parameters. The extra complexity makes the Cartesian
125 coordinates based analysis [13] non-applicable to our
126 setting. Towards this goal, we have developed a new polar

127 coordinates based analysis to control the model complex-
128 ity. We have also developed a new angle-based iteration
129 algorithm to achieve optimal clustering rates *without the*
130 *need of estimating nuisance degree parameters.*

- 131 • *Degree-corrected block model.* The hypergraph
132 degree-corrected block model (hDCBM) and its
133 variant have been proposed in the literature [9],
134 [17]. For this popular model, however, the optimal
135 statistical-computational rates remain an open problem.
136 Our main contribution is to provide a sharp statistical
137 and computational critical phase transition in dTBM
138 literature. In addition, our algorithm results in a faster
139 *exponential* error rate, in contrast to the *polynomial*
140 rate in [9]. The original hDCBM [9] is designed for
141 binary observations only, and we extend the model to
142 both continuous and binary observations. We believe
143 our results are novel and helpful to the community. See
144 Figure 2 for overview of our results.
- 145 • *Global-to-local algorithm strategy.* Our methods gen-
146 eralize the recent global-to-local strategy for matrix
147 learning [15], [18], [19] to tensors [13], [16], [20].
148 Despite the conceptual similarity, we address several
149 fundamental challenges associated with this non-convex,
150 non-continuous problem. We show the insufficiency of
151 the conventional tensor HOSVD [21], and we develop
152 a weighted higher-order initialization that relaxes the
153 singular-value gap separation condition. Furthermore,
154 our local iteration leverages the angle-based clustering
155 in order to avoid explicit estimation of degree heteroge-
156 neity. Our bounds reveal the interesting interplay between
157 the computational and statistical errors. We show that
158 our final estimate *provably* achieves the exact clustering
159 within only polynomial-time complexity.

160 C. Notation

161 We use lower-case letters (e.g., a, b) for scalars, lower-case
162 boldface letters (e.g., $\mathbf{a}, \boldsymbol{\theta}$) for vectors, upper-case boldface
163 letters (e.g., \mathbf{X}, \mathbf{Y}) for matrices, and calligraphy letters (e.g.,
164 \mathcal{X}, \mathcal{Y}) for tensors of order three or greater. We use $\mathbf{1}_p$ to denote
165 a vector of length p with all entries to be 1. We use $|\cdot|$ for
166 the cardinality of a set and $\mathbf{1}\{\cdot\}$ for the indicator function. For
167 an integer $p \in \mathbb{N}_+$, we use the shorthand $[p] = \{1, 2, \dots, p\}$.
168 For a length- p vector \mathbf{a} , we use $a(i) \in \mathbb{R}$ to denote the i -th
169 entry of \mathbf{a} , and use \mathbf{a}_I to denote the sub-vector by restricting
170 the indices in the set $I \subset [p]$. We use $\|\mathbf{a}\| = \sqrt{\sum_i a^2(i)}$ to
171 denote the ℓ_2 -norm, $\|\mathbf{a}\|_1 = \sum_i |a_i|$ to denote the ℓ_1 norm of

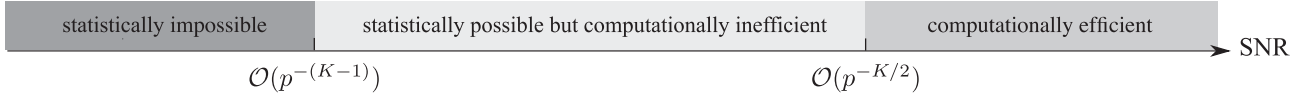


Fig. 2. SNR thresholds for statistical and computational limits in order- K dTBM with dimension (p, \dots, p) and $K \geq 2$. The SNR gap between statistical possibility and computational efficiency exists only for tensors with $K \geq 3$.

TABLE I

COMPARISON BETWEEN PREVIOUS METHODS WITH OUR METHOD. *WE LIST THE RESULT FOR ORDER- K TENSORS WITH $K \geq 3$ AND GENERAL NUMBER OF COMMUNITIES $r = \mathcal{O}(1)$. **THE PARAMETER $\alpha = f(p) > 0$ DENOTES THE SPARSITY LEVEL WHICH IS SOME FUNCTION OF DIMENSION p

	Gao et al. (2018)[15]	Ahn et al. (2018)[16]	Han et al. (2022)[13]	Ghoshdastidar et al. (2019)[7]	Ke et al. (2019)[9]	Ours
Allow tensors of arbitrary order	×	✓	✓	✓	✓	✓
Allow degree heterogeneity	✓	✗	✗	✓	✓	✓
Singular-value gap-free clustering	✓	✓	✓	✗	✗	✓
Misclustering rate (for order K^*)	-	$p^{-(K-1)}\alpha^{-1}**$	$\exp(-p^{K/2})$	p^{-1}	p^{-2}	$\exp(-p^{K/2})$
Consider sparse observation	✗	✓	✗	✗	✗	✗

- 172 a. For two vector \mathbf{a}, \mathbf{b} of the same dimension, we denote the
173 angle between \mathbf{a}, \mathbf{b} by

$$174 \cos(\mathbf{a}, \mathbf{b}) = \frac{\langle \mathbf{a}, \mathbf{b} \rangle}{\|\mathbf{a}\| \|\mathbf{b}\|},$$

175 where $\langle \mathbf{a}, \mathbf{b} \rangle$ is the inner product of two vectors and
176 $\cos(\mathbf{a}, \mathbf{b}) \in [-1, 1]$. We make the convention that $\cos(\mathbf{a}, \mathbf{b}) =$
177 $\cos(\mathbf{a}^T, \mathbf{b}^T)$.

178 Let $\mathcal{Y} \in \mathbb{R}^{p_1 \times \dots \times p_K}$ be an order- K (p_1, \dots, p_K) -
179 dimensional tensor. We use $\mathcal{Y}(i_1, \dots, i_K)$ to denote the
180 (i_1, \dots, i_K) -th entry of \mathcal{Y} . The multilinear multiplication of a
181 tensor $\mathcal{S} \in \mathbb{R}^{r_1 \times \dots \times r_K}$ by matrices $\mathbf{M}_k \in \mathbb{R}^{p_k \times r_k}$ results in
182 an order- K (p_1, \dots, p_K) -dimensional tensor \mathcal{X} , denoted

$$183 \mathcal{X} = \mathcal{S} \times_1 \mathbf{M}_1 \times \dots \times_K \mathbf{M}_K,$$

184 where the entries of \mathcal{X} are defined by

$$185 \mathcal{X}(i_1, \dots, i_K) \\ 186 = \sum_{(j_1, \dots, j_K)} \mathcal{S}(j_1, \dots, j_K) \mathbf{M}_1(i_1, j_1) \dots \mathbf{M}_K(i_K, j_K).$$

187 For a matrix \mathbf{Y} , we use $\mathbf{Y}_{:i}$ (respectively, $\mathbf{Y}_{i:}$) to denote the
188 i -th row (respectively, i -th column) of the matrix. Similarly,
189 for an order-3 tensor, we use $\mathcal{Y}_{::i}$ to denote the i -th matrix
190 slide of the tensor. We use $\text{Ave}(\cdot)$ to denote the operation of
191 taking averages across elements and $\text{Mat}_k(\cdot)$ to denote the
192 unfolding operation that reshapes the tensor along mode k
193 into a matrix. For a symmetric tensor $\mathcal{X} \in \mathbb{R}^{p \times \dots \times p}$, we omit
194 the subscript and use $\text{Mat}(\mathcal{X}) \in \mathbb{R}^{p \times p^{K-1}}$ to denote the
195 unfolding. For two sequences $\{a_p\}, \{b_p\}$, we denote $a_p \lesssim b_p$
196 or $a_p = \mathcal{O}(b_p)$ if $\lim_{p \rightarrow \infty} a_p/b_p \leq c$, $a_p \gtrsim b_p$ or $a_p = \Omega(b_p)$
197 if $\lim_{p \rightarrow \infty} a_p/b_p \geq c$, for some constant $c > 0$, $a_p = o(b_p)$
198 if $\lim_{p \rightarrow \infty} a_p/b_p = 0$, and $a_p \asymp b_p$ if both $b_p \lesssim a_p$ and
199 $a_p \lesssim b_p$. Throughout the paper, we use the terms ‘‘community’’
200 and ‘‘clusters’’ exchangeably.

201 1) *Organization:* The rest of this paper is organized as
202 follows. Section II introduces the degree-corrected tensor
203 block model (dTBM) with three motivating examples and
204 presents the identifiability of dTBM under the angle gap
205 condition. We show the phase transition and the existence of
206 statistical-computational gaps for the higher-order dTBM in
207 Section III. In Section IV, we provide a polynomial-time two-
208 stage algorithm with misclustering rate guarantees. Extension

209 to Bernoulli models is also presented. In Section V, we com-
210 pare our work with non-degree tensor block models. Numer-
211 ical studies including the simulation, comparison with other
212 methods, and two real dataset analyses are in Sections VI-VII.
213 The main technical ideas we develop for addressing main
214 theorems are provided in Section VIII. Detailed proofs and
215 extra theoretical results are provided in Appendix.

II. MODEL FORMULATION AND MOTIVATIONS

A. Degree-Corrected Tensor Block Model

Suppose that we have an order- K data tensor $\mathcal{Y} \in \mathbb{R}^{p \times \dots \times p}$.
Assume that there exist $r \geq 1$ disjoint communities among the
p nodes. We represent the community assignment by a function
 $z: [p] \mapsto [r]$, where $z(i) = a$ for i -th node that belongs to
the a -th community. Then, $z^{-1}(a) = \{i \in [p]: z(i) = a\}$
denotes the set of nodes that belong to the a -th community,
and $|z^{-1}(a)|$ denotes the number of nodes in the a -th community.
Let $\boldsymbol{\theta} = (\theta(1), \dots, \theta(p))^T$ denote the degree heterogeneity for
p nodes. We consider the order- K dTBM [7], [9],

$$\mathcal{Y}(i_1, \dots, i_K) = \mathcal{S}(z(i_1), \dots, z(i_K)) \prod_{k=1}^K \theta_{i_k} + \mathcal{E}(i_1, \dots, i_K),$$

where $\mathcal{S} \in \mathbb{R}^{r \times \dots \times r}$ is an order- K tensor collecting the block
means among communities, and $\mathcal{E} \in \mathbb{R}^{p \times \dots \times p}$ is a noise tensor
consisting of independent zero-mean sub-Gaussian entries
with variance bounded by σ^2 . The unknown parameters are z ,
 \mathcal{S} , and $\boldsymbol{\theta}$. The dTBM can be equivalently written in a compact
form of tensor-matrix product:

$$\mathbb{E}\mathcal{Y} = \mathcal{S} \times_1 \boldsymbol{\Theta} \mathbf{M} \times_2 \dots \times_K \boldsymbol{\Theta} \mathbf{M}, \quad (1)$$

where $\boldsymbol{\Theta} = \text{diag}(\theta(1), \dots, \theta(p)) \in \mathbb{R}^{p \times p}$ is a diagonal matrix,
 $\mathbf{M} \in \{0, 1\}^{p \times r}$ is the membership matrix associated with
community assignment z such that $\mathbf{M}(i, j) = 1\{z(i) = j\}$.
By definition, each row of \mathbf{M} has one copy of 1’s and
0’s elsewhere. Note that the discrete nature of \mathbf{M} renders
our model (1) more challenging than Tucker decomposition.
We call a tensor \mathcal{Y} an r -block tensor with degree $\boldsymbol{\theta}$ if \mathcal{Y} admits
dTBM (1) and let $\mathcal{X} = \mathbb{E}\mathcal{Y}$ denote the mean tensor. The goal
of clustering is to estimate z from a single noisy tensor \mathcal{Y} .
We are particularly interested in the high-dimensional regime
where p grows whereas $r = \mathcal{O}(1)$.

For ease of notation, we have focused on the case with symmetric mean tensor $\mathbb{E}\mathcal{Y}$. This assumption simplifies the notation because all modes have the same (Θ, M, z) ; the noise tensor \mathcal{E} and the data tensor \mathcal{Y} are still possibly asymmetric. In general, we allow asymmetric mean tensors with $\{(\Theta_k, M_k, z_k)\}_{k=1}^K$, one for each mode. The extension can be found in Appendix B.

B. Motivating Examples

Here, we provide four applications to illustrate the practical necessity of dTBM.

1) *Tensor Block Model*: Consider the model (1). Let $\theta(i) = 1$ for all $i \in [p]$. The model (1) reduces to the tensor block model, which is widely used in previous clustering algorithms [10], [12], [13]. The theoretical results in TBM serve as benchmarks for dTBM.

2) *Community Detection in Hypergraphs*: The hypergraph network is a powerful tool to represent the complex entity relations with higher-order interactions [9]. A typical undirected hypergraph is denoted as $H = (V, E)$, where $V = [p]$ is the set of nodes and E is the set of undirected hyperedges. Each hyperedge in E is a subset of V , and we call the hyperedge an order- K edge if the corresponding subset involves K nodes. We call H a K -uniform hypergraph if E only contains order- K edges.

It is natural to represent the K -uniform hypergraph using a binary order- K adjacency tensor. Let $\mathcal{Y} \in \{0, 1\}^{p \times \dots \times p}$ denote the adjacency tensor, where the entries encode the presence or absence of order- K edges among p nodes. Specifically, for all $(i_1, \dots, i_K) \in [p]^K$, we have

$$\mathcal{Y}(i_1, \dots, i_K) = \begin{cases} 1 & \text{if } (i_1, \dots, i_K) \in E, \\ 0 & \text{if } (i_1, \dots, i_K) \notin E. \end{cases}$$

Assume that there exist r disjoint communities among p nodes, and the connection probabilities depend on the community assignments and node-specific parameters. Then, the equation (1) models $\mathbb{E}\mathcal{Y}$ with unknown degree heterogeneity θ and sub-Gaussianity parameter $\sigma^2 = 1/4$. **Multilayer or multilayer**

3) *Multi-Layer Weighted Network*: Multi-layer weighted network data consists of multiple networks over the same set of nodes. One representative example is the brain connectome data [22]. The multi-layer weighted network \mathcal{Y} has dimension of $p \times p \times L$, where p denotes the number of brain regions of interest, and L denotes the number of layers (networks). Each of the L networks describes one aspect of the brain connectivity, such as functional connectivity or structural connectivity. The resulting tensor \mathcal{Y} consists of a mixture of slices with various data types.

Assume that there exist r disjoint communities among p nodes and r_l disjoint communities among the L layers. The multi-layer network community detection is modeled by the general asymmetric dTBM model (1)

$$\mathbb{E}\mathcal{Y} = \mathcal{S} \times_1 \Theta M \times_2 \Theta M \times_3 \Theta_l M_l,$$

where $(\Theta \in \mathbb{R}^p, M \in \{0, 1\}^{p \times r})$ and $(\Theta_l \in \mathbb{R}^L, M_l \in \{0, 1\}^{L \times r_l})$ are the degree heterogeneity and membership matrices corresponding to the community structure for p nodes and L layers, respectively.

4) *Gaussian Higher-Order Clustering*: Datasets in various fields such as medical image, genetics, and computer science are formulated as Gaussian tensors. One typical example is the multi-tissue gene expression dataset, which records different gene expressions in different individuals and different tissues. The dataset, denoted as $\mathcal{Y} \in \mathbb{R}^{p \times n \times t}$, consists of the expression data for p genes of n individuals in t tissues.

Assume that there exist r_1, r_2, r_3 disjoint clusters for p genes, n individuals, and t tissues, respectively. We apply the general asymmetric dTBM model (1)

$$\mathbb{E}\mathcal{Y} = \mathcal{S} \times_1 \Theta_1 M_1 \times_2 \Theta_2 M_2 \times_3 \Theta_3 M_3,$$

where $\{(\Theta_k, M_k)\}_{k=1}^3$ represents the degree heterogeneity and membership for genes, individuals, and tissues.

Remark 1 (Comparison With Non-Degree Models): Our dTBM uses fewer block parameters than TBM. In particular, every non-degree r_1 -block tensor can be represented by a *degree-corrected* r_2 -block tensor with $r_2 \leq r_1$. In particular, there exist tensors with $r_1 = p$ but $r_2 = 1$, so the reduction in model complexity can be dramatic from p to 1. This fact highlights the benefits of introducing degree heterogeneity in higher-order clustering tasks.

C. Identifiability Under Angle Gap Condition

The goal of clustering is to estimate the partition function z from model (1). For ease of notation, we focus on symmetric tensors; the extension to non-symmetric tensors are similar. We use \mathcal{P} to denote the following parameter space for (z, \mathcal{S}, θ) ,

$$\begin{aligned} \mathcal{P} = & \left\{ (z, \mathcal{S}, \theta) : \theta \in \mathbb{R}_+^p, \frac{c_1 p}{r} \leq |z^{-1}(a)| \leq \frac{c_2 p}{r}, \right. \\ & \left. c_3 \leq \|\text{Mat}(\mathcal{S})_{:a}\| \leq c_4, \|\theta_{z^{-1}(a)}\|_1 = |z^{-1}(a)|, a \in [r] \right\} \end{aligned}$$

where $c_i > 0$'s are universal constants. We briefly describe the rationale of the constraints in (2). First, the entrywise positivity constraint on $\theta \in \mathbb{R}_+^p$ is imposed to avoid sign ambiguity between entries in $\theta_{z^{-1}(a)}$ and \mathcal{S} . This constraint allows the trigonometric cos to describe the angle similarity in the Assumption 1 below and Sub-algorithm 2 in Section IV. Note that the positivity constraint can be achieved without sacrificing model flexibility, by using a slightly larger dimension of \mathcal{S} in the factorization (1); see Example 1 below. Second, recall that the quantity $|z^{-1}(a)|$ denotes the number of nodes in the a -th community. The constants c_1, c_2 in the $|z^{-1}(a)|$ bounds assume the roughly balanced size across r communities. Third, the constant c_3 requires that all slides in \mathcal{S} have non-degenerate norm. Particularly, the lower bound c_3 excludes the purely zero slide to avoid trivial non-identifiability of model (1); see Example 2 below. The upper bound c_4 is a technical constraint to avoid the slides with diverging norm as dimension grows. Lastly, the ℓ_1 normalization $\|\theta_{z^{-1}(a)}\|_1 = |z^{-1}(a)|$ is imposed to avoid the scalar ambiguity between $\theta_{z^{-1}(a)}$ and \mathcal{S} . This constraint, again, incurs no restriction to model flexibility but makes our presentation cleaner. Our constraints in \mathcal{P} are mild compared with previous literature; see Table II for comparison.

352 *Example 1 (Positivity of Degree Parameters):* Here we
 353 provide an example to show the positivity constraint
 354 on $\boldsymbol{\theta}$ incurs no loss on the model flexibility. Consider
 355 an order-3 dTBM with core tensor $\mathcal{S} = 1$ and degree
 356 $\boldsymbol{\theta} = (1, 1, -1, -1)^T$. We have the mean tensor

$$357 \quad \mathcal{X} = \mathcal{S} \times_1 \boldsymbol{\Theta} \mathbf{M} \times_2 \boldsymbol{\Theta} \mathbf{M} \times_3 \boldsymbol{\Theta} \mathbf{M},$$

358 where $\boldsymbol{\Theta} = \text{diag}(\boldsymbol{\theta})$ and $\mathbf{M} = (1, 1, 1, 1)^T$. Note that $\mathcal{X} \in$
 359 $\mathbb{R}^{4 \times 4 \times 4}$ is a 1-block tensor with *mixed-signed* degree $\boldsymbol{\theta}$, and
 360 the mode-3 slices of \mathcal{X} are

$$361 \quad \mathcal{X}_{::1} = \mathcal{X}_{::2} = -\mathcal{X}_{::3} = -\mathcal{X}_{::4} = \begin{bmatrix} 1 & 1 & -1 & -1 \\ 1 & 1 & -1 & -1 \\ -1 & -1 & 1 & 1 \\ -1 & -1 & 1 & 1 \end{bmatrix}.$$

362 Now, instead of original decomposition, we encode \mathcal{X} as
 363 a 2-block tensor with *positive-signed* degree. Specifically,
 364 we write

$$365 \quad \mathcal{X} = \mathcal{S}' \times_1 \boldsymbol{\Theta}' \mathbf{M}' \times_2 \boldsymbol{\Theta}' \mathbf{M}' \times_3 \boldsymbol{\Theta}' \mathbf{M}',$$

366 where $\boldsymbol{\Theta}' = \text{diag}(\boldsymbol{\theta}') = \text{diag}(1, 1, 1, 1)$, the core tensor $\mathcal{S}' \in$
 367 $\mathbb{R}^{2 \times 2 \times 2}$ has following mode-3 slices, and the membership
 368 matrix $\mathbf{M}' \in \{0, 1\}^{4 \times 2}$ defines the clustering $z' : [4] \rightarrow [2]$;
 369 i.e.,

$$370 \quad \mathcal{S}'_{::1} = -\mathcal{S}'_{::2} = \begin{bmatrix} 1 & -1 \\ -1 & 1 \end{bmatrix}, \quad \mathbf{M}' = \begin{bmatrix} 1 & 0 \\ 1 & 0 \\ 0 & 1 \\ 0 & 1 \end{bmatrix}.$$

371 The triplet $(z', \mathcal{S}', \boldsymbol{\theta}')$ lies in our parameter space (2). In general, we can always reparameterize an r -block tensor with mixed-signed degree using a $2r$ -block tensor with positive-signed degree. Since we assume $r = \mathcal{O}(1)$ throughout the paper, the splitting does not affect the error rates of our interest.

377 *Example 2 (Non-Identifiability With Purely Zero Core Slice):*
 378 Consider an order-2 dTBM with core tensor $\mathcal{S} = \begin{pmatrix} 0 & 0 \\ 1 & -1 \end{pmatrix}$
 379 degree matrices $\boldsymbol{\Theta}_1 = \boldsymbol{\Theta}_2 = \text{diag}(1, 1, 1, 1)$, and mean tensor

$$380 \quad \mathcal{X} = \boldsymbol{\Theta}_1 \mathbf{M} \mathcal{S} \mathbf{M}^T \boldsymbol{\Theta}_2, \quad \text{with } \mathbf{M} = \begin{bmatrix} 1 & 0 \\ 1 & 0 \\ 0 & 1 \\ 0 & 1 \end{bmatrix}.$$

381 Replacing $\boldsymbol{\Theta}_1$ by $\boldsymbol{\Theta}'_1 = (3/2, 1/2, 1, 1)$ leads to the same
 382 mean tensor \mathcal{X} .

383 We now provide the identifiability conditions for our model
 384 before estimation procedures. When $r = 1$, the decomposition
 385 in (1) is always unique (up to cluster label permutation) in \mathcal{P} ,
 386 because dTBM is equivalent to the rank-1 tensor family under
 387 this case. When $r \geq 2$, the Tucker rank of signal tensor $\mathbb{E}\mathcal{Y}$
 388 in (1) is bounded by, but not necessarily equal to, the number
 389 of blocks r [10]. Therefore, one can not apply the classical
 390 identifiability conditions for low-rank tensors to dTBM. Here,
 391 we introduce a key separation condition on the core tensor.

392 *Assumption 1 (Angle Gap):* Let $\mathbf{S} = \text{Mat}(\mathcal{S})$. Assume that
 393 the minimal gap between normalized rows of \mathbf{S} is bounded

away from zero; i.e.,

$$394 \quad \Delta_{\min} := \min_{a \neq b \in [r]} \left\| \frac{\mathbf{S}_{a:}}{\|\mathbf{S}_{a:}\|} - \frac{\mathbf{S}_{b:}}{\|\mathbf{S}_{b:}\|} \right\| > 0, \quad \text{for } r \geq 2. \quad (3)$$

We make the convention $\Delta_{\min} = 1$ for $r = 1$. Equivalently, (3) says that none of the two rows in \mathbf{S} are parallel; i.e., $\max_{a \neq b \in [r]} \cos(\mathbf{S}_{a:}, \mathbf{S}_{b:}) = 1 - \Delta_{\min}^2/2 < 1$. The quantity Δ_{\min} characterizes the non-redundancy among clusters measured by angle separation. The denominators involved in definition (3) are well posed because of the lower bound on $\|\mathbf{S}_{a:}\|$ in (2).

Our first main result is the following theorem showing the sufficiency and necessity of the angle gap separation condition for the parameter identifiability under dTBM.

Theorem 1 (Model Identifiability): Consider the dTBM with $r \geq 2$ and $K \geq 2$. The parameterization (1) is unique in \mathcal{P} up to cluster label permutations, if and only if Assumption 1 holds.

The identifiability guarantee for the dTBM is stronger than classical Tucker model. In the Tucker model, the factor matrix \mathbf{M} is identifiable only up to orthogonal rotations. In contrast, our model does not suffer from rotational invariance. As we will show in Section IV, each column of the membership matrix \mathbf{M} can be precisely recovered under our algorithm. This property benefits the interpretation of dTBM in practice.

III. STATISTICAL-COMPUTATIONAL CRITICAL VALUES FOR HIGHER-ORDER TENSORS

A. Assumptions

We propose the signal-to-noise ratio (SNR),

$$417 \quad \text{SNR} := \Delta_{\min}^2 / \sigma^2 = p^\gamma, \quad (4)$$

422 with varying $\gamma \in \mathbb{R}$ that quantifies different regimes of
 423 interest. We call γ the *signal exponent*. Intuitively, a larger
 424 SNR, or equivalently a larger γ , benefits the clustering in the
 425 presence of noise. With quantification (4), we consider the
 426 following parameter space,

$$427 \quad \mathcal{P}(\gamma) = \mathcal{P} \cap \{\mathcal{S} \text{ satisfies SNR condition (4) with } \gamma\}. \quad (5)$$

428 The 1-block dTBM does not belong to the space $\mathcal{P}(\gamma)$ when
 429 $\gamma < 0$, due to the convention in Assumption 1. Our goal is to
 430 characterize the clustering accuracy with respect to γ under
 431 the space $\mathcal{P}(\gamma)$.

432 In our algorithmic development, we often refer to the
 433 regime of balanced degree heterogeneity. We call the degree
 434 $\boldsymbol{\theta}$ *balanced* if

$$435 \quad \min_{a \in [r]} \|\boldsymbol{\theta}_{z^{-1}(a)}\| = (1 + o(1)) \max_{a \in [r]} \|\boldsymbol{\theta}_{z^{-1}(a)}\|. \quad (6)$$

436 The following lemma provides the rationale of balanced degree
 437 assumption. We show the close relation between angle gaps
 438 in the mean tensor \mathcal{X} and the core tensor \mathcal{S} under balanced
 439 degree heterogeneity.

440 *Lemma 1 (Angle Gaps in \mathcal{X} and \mathcal{S}):* Consider the dTBM
 441 model (1) under the parameter space \mathcal{P} in (2) with $r \geq 2$.
 442 Suppose $\boldsymbol{\theta}$ is balanced satisfying (6) and $\min_{i \in [p]} \theta(i) \geq c$

TABLE II
PARAMETER SPACE COMPARISON BETWEEN PREVIOUS WORK WITH OUR ASSUMPTION

Assumptions in parameter space	Gao et al. (2018)[15]	Han et al. (2022)[13]	Ke et al. (2019)[9]	Ours
Balanced community sizes	✓	✓	✓	✓
Bounded core tensors	✓	✗	✓	✓
Balanced degrees	✓	-	✓	✓
Flexible in-group connections	✗	✓	✓	✓
Gaps among cluster centers	In-between cluster difference	Euclidean gap	Eigen gap	Angle gap

from some constant $c > 0$. Then, as $p \rightarrow \infty$, for all i, j such that $z(i) \neq z(j)$, we have

$$\cos(\mathbf{X}_{i:}, \mathbf{X}_{j:}) \asymp \cos(\mathbf{S}_{z(i):}, \mathbf{S}_{z(j):}),$$

where $\mathbf{X} = \text{Mat}(\mathcal{X})$ and $\mathbf{S} = \text{Mat}(\mathcal{S})$.

In practice, an estimation algorithm has access to a noisy version of \mathcal{X} but not \mathcal{S} . Our goal is to establish the algorithm performance with respect to the signal Δ_{\min}^2 in the core tensor. By Lemma 1, the mapping from the core tensor $\mathbf{S}_{z(i)}$ to the mean tensor $\mathbf{X}_{z(i)}$ preserves the angle information Δ_{\min}^2 under balanced degree heterogeneity (6). Therefore, the balanced degree assumption helps to exclude the cases in which the degree heterogeneity distorts the algorithm guarantees.

Here, we provide an example to illustrate the insufficiency of Δ_{\min}^2 in the absence of balanced degrees.

Example 3 (Insufficiency of Δ_{\min}^2 in the Absence of Balanced Degrees): Consider an order-2 (p, p) -dimensional dTBM with core matrix

$$\mathbf{S} = \begin{pmatrix} 1 & a \\ 1 & -a \end{pmatrix}, \quad (7)$$

and $\boldsymbol{\theta}$ such that $\|\boldsymbol{\theta}_{z^{-1}(1)}\|^2 = p^m \|\boldsymbol{\theta}_{z^{-1}(2)}\|^2$, where $m \in [-1, 1]$ is a scalar parameter controlling the skewness of degrees. Let $\Delta_{\mathbf{X}}^2$ denote the minimal angle gap of the mean tensor, defined by

$$\Delta_{\mathbf{X}}^2 := \min_{i,j \in [p], z(i) \neq z(j)} \left\| \frac{\mathbf{X}_{i:}}{\|\mathbf{X}_{i:}\|} - \frac{\mathbf{X}_{j:}}{\|\mathbf{X}_{j:}\|} \right\|, \quad (8)$$

where $\mathbf{X} = \text{Mat}(\mathcal{X})$. Take $a = p^{-1/4}$ in the model setup (7). We have

$$\begin{aligned} \Delta_{\min}^2 &= \frac{2a^2}{1+a^2} \asymp p^{-1/2}, \\ \Delta_{\mathbf{X}}^2 &= \frac{2\|\boldsymbol{\theta}_{z^{-1}(2)}\|^2 a^2}{\|\boldsymbol{\theta}_{z^{-1}(1)}\|^2 + \|\boldsymbol{\theta}_{z^{-1}(2)}\|^2 a^2} \asymp p^{-1/2-m}. \end{aligned}$$

Based on the Theorem 2 in Section III, the dTBM is impossible to solve when $\Delta_{\mathbf{X}}^2 \lesssim p^{-1}$ even though $\Delta_{\min}^2 \asymp p^{-1/2}$; that is, the dTBM estimation depends on the relative magnitude of m vs. $1/2$. In such a setting, the proposed signal notion Δ_{\min}^2 alone fails to fully characterize dTBM.

Remark 2 (Flexibility in Balanced Degree Assumption): One important note is that our balance assumption (6) does not preclude the mild degree heterogeneity. In fact, within each of the clusters, we allow the highest degree at the order $\mathcal{O}(p)$, whereas the lowest degree at the order $\Omega(1)$. This range is more relaxed than previous work [15] that restricts the highest degree in the sub-linear regime $o(p)$ and the lowest degree at the order $\Omega(1)$.

Remark 3 (Similar Assumptions in Literature): Similar degree regulations are not rare in literature. In higher-order tensor model [9], the degree assumption $\max_{a \in [r]} \|\boldsymbol{\theta}_{z^{-1}(a)}\| \leq C \min_{a \in [r]} \|\boldsymbol{\theta}_{z^{-1}(a)}\|$ is made to ensure degree balance across communities. In [15], the degree distribution is restricted to $\frac{1}{|z^{-1}(a)|} \sum_{i \in z^{-1}(a)} \theta_i = 1 + o(1)$ for all communities.

Last, let \hat{z} and z be the estimated and true clustering functions in the family (2). Define the misclustering error by

$$\ell(\hat{z}, z) = \frac{1}{p} \min_{\pi \in \Pi} \sum_{i \in [p]} \mathbb{1}\{\hat{z}(i) \neq \pi \circ z(i)\}, \quad (492)$$

where $\pi : [r] \mapsto [r]$ is a permutation of cluster labels, \circ denotes the composition operation, and Π denotes the collection of all possible permutations. The infimum over all permutations accounts for the ambiguity in cluster label permutation.

In Sections III-B and III-C, we provide the phase transition of $\ell(\hat{z}, z)$ for general Gaussian dTBMs (1) without symmetric assumptions. For general (asymmetric) Gaussian dTBMs, we assume Gaussian noise $\mathcal{E}(i_1, \dots, i_K) \stackrel{\text{i.i.d.}}{\sim} N(0, \sigma^2)$, and we extend the parameter space (2) to allow K clustering functions $\{z_k\}_{k \in [K]}$, one for each mode. For notational simplicity, we still use z and $\mathcal{P}(\gamma)$ for this general (asymmetric) model. All results should be interpreted as the worst-case results across K modes.

B. Statistical Critical Value

The statistical critical value means the SNR required for solving dTBMs with *unlimited computational cost*. Our following result shows the minimax lower bound for exact recovery and the matching upper bound for maximum likelihood estimator (MLE). We consider the Gaussian MLE, denoted as $(\hat{z}_{\text{MLE}}, \hat{\mathcal{S}}_{\text{MLE}}, \hat{\boldsymbol{\theta}}_{\text{MLE}})$, over the estimation space \mathcal{P} , where

$$(\hat{z}_{\text{MLE}}, \hat{\mathcal{S}}_{\text{MLE}}, \hat{\boldsymbol{\theta}}_{\text{MLE}}) = \arg \min_{(z, \mathcal{S}, \boldsymbol{\theta}) \in \mathcal{P}} \|\mathcal{Y} - \mathcal{X}(z, \mathcal{S}, \boldsymbol{\theta})\|_F^2. \quad (9)$$

Theorem 2 (Statistical critical value): Consider general Gaussian dTBMs with parameter space $\mathcal{P}(\gamma)$ and $K \geq 2$. Then, we have the following statistical phase transition.

• Impossibility. Assume $p \rightarrow \infty$ and $2 \leq r \lesssim p^{1/3}$. Let $\mathcal{P}_{\mathcal{S}}(\gamma) := \{\mathcal{S} : c_3 \leq \|\text{Mat}(\mathcal{S})_{:a}\| \leq c_4, a \in [r]\} \cap \{\mathcal{S} : \Delta_{\min}^2 = p^\gamma\}$ denote the space for valid \mathcal{S} satisfying SNR condition (4), and $\mathcal{P}_{z, \boldsymbol{\theta}} := \{\boldsymbol{\theta} \in \mathbb{R}_+^p, \frac{c_1 p}{r} \leq |z^{-1}(a)| \leq \frac{c_2 p}{r}, \|\boldsymbol{\theta}_{z^{-1}(a)}\|_1 = |z^{-1}(a)|, a \in [r]\}$ denote the space for valid $(z, \boldsymbol{\theta})$, where c_1, c_2, c_3, c_4 are the constants in parameter space (2). If the signal exponent satisfies $\gamma < -(K-1)$, then, for any true core tensor $\mathcal{S} \in \mathcal{P}_{\mathcal{S}}(\gamma)$, no estimator \hat{z}_{stat} achieves exact recovery in expectation;

526 that is, when $\gamma < -(K - 1)$, we have

$$\liminf_{p \rightarrow \infty} \inf_{\mathcal{S} \in \mathcal{P}_S(\gamma)} \inf_{\hat{z}_{\text{stat}}} \sup_{(z, \theta) \in \mathcal{P}_{z, \theta}} \mathbb{E} [p\ell(\hat{z}_{\text{stat}}, z)] \geq 1. \quad (10)$$

528 Further, we define the parameter space $\mathcal{P}'(\gamma') := \mathcal{P} \cap$
529 $\{\Delta_X^2 = p^{\gamma'}\}$, where Δ_X^2 is the mean tensor minimal gap
530 in (8). When $\gamma' < -(K - 1)$, we have

$$\liminf_{p \rightarrow \infty} \inf_{\hat{z}_{\text{stat}}} \sup_{(z, \mathcal{S}, \theta) \in \mathcal{P}'(\gamma')} \mathbb{E} [p\ell(\hat{z}_{\text{stat}}, z)] \geq 1.$$

- 532 • **MLE achievability.** Suppose that the signal exponent
533 satisfies $\gamma > -(K - 1) + c_0$ for an arbitrary constant
534 $c_0 > 0$. Furthermore, assume that θ is balanced and
535 $\min_{i \in [p]} \theta(i) \geq c$ from some constant $c > 0$. Then, when
536 $p \rightarrow \infty$, for fixed $r \geq 1$, the MLE in (9) achieves exact
537 recovery in high probability; that is,

$$\ell(\hat{z}_{\text{MLE}}, z) \lesssim \text{SNR}^{-1} \exp\left(-\frac{p^{K-1} \text{SNR}}{r^{K-1}}\right) \rightarrow 0,$$

539 with probability going to 1.

540 The proofs for the two parts in Theorem 2 are in the
541 Appendix B, Section B-D and Section B-G, respectively.
542 The first part of Theorem 2 demonstrates impossibility of
543 exact recovery whenever the core tensor \mathcal{S} satisfies SNR
544 condition (4) with exponent $\gamma < -(K - 1)$. The proof is
545 information-theoretical, and therefore the results apply to all
546 statistical estimators, including but not limited to MLE and
547 trace maximization [6]. The minimax bound (10) indicates the
548 worst case impossibility for a particular core tensor \mathcal{S} with
549 signal exponent $\gamma < -(K - 1)$; i.e., under the assumptions of
550 Theorem 2, when $\gamma < -(K - 1)$, we have

$$\liminf_{p \rightarrow \infty} \inf_{\hat{z}_{\text{stat}}} \sup_{(z, \mathcal{S}, \theta) \in \mathcal{P}(\gamma)} \mathbb{E} [p\ell(\hat{z}_{\text{stat}}, z)] \geq 1.$$

552 Such worst case impossibility is studied in related works [13],
553 [15] while our lower bound (10) provides a stronger impossibility
554 statement for arbitrary core tensors with weak signals.
555 The second part of Theorem 2 shows the exact recovery of
556 MLE when $\gamma > -(K - 1) + c_0$ for an arbitrary constant
557 $c_0 > 0$. Combining the impossibility and achievability results,
558 we conclude that the boundary $\gamma_{\text{stat}} := -(K - 1)$ is the critical
559 value for statistical performance of dTBM with respect to our
560 SNR.

561 C. Computational Critical Value

562 The computational critical value means the minimal SNR
563 required for exact recovery with *polynomial-time* computa-
564 tional cost. An important ingredient to establish the computa-
565 tional limits is the *hypergraphic planted clique (HPC) conjec-*
566 *ture* [23], [24]. The HPC conjecture indicates the impossibility
567 of fully recovering the planted cliques with polynomial-time
568 algorithm when the clique size is less than the number of ver-
569 tices in the hypergraph. The formal statement of HPC detection
570 conjecture is provided in Definition 1 and Conjecture 1 as
571 follows.

572 *Definition 1 (Hypergraphic Planted Clique (HPC) Detec-*
573 *tion):* Consider an order- K hypergraph $H = (V, E)$ where

574 $V = [p]$ collects vertices and E collects all the order- K
575 edges. Let $\mathcal{H}_k(p, 1/2)$ denote the Erdős-Rényi K -hypergraph
576 where the edge (i_1, \dots, i_K) belongs to E with probability
577 $1/2$. Further, we let $\mathcal{H}_K(p, 1/2, \kappa)$ denote the hyhpergraph
578 with planted cliques of size κ . Specifically, we generate a
579 hypergraph from $\mathcal{H}_k(p, 1/2)$, pick κ vertices uniformly from
580 $[p]$, denoted K , and then connect all the hyperedges with
581 vertices in K . Note that the clique size κ can be a function of
582 p , denoted κ_p . The order- K HPC detection aims to identify
583 whether there exists a planted clique hidden in an Erdős-
584 Rényi K -hypergraph. The HPC detection is formulated as the
585 following hypothesis testing problem

$$H_0 : H \sim \mathcal{H}_k(p, 1/2) \quad \text{versus} \quad H_1 : H \sim \mathcal{H}_K(p, 1/2, \kappa_p).$$

587 *Conjecture 1 (HPC Conjecture):* Consider the HPC detec-
588 tion problem in Definition 1 with $K \geq 2$. Suppose the
589 sequence $\{\kappa_p\}$ such that $\limsup_{p \rightarrow \infty} \log \kappa_p / \log \sqrt{p} \leq (1 - \tau)$
590 for any $\tau > 0$. Then, for every sequence of polynomial-time
591 test $\{\varphi_p\} : H \mapsto \{0, 1\}$ we have

$$\liminf_{p! \rightarrow \infty} \mathbb{P}_{H_0} (\varphi_p(H) = 1) + \mathbb{P}_{H_1} (\varphi_p(H) = 0) > \frac{1}{2}.$$

593 Under the HPC conjecture, we establish the SNR lower
594 bound that is necessary for any *polynomial-time* estimator to
595 achieve exact clustering.

596 *Theorem 3 (Computational Critical Value):* Consider gen-
597 eral Gaussian dTBMs under the parameter space \mathcal{P} with
598 $K \geq 2$. Then, we have the following computational phase
599 transition.

- 600 • **Impossibility.** Assume HPC conjecture holds and $r \geq$
601 2. If the signal exponent satisfies $\gamma < -K/2$, then,
602 no *polynomial-time estimator* \hat{z}_{comp} achieves exact recov-
603 ery in expectation as $p \rightarrow \infty$; that is, when $\gamma < -K/2$,
604 we have

$$\liminf_{p \rightarrow \infty} \sup_{(z, \mathcal{S}, \theta) \in \mathcal{P}(\gamma)} \mathbb{E} [p\ell(\hat{z}_{\text{comp}}, z)] \geq 1.$$

- 605 • **Polynomial-time algorithm achievability.** Suppose that
606 we have fixed $r \geq 1$, and the signal exponent satisfies
607 $\gamma > -K/2 + c_0$ for an arbitrary constant $c_0 > 0$.
608 Furthermore, assume that the degree θ is balanced, lower
609 bounded in that $\min_{i \in [p]} \theta_i \geq c$ for some constant $c > 0$,
610 and satisfies the locally linear stability in Definition 2 in
611 the neighborhood $\mathcal{N}(z, \varepsilon)$ for all $\varepsilon \leq E_0$ and some $E_0 \gtrsim$
612 $\log^{-1} p$. Then, as $p \rightarrow \infty$, there exists a polynomial-time
613 algorithm \hat{z}_{ploy} that achieves exact recovery in high prob-
614 ability; that is,

$$\ell(\hat{z}_{\text{poly}}, z) \lesssim \text{SNR}^{-1} \exp\left(-\frac{p^{K-1} \text{SNR}}{r^{K-1}}\right) \rightarrow 0,$$

617 with probability going to 1.

618 The proofs for the two parts in Theorem 3 are in the
619 Appendix B, Section B-E and Section B-G, respectively. The
620 first part of Theorem 3 indicates the impossibility of exact
621 recovery by polynomial-time algorithms when $\gamma < -K/2$,
622 and the second part shows the existence of such algorithm
623 when $\gamma > -K/2 + c_0$ for an arbitrary constant $c_0 > 0$ under
624 extra technical assumptions. In Section IV, we will present an

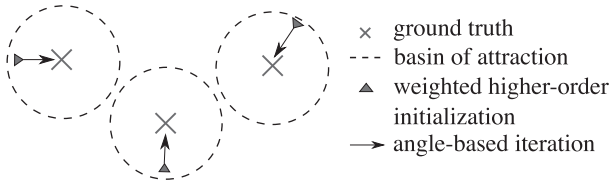


Fig. 3. Illustration of our global-to-local algorithm.

efficient polynomial-time algorithm in this setting. Therefore, we conclude that $\gamma_{\text{comp}} := -K/2$ is the critical value for computational performance of dTBM with respect to our SNR.

Remark 4 (Statistical-Computational Gaps): Now, we have established the phase transition of exact clustering under order- K dTBM by combining Theorems 2 and 3. Figure 2 summarizes our results of critical SNRs when $K \geq 2$. In the weak SNR region $\gamma < -(K-1)$, no statistical estimator succeeds in degree-corrected higher-order clustering. In the strong SNR region $\gamma > -K/2$, our proposed algorithm precisely recovers the clustering in polynomial time. In the moderate SNR regime, $-(K-1) \leq \gamma \leq -K/2$, the degree-corrected clustering problem is statistically easy but computationally hard. Particularly, dTBM reduces to matrix degree-corrected model when $K = 2$, and the statistical and computational bounds show the same critical value. When $K = 1$, dTBM reduces to the degree-corrected sub-Gaussian mixture model (GMM) with model

$$Y = \Theta M S + E,$$

where $Y \in \mathbb{R}^{p \times d}$ collects n data points in \mathbb{R}^d , $S \in \mathbb{R}^{r \times d}$ collects the d -dimensional centroids for r clusters, and $\Theta \in \mathbb{R}^{p \times p}$, $M \in \{0, 1\}^{p \times r}$, $E \in \mathbb{R}^{p \times d}$ have the same meaning as in dTBM. [25] implies that polynomial-time algorithms are able to achieve the statistical minimax lower bound in GMM. Therefore, we conclude that the statistical-computational gap emerges only for higher-order tensors with $K \geq 3$. The result reveals the intrinsic distinctions among (vector) one-dimensional clustering, (matrix) biclustering, and (tensor) higher-order clustering.

IV. POLYNOMIAL-TIME ALGORITHM UNDER MILD SNR

In this section, we present an efficient polynomial-time clustering algorithm under mild SNR. The procedure takes a global-to-local approach. See Figure 3 for illustration. The global step finds the basin of attraction with polynomial misclustering error, whereas the local iterations improve the initial clustering to exact recovery. Both steps are critical to obtain a satisfactory algorithm output. In what follows, we first use the symmetric tensor as a working example to describe the algorithm procedures to gain insight. Our theoretical analysis focuses on dTBMs with symmetric mean tensor and independent sub-Gaussian noises such as Gaussian and uniform observations. The extensions for Bernoulli observations and other practical issues are in Sections IV-C and IV-D.

To construct algorithm guarantees, we introduce the misclustering loss between an estimator \hat{z} and the true z :

$$L(\hat{z}, z) = \frac{1}{p} \sum_{i \in [p]} \theta(i) \sum_{b \in [r]} \mathbb{1}\{\hat{z}(i) = b\} \cdot \|[\mathbf{S}_{z(i)}]_b^s - [\mathbf{S}_b]_b^s\|^2, \quad (11)$$

where the superscript \cdot^s denotes the normalized vector; i.e., $\mathbf{a}^s := \mathbf{a}/\|\mathbf{a}\|$ if $\mathbf{a} \neq 0$ and $\mathbf{a}^s = 0$ if $\mathbf{a} = 0$ for any vector \mathbf{a} . The following lemma indicates the close relationship between the loss $L(\hat{z}, z)$ and error $\ell(\hat{z}, z)$. The loss $L(\hat{z}, z)$ serves as an important intermediate quantity to control the misclustering error.

Lemma 2 (Relationship Between Misclustering Error and Loss): Consider the dTBM under the parameter space \mathcal{P} . Suppose $\min_{i \in [p]} \theta(i) > c$ for some constant $c > 0$. We have $\ell(\hat{z}, z) \Delta_{\min}^2 \leq L(\hat{z}, z)$.

A. Weighted Higher-Order Initialization

We start with weighted higher-order clustering algorithm as initialization. We take an order-3 tensor and the clustering on the first mode as illustration for insight. Consider noiseless case with $\mathcal{X} = \mathbb{E}\mathcal{Y}$ and $\mathbf{X} = \text{Mat}(\mathcal{X})$. By model (1), for all $i \in [p]$, we have

$$\theta(i)^{-1} \mathbf{X}_{i:} = [\text{Mat}(\mathcal{S} \times_2 \Theta M \times_3 \Theta M)]_{z(i)} : .$$

This implies that, all node i belonging to the a -th community (i.e., $z(i) = a$) share the same normalized mean vector $\theta(i)^{-1} \mathbf{X}_{i:}$, and vice versa. Intuitively, one can apply k -means clustering to the vectors $\{\theta(i)^{-1} \mathbf{X}_{i:}\}_{i \in [p]}$, which leads to main idea of our Sub-algorithm 1.

Specifically, our initialization consists of the denoising step and the clustering step. The denoising step (lines 1-2 in Sub-algorithm 1) estimates \mathcal{X} from \mathcal{Y} by a double projection spectral method. The first projection performs HOSVD [21] via $\mathbf{U}_{\text{pre},k} = \text{SVD}_r(\text{Mat}_k(\mathcal{Y}))$, $k \in [3]$, where $\text{SVD}_r(\cdot)$ returns the top- r left singular vectors. The second projection performs HOSVD on the projected \mathcal{Y} onto the multilinear Kronecker space $\mathbf{U}_{\text{pre},k} \otimes \mathbf{U}_{\text{pre},k}$; i.e.,

$$\hat{\mathbf{U}}_1 = \text{SVD}_r(\text{Mat}_1(\mathcal{Y} \times_2 \mathbf{U}_{\text{pre},2} \mathbf{U}_{\text{pre},2}^T \times_3 \mathbf{U}_{\text{pre},3} \mathbf{U}_{\text{pre},3}^T)) .$$

and similar for $\hat{\mathbf{U}}_2, \hat{\mathbf{U}}_3$. The final denoised tensor $\hat{\mathcal{X}}$ is defined by

$$\hat{\mathcal{X}} = \mathcal{Y} \times_1 \hat{\mathbf{U}}_1 \hat{\mathbf{U}}_1^T \times_2 \hat{\mathbf{U}}_2 \hat{\mathbf{U}}_2^T \times_3 \hat{\mathbf{U}}_3 \hat{\mathbf{U}}_3^T .$$

The double projection improves usual matrix spectral methods in order to alleviate the noise effects for $K \geq 3$ [13].

The clustering step (lines 3-5 in Sub-algorithm 1) performs the weighted k -means clustering. We write $\hat{\mathbf{X}} = \text{Mat}_1(\hat{\mathcal{X}})$, and normalize the rows into $\hat{\mathbf{X}}_{i:}^s = \|\hat{\mathbf{X}}_{i:}\|^{-1} \hat{\mathbf{X}}_{i:}$ as a surrogate of $\theta(i)^{-1} \mathbf{X}_{i:}$. Then, a weighted k -means clustering is performed on the normalized rows with weights equal to $\|\hat{\mathbf{X}}_{i:}\|^2$. The choice of weights is to bound the k -means objective function by the Frobenius-norm accuracy of $\hat{\mathcal{X}}$. Unlike existing clustering algorithm [9], we apply the clustering on the unfolded tensor $\hat{\mathbf{X}}$ rather than on the factors $\hat{\mathbf{U}}_k$. This strategy relaxes the singular-value gap condition [13], [15]. We assign

718 degenerate rows with purely zero entries to an arbitrarily
 719 random cluster; these nodes are negligible in high-dimensions
 720 because of the lower bound on $\|\text{Mat}(\mathcal{S})_{a,:}\|$ in (2). The final
 721 result gives the initial cluster assignment $z^{(0)}$. Full procedures
 722 for clustering are provided in Sub-algorithm 1.

723 We now establish the misclustering error rate of initialization.
 724

725 *Theorem 4 (Error for Weighted Higher-Order Initialization):*
 726 Consider the general sub-Gaussian dTBM with fixed $r \geq 1$,
 727 $K \geq 2$, i.i.d. noise under the parameter space \mathcal{P} , and
 728 Assumption 1. Assume $\min_{i \in [p]} \theta(i) \geq c$ for some constant
 729 $c > 0$. Let Δ_X denote the minimal gap in mean tensor defined
 730 in (8), and let $z_k^{(0)}$ denote the output of Sub-algorithm 1.
 731 With probability going to 1, as $p \rightarrow \infty$, we have

$$\ell(z_k^{(0)}, z) \lesssim \frac{\sigma^2 r^K p^{-K/2}}{\Delta_X^2}.$$

732 Further, assume that θ is balanced as (6). We have

$$\ell(z_k^{(0)}, z) \lesssim \frac{r^K p^{-K/2}}{\text{SNR}} \quad \text{and} \quad L(z_k^{(0)}, z) \lesssim \sigma^2 r^K p^{-K/2}, \quad (12)$$

733 with probability going to 1 as $p \rightarrow \infty$.

734 *Remark 5 (Comparison to Previous Results):* For fixed
 735 SNR, our initialization error rate with $K = 2$ agrees with
 736 the initialization error rate $\mathcal{O}(p^{-1})$ in matrix models [15].
 737 Furthermore, in the special case of non-degree TBMs with
 738 $\theta = \mathbf{1}_p$, we achieve the same initial misclustering error
 739 $\mathcal{O}(p^{-K/2})$ as in non-degree models [13]. Theorem 4 implies
 740 the advantage of our algorithm in achieving both accuracy
 741 and model flexibility.

742 *Remark 6 (Failure of Conventional Tensor HOSVD):* If
 743 we use conventional HOSVD for tensor denoising; that is,
 744 we use $\mathbf{U}_{\text{pre},k}$ in place of $\hat{\mathbf{U}}_k$ in line 2, then the misclustering
 745 rate becomes $\mathcal{O}(p^{-1})$ for all $K \geq 2$. This rate is substantially
 746 worse than our current rate (12).

747 *Remark 7 (Singular-Value Gap-Free Clustering):* Note
 748 that our clustering directly applies to the estimated mean
 749 tensor $\hat{\mathcal{X}}$ rather than the leading tensor factors $\hat{\mathbf{U}}_k$.
 750 Applying clustering to the tensor factors suffers from the
 751 non-identifiability issue due to the infinitely many orthogonal
 752 rotations when the number of blocks $r \geq 3$ in the absence
 753 of singular-value gaps. Such ambiguity causes the trouble
 754 for effective clustering [26]. In contrast, our initialization
 755 algorithm applies the clustering to the overall mean tensor $\hat{\mathcal{X}}$.
 756 This strategy avoids the non-identifiability issue regardless of
 757 the number of blocks and singular-value gaps.

760 B. Angle-Based Iteration

761 Our Theorem 4 has shown the polynomially decaying error
 762 rate from our initialization. Now we improve the error rate
 763 to exponential decay using local iterations. We propose an
 764 angle-based local iteration to improve the outputs from Sub-
 765 algorithm 1. To gain the intuition, consider an one-dimensional
 766 degree-corrected clustering problem with data vectors $\mathbf{x}_i =$
 767 $\theta(i)\mathbf{s}_{z(i)} + \epsilon_i, i \in [p]$, where \mathbf{s}_i 's are known cluster centroids,
 768 $\theta(i)$'s are unknown positive degrees, and $z: [p] \mapsto [r]$ is
 769 the cluster assignment of interest. The angle-based k -means

770 algorithm estimates the assignment z by minimizing the angle
 771 between data vectors and centroids; i.e.,
 772

$$z(i) = \arg \max_{a \in [r]} \cos(\mathbf{x}_i, \mathbf{s}_a), \quad \text{for all } i \in [p]. \quad (13)$$

773 The classical Euclidean-distance based clustering [13] fails
 774 to recover z in the presence of degree heterogeneity, even
 775 under noiseless case. In contrast, the proposed angle-based
 776 k -means algorithm achieves accurate recovery without the
 777 explicit estimation of θ .

778 Our Sub-algorithm 2 shares the same spirit as in the angle-
 779 based k -means. We still take the order-3 tensor for illustration.
 780 Specifically, Sub-algorithm 2 updates estimated core tensor
 781 and cluster assignment in each iteration. We use superscript
 782 (t) to denote the estimate from the t -th iteration, where $t =$
 783 $1, 2, \dots$. For core tensor, we consider the following update
 784 strategy

$$\mathcal{S}^{(t)}(a_1, a_2, a_3) = \text{Ave}\{\mathcal{Y}(i_1, i_2, i_3): z_k^{(t)}(i_k) = a_k, k \in [3]\}.$$

785 Intuitively, $\mathcal{S}^{(t)}$ becomes closer to the true core \mathcal{S} as $z_k^{(t)}$ is
 786 more precise. For cluster assignment, we first aggregate the
 787 slices of \mathcal{Y} and obtain the reduced tensor $\mathcal{Y}_1^d \in \mathbb{R}^{p \times r \times r}$ on
 788 the first mode with given $z_k^{(t)}$, where

$$\mathcal{Y}_1^d(i, a_2, a_3) = \text{Ave}\{\mathcal{Y}(i, i_2, i_3): z_k^{(t)}(i_k) = a_k, k \neq 1\}.$$

789 Similarly, we also obtain $\mathcal{Y}_2^d, \mathcal{Y}_3^d$. We use \mathbf{Y}_k^d and $\mathbf{S}_k^{(t)}$ to
 790 denote the $\text{Mat}_k(\mathcal{Y}^d)$ and $\text{Mat}_k(\mathcal{S}^{(t)})$. The rows $\mathbf{Y}_{k,i,:}^d$ and
 791 $\mathbf{S}_{k,a,:}^{(t)}$ correspond to the \mathbf{x}_i and \mathbf{s}_a in the one-dimensional
 792 clustering (13). Then, we obtain the updated assignment by

$$z_k(i)^{(t+1)} = \arg \max_{a \in [r]} \cos(\mathbf{Y}_{k,i,:}^d, \mathbf{S}_{k,a,:}^{(t)}), \quad \text{for all } i \in [p],$$

793 provided that $\mathbf{S}_{k,a,:}^{(t)}$ is a non-zero vector. Otherwise, if $\mathbf{S}_{k,a,:}^{(t)}$ is
 794 a zero vector, then we make the convention to assign $z_k^{(t+1)}(i)$
 795 randomly in $[r]$. Full procedures for our angle-based iteration
 796 are described in Sub-algorithm 2.

797 We now establish the misclustering error rate of iterations
 798 under the stability assumption.

800 *Definition 2 (Locally Linear Stability):* Define the ε -
 801 neighborhood of z by $\mathcal{N}(z, \varepsilon) = \{\bar{z}: \ell(\bar{z}, z) \leq \varepsilon\}$. Let
 802 $\bar{z}: [p] \rightarrow [r]$ be a clustering function. We define two vectors
 803 associated with \bar{z} ,

$$\begin{aligned} \mathbf{p}(\bar{z}) &= (|\bar{z}^{-1}(1)|, \dots, |\bar{z}^{-1}(r)|)^T, \\ \mathbf{p}_\theta(\bar{z}) &= (\|\theta_{\bar{z}^{-1}(1)}\|_1, \dots, \|\theta_{\bar{z}^{-1}(r)}\|_1)^T. \end{aligned}$$

804 We call the degree is ε -locally linearly stable if and only if

$$\sin(\mathbf{p}(\bar{z}), \mathbf{p}_\theta(\bar{z})) \lesssim \varepsilon \Delta_{\min}, \quad \text{for all } \bar{z} \in \mathcal{N}(z, \varepsilon). \quad (14)$$

819 Roughly speaking, the vector $\mathbf{p}(\bar{z})$ represents the raw cluster
 820 sizes, and $\mathbf{p}_\theta(\bar{z})$ represents the relative cluster sizes weighted
 821 by degrees. The local stability holds trivially for $\varepsilon = 0$ based
 822 on the construction of parameter space (2). The condition (14)
 823 controls the impact of node degree to the $\mathbf{p}_\theta(\cdot)$ with respect
 824 to the misclustering rate ε and angle gap. Intuitively, the
 825 condition (14) controls the skewness of degree so that the
 826 angle between raw cluster size and degree-weighted cluster
 827

Algorithm 1 Multiway Spherical Clustering for Degree-Corrected Tensor Block Model**Sub-algorithm 1: Weighted higher-order initialization**

Input: Observation $\mathcal{Y} \in \mathbb{R}^{p \times \dots \times p}$, cluster number r , relaxation factor $\eta > 1$ in k -means clustering.

1: Compute factor matrices $\mathbf{U}_{\text{pre},k} = \text{SVD}_r(\text{Mat}_k(\mathcal{Y}))$, $k \in [K]$ and the $(K-1)$ -mode projections

$$\mathcal{X}_{\text{pre},k} = \mathcal{Y} \times_1 \mathbf{U}_{\text{pre},1} \mathbf{U}_{\text{pre},1}^T \times_2 \dots \times_{k-1} \mathbf{U}_{\text{pre},k-1} \mathbf{U}_{\text{pre},k-1}^T \times_{k+1} \mathbf{U}_{\text{pre},k+1} \mathbf{U}_{\text{pre},k+1}^T \times_{k+2} \dots \times_K \mathbf{U}_{\text{pre},K} \mathbf{U}_{\text{pre},K}^T.$$

2: Compute factor matrices $\hat{\mathbf{U}}_k = \text{SVD}_r(\text{Mat}_k(\mathcal{X}_{\text{pre},k}))$, $k \in [K]$ and the denoised tensor

$$\hat{\mathcal{X}} = \mathcal{Y} \times_1 \hat{\mathbf{U}}_1 \hat{\mathbf{U}}_1^T \times_2 \dots \times_K \hat{\mathbf{U}}_K \hat{\mathbf{U}}_K^T.$$

3: **for** $k \in [K]$ **do**

4: Let $\hat{\mathbf{X}} = \text{Mat}_k(\hat{\mathcal{X}})$ and $S_0 = \{i \in [p] : \|\hat{\mathbf{X}}_{i:\}\| = 0\}$. Set $\hat{z}(i)$ randomly in $[r]$ for $i \in S_0$.

5: For all $i \in S_0^c$, compute normalized rows $\hat{\mathbf{X}}_{i:\}^s := \|\hat{\mathbf{X}}_{i:\}\|^{-1} \hat{\mathbf{X}}_{i:\}$.

6: Solve the clustering $\hat{z}_k : [p] \rightarrow [r]$ and centroids $\{\hat{x}_j\}_{j \in [r]}$ using weighted k -means, such that

$$\sum_{i \in S_0^c} \|\hat{\mathbf{X}}_{i:\}\|^2 \|\hat{\mathbf{X}}_{i:\}^s - \hat{\mathbf{x}}_{\hat{z}_k(i)}\|^2 \leq \eta \min_{\bar{\mathbf{x}}_j, j \in [r], \bar{z}_k(i), i \in S_0^c} \sum_{i \in S_0^c} \|\hat{\mathbf{X}}_{i:\}\|^2 \|\hat{\mathbf{X}}_{i:\}^s - \bar{\mathbf{x}}_{\bar{z}_k(i)}\|^2.$$

7: **end for**

Output: Initial clustering $z_k^{(0)} \leftarrow \hat{z}_k$, $k \in [K]$.

Sub-algorithm 2: Angle-based iteration

Input: Observation $\mathcal{Y} \in \mathbb{R}^{p \times \dots \times p}$, initialization $z_k^{(0)} : [p] \rightarrow [r]$, $k \in [K]$ from Sub-algorithm 1, iteration number T .

8: **for** $t = 0$ to $T-1$ **do**

9: Update the block tensor $\mathcal{S}^{(t)}$ via $\mathcal{S}^{(t)}(a_1, \dots, a_K) = \text{Ave}\{\mathcal{Y}(i_1, \dots, i_K) : z_k^{(t)}(i_k) = a_k, k \in [K]\}$.

10: **for** $k \in [K]$ **do**

11: Calculate the reduced tensor $\mathcal{Y}_k^d \in \mathbb{R}^{r \times \dots \times r \times p \times r \times \dots \times r}$ via

$$\mathcal{Y}_k^d(a_1, \dots, a_{k-1}, i, a_{k+1}, \dots, a_K) = \text{Ave}\{\mathcal{Y}(i_1, \dots, i_{k-1}, i, i_{k+1}, \dots, i_K) : z^{(t)}(i_j) = a_j, j \neq k\}$$

12: Let $\mathbf{Y}_k^d = \text{Mat}_k(\mathcal{Y}_k^d)$ and $J_0 = \{i \in [p] : \|\mathbf{Y}_{i:\}\| = 0\}$. Set $z_k^{(t+1)}(i)$ randomly in $[r]$ for $i \in J_0$.

13: Let $\mathbf{S}_k^{(t)} = \text{Mat}_k(\mathcal{S}^{(t)})$. For all $i \in J_0^c$, update the cluster assignment by

$$z(i)_k^{(t+1)} = \arg \max_{a \in [r]} \cos \left(\mathbf{Y}_{k,i:\}, \mathbf{S}_{k,a:\}^{(t)} \right).$$

14: **end for**

15: **end for**

Output: Estimated clustering $z_k^{(T)} : [p] \mapsto [r]$, $k \in [K]$.

size is well controlled. The stability assumption is proposed for technical convenience, and we relax this condition in numerical studies; see Section VI.

Theorem 5 (Error for Angle-Based Iteration): Consider the general sub-Gaussian dTBM with fixed $r \geq 1$, $K \geq 2$, independent noise under the parameter space \mathcal{P} , and Assumption 1. Assume that the locally linear stability of degree holds in the neighborhood $\mathcal{N}(z, \varepsilon)$ for all $\varepsilon \leq E_0$ and some $E_0 \gtrsim \log^{-1} p$. Let $\{z_k^{(0)}\}_{k=1}^K$ be the initialization for Sub-algorithm 2 and $z_k^{(t)}$ be the t -th iteration output on the k -th mode. Suppose $\min_{i \in [p]} \theta(i) \geq c$ for some constant $c > 0$, the SNR $\geq \tilde{C} p^{-(K-1)} \log p$ for some sufficiently large positive constant \tilde{C} , and the initialization satisfies

$$L(z_k^{(0)}, z) \lesssim \frac{\Delta_{\min}^2}{r \log p}, \quad k \in [K].$$

With probability going to 1 as $p \rightarrow \infty$, there exists a contraction parameter $\rho \in (0, 1)$ such that

$$\ell(z, \hat{z}_k^{(t+1)}) \lesssim \underbrace{\text{SNR}^{-1} \exp \left(-\frac{p^{K-1} \text{SNR}}{r^{K-1}} \right)}_{\text{statistical error}} + \underbrace{\rho^t \ell(z, z_k^{(0)})}_{\text{computational error}}. \quad (15)$$

From the conclusion (15), we find that the iteration error is decomposed into two parts: statistical error and computational error. The statistical error is unavoidable with noisy data regardless t , whereas the computational error decays in an exponential rate as the number of iterations $t \rightarrow \infty$.

Corollary 1 (Exact recovery of dTBM with weighted higher-order initialization): Let the initialization $\{z_k^{(0)}\}_{k=1}^K$ be the output from Sub-algorithm 1. Assume $\text{SNR} \gtrsim p^{-K/2} \log p$. Combining all parameter assumptions and the results in Theorems 4 and 5, with probability going to 1 as $p \rightarrow \infty$, our estimate $z_k^{(T)}$ achieves exact recovery within polynomial

iterations; more precisely,

$$z_k^{(T)} = \pi_k \circ z, \quad \text{for all } T \gtrsim \log_{1/\rho} p \text{ and } k \in [K].$$

for some permutation $\pi_k \in \Pi$.

Therefore, our combined algorithm is *computationally efficient* as long as $\text{SNR} \gtrsim p^{-K/2} \log p$. Note that, ignoring the logarithmic term, the minimal SNR requirement, $p^{-K/2}$, coincides with the computational critical value in Theorem 3. Therefore, our algorithm is optimal regarding the signal requirement and lies in the sharpest *computationally efficient* regime in Figure 2.

856 C. Extension to Bernoulli Observations

Bernoulli or network observations are common in multiple fields. Our iteration Theorem 5 holds for Bernoulli models, but our initialization Theorem 4 does not. Moreover, our current dTBM is insufficient to address sparsity with decaying mean tensor. Here, we provide extra discussions for Bernoulli initialization and strategies under sparse settings.

- *Extension to dense binary dTBMs.* The main difficulty to establish initialization guarantees for Bernoulli observations lies in the denoising step (lines 1-2 in Sub-algorithm 1). We now provide a high-level explanation for the technical difficulty when applying Theorem 4 to Bernoulli observations.

The derivation of Theorem 4 relies on the upper bound of the estimation error for the mean tensor in Lemma 7; i.e., with high probability

$$\|\hat{\mathcal{X}} - \mathcal{X}\|_F^2 \lesssim p^{K/2}, \quad (16)$$

where $\mathcal{X} = \mathbb{E}\mathcal{Y}$ and $\hat{\mathcal{X}}$ is defined in Step 2 of Sub-algorithm 1. Unfortunately, the inequality (16) holds only for i.i.d. sub-Gaussian observations, while Bernoulli observations are generally not identically distributed.

One possible remedy is to apply singular value decomposition to the *square unfolding* [27], $\text{Mat}_{sq}(\cdot)$, of Bernoulli tensor $\mathcal{Y} \in \{0, 1\}^{p_1 \times \dots \times p_K}$. Specifically, the square matricization $\text{Mat}_{sq}(\mathcal{Y}) \in \{0, 1\}^{p^{\lfloor K/2 \rfloor} \times p^{\lceil K/2 \rceil}}$ has entries $[\text{Mat}_{sq}(\mathcal{Y})](j_1, j_2) = \mathcal{Y}(i_1, \dots, i_K)$, where

$$\begin{aligned} j_1 &= i_1 + p_1(i_2 - 1) + \dots + p_{\lfloor K/2 \rfloor - 1}(i_{\lfloor K/2 \rfloor} - 1), \\ j_2 &= i_{\lceil K/2 \rceil} + p_{\lceil K/2 \rceil}(i_{\lceil K/2 \rceil + 1} - 1) + \dots \\ &\quad + p_{\lceil K/2 \rceil} \cdot p_{K-1}(i_K - 1). \end{aligned}$$

The matrix $\text{Mat}_{sq}(\mathcal{Y})$ is asymmetric. We interpret $\text{Mat}_{sq}(\mathcal{Y})$ as the adjacency matrix for a bipartite network with connections between two groups of nodes. The two groups of nodes in the bipartite network have $p_1 \cdots p_{\lfloor K/2 \rfloor}$ and $p_{\lceil K/2 \rceil} \cdots p_K$ nodes, respectively. The entry $[\text{Mat}_{sq}(\mathcal{Y})](j_1, j_2)$ refers to the presence of connection between the nodes indexed by combinations $(i_1, \dots, i_{\lfloor K/2 \rfloor})$ and $(i_{\lceil K/2 \rceil}, \dots, i_K)$. We summarize the procedure in Sub-algorithm 3.

894 Proposition 1 (Error for Bernoulli Initialization):

Consider the Bernoulli dTBM in the parameter space \mathcal{P} with fixed $r \geq 1, K \geq 2$. Assume that Assumption 1 holds, $\boldsymbol{\theta}$ is balanced, and $\min_{i \in [p]} \theta(i) \geq c$ for some

Algorithm 2 Sub-algorithm 3: Weighted Higher-Order Initialization for Bernoulli Observation

Input: Bernoulli tensor $\mathcal{Y} \in \{0, 1\}^{p \times \dots \times p}$, cluster number r , relaxation factor $\eta > 1$ in k -means clustering.

- 1: Let the matrix $\text{Mat}_{sq}(\mathcal{Y}) \in \{0, 1\}^{p^{\lfloor K/2 \rfloor} \times p^{\lceil K/2 \rceil}}$ denote the nearly square unfolded tensor. Compute the estimate $\hat{\mathcal{X}}$, where

$$\hat{\mathcal{X}}' = \arg \min_{\text{rank}(\text{Mat}_{sq}(\hat{\mathcal{X}}')) \leq r^{\lceil K/2 \rceil}} \|\text{Mat}_{sq}(\hat{\mathcal{X}}') - \text{Mat}_{sq}(\mathcal{Y})\|_F^2. \quad (17)$$

- 2: Implement lines 3-5 of Sub-algorithm 1 with $\hat{\mathcal{X}}$ replaced by $\hat{\mathcal{X}}'$ in (17).

Output: Initial clustering $z_k^{(0)} \leftarrow \hat{z}_k, k \in [K]$.

constant $c > 0$. Let $z_k^{(0)}$ denote the output of Sub-algorithm 3. With probability going to 1 as $p \rightarrow \infty$, we have

$$\ell(z_k^{(0)}, z_k) \lesssim \frac{r^K p^{-\lfloor K/2 \rfloor}}{\text{SNR}}, \quad \text{and } L(z_k^{(0)}, z_k) \lesssim \sigma^2 r^K p^{-\lfloor K/2 \rfloor}.$$

Remark 8 (Comparison with Gaussian model): The Bernoulli bound $\mathcal{O}(p^{-\lfloor K/2 \rfloor})$ in Proposition 1 is relatively looser than the Gaussian bound $\mathcal{O}(p^{-K/2})$ in Theorem 4. The gap between Bernoulli and Gaussian error decreases as the order K increases. Nevertheless, combining with angle iteration Sub-algorithm 2, Bernoulli clustering still achieves exponential error rate $\exp(-p^{(K-1)})$ at a price of a larger SNR. The investigation of the gap between upper bound $p^{-\lfloor K/2 \rfloor}$ and the lower bound $p^{-K/2}$ for Bernoulli tensors will be left as future work. In numerical experiments, we will use our original initialization, Sub-algorithm 1, to verify the robustness to Bernoulli observations.

914 Remark 9 (Comparison With Previous Methods):

Previous work [9] develops a spectral clustering method for Bernoulli dTBM. [9] adopts a different signal notion based on the singular gap in the core tensor, denoted as Δ_{singular} . By [9, Theorem 1], the spectral method achieves exact recovery with $\Delta_{\text{singular}} \gtrsim p^{-1/2}$. However, we are not able to infer the exact recovery of spectral method by our angle-base SNR condition. Consider an order-2 dTBM with $p > 2, \sigma^2 = 1, \boldsymbol{\theta} = \mathbf{1}_p$, equal size assignment $|z^{-1}(a)| = p/r$ for all $a \in [r]$, and core matrix equal to the 2-dimensional identity matrix $\mathbf{S} = \mathbf{I}_2$. The singular gap under this setting is $\Delta_{\text{singular}} = \min\{\lambda_1 - \lambda_2, \lambda_2\} = 0$, where $\lambda_1 \geq \lambda_2$ are singular values of \mathbf{S} . In contrast, our angle gap $\Delta_{\text{min}}^2 = 2$ satisfies the SNR condition in Theorem 5. Then, our algorithm achieves the exact recovery, but the spectral method in [9] fails.

Hence, for fair comparison, we compare the best performance of our algorithm and [9] under the strongest signal setting of each model. Since both methods contain an iteration procedure, we set the iteration number to infinity to avoid the computational error. Considering the largest angle-based SNR $\asymp 1$ in Theorem 5, our Bernoulli clustering achieves exponential error rate of order $\exp(-p^{(K-1)})$; considering the largest singular

gap $\Delta_{\text{singular}} \asymp 1$ in Theorem 1 of [9], the spectral clustering has a polynomial error rate of order p^{-2} . Our algorithm still shows a better theoretical accuracy than the competitive work for Bernoulli observations.

- *Extension to sparse binary dTBMs.* The sparsity is often a popular feature in hypergraphs [9], [16], [28]. Specifically, the sparse binary dTBM assumes that, the entries of \mathcal{Y} follow independent Bernoulli distributions with the mean

$$\mathbb{E}\mathcal{Y} = \alpha_p \mathcal{S} \times_1 \Theta M \times_2 \cdots \times_K \Theta M, \quad (18)$$

where the extra scalar parameter $\alpha_p \in (0, 1]$ is function of p that controls the sparsity. A smaller α_p indicates a higher level of sparsity. Our current work focuses on dense dTBM with $\alpha_p = 1$. While sparse dTBM is an interesting application, the algorithm and its analysis require different techniques. Below, we discuss possible modifications of the algorithm.

The sparsity affects our initialization guarantee in our Theorem 4. In our initialization, the spectral denoising step (lines 1-2 in Sub-algorithm 1) implements matrix SVD to unfolded tensors. However, SVD-based methods are believed to fail in extremely sparse SBM due to the localization phenomenon in the singular vectors [28]. Inspired by [28], we adopt the diagonal-deleted HOSVD (D-HOSVD) [9] as the initialization in our higher-order clustering.

The sparsity also affects the iteration guarantee in our Theorem 5. The decaying mean tensor leads to a worse statistical error of order $\mathcal{O}(-\alpha_p p^{K-1})$ on $\hat{\mathcal{X}}$. The theoretical analyses for sparse binary dTBM and algorithms are left as future directions. Instead, we add numerical experiments to evaluate the robustness of our algorithm and the improvement of D-HOSVD initialization in the sparse dTBM; see Appendix A.

D. Practical Issues

1) *Computational Complexity:* Our two-stage algorithm has a computational cost polynomial in tensor dimension p . Specifically, the complexity of Sub-algorithm 1 is $\mathcal{O}(Kp^{K+1} + Kp^K)$, where the first term is contributed by the double projection and the calculation of $\hat{\mathcal{X}}$, and the second term comes from normalization and the k -means. The cost of each update in Sub-algorithm 2 is $\mathcal{O}(p^K + pr^K)$, where p^K comes from the calculation of $\mathcal{S}^{(t)}$ and \mathcal{Y}_k^d , and pr^K comes from the normalization of \mathcal{Y}_k^d , the calculation of $\mathcal{S}^{(t)}$, and the cluster assignment update in Step 13.

2) *Hyper-Parameter Selection:* In our theoretical analysis, we have assumed the true cluster number r is given to our algorithm. In practice, the cluster number r is often unknown, and we now propose a method to choose r from data. We impose the Bayesian information criterion (BIC) and choose the cluster number that minimizes BIC; i.e., under the symmetric Gaussian dTBM (1),

$$\hat{r} = \arg \min_{r \in \mathbb{Z}_+} \left(p^K \log(\|\hat{\mathcal{X}} - \mathcal{Y}\|_F^2) + p_e(r)K \log p \right), \quad (19)$$

with $\hat{\mathcal{X}} = \hat{\mathcal{S}}(r) \times_1 \hat{\Theta}(r) \hat{M}(r) \times_2 \cdots \times_K \hat{\Theta}(r) \hat{M}(r)$, where the triplet $(\hat{z}(r), \hat{\mathcal{S}}(r), \hat{\Theta}(r))$ are estimated parameters with cluster number r , and $p_e(r) = r^K + p(\log r + 1) - r$ is the effective number of parameters. Note that we have added the argument (r) to related quantities as functions of r . In particular, the estimate $\hat{\Theta}(r)$ in (19) is obtained by first calculating the reduced tensor $\hat{\mathcal{Y}}^d$ with $\hat{z}(r)$, and then normalizing the row norms $\|\hat{\mathcal{Y}}_{i:}^d\|$ to 1 in each cluster; i.e.,

$$\hat{\theta}(r) = (\hat{\theta}(1, r), \dots, \hat{\theta}(p, r))^T, \quad 1001$$

with $\hat{\theta}(i, r) = \|\hat{\mathcal{Y}}^d(r)_{i:}\| / \sum_{j: \hat{z}(j, r) = \hat{z}(i, r)} \|\hat{\mathcal{Y}}^d(r)_{j:}\|$, $\hat{\mathcal{Y}}^d(r) = \text{Mat}(\hat{\mathcal{Y}}^d(r))$, $\hat{\mathcal{Y}}^d(r)(i, a_2, \dots, a_K) = \text{Ave}\{\mathcal{Y}(i, i_2, \dots, i_K) : \hat{z}(i_k, r) = a_k, k \neq 1\}$, and $\hat{z}(i, r)$ denotes the community label for the i -th node with given cluster number r . We evaluate the performance of the BIC criterion in Section VI-A.

V. COMPARISON WITH NON-DEGREE TENSOR BLOCK MODEL

We discuss the connections and differences between dTBM and TBM [13] from three aspects: signal notions, theoretical results, and algorithms. Without loss of generality, let $\sigma^2 = 1$.

- *Signal notion.* The signal levels in both TBM [13] and our dTBM are functions of the core tensor \mathcal{S} . We emphasize that the signal notions are different between the two models. In particular, the Euclidean-based signal notion in TBM [13] fails to accurately describe the phase transition in our dTBM due to the possible heterogeneity in degree θ . To compare, we denote our angle-based signal notion in (4) and the Euclidean-based SNR in [13] as Δ_{ang}^2 and Δ_{Euc}^2 , respectively:

$$\Delta_{\text{ang}}^2 = 2(1 - \max_{a \neq b \in [r]} \cos(\mathbf{S}_{a:}, \mathbf{S}_{b:})), \quad 1021$$

$$\Delta_{\text{Euc}}^2 = \min_{a \neq b \in [r]} \|\mathbf{S}_{a:} - \mathbf{S}_{b:}\|^2. \quad 1022$$

By Lemma 4 in the Appendix B, we have

$$\Delta_{\text{ang}}^2 \max_{a \in [r]} \|\mathbf{S}_{a:}\|^2 \leq \Delta_{\text{Euc}}^2. \quad 1024$$

The above inequality indicates that the condition $\Delta_{\text{Euc}}^2 \leq p^\gamma$ is sufficient but not necessary for $\Delta_{\text{ang}}^2 \leq p^\gamma$. In fact, if we were to use Δ_{Euc}^2 for both models, then the phase transition of dTBM can be arbitrarily worse than that for TBM.

Here, we provide an example to illustrate the dramatical difference between TBM and dTBM with the same core tensor.

Example 4 (Comparison With Euclidean-Based Signal Notion): Consider a biclustering model with $\theta = 1$ and an order-2 core matrix

$$\mathbf{S} = \begin{pmatrix} p^{(\gamma+1)/2} + 2 & 2 \\ 2 & 4 \end{pmatrix}, \quad \text{with } \gamma \leq -1. \quad 1036$$

The core matrix \mathbf{S} lies in the parameter spaces of TBM and our dTBM. Here, the constraint $\gamma \leq -1$ is added to ensure the bounded condition of \mathbf{S} in our parameter

space in (2). The angle-based and Euclidean-based signal levels of \mathcal{S} are

$$\Delta_{\text{ang}}^2(\mathcal{S}) = 0 \ (\leq p^\gamma), \quad \Delta_{\text{Euc}}^2(\mathcal{S}) = 5 p^{\gamma+1} \ (\geq p^\gamma).$$

We conclude that TBM with \mathcal{S} achieves exact recovery with a polynomial-time algorithm; see [13, Theorem 4]. By contrast, the dTBM with the same \mathcal{S} and input $r = 2$ violates the identifiability condition, and thus fails to be solved by all estimators; see our Theorem 1.

- *Theoretical results.* In both works, we study the phase transition of TBM and dTBM with respect to the Euclidean and angle-based SNRs. We briefly summarize the results in [13] and compare with ours.

Statistical critical value:

Ours: $\Delta_{\text{ang}}^2 \lesssim p^{-(K-1)} \Rightarrow$ statistically impossible;
 $\Delta_{\text{ang}}^2 \gtrsim p^{-(K-1)} \Rightarrow$ MLE achieves exact recovery;

Han's: $\Delta_{\text{Euc}}^2 \lesssim p^{-(K-1)} \Rightarrow$ statistically impossible;
 $\Delta_{\text{Euc}}^2 \gtrsim p^{-(K-1)} \Rightarrow$ MLE achieves exact recovery.

Computational critical value:

Ours: $\Delta_{\text{ang}}^2 \lesssim p^{-K/2} \Rightarrow$ computationally impossible;
 $\Delta_{\text{ang}}^2 \gtrsim p^{-K/2} \Rightarrow$ computationally efficient;

Han's: $\Delta_{\text{Euc}}^2 \lesssim p^{-K/2} \Rightarrow$ computationally impossible;
 $\Delta_{\text{Euc}}^2 \gtrsim p^{-K/2} \Rightarrow$ computationally efficient.

The above comparison reveals four major differences. First, none of our results in Section III are corollaries of [13]. Both models show the similar conclusion but under different conditions. While the TBM impossibility [13] provides a necessary condition for our dTBM impossibility, we find that such a condition is often loose. There exists a regime of \mathcal{S} in which TBM problems are computationally efficient but dTBM problems are statistically impossible; see Example 4. This observation has motivated us to develop the new signal notion Δ_{ang}^2 for sharp dTBM phase transition conditions.

Second, to find the phase transition, we need to show both the impossibility and achievability when SNR is below and above the critical value, respectively. While the TBM impossibility can serve as a loose condition of our dTBM impossibility, more efforts are required to show the achievability. In particular, since TBM is a more restrictive model than dTBM, the achievability in [13] does not imply the achievability of dTBM in a larger parameter space. The latter requires us to develop new MLE and polynomial algorithms for dTBM achievability. Third, from the perspective of proofs, we develop new dTBM-specific techniques to handle the extra degree heterogeneity. In our Theorem 2, we construct a special non-trivial degree heterogeneity to establish the lower bound for arbitrary core tensor with small angle gap, while, TBM [13] considers the constructions without degree parameter. In our Theorem 3, we construct a rank-2 tensor to relate HPC conjecture to Δ_{ang}^2 , while TBM [13] constructs a rank-1 tensor to relate HPC

conjecture to Δ_{Euc}^2 . The asymptotic non-equivalence between Δ_{ang}^2 and Δ_{Euc}^2 renders our proof technically more involved.

Last, we discuss the statistical impossibility statements. Our Theorem 2 implies the statistical impossibility whenever the core tensor \mathcal{S} leads to an angle-based SNR below the critical value, while, Theorem 6 in [13] implies the worst case statistical impossibility for a particular core tensor \mathcal{S} with Euclidean-based SNR below the statistical limit. Hence, our Theorem 2 shows a stronger statistical impossibility for dTBM than that presented in TBM [13, Theorem 6]. However, inspecting the proof of [13], the proof of Theorem 6 indeed implies a stronger TBM impossibility statement for arbitrary core tensor; i.e., when $\gamma < -(K - 1)$

$$\liminf_{p \rightarrow \infty} \inf_{\mathcal{S} \in \mathcal{P}_{\mathcal{S}, \text{TBM}} \cap \{\Delta_{\text{Euc}}^2 = p^\gamma\}} \inf_{\hat{z}_{\text{stats}}} \sup_{z \in \mathcal{P}_{z, \text{TBM}}} \mathbb{E}[\ell(\hat{z}_{\text{stats}}, z)] \geq 1,$$

where $\mathcal{P}_{\mathcal{S}, \text{TBM}}$ and $\mathcal{P}_{z, \text{TBM}}$ refer to the space for core tensor \mathcal{S} and assignment z under TBM, respectively. Again, in terms of the strong statistical impossibility, both models show the similar conclusion but under different conditions. Since two impossibilities consider different core tensor regimes with non-equivalent Δ_{ang}^2 and Δ_{Euc}^2 , we emphasize that different proof techniques are required to obtain these similar conclusions. See our proof sketch in Section VIII-A, Appendices B-D and B-E for detail technical differences.

- *Algorithms.* Both [13] and our work propose the two-step algorithm, which combines warm initialization and iterative refinement to achieve exact recovery. This local-to-global strategy is not new in clustering literature [29], [30]. The highlight of our algorithm is the angle-based update in lines 10-14, Sub-algorithm 2, which is specifically designed for dTBM to avoid the estimation of θ . This angle-based update brings new proof challenges. We develop polar-coordinate based techniques to establish the error rate for the proposed algorithm.

VI. NUMERICAL STUDIES

We evaluate the performance of the weighted higher-order initialization and angle-based iteration in this section. We report average errors and standard deviations across 30 replications in each experiment. Clustering accuracy is assessed by clustering error rate (CER, i.e., one minus rand index). The CER between (\hat{z}, z) is equivalent to misclustering error $\ell(\hat{z}, z)$ up to constant multiplications [31], and a lower CER indicates a better performance.

We generate order-3 tensors with *assortative* [15] core tensors to control SNR; i.e., we set $\mathcal{S}_{aaa} = s_1$ for $a \in [r]$ and others be s_2 , where $s_1 > s_2 > 0$. Let $\alpha = s_1/s_2$. We set α close to 1 such that $1 - \alpha = o(p)$. In particular, we have $\alpha = 1 + \Omega(p^{\gamma/2})$ with $\gamma < 0$ by Assumption 1 and definition (4). Hence, we easily adjust SNR via varying α . The assortative setting is proposed for simulations, and our algorithm is applicable for general tensors in practice. The cluster assignment z is randomly generated with equal

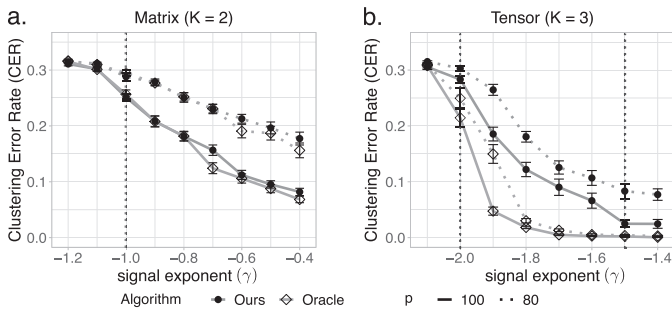


Fig. 4. SNR phase transitions for clustering in dTBM with $p = \{80, 100\}$, $r = 5$ under (a) matrix case with $\gamma \in [-1.2, -0.4]$ and (b) tensor case with $\gamma \in [-2.1, -1.4]$.

probability across r clusters for each mode. Without further explanation, we generate degree heterogeneity θ from absolute normal distribution by $\theta(i) = |X_i| + 1 - 1/\sqrt{2\pi}$ with $|X_i| \stackrel{\text{i.i.d.}}{\sim} N(0, 1)$, $i \in [p]$ and normalize θ to satisfy (2). Also, we set $\sigma^2 = 1$ for Gaussian data without further specification.

A. Verification of Theoretical Results

The first experiment verifies statistical-computational gap described in Section III. Consider the Gaussian model with $p = \{80, 100\}$, $r = 5$. We vary γ in $[-1.2, -0.4]$ and $[-2.1, -1.4]$ for matrix ($K = 2$) and tensor ($K = 3$) clustering, respectively. Note that finding MLE under dTBM is computationally intractable. We approximate MLE using an oracle estimator, i.e., the output of Sub-algorithm 2 initialized from true assignment. Figure 4a shows that both our algorithm and oracle estimator start to decrease around the critical value $\gamma_{\text{stat}} = \gamma_{\text{comp}} = -1$ in matrix case. In contrast, Figure 4b shows a significant gap in the phase transitions between the algorithm estimator and oracle estimator in tensor case. The oracle error rapidly decreases to 0 when $\gamma_{\text{stat}} = -2$, whereas the algorithm estimator tends to achieve exact clustering when $\gamma_{\text{comp}} = -1.5$. Figure 4 confirms the existence of the statistical-computational gap in our Theorems 2 and 3.

The second experiment verifies the performance guarantees of two algorithms: (i) weighted higher-order initialization; (ii) combined algorithm of weighted higher-order initialization and angle-based iteration. We consider both the Gaussian and Bernoulli models with $p = \{80, 100\}$, $r = 5$, $\gamma \in [-2.1, -1.4]$. Figure 5 shows the substantial improvement of combined algorithm over initialization, especially under weak and intermediate signals. This phenomenon agrees with the error rates in Theorems 4 and 5 and confirms the necessity of the local iterations.

The third experiment evaluates the empirical performance of the BIC criterion to select unknown cluster number. We generate the data from an order-3 Gaussian model with $p = \{50, 80\}$, $r = \{2, 4\}$, and noise level $\sigma^2 \in \{0.25, 1\}$. Table III shows that our BIC criterion well chooses the true r under most settings. Note that the BIC slightly underestimates the true cluster number ($r = 4$) with smaller dimension and higher noise ($p = 50, \sigma^2 = 1$), and the accuracy immediately increases with larger dimension $p = 80$. The improvement follows from the fact that a larger dimension p indicates

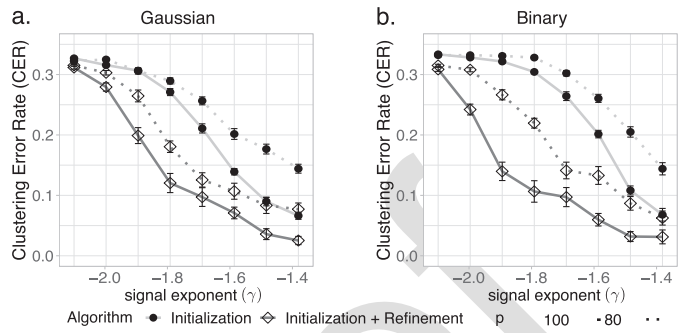


Fig. 5. CER versus signal exponent (γ) for initialization only and for combined algorithm. We set $p = \{80, 100\}$, $r = 5$, $\gamma \in [-2.1, -1.4]$ under (a) Gaussian models and (b) Bernoulli models.

a larger sample size in the tensor block model. Therefore, we conclude that BIC criterion is a reasonable way to tune the cluster number.

B. Comparison With Other Methods

We compare our algorithm with following higher-order clustering methods:

- **HOSVD**: HOSVD on data tensor and k -means on the rows of the factor matrix;
- **HOSVD+**: HOSVD on data tensor and k -means on the ℓ_2 -normalized rows of the factor matrix;
- **HLloyd** [13]: High-order clustering algorithm developed for non-degree tensor block models;
- **SCORE** [9]: Tensor-SCORE for clustering developed for sparse binary tensors.

Among the four alternative algorithms, the **SCORE** is the closest method to ours. We set the tuning parameters of **SCORE** as in previous literature [9]. The methods **SCORE** and **HOSVD+** are designed for degree models, whereas **HOSVD** and **HLloyd** are designed for non-degree models. We conduct two experiments to assess the impacts of (i) signal strength and (ii) degree heterogeneity, based on Gaussian and Bernoulli models with $p = 100, r = 5$. We refer to our algorithm as **dTBM** in the comparison.

We investigate the effects of signal to clustering performance by varying $\gamma \in [-1.5, -1.1]$. Figure 6 shows that our method **dTBM** outperforms all other algorithms. The sub-optimality of **SCORE** and **HOSVD+** indicates the necessity of local iterations on the clustering. Furthermore, Figure 6 shows the inadequacy of non-degree algorithms in the presence of mild degree heterogeneity. The experiment demonstrates the benefits of addressing heterogeneity in higher-order clustering tasks.

The only exception in Figure 6 is the slightly better performance of **HLloyd** over **HOSVD+** under Gaussian model. However, we find the advantage of **HLloyd** disappears with higher degree heterogeneity. We perform extra simulations to verify the impact of degree effects. We use the same setting as in the first experiment in the Section VI-B, except that we now generate the degree heterogeneity θ from Pareto distribution prior to normalization. The density function of Pareto distribution is $f(x|a, b) = ab^a x^{-(a+1)} \mathbb{1}\{x \geq b\}$, where

TABLE III

ESTIMATED CLUSTER NUMBER GIVEN BY BIC CRITERION UNDER THE LOW NOISE LEVEL ($\sigma^2 = 0.25$) AND HIGH NOISE LEVEL ($\sigma^2 = 0.5$) SETTINGS. NUMBERS IN PARENTHESES ARE STANDARD DEVIATIONS OF \hat{r} OVER 30 REPLICATIONS

Settings	$p = 50, \sigma^2 = 0.25$		$p = 50, \sigma^2 = 1$		$p = 80, \sigma^2 = 0.25$		$p = 80, \sigma^2 = 1$	
	2	4	2	4	2	4	2	4
True cluster number r								
Estimated cluster number \hat{r}	2(0)	3.9(0.25)	2(0)	3.1(0.52)	2(0)	4(0)	2(0)	3.9(0.31)

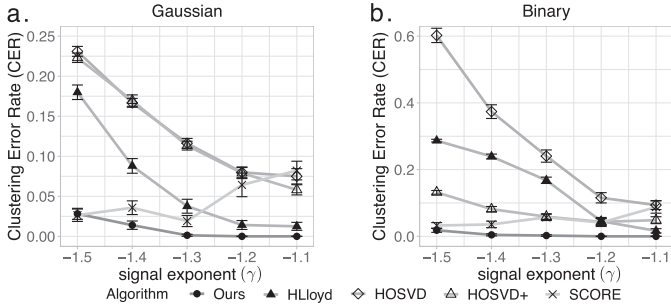


Fig. 6. CER versus signal exponent (denoted γ) for different methods. We set $p = 100, r = 5, \gamma \in [-1.5, -1.1]$ under (a) Gaussian and (b) Bernoulli models.

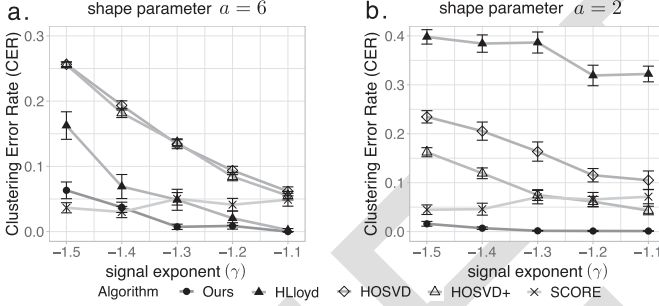


Fig. 7. CER comparison versus signal exponent (denoted γ) under (a) low (shape parameter $a = 6$) (b) high (shape parameter $a = 2$) degree heterogeneity. We set $p = 100, r = 5, \gamma \in [-1.5, -1.1]$ under Gaussian model.

1229 a is called *shape parameter*. We vary $a \in \{2, 6\}$ and choose b
1230 such that $\mathbb{E}X = a(a-1)^{-1}b = 1$ for X following $\text{Pareto}(a, b)$.
1231 Note that a smaller a leads to a larger variance in θ and hence a
1232 larger degree heterogeneity. We consider the Gaussian model
1233 under low ($a = 6$) and high ($a = 2$) degree heterogeneity.
1234 Figure 7 shows that the errors for non-degree algorithms
1235 (**HLloyd**, **HOSVD**) increase with degree heterogeneity. In addition,
1236 the advantage of **HLloyd** over **HOSVD+** disappears with
1237 higher degree heterogeneity.

1238 The last experiment investigates the effects of degree hetero-
1239 geneity to clustering performance. We fix the signal exponent
1240 $\gamma = -1.2$ and vary the extent of degree heterogeneity.
1241 In this experiment, we generate θ from Pareto distribution
1242 prior to normalization. We vary the shape parameter $a \in$
1243 $[3, 6]$ in the Pareto distribution to investigate a range of
1244 degree heterogeneities. Figure 8 demonstrates the stability
1245 of degree-corrected algorithms (**dTBM**, **SCORE**, **HOSVD+**)
1246 over the entire range of degree heterogeneity under consid-
1247 eration. In contrast, non-degree algorithms (**HLloyd**, **HOSVD**)
1248 show poor performance with large heterogeneity, especially in
1249 Bernoulli cases. This experiment, again, highlights the benefit
1250 of addressing degree heterogeneity in higher-order clustering.

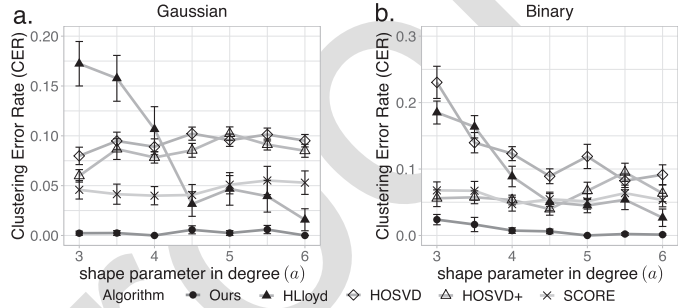


Fig. 8. CER versus shape parameter in degree ($a \in [3, 6]$) for different methods. We set $p = 100, r = 5, \gamma = -1.2$ under (a) Gaussian and (b) Bernoulli models.

VII. REAL DATA APPLICATIONS

A. Human Brain Connectome Data Analysis

The Human Connectome Project (HCP) aims to construct the structural and functional neural connections in human brains [32]. We preprocess the original dataset following [33] and partition the brain into 68 regions. The cleaned dataset includes brain networks for 136 individuals. Each brain network is represented by a 68-by-68 binary symmetric matrix, where the entry with value 1 indicates the presence of connection between node pairs, while the value 0 indicates the absence. We use $\mathcal{Y} \in \{0, 1\}^{68 \times 68 \times 136}$ to denote the binary tensor. Individual attributes such as gender and sex are recorded.

We apply our general asymmetric algorithm to the HCP data with the numbers of clusters on three modes $r_1 = r_2 = 4$ and $r_3 = 3$. The selection of r_1 and r_2 follows the human brain anatomy and the symmetry in the brain network, and the r_3 is specified following previous analysis [34]. Because of the symmetry in the data, the estimated brain node clustering results are the same on the first and second modes. Figure 9 shows that brain connection exhibits a strong spatial separation structure. Specifically, the first cluster, named *L.Hemis*, involves all the nodes in the left hemisphere. The nodes in the right hemisphere are further separated into three clusters led by the middle-part tissues in Temporal and Parietal lobes (*R.Temporal*), the back-part tissues in Occipital lobe (*R.Occipital*), and the front-part tissues in Frontal and Parietal lobes (*R.Supra*). This clustering result is reasonable since the left and right hemispheres often play different roles in human brains.

Figure 10 illustrates the estimated core tensor $\hat{\mathcal{S}}$ with estimated clustering, and Figure 11 visualizes the average brain connections and the connection enrichment in contrast to average networks in each group. In general, we find

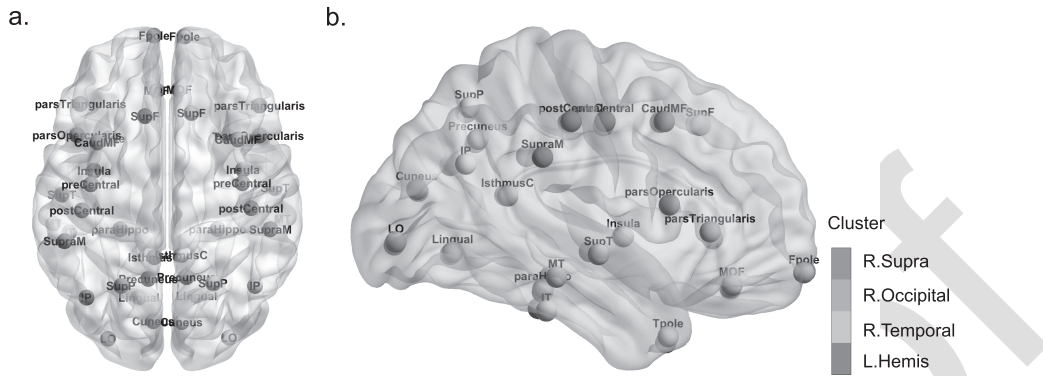


Fig. 9. Illustration of brain node clustering results for HCP data with (a) top and (b) side views.

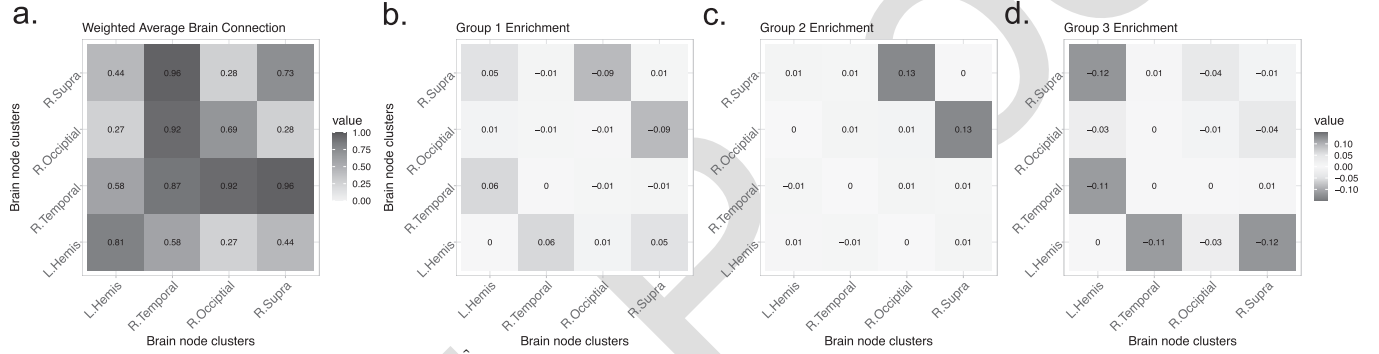


Fig. 10. Mode 3 slices of estimated core tensor $\hat{\mathcal{S}}$. (a) Average estimated slice weighted by the group size; (b)-(d) Group-specified enrichment, i.e., the difference between each slice of $\hat{\mathcal{S}}$ and the averaged slice.

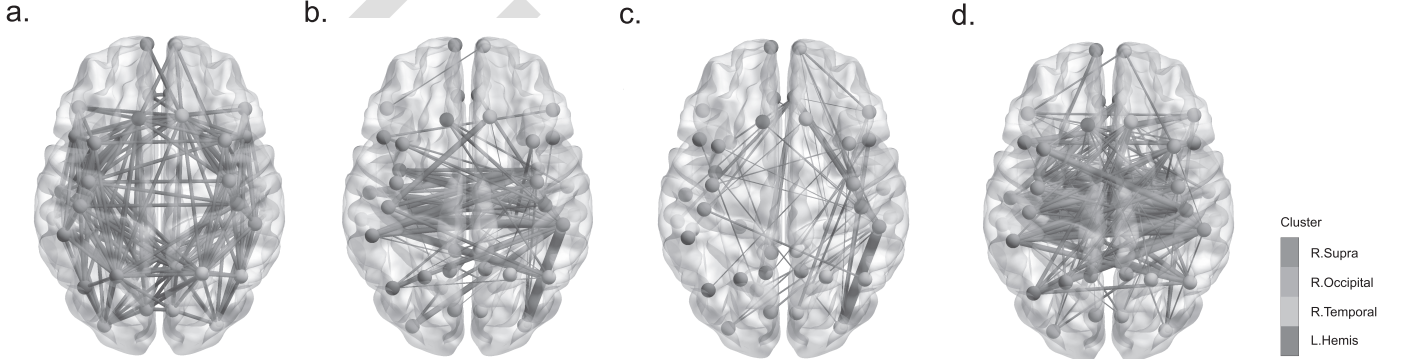


Fig. 11. Observed brain connections in the population and each group of individuals. (a) Average brain network; (b)-(d) Group-specified brain network enrichments in Groups 1-3. Red edges represent the positive enrichment and blue edges represent the negative enrichment.

that the inner-hemisphere connection has stronger connection compared to inter-hemisphere connections (Figure 10a). Also, the back and front parts (*R.Occipital*, *R.Supra*) are shown to have more interactions with temporal tissues than inner-cluster connections. In addition, the group 1 with 54% females shows an enrichment on the inter-hemisphere connections (Figure 10b), while group 4 with only 36% females exhibits a reduction (Figure 10d). This result agrees with previous findings in [34]. The enrichment on the back-front connection is also recognized in group 3 (Figure 10c). The interpretive patterns in our results demonstrate the usefulness of our clustering methods in the human brain connectome data application.

B. Peru Legislation Data Analysis

We also apply our method to the legislation networks in the Congress of the Republic of Peru [35]. Because of the frequent political power shifts in the Peruvian Congress during 2006-2011, we choose to focus on the data for the first half of 2006-2007 year. The dataset records the co-sponsorship of 116 legislators from top 5 parties and 802 bill proposals. We reconstruct legislation network as an order-3 binary tensor $\mathcal{Y} \in \{0, 1\}^{116 \times 116 \times 116}$, where $\mathcal{Y}_{ijk} = 1$ if the legislators (i, j, k) have sponsored the same bill, and $\mathcal{Y}_{ijk} = 0$ otherwise. The true party affiliations of legislators are provided and serve as the ground truth. We apply various higher-order

TABLE IV
CLUSTERING ERRORS (MEASURED BY CER) FOR VARIOUS METHODS IN
THE ANALYSIS OF PERU LEGISLATION DATASET

Method	dTBM	HOSVD	HOSVD+	HLloyd	SCORE
CER	0.116	0.22	0.213	0.149	0.199

clustering methods to \mathcal{Y} with $r = 5$. Table IV shows that our **dTBM** achieves the best performance compared to others. The second best method is the two-stage algorithm **HLloyd**, followed by the spectral methods **SCORE** and **HOSVD+**. This result is consistent with our simulations under strong signal and moderate degree heterogeneity. The comparison suggests that our method **dTBM** is more appealing in real-world applications.

VIII. PROOF SKETCHES

In this section, we provide the proof sketches for the main Theorem 2 (Impossibility), Theorem 3 (Impossibility), and Theorems 4-5. Detail proofs and extra theoretical results are provided in Appendix B.

A. Proof Sketch of Theorem 2 (Impossibility) and Theorem 3 (Impossibility)

The proofs of impossibility in Theorems 2 and 3 share the same proof idea with [13, Theorems 6 and 7] and [15, Theorem 2]. In both proofs of statistical and computational impossibilities, the key idea is to construct a particular set of parameters to lower bound the minimax rate. Specifically, for statistical impossibility in Theorem 2, we construct a particular $(z_{\text{stats}}^*, \theta_{\text{stats}}^*) \in \mathcal{P}_{z,\theta}$ such that for all $\mathcal{S}^* \in \mathcal{P}_S(\gamma)$

$$\begin{aligned} & \inf_{\hat{z}_{\text{stats}}} \sup_{(z,\theta) \in \mathcal{P}_{z,\theta}} \mathbb{E}[p\ell(\hat{z}_{\text{stats}}, z)] \\ & \geq \inf_{\hat{z}_{\text{stats}}} \mathbb{E}[p\ell(\hat{z}_{\text{stats}}, z_{\text{stats}}^*) | (z_{\text{stats}}^*, \mathcal{S}^*, \theta_{\text{stats}}^*)] \geq 1; \end{aligned} \quad (20)$$

for computational impossibility in Theorem 3, we construct a particular $(z_{\text{comp}}^*, \mathcal{S}_{\text{comp}}^*, \theta_{\text{comp}}^*) \in \mathcal{P}(\gamma)$ such that

$$\begin{aligned} & \inf_{\hat{z}_{\text{comp}}} \sup_{(z,\mathcal{S},\theta) \in \mathcal{P}(\gamma)} \mathbb{E}[p\ell(\hat{z}_{\text{comp}}, z)] \\ & \geq \inf_{\hat{z}_{\text{comp}}} \mathbb{E}[p\ell(\hat{z}_{\text{comp}}, z_{\text{comp}}^*) | (z_{\text{comp}}^*, \mathcal{S}_{\text{comp}}^*, \theta_{\text{comp}}^*)] \geq 1. \end{aligned}$$

The constructions of $(z_{\text{stats}}^*, \theta_{\text{stats}}^*)$ and $(z_{\text{comp}}^*, \mathcal{S}_{\text{comp}}^*, \theta_{\text{comp}}^*)$ are the most critical steps. With good constructions, the lower bound “ ≥ 1 ” can be verified by classical statistical conclusions (e.g. Neyman-Pearson Lemma) or prior work (e.g. HPC Conjecture).

A notable detail in the proof of statistical impossibility is the arbitrariness of \mathcal{S}^* . The first infimum over $\mathcal{P}_S(\gamma)$ in the minimax rate (10) requires that the lower bound (20) holds for any $\mathcal{S}^* \in \mathcal{P}_S(\gamma)$. The arbitrary choice of \mathcal{S}^* brings extra difficulties in the parameter construction, and consequently a non-trivial $\theta_{\text{stats}}^* \neq 1$ is chosen to address the arbitrariness. Previous TBM construction in the proof of [13, Theorem 6] with $\theta_{\text{stats}}^* = 1$ is no longer applicable in our case. Meanwhile, our construction $(z_{\text{comp}}^*, \mathcal{S}_{\text{comp}}^*, \theta_{\text{comp}}^*)$ leads to a rank-2 mean tensor to relate the HPC Conjecture while TBM [13, Theorem

7] constructs a rank-1 mean tensor. Hence, we emphasize that dTBM-specific techniques are required to obtain our impossibility results, though the proof idea is common for minimax lower bound analysis.

B. Proof Sketch of Theorem 4

The proof of Theorem 4 is inspired by the proof idea of [15, Lemma 1]. The extra difficulties are the angle gap characterization and multilinear algebra property in tensors; we address both challenges in our proof. Specifically, we control the misclustering error by the estimation error of $\hat{\mathcal{X}}$ calculated in Step 2 of Sub-algorithm 1. We prove the following inequality

$$\begin{aligned} \ell(z^{(0)}, z) & \lesssim \frac{1}{p} \min_{\pi \in \Pi} \sum_{i: z^{(0)}(i) \neq \pi(z(i))} \theta(i)^2 \\ & \lesssim \frac{\sigma^2 r^{K-1}}{\Delta_{\min}^2 p^K} \|\hat{\mathcal{X}} - \mathcal{X}\|_F^2 \\ & \lesssim \frac{r^K p^{-K/2}}{\text{SNR}}, \end{aligned} \quad (21)$$

where $\mathcal{X} = \mathbb{E}\mathcal{Y}$ is the true mean. The first inequality in (21) holds with the assumption $\min_{i \in [p]} \theta(i) \geq c > 0$ in Theorem 4. The second inequality relies on the key Lemma 1, which indicates

$$\min_{z(i) \neq z(j)} \|[\mathbf{X}_{i:}]^s - [\mathbf{X}_{j:}]^s\| \gtrsim \Delta_{\min}, \quad (22)$$

where $\mathbf{X} = \text{Mat}(\mathcal{X})$. The most challenging part in the proof of Theorem 4 lies in the derivation of inequality (22) (or the proof of Lemma 1), in which the proof of [15] is no longer applicable due to different angle gap assumption in our dTBM. To address the angle gap notion, we develop the extra padding technique in Lemma 5 and balance assumption (6). Last, we finish the proof of Theorem 4 by showing the third inequality of (21) using [13, Proposition 1].

C. Proof Sketch of Theorem 5

The proof of Theorem 5 is inspired by the proof idea of [13, Theorem 2]. We develop extra polar-coordinate based techniques with angle gap characterization to address the nuisance degree heterogeneity. Recall the intermediate quantity, misclustering loss, defined in (11)

$$\begin{aligned} L^{(t)} & := L(z, z^{(t)}) \\ & = \frac{1}{p} \sum_{i \in [p]} \theta(i) \sum_{b \in [r]} \mathbb{1}\left\{z^{(t)}(i) = b\right\} \|[\mathbf{S}_{z(i)}]_b^s - [\mathbf{S}_b]_i^s\|^2. \end{aligned}$$

We show that $L^{(t)}$ provides an upper bound for the misclustering error of interest via the inequality $\ell^{(t)} \leq \frac{L^{(t)}}{\Delta_{\min}^2}$ in Lemma 2. Therefore, it suffices to control $L^{(t)}$. Further, we introduce the oracle estimators for core tensor under the true cluster assignment via

$$\tilde{\mathcal{S}} = \mathcal{Y} \times_1 \mathbf{W}^T \times_2 \cdots \times_K \mathbf{W}^T,$$

where $\mathbf{W} = \mathbf{M} (\text{diag}(\mathbf{1}_p^T \mathbf{M}))^{-1}$ is the weighted true membership matrix. Let $\mathbf{V} = \mathbf{W}^{\otimes(K-1)}$ denote the Kronecker product of $(K-1)$ copies of \mathbf{W} matrices, and we define the

1397 t -th iteration quantities $\mathbf{W}^{(t)}, \mathbf{V}^{(t)}$ corresponding to $\mathbf{M}^{(t)}$ (or
 1398 equivalently $z^{(t)}$). To evaluate $L^{(t+1)}$, we prove the bound

$$\begin{aligned} 1399 & \mathbb{1} \left\{ z^{(t+1)}(i) = b \right\} \\ 1400 & = \mathbb{1} \left\{ \|[\mathbf{Y}_{i:} \mathbf{V}^{(t)}]^s - [\mathbf{S}_{b:}^{(t)}]^s\|^2 \leq \|[\mathbf{Y}_{i:} \mathbf{V}^{(t)}]^s - [\mathbf{S}_{z(i):}^{(t)}]^s\|^2 \right\} \\ 1401 & \leq A_{ib} + B_{ib}, \end{aligned} \quad (23)$$

1402 where $\mathbf{Y} = \text{Mat}(\mathcal{Y}), \mathbf{S} = \text{Mat}(\mathcal{S}), \mathbf{S}^{(t)} = \text{Mat}(\mathcal{S}^{(t)})$ and

$$\begin{aligned} 1403 & A_{ib} = \mathbb{1} \left\{ \left\langle \mathbf{E}_{i:} \mathbf{V}, [\tilde{\mathbf{S}}_{z(i):}]^s - [\tilde{\mathbf{S}}_{b:}]^s \right\rangle \lesssim -\|[\mathbf{S}_{z(i):}]^s - [\mathbf{S}_{b:}]^s\|^2 \right\}, \\ 1404 & B_{ib} = \mathbb{1} \left\{ \|[\mathbf{S}_{z(i):}]^s - [\mathbf{S}_{b:}]^s\|^2 \lesssim F_{ib}^{(t)} + G_{ib}^{(t)} + H_{ib}^{(t)} \right\}. \end{aligned}$$

1405 The terms $F_{ib}^{(t)}, G_{ib}^{(t)}, H_{ib}^{(t)}$ are controlled by $z^{(t)}, \mathcal{S}^{(t)}$; see the
 1406 detailed definitions in (68), (69), (70). Note that the event A_{ib}
 1407 only involves the oracle estimator independent of t , while all
 1408 the terms related to the t -th iteration are in B_{ib} . Thus, the
 1409 inequality (23) decomposes the misclustering loss in the $(t +$
 1410 1)-th iteration into the oracle loss and the loss in t -th iteration.
 1411 This decomposition leads to the separation of statistical error
 1412 and computational error in the final upper bound of Theorem 5.
 1413 Specifically, we prove the contraction inequality

$$\begin{aligned} 1414 & L^{(t+1)} \leq M\xi + \rho L^{(t)}, \\ 1415 & \text{with } \xi = \frac{1}{p} \sum_{i \in [p]} \theta(i) \sum_{b \in [r]} A_{ib} \|[\mathbf{S}_{z(i):}]^s - [\mathbf{S}_{b:}]^s\|^2, \end{aligned} \quad (24)$$

1416 where M is a positive constant, $\rho \in (0, 1)$ is the contraction
 1417 parameter, and we call ξ the oracle loss. Controlling the
 1418 probability of event B_{ib} and obtaining the $\rho L^{(t)}$ term in the
 1419 right hand side of (24) are the most challenging parts in
 1420 the proof of Theorem 5. Note that the true and estimated
 1421 core tensors are involved via their normalized rows such
 1422 as $\mathbf{S}_{a:}^s, \tilde{\mathbf{S}}_{a:}^s, [\mathbf{S}_{a:}^{(t)}]^s$. The Cartesian coordinate based analysis
 1423 in [13] is no longer applicable in our case. Instead, we use
 1424 the polar-coordinate based analysis and the geometry property
 1425 of trigonometric functions to derive the high probability upper
 1426 bounds for $F_{ib}^{(t)}, G_{ib}^{(t)}, H_{ib}^{(t)}$.

1427 Further, by sub-Gaussian concentration, we prove the high
 1428 probability upper bound for oracle loss

$$\xi \lesssim \text{SNR}^{-1} \exp \left(-\frac{p^{K-1} \text{SNR}}{r^{K-1}} \right). \quad (25)$$

1430 Combining the decomposition (24) and the oracle bound (25),
 1431 we finish the proof of Theorem 5.

1432 The proof of MLE error shares the similar idea as Theorems 4-5. We first show a weaker polynomial rate for MLE
 1433 and then improve the rate from polynomial to exponential
 1434 through the iterations. The only difference is that the MLE
 1435 remains the same over iterations due to its global optimality.
 1436 See Appendix B, Section B-G for the detailed proof.

APPENDIX A

ADDITIONAL NUMERICAL EXPERIMENTS

A. Bernoulli Phase Transition

1441 The first additional experiment verifies the
 1442 statistical-computational gap in Section III under the Bernoulli
 1443 model. Consider the Bernoulli model with $p = \{80, 100\}$,

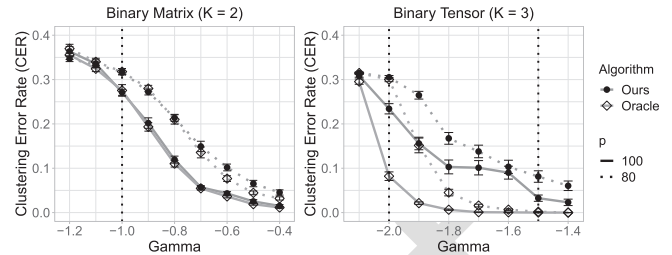


Fig. 12. SNR phase transitions for Bernoulli dTBM with $p = \{80, 100\}, r = 5$ under (a) matrix case with $\gamma \in [-1.2, -0.4]$ and (b) tensor case with $\gamma \in [-2.0, -1.4]$.

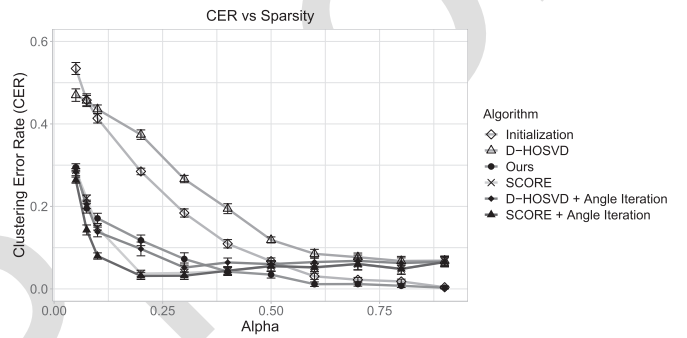


Fig. 13. CER comparison versus sparsity parameter α_p in $[0.05, 0.9]$. We set $p = 100, r = 5$ and $\gamma = -1.2$ under sparse binary dTBM.

1444 $r = 5$. We vary γ in $[-1.2, -0.4]$ and $[-2.1, -1.4]$ for
 1445 matrix ($K = 2$) and tensor ($K = 3$) clustering, respectively.
 1446 We approximate MLE using an oracle estimator, i.e., the
 1447 output of Sub-algorithm 2 initialized from the true assignment.
 1448 Figure 12 shows a similar pattern as Figure 4. The algorithm
 1449 and oracle estimators have no gap in the matrix case, while an
 1450 error gap emerges between the critical values $\gamma_{\text{stat}} = -2$ and
 1451 $\gamma_{\text{comp}} = -1.5$ in the tensor case. Figure 4 suggests the
 1452 statistical-computational gap in Bernoulli models.
 1453

B. Sparsity

1454 The second additional experiment evaluates the algorithm
 1455 performances under the sparse binary dTBM (18). We fix the
 1456 signal exponent $\gamma = -1.2$ and vary the sparsity parameter
 1457 $\alpha_p \in [0.05, 0.9]$. A smaller α_p leads to a higher probability
 1458 of zero entries in the observation. In addition to the three
 1459 algorithms mentioned in Section VI-B (denoted **Initialization**,
 1460 **dTBM**, and **SCORE**), we consider other three algorithms based
 1461 on the discussion in Section IV-C:

- **D-HOSVD**, the diagonal-deleted HOSVD in [9];
- **D-HOSVD + Angle**, the combined algorithm of our
 1463 angle-based iteration with initialization from **D-HOSVD**;
- **SCORE + Angle**, the combined algorithms of our
 1465 angle-based iteration with initialization from **SCORE**.

1466 Figure 13 shows a slightly larger error in **dTBM** than that in
 1467 **SCORE**, **D-HOSVD + Angle**, and **SCORE + Angle** under the
 1468 sparse setting with $\alpha_p < 0.3$. The small gap between **dTBM**
 1469 and other sparse-specific methods implies the robustness of our
 1470 algorithm. In addition, comparing **SCORE** versus **SCORE + Angle** (or **D-HOSVD** versus **D-HOSVD + Angle**) indicates the
 1471 benefit of our angle iterations under the sparse dTBM. In the
 1472

intermediate and dense cases with $\alpha_p \geq 0.3$, our proposed **dTBM** has a clear improvement over others, which again verifies the success of our algorithm in dense settings.

APPENDIX B PROOFS

We provide the proofs for all the theorems in our main paper. In each sub-section, we first show the proof of main theorem and then collect the useful lemmas in the end. We combine the proofs of MLE achievement in Theorem 2 and polynomial-time achievement in Theorem 5 in the last section due to the similar idea.

A. Notation

Before the proofs, we first introduce the notation used throughout the appendix and the general dTBM without symmetric assumptions. The parameter space and minimal gap assumption are also extended for the general asymmetric dTBM.

1) *Preliminaries:* 1) For mode $k \in [K]$, denote mode- k tensor matricizations by

$$\begin{aligned} \mathbf{Y}_k &= \text{Mat}_k(\mathcal{Y}), \quad \mathbf{S}_k = \text{Mat}_k(\mathcal{S}), \\ \mathbf{E}_k &= \text{Mat}_k(\mathcal{E}), \quad \mathbf{X}_k = \text{Mat}_k(\mathcal{X}). \end{aligned}$$

2) For a vector \mathbf{a} , let $\mathbf{a}^s := \mathbf{a}/\|\mathbf{a}\|$ denote the normalized vector. We make the convention that $\mathbf{a}^s = \mathbf{0}$ if $\mathbf{a} = \mathbf{0}$.

3) For a matrix $\mathbf{A} \in \mathbb{R}^{n \times m}$, let $\mathbf{A}^{\otimes K} := \mathbf{A} \otimes \cdots \otimes \mathbf{A} \in \mathbb{R}^{n^K \times m^K}$ denote the Kronecker product of K copies of matrices \mathbf{A} .

4) For a matrix \mathbf{A} , let $\|\mathbf{A}\|_\sigma$ denote the spectral norm of matrix \mathbf{A} , which is equal to the maximal singular value of \mathbf{A} ; let $\lambda_k(\mathbf{A})$ denote the k -th largest singular value of \mathbf{A} ; let $\|\mathbf{A}\|_F$ denote the Frobenius norm of matrix \mathbf{A} .

2) *Extension to General Asymmetric dTBM.:* The general order- K (p_1, \dots, p_K)-dimensional dTBM with r_k communities and degree heterogeneity $\boldsymbol{\theta}_k = [\theta_k(i)] \in \mathbb{R}_+^{p_k}$ is represented by

$$\mathcal{Y} = \mathcal{X} + \mathcal{E}, \quad \text{where } \mathcal{X} = \mathcal{S} \times_1 \boldsymbol{\Theta}_1 \mathbf{M}_1 \times_2 \cdots \times_K \boldsymbol{\Theta}_K \mathbf{M}_K, \quad (26)$$

where $\mathcal{Y} \in \mathbb{R}^{p_1 \times \cdots \times p_K}$ is the data tensor, $\mathcal{X} \in \mathbb{R}^{p_1 \times \cdots \times p_K}$ is the mean tensor, $\mathcal{S} \in \mathbb{R}^{r_1 \times \cdots \times r_K}$ is the core tensor, $\mathcal{E} \in \mathbb{R}^{p_1 \times \cdots \times p_K}$ is the noise tensor consisting of independent zero-mean sub-Gaussian entries with variance bounded by σ^2 , $\boldsymbol{\Theta}_k = \text{diag}(\boldsymbol{\theta}_k)$, and $\mathbf{M}_k \in \{0, 1\}^{p_k \times r_k}$ is the membership matrix corresponding to the assignment $z_k : [p_k] \mapsto [r_k]$, for all $k \in [K]$.

For ease of notation, we use $\{z_k\}$ to denote the collection $\{z_k\}_{k=1}^K$, and $\{\boldsymbol{\theta}_k\}$ to denote the collection $\{\boldsymbol{\theta}_k\}_{k=1}^K$. Correspondingly, we consider the parameter space for the triplet $(\{z_k\}, \mathcal{S}, \{\boldsymbol{\theta}_k\})$,

$$\begin{aligned} \mathcal{P}(\{r_k\}) &= \left\{ (\{z_k\}, \mathcal{S}, \{\boldsymbol{\theta}_k\}) : \boldsymbol{\theta}_k \in \mathbb{R}_+^p, \frac{c_1 p_k}{r_k} |z_k^{-1}(a)| \leq \frac{c_2 p_k}{r_k}, \right. \\ &\quad c_3 \leq \|\mathbf{S}_{k,a,:}\| \leq c_4, \|\boldsymbol{\theta}_{k,z_k^{-1}(a)}\|_1 = |z_k^{-1}(a)|, \\ &\quad \left. \text{for all } a \in [r_k], k \in [K] \right\}. \end{aligned} \quad (27)$$

We call the degree heterogeneity $\{\boldsymbol{\theta}_k\}$ is balanced if for all $k \in [K]$,

$$\min_{a \in [r]} \|\boldsymbol{\theta}_{k,z_k^{-1}(a)}\| = (1 + o(1)) \max_{a \in [r]} \|\boldsymbol{\theta}_{k,z_k^{-1}(a)}\|. \quad (1526)$$

We also consider the generalized Assumption 1 on angle gap.

Assumption 2 (Generalized Angle Gap): Recall $\mathbf{S}_k = \text{Mat}_k(\mathcal{S})$. We assume the minimal gap between normalized rows of \mathbf{S}_k is bounded away from zero for all $k \in [K]$; i.e.,

$$\Delta_{\min} := \min_{k \in [K]} \min_{a \neq b \in [r_k]} \|\mathbf{S}_{k,a,:}^s - \mathbf{S}_{k,b,:}^s\| > 0. \quad (1533)$$

Similarly, let $\text{SNR} = \Delta_{\min}^2/\sigma^2$ with the generalized minimal gap Δ_{\min}^2 defined in Assumption 2. We define the regime

$$\mathcal{P}(\gamma) = \mathcal{P}(\{r_k\}) \cap \{\mathcal{S} \text{ satisfies } \text{SNR} = p^\gamma \text{ and } p_k \asymp p, k \in [K]\}. \quad (1536)$$

B. Proof of Theorem 1

Proof of Theorem 1: To study the identifiability, we consider the noiseless model with $\mathcal{E} = 0$. Assume that there exist two parameterizations satisfying

$$\begin{aligned} \mathcal{X} &= \mathcal{S} \times_1 \boldsymbol{\Theta}_1 \mathbf{M}_1 \times_2 \cdots \times_K \boldsymbol{\Theta}_K \mathbf{M}'_K \\ &= \mathcal{S}' \times_1 \boldsymbol{\Theta}'_1 \mathbf{M}'_1 \times_2 \cdots \times_K \boldsymbol{\Theta}'_K \mathbf{M}'_K, \end{aligned} \quad (1541)$$

where $(\{z_k\}, \mathcal{S}, \{\boldsymbol{\theta}_k\}) \in \mathcal{P}(\{r_k\})$ and $(\{z'_k\}, \mathcal{S}', \{\boldsymbol{\theta}'_k\}) \in \mathcal{P}(\{r'_k\})$ are two sets of parameters. We prove the sufficient and necessary conditions separately.

(\Leftarrow) For the necessity, it suffices to construct two distinct parameters up to cluster label permutation, if the model (26) violates Assumption 2. Note that $\Delta_{\min}^2 = 1$ when there exists $k \in [K]$ such that $r_k = 1$. Hence, we consider the case that $r_k \geq 2$ for all $k \in [K]$. Without loss of generality, we assume $\|\mathbf{S}_{1,1,:}^s - \mathbf{S}_{1,2,:}^s\| = 0$.

By constraints in parameter space (27), neither $\mathbf{S}_{1,1,:}$ nor $\mathbf{S}_{1,2,:}$ is a zero vector. There exists a positive constant c such that $\mathbf{S}_{1,1,:} = c \mathbf{S}_{1,2,:}$. Thus, there exists a core tensor $\mathcal{S}_0 \in \mathbb{R}^{r_1-1 \times \cdots \times r_K}$ such that

$$\mathcal{S} = \mathcal{S}_0 \times_1 \mathbf{C} \mathbf{R}, \quad (1556)$$

where $\mathbf{C} = \text{diag}(1, c, 1, \dots, 1) \in \mathbb{R}^{r_1 \times r_1}$ and

$$\mathbf{R} = \begin{pmatrix} 1 & 0 \\ 1 & 0 \\ 0 & \mathbf{1}_{r_1-2} \end{pmatrix} \in \mathbb{R}^{r_1 \times (r_1-1)}. \quad (1558)$$

Let $\mathbf{D} = \text{diag}(1 + c, 1, \dots, 1) \in \mathbb{R}^{r_1-1 \times r_1-1}$. Consider the parameterization $\mathbf{M}'_1 = \mathbf{M}_1 \mathbf{R}$, $\mathcal{S}' = \mathcal{S}_0 \times_1 \mathbf{D}$, and

$$\theta'_1(i) = \begin{cases} \frac{1}{1+c} \theta_1(i) & i \in z_1^{-1}(1), \\ \frac{c}{1+c} \theta_1(i) & i \in z_1^{-1}(2), \\ \theta_1(i) & \text{otherwise,} \end{cases} \quad (1561)$$

and $\mathbf{M}'_k = \mathbf{M}_k$, $\boldsymbol{\theta}'_k = \boldsymbol{\theta}_k$ for all $k = 2, \dots, K$. Then we have constructed a triplet $(\{z'_k\}, \mathcal{S}', \{\boldsymbol{\theta}'_k\})$ that is distinct from $(\{z_k\}, \mathcal{S}, \{\boldsymbol{\theta}_k\})$ up to label permutation.

(\Rightarrow) For the sufficiency, it suffices to show that all possible triplets $(\{z'_k\}, \mathcal{S}', \{\boldsymbol{\theta}'_k\})$ are identical to $(\{z_k\}, \mathcal{S}, \{\boldsymbol{\theta}_k\})$ up

to label permutation if the model (26) satisfies Assumption (2). We show the uniqueness of the three parameters, $\{\mathbf{M}_k\}, \{\mathcal{S}\}, \{\boldsymbol{\theta}_k\}$ separately.

First, we show the uniqueness of \mathbf{M}_k for all $k \in [K]$. When $r_k = 1$, all possible \mathbf{M}_k 's are equal to the vector $\mathbf{1}_{p_k}$, and the uniqueness holds trivially. Hence, we consider the case that $r_k \geq 2$. Without loss of generality, we consider $k = 1$ with $r_1 \geq 2$ and show the uniqueness of the first mode membership matrix; i.e., $\mathbf{M}'_1 = \mathbf{M}_1 \mathbf{P}_1$ where \mathbf{P}_1 is a permutation matrix. The conclusion for $k \geq 2$ can be showed similarly and thus omitted.

Consider an arbitrary node pair (i, j) . If $z_1(i) = z_1(j)$, then we have $\|\mathbf{X}_{1,z_1(i)}^s - \mathbf{X}_{1,z_1(j)}^s\| = 0$ and thus $\|(\mathbf{S}')_{1,z'_1(i)}^s - (\mathbf{S}')_{1,z'_1(j)}^s\| = 0$ by Lemma 3. Then, by Assumption (2), we have $z'_1(i) = z'_1(j)$. Conversely, if $z_1(i) \neq z_1(j)$, then we have $\|\mathbf{X}_{1,i}^s - \mathbf{X}_{1,j}^s\| \neq 0$ and thus $\|(\mathbf{S}')_{1,z'_1(i)}^s - (\mathbf{S}')_{1,z'_1(j)}^s\| \neq 0$ by Lemma 3. Hence, we have $z'_1(i) \neq z'_1(j)$. Therefore, we have proven that z'_1 is identical z_1 up to label permutation.

Next, we show the uniqueness of $\boldsymbol{\theta}_k$ for all $k \in [K]$ provided that $z_k = z'_k$. Similarly, consider $k = 1$ only, and omit the procedure for $k \geq 2$.

Consider an arbitrary $j \in [p_1]$ such that $z_1(j) = a$. Then for all the nodes $i \in z_1^{-1}(a)$ in the same cluster of j , we have

$$\frac{\mathbf{X}_{1,z_1(i)}^s}{\mathbf{X}_{1,z_1(j)}^s} = \frac{\mathbf{X}'_{1,z_1(i)}^s}{\mathbf{X}'_{1,z_1(j)}^s}, \text{ which implies } \frac{\theta_1(j)}{\theta_1(i)} = \frac{\theta'_1(j)}{\theta'_1(i)}. \quad (29)$$

Let $\theta'_1(j) = c\theta_1(j)$ for some positive constant c . By equation (29), we have $\theta'_1(i) = c\theta_1(i)$ for all $i \in z_1^{-1}(a)$. By the constraint $(\{z_k\}, \mathcal{S}', \{\boldsymbol{\theta}'_k\}) \in \mathcal{P}(\{r_k\})$, we have

$$\sum_{j \in z_1^{-1}(a)} \theta'_1(j) = c \sum_{j \in z_1^{-1}(a)} \theta_1(j) = 1,$$

which implies $c = 1$. Hence, we have proven $\boldsymbol{\theta}_1 = \boldsymbol{\theta}'_1$ provided that $z_1 = z'_1$.

Last, we show the uniqueness of \mathcal{S} ; i.e., $\mathcal{S}' = \mathcal{S} \times_1 \mathbf{P}_1^{-1} \times_2 \cdots \times_K \mathbf{P}_K^{-1}$, where \mathbf{P}_k 's are permutation matrices for all $k \in [K]$. Provided $z'_k = z_k, \boldsymbol{\theta}'_k = \boldsymbol{\theta}_k$, we have $\mathbf{M}'_k = \mathbf{M}_k \mathbf{P}_k$ and $\boldsymbol{\Theta}'_k = \boldsymbol{\Theta}_k$ for all $k \in [K]$.

Let $\mathbf{D}_k = [(\boldsymbol{\Theta}'_k \mathbf{M}'_k)^T (\boldsymbol{\Theta}'_k \mathbf{M}'_k)]^{-1} (\boldsymbol{\Theta}'_k \mathbf{M}'_k)^T, k \in [K]$. By the parameterization (28), we have

$$\begin{aligned} \mathcal{S}' &= \mathcal{X} \times_1 \mathbf{D}_1 \times_2 \cdots \times_K \mathbf{D}_K \\ &= \mathcal{S} \times_1 \mathbf{D}_1 \boldsymbol{\Theta}_1 \mathbf{M}_1 \times_1 \cdots \times_K \mathbf{D}_K \boldsymbol{\Theta}_K \mathbf{M}_K \\ &= \mathcal{S} \times_1 \mathbf{P}_1^{-1} \times_2 \cdots \times_K \mathbf{P}_K^{-1}. \end{aligned}$$

Therefore, we finish the proof of Theorem 1. \square

1) Useful Lemma for the Proof of Theorem 1:

Lemma 3 (Motivation of Angle-Based Clustering):

Consider the signal tensor \mathcal{X} in the general asymmetric dTBM (26) with $(\{z_k\}, \mathcal{S}, \{\boldsymbol{\theta}_k\}) \in \mathcal{P}(\{r_k\})$ and $r_k \geq 2, k \in [K]$. Then, for any $k \in [K]$ and index pair $(i, j) \in [p_k]^2$, we have

$$\begin{aligned} \left\| \mathbf{S}_{k,z_k(i)}^s - \mathbf{S}_{k,z_k(j)}^s \right\| &= 0 \quad \text{if and only if} \\ \left\| \mathbf{X}_{k,z_k(i)}^s - \mathbf{X}_{k,z_k(j)}^s \right\| &= 0. \end{aligned}$$

Proof of Lemma 3: Without loss of generality, we prove $k = 1$ only and drop the subscript k in $\mathbf{X}_k, \mathbf{S}_k$ for notational convenience. By tensor matricization, we have

$$\mathbf{X}_{j:} = \theta_1(j) \mathbf{S}_{z_1(j):} [\boldsymbol{\Theta}_2 \mathbf{M}_2 \otimes \cdots \otimes \boldsymbol{\Theta}_K \mathbf{M}_K]^T. \quad (1619)$$

Let $\tilde{\mathbf{M}} = \boldsymbol{\Theta}_2 \mathbf{M}_2 \otimes \cdots \otimes \boldsymbol{\Theta}_K \mathbf{M}_K$. Notice that for two vectors \mathbf{a}, \mathbf{b} and two positive constants $c_1, c_2 > 0$, we have

$$\|\mathbf{a}^s - \mathbf{b}^s\| = \|(c_1 \mathbf{a})^s - (c_2 \mathbf{b})^s\|. \quad (1622)$$

Thus it suffices to show the following statement holds for any index pair $(i, j) \in [p_1]^2$,

$$\left\| \mathbf{S}_{z_1(i):}^s - \mathbf{S}_{z_1(j):}^s \right\| = 0 \quad \text{if and only if} \quad (1625)$$

$$\left\| [\mathbf{S}_{z_1(i):} \tilde{\mathbf{M}}^T]^s - [\mathbf{S}_{z_1(j):} \tilde{\mathbf{M}}^T]^s \right\| = 0. \quad (1626)$$

$$(\Leftarrow) \text{ Suppose } \left\| [\mathbf{S}_{z_1(i):} \tilde{\mathbf{M}}^T]^s - [\mathbf{S}_{z_1(j):} \tilde{\mathbf{M}}^T]^s \right\| = 0. \quad (1627)$$

There exists a positive constant c such that $\mathbf{S}_{z_1(i):} \tilde{\mathbf{M}}^T = c \mathbf{S}_{z_1(j):} \tilde{\mathbf{M}}^T$. Note that

$$\mathbf{S}_{z_1(i):} = \mathbf{S}_{z_1(i):} \tilde{\mathbf{M}}^T \left[\tilde{\mathbf{M}} \left(\tilde{\mathbf{M}}^T \tilde{\mathbf{M}} \right)^{-1} \right], \quad (1630)$$

where $\tilde{\mathbf{M}}^T \tilde{\mathbf{M}}$ is an invertible diagonal matrix with positive diagonal elements. Thus, we have $\mathbf{S}_{z_1(i):} = c \mathbf{S}_{z_1(j):}$, which implies $\left\| \mathbf{S}_{z_1(i):}^s - \mathbf{S}_{z_1(j):}^s \right\| = 0$.

(\Rightarrow) Suppose $\left\| \mathbf{S}_{z_1(i):}^s - \mathbf{S}_{z_1(j):}^s \right\| = 0$. There exists a positive constant c such that $\mathbf{S}_{z_1(i):} = c \mathbf{S}_{z_1(j):}$, and thus $\mathbf{S}_{z_1(i):} \tilde{\mathbf{M}}^T = c \mathbf{S}_{z_1(j):} \tilde{\mathbf{M}}^T$, which implies $\left\| [\mathbf{S}_{z_1(i):} \tilde{\mathbf{M}}^T]^s - [\mathbf{S}_{z_1(j):} \tilde{\mathbf{M}}^T]^s \right\| = 0$.

Therefore, we finish the proof of Lemma 3. \square

C. Proof of Lemma 1 and Lemma 2

Proof of Lemma 1: Note that the vector $\mathbf{S}_{z(i):}$ can be folded to a tensor $\mathcal{S}' = [\mathcal{S}'_{a_2, \dots, a_K}] \in \mathbb{R}^{r^{K-1}}$; i.e., $\text{vec}(\mathcal{S}') = \mathbf{S}_{z(i):}$. Define weight vectors $\mathbf{w}_{a_2, \dots, a_K}$ corresponding to the elements in $\mathcal{S}'_{a_2, \dots, a_K}$ by

$$\begin{aligned} \mathbf{w}_{a_2 \dots a_K} &= [\theta_{z^{-1}(a_2)}^T \otimes \cdots \otimes \theta_{z^{-1}(a_K)}^T] \in \mathbb{R}^{|z^{-1}(a_2)| \times \cdots \times |z^{-1}(a_K)|}, \end{aligned} \quad (1645)$$

for all $a_k \in [r], k = 2, \dots, K$, where \otimes denotes the Kronecker product. Therefore, we have $\mathbf{X}_{i:} = \theta(i) \text{Pad}_{\mathbf{w}}(\mathbf{S}_{z(i)})$ where $\mathbf{w} = \{\mathbf{w}_{a_2, \dots, a_K}\}_{a_k \in [r], k \in [K]/\{1\}}$. Specifically, we have $\|\mathbf{w}_{a_2, \dots, a_K}\|^2 = \prod_{k=2}^K \|\theta_{z^{-1}(a_k)}\|^2$, and by the balanced assumption (6) we have

$$\max_{(a_2, \dots, a_K)} \|\mathbf{w}_{a_2, \dots, a_K}\|^2 = (1 + o(1)) \min_{(a_2, \dots, a_K)} \|\mathbf{w}_{a_2, \dots, a_K}\|^2. \quad (30)$$

Consider the inner product of $\mathbf{X}_{i:}$ and $\mathbf{X}_{j:}$ for $z(i) \neq z(j)$. By the definition of weighted padding operator (56) and the balanced assumption (30), we have

$$\begin{aligned} &\langle \mathbf{X}_{i:}, \mathbf{X}_{j:} \rangle \\ &= \theta(i)\theta(j) \langle \text{Pad}_{\mathbf{w}}(\mathbf{S}_{z(i)}), \text{Pad}_{\mathbf{w}}(\mathbf{S}_{z(j)}) \rangle \\ &= \theta(i)\theta(j) \min_{(a_2, \dots, a_K)} \|\mathbf{w}_{a_2, \dots, a_K}\|^2 \langle \mathbf{S}_{z(i)}, \mathbf{S}_{z(j)} \rangle (1 + o(1)). \end{aligned} \quad (1657)$$

Therefore, when p large enough, the inner product $\langle \mathbf{X}_{i:}, \mathbf{X}_{j:} \rangle$ has the same sign as $\langle \mathbf{S}_{z(i):}, \mathbf{S}_{z(j):} \rangle$.

Then, we have

$$\begin{aligned} \cos(\mathbf{S}_{z_1(i):}, \mathbf{S}_{z_1(j):}) &= \frac{\langle \mathbf{S}_{z_1(i):}, \mathbf{S}_{z_1(j):} \rangle}{\|\mathbf{S}_{z_1(i):}\| \|\mathbf{S}_{z_1(j):}\|} \\ &= (1 + o(1)) \frac{\langle \mathbf{X}_{i:}, \mathbf{X}_{j:} \rangle}{\|\mathbf{X}_{i:}\| \|\mathbf{X}_{j:}\|} \\ &= (1 + o(1)) \cos(\mathbf{X}_{i:}, \mathbf{X}_{j:}), \end{aligned}$$

where the second inequality follows by the balance assumption on θ .

Further, notice that $\|\mathbf{v}_1^s - \mathbf{v}_2^s\|^2 = 2(1 - \cos(\mathbf{v}_1, \mathbf{v}_2))$. For all i, j such that $z(i) \neq z(j)$, when $p \rightarrow \infty$, we have

$$\|\mathbf{X}_{i:}^s - \mathbf{X}_{j:}^s\| \asymp \|\mathbf{S}_{z_1(i):}^s - \mathbf{S}_{z_1(j):}^s\| \gtrsim \Delta_{\min}.$$

Combining the inequalities (12) and (12) in the proof of Theorem 2 in [15], we have

$$\begin{aligned} \inf_{\hat{z}_1} \mathbb{E} [\ell(\hat{z}_1, z_1^*) | (z_k^*, \mathcal{S}^*, \boldsymbol{\theta}_k^*)] &\geq \\ \frac{C}{r^3 |T_1^c|} \sum_{i \in T_1^c} \inf_{\hat{z}_1(i)} \{ \mathbb{P}[\hat{z}_1(i) = 1 | z_1^*(i) = 2, z_k^*, \mathcal{S}^*, \boldsymbol{\theta}_k^*] \\ &\quad + \mathbb{P}[\hat{z}_1(i) = 2 | z_1^*(i) = 1, z_k^*, \mathcal{S}^*, \boldsymbol{\theta}_k^*] \}, \end{aligned} \quad (31)$$

where C is some positive constant, \hat{z}_1 on the left hand side denote the generic assignment functions in $\mathcal{P}(\gamma)$, and the infimum on the right hand side is taken over the generic assignment function family of $\hat{z}_1(i)$ for all nodes $i \in T_1^c$. Here, the factor $r^3 = r \cdot r^2$ in (31) comes from two sources: $r^2 \asymp \binom{r}{2}$ comes from the multiple testing burden for all pairwise comparisons among r clusters; and another r comes from the number of elements $|T_k^c| \asymp p/r$ to be clustered.

Proof of Lemma 2: By the definition of minimal gap in Assumption 1, we have

Next, we need to find the lower bound of the rightmost side in (31).

We consider the hypothesis test based on model (26). First, we reparameterize the model under the construction (i)-(ii).

$$\mathbf{x}_a^* = [\text{Mat}_1(\mathcal{S}^* \times_2 \boldsymbol{\Theta}_2^* \mathbf{M}_2^* \times_3 \cdots \times_K \boldsymbol{\Theta}_K^* \mathbf{M}_K^*)]_{a:},$$

$$\begin{aligned} L^{(t)} &= \frac{1}{p} \sum_{i \in [p]} \theta(i) \sum_{b \in [r]} \mathbf{1}\{z^{(t)}(i) = b\} \|[\mathbf{S}_{z(i):}]^s - [\mathbf{S}_b:]^s\|^2 \\ &\geq \frac{1}{p} \sum_{i \in [p]} \theta(i) \sum_{b \in [r]} \mathbf{1}\{z^{(t)}(i) = b\} \Delta_{\min}^2 \\ &\geq c\ell^{(t)} \Delta_{\min}^2, \end{aligned}$$

where the last inequality follows from the assumption $\min_{i \in [p]} \theta(i) \geq c > 0$. \square

for all $a \in [r]$, where \mathbf{x}_a^* 's are centroids in $\mathbb{R}^{p^{K-1}}$. Without loss of generality, we consider the lower bound for the summand in (31) for $i = 1$. The analysis for other $i \in T_1^c$ are similar. For notational simplicity, we suppress the subscript i and write $\mathbf{y}, \boldsymbol{\theta}^*, z$ in place of $\mathbf{y}_1, \boldsymbol{\theta}_1^*(1)$ and $z_1(1)$, respectively. The equivalent vector problem for assessing the summand in (31) is

$$\mathbf{y} = \boldsymbol{\theta}^* \mathbf{x}_z^* + \mathbf{e}, \quad (32)$$

D. Proof of Theorem 2 (Impossibility)

Proof of Theorem 2 (Impossibility): Consider the general asymmetric dTBM (26) in the special case that $p_k = p$ and $r_k = r$ for all $k \in [K]$ with $K \geq 2$, $2 \leq r \lesssim p^{1/3}$ as $p \rightarrow \infty$. For simplicity, we show the minimax rate for the estimation on the first mode \hat{z}_1 ; the proof for other modes are essentially the same.

To prove the minimax rate (10), it suffices to take an arbitrary $\mathcal{S}^* \in \mathcal{P}_S(\gamma)$ with $\gamma < -(K-1)$ and construct $(z_k^*, \boldsymbol{\theta}_k^*)$ such that

$$\inf_{\hat{z}_1} \mathbb{E} [\ell(\hat{z}_1, z_1^*) | (z_k^*, \mathcal{S}^*, \boldsymbol{\theta}_k^*)] \geq 1.$$

We first define a subset of indices $T_k \subset [p_k]$, $k \in [K]$ in order to avoid the complication of label permutation. Based on [13, Proof of Theorem 6], we consider the restricted family of \hat{z}_k 's for which the following three conditions are satisfied:

- (a) $\hat{z}_k(i) = z_k(i)$ for all $i \in T_k$; (b) $|T_k^c| \asymp \frac{p}{r}$;
- (c) $\min_{\pi \in \Pi} \sum_{i \in [p]} \mathbf{1}\{\hat{z}_k(i) \neq \pi \circ z_k(i)\} = \sum_{i \in [p]} \mathbf{1}\{\hat{z}_k(i) \neq z_k(i)\}$,

for all $k \in [K]$. Now, we consider the construction:

- (i) $\{z_k^*\}$ satisfies properties (a)-(c) with misclassification sets T_k^c for all $k \in [K]$;
- (ii) $\{\boldsymbol{\theta}_k^*\}$ such that $\boldsymbol{\theta}_k^*(i) \leq \sigma r^{(K-1)/2} p^{-(K-1)/2}$ for all $i \in T_k^c$, $k \in [K]$ and $\max_{k \in [K], a \in [r]} \|\boldsymbol{\theta}_{k,z_k^{*, -1}(a)}\|_2^2 \asymp p/r$.

where $z \in \{1, 2\}$ is an unknown parameter, $\boldsymbol{\theta}^* \in \mathbb{R}_+$ is the given heterogeneity degree, $\mathbf{x}_1^*, \mathbf{x}_2^* \in \mathbb{R}^{p^{K-1}}$ are given centroids, and $\mathbf{e} \in \mathbb{R}^{p^{K-1}}$ consists of i.i.d. $N(0, \sigma^2)$ entries. Then, we consider the hypothesis testing under the model (32):

$$H_0 : z = 1, \mathbf{y} = \boldsymbol{\theta}^* \mathbf{x}_1^* + \mathbf{e} \leftrightarrow H_1 : z = 2, \mathbf{y} = \boldsymbol{\theta}^* \mathbf{x}_2^* + \mathbf{e}, \quad (33)$$

The hypothesis testing (33) is a simple versus simple testing, since the assignment z is the only unknown parameter in the test. By Neyman-Pearson lemma, the likelihood ratio test is optimal with minimal Type I + II error. Under Gaussian model, the likelihood ratio test of (33) is equivalent to the least square estimator $\hat{z}_{LS} = \arg \min_{a=\{1,2\}} \|\mathbf{y} - \boldsymbol{\theta}^* \mathbf{x}_a^*\|_F^2$.

Let $\mathbf{S} = \text{Mat}_1(\mathcal{S})$. Note that

$$\begin{aligned} &\|\boldsymbol{\theta}^* \mathbf{x}_1^* - \boldsymbol{\theta}^* \mathbf{x}_2^*\|_F \\ &\leq \boldsymbol{\theta}^* \|\mathbf{S}_{1:}^* - \mathbf{S}_{2:}^*\|_F \prod_{k=2}^K \lambda_{\max}(\boldsymbol{\Theta}_k^* \mathbf{M}_k^*) \\ &\leq \boldsymbol{\theta}^* \|\mathbf{S}_{1:}^* - \mathbf{S}_{2:}^*\|_F \max_{k \in [K]/\{1\}, a \in [r]} \|\boldsymbol{\theta}_{k,z_k^{*, -1}(a)}\|_2^{K-1} \\ &\leq \sigma r^{(K-1)/2} p^{-(K-1)/2} 2 c_4 p^{(K-1)/2} r^{-(K-1)/2} \\ &\leq 2 c_4 \sigma, \end{aligned}$$

where $\lambda_{\max}(\cdot)$ denotes the maximal singular value, the second inequality follows from Lemma 6, and the third inequality

follows from property (ii) and the boundedness constraint in $\mathcal{P}_S(\gamma)$ such that $\|\mathbf{S}_{1:}^* - \mathbf{S}_{2:}^*\|_F \leq \|\mathbf{S}_{1:}^*\|_F + \|\mathbf{S}_{2:}^*\|_F \leq 2c_4$. Hence, we have

$$\begin{aligned} & \inf_{\hat{z}_1(1)} \{\mathbb{P}[\hat{z}_1(1) = 1 | z_1^*(1) = 2, z_k^*, \mathcal{S}^*, \boldsymbol{\theta}_k^*] \\ & \quad + \mathbb{P}[\hat{z}_1(1) = 2 | z_1^*(1) = 1, z_k^*, \mathcal{S}^*, \boldsymbol{\theta}_k^*]\} \\ &= 2\mathbb{P}[\hat{z}_{LS} = 1 | z_1^*(1) = 2, z_k^*, \mathcal{S}^*, \boldsymbol{\theta}_k^*] \\ &= 2\mathbb{P}[\|\mathbf{y} - \boldsymbol{\theta}^* \mathbf{x}_1^*\|_F^2 \leq \|\mathbf{y} - \boldsymbol{\theta}^* \mathbf{x}_2^*\|_F^2 | z_1^*(1) = 2, z_k^*, \mathcal{S}^*, \boldsymbol{\theta}_k^*] \\ &= 2\mathbb{P}[2\langle \mathbf{e}, \boldsymbol{\theta}^* \mathbf{x}_1^* - \boldsymbol{\theta}^* \mathbf{x}_2^* \rangle \geq \|\boldsymbol{\theta}^* \mathbf{x}_1^* - \boldsymbol{\theta}^* \mathbf{x}_2^*\|_F^2] \\ &= 2\mathbb{P}[N(0, 1) \geq \boldsymbol{\theta}^* \|\mathbf{x}_1^* - \mathbf{x}_2^*\|_F / (2\sigma)] \\ &\geq 2\mathbb{P}[N(0, 1) \geq c_4] \geq c, \end{aligned} \quad (34)$$

where the first equation holds by symmetry, the third equation holds by rearrangement, the fourth equation holds from the fact that $\langle \mathbf{e}, \boldsymbol{\theta}^* \mathbf{x}_1^* - \boldsymbol{\theta}^* \mathbf{x}_2^* \rangle \sim N(0, \sigma \|\boldsymbol{\theta}^* \mathbf{x}_1^* - \boldsymbol{\theta}^* \mathbf{x}_2^*\|_F)$, and c is some positive constant in the last inequality.

Plugging the inequality (34) into the inequality (31) for all $i \in T_1^c$, then, we have

$$\liminf_{p \rightarrow \infty} \inf_{\hat{z}_1} \mathbb{E}[\rho(\hat{z}_1, z_1^*) | z_k^*, \boldsymbol{\theta}_k^*, \mathcal{S}^*] \geq \liminf_{p \rightarrow \infty} \frac{Ccp}{r^3} \geq Cc,$$

where the last inequality follows by the condition $r = o(p^{1/3})$. By the discrete nature of the misclustering error, we obtain our conclusion

$$\liminf_{p \rightarrow \infty} \inf_{\mathcal{S}^* \in \mathcal{P}_S(\gamma)} \inf_{\hat{z}_{\text{stat}}} \sup_{(z^*, \boldsymbol{\theta}^*) \in \mathcal{P}_{z, \boldsymbol{\theta}}} \mathbb{E}[\rho(\hat{z}_{\text{stat}}, z)] \geq 1.$$

Last, with constructed $z_k^*, \boldsymbol{\theta}_k^*$ satisfying properties (i) and (ii) and $\gamma' < -(K-1)$, we construct a core tensor \mathcal{S}^* such that $\Delta_{\mathbf{X}^*}^2 \leq p^{-(K-1)}$. Based on the property (ii) and the boundedness constraint of \mathcal{S}^* in \mathcal{P} , we still have $\|\boldsymbol{\theta}^* \mathbf{x}_1^* - \boldsymbol{\theta}^* \mathbf{x}_2^*\|_F \leq 2c_4\sigma$. Hence, we obtain the desired result

$$\begin{aligned} & \liminf_{p \rightarrow \infty} \inf_{\hat{z}_1} \sup_{(z, \mathcal{S}, \boldsymbol{\theta}) \in \mathcal{P}'(\gamma')} \mathbb{E}[\rho(\hat{z}_1, z_1)] \\ & \geq \liminf_{p \rightarrow \infty} \inf_{\hat{z}_{\text{stat}}} \mathbb{E}[\rho(\hat{z}_1, z_1^*) | z_k^*, \mathcal{S}^*, \boldsymbol{\theta}_k^*] \geq 1. \end{aligned}$$

□

E. Proof of Theorem 3 (Impossibility)

Proof of Theorem 3 (Impossibility): The idea of proving computational hardness is to show the computational lower bound for a special class of degree-corrected tensor clustering model with $K \geq 2$ and $r \geq 2$. We construct the following special class of higher-order degree-corrected tensor clustering model. For a given signal level $\gamma \in \mathbb{R}$ and noise variance σ , define a rank-2 symmetric tensor $\mathcal{S} \in \mathbb{R}^{3 \times \dots \times 3}$ subject to

$$\mathcal{S} = \mathcal{S}(\gamma) = \begin{bmatrix} 1 \\ 1 \\ 1 \end{bmatrix}^{\otimes K} + \sigma p^{-\gamma/2} \begin{bmatrix} 1 \\ -1 \\ 0 \end{bmatrix}^{\otimes K}. \quad (35)$$

Then, we consider the signal tensor family

$\mathcal{P}_{\text{shifted}}(\gamma) = \{\mathcal{X} : \mathcal{X} = \mathcal{S} \times_1 \mathbf{M}_1 \times_2 \dots \times_K \mathbf{M}_K\}$, where membership matrix $\mathbf{M}_k \in \{0, 1\}^{p \times 3}$ satisfies $|\mathbf{M}_k(:, i)| \asymp p$ for all $i \in [3]$ and $k \in [K]$.

We claim that the constructed family satisfies the following two properties:

- (i) For every $\gamma \in \mathbb{R}$, $\mathcal{P}_{\text{shifted}}(\gamma) \subset \mathcal{P}(\gamma)$, where $\mathcal{P}(\gamma)$ is the degree-corrected cluster tensor family (5). 1788
- (ii) For every $\gamma \in \mathbb{R}$, $\{\mathcal{X} - 1 : \mathcal{X} \in \mathcal{P}_{\text{shifted}}(\gamma)\} \subset \mathcal{P}_{\text{non-degree}}(\gamma)$, where $\mathcal{P}_{\text{non-degree}}(\gamma)$ denotes the sub-family of rank-one tensor block model constructed in the proof of [13, Theorem 7]. 1789

The verification of the above two properties is provided in the end of this proof. 1793

Now, following the proof of [13, Theorem 7], when $\gamma < -K/2$, every polynomial-time algorithm estimator $(\hat{\mathbf{M}}_k)_{k \in [K]}$ obeys 1795

$$\liminf_{p \rightarrow \infty} \sup_{\mathcal{X} \in \mathcal{P}_{\text{non-degree}}(\gamma)} \mathbb{P}(\exists k \in [K], \hat{\mathbf{M}}_k \neq \mathbf{M}_k) \geq 1/2, \quad (36) \quad 1797$$

under the HPC Conjecture 1. The inequality (36) implies 1798

$$\liminf_{p \rightarrow \infty} \sup_{\mathcal{X} \in \mathcal{P}_{\text{non-degree}}(\gamma)} \max_{k \in [K]} \mathbb{E}[\rho(\mathbf{z}_k, \hat{\mathbf{z}}_k)] \geq 1. \quad 1799$$

Based on properties (i)-(ii), we conclude that 1800

$$\liminf_{p \rightarrow \infty} \sup_{\mathcal{X} \in \mathcal{P}(\gamma)} \max_{k \in [K]} \mathbb{E}[\rho(\mathbf{z}_k, \hat{\mathbf{z}}_k)] \geq 1. \quad 1801$$

We complete the proof by verifying the properties (i)-(ii). For (i), we verify that the angle gap for the core tensor \mathcal{S} in (35) is on the order of $\sigma p^{-\gamma/2}$. Specifically, write $\mathbf{1} = (1, 1, 1)$ and $\mathbf{e} = (1, -1, 0)$. 1802

We have 1803

$$\text{Mat}(\mathcal{S}) = \begin{bmatrix} \text{Vec}(\mathbf{1}^{\otimes K-1}) + \sigma p^{-\gamma/2} \text{Vec}\left(\mathbf{e}^{\otimes(K-1)}\right) \\ \text{Vec}(\mathbf{1}^{\otimes K-1}) - \sigma p^{-\gamma/2} \text{Vec}\left(\mathbf{e}^{\otimes(K-1)}\right) \\ \text{Vec}(\mathbf{1}^{\otimes K-1}) \end{bmatrix}. \quad 1804$$

Based on the orthogonality $\langle \mathbf{1}, \mathbf{e} \rangle = 0$, the minimal angle gap among rows of $\text{Mat}(\mathcal{S})$ is 1805

$$\begin{aligned} \Delta_{\min}^2(\mathcal{S}) &\asymp \tan^2(\text{Mat}(\mathcal{S})_{1:}, \text{Mat}(\mathcal{S})_{3:}) \\ &= \left(\frac{\|\mathbf{e}\|_2}{\|\mathbf{1}\|_2}\right)^{2(K-1)} \sigma^2 d^{-\gamma} \\ &\asymp \sigma^2 d^{-\gamma}. \end{aligned} \quad 1806$$

Therefore, we have shown that $\mathcal{P}_{\text{shifted}}(\gamma) = \mathcal{P}(\gamma)$. Finally, the property (ii) follows directly by comparing the definition of \mathcal{S} in (35) with that in the proof of [13, Theorem 7]. □ 1812

F. Proof of Theorem 4 and Proposition 1

Proof of Theorem 4: We prove Theorem 4 under the dTBM (1) with symmetric mean tensor, parameters $(z, \mathcal{S}, \boldsymbol{\theta})$, fixed $r \geq 1, K \geq 2$, and i.i.d. noise. For the case $r = 1$, we have $L(z^{(0)}, z) = 0, \ell(z^{(0)}, z) = 0$ trivially. Hence, we focus on the proof of the first mode clustering $z_1^{(0)}$ with $r \geq 2$; the proofs for the other modes can be extended similarly. We drop the subscript k in the matricizations $\mathbf{M}_k, \mathbf{X}_k, \mathbf{S}_k$ and in the estimate $z_1^{(0)}$. We firstly show the proof with balanced $\boldsymbol{\theta}$.

1) *We Firstly Show the Upper Bound for Misclustering Error $\ell(z^{(0)}, z)$:* First, by Lemma 1, there exists a positive constant such that $\min_{z(i) \neq z(j)} \|\mathbf{X}_i^s - \mathbf{X}_j^s\| \geq c_0 \Delta_{\min}$. By the balance assumption on $\boldsymbol{\theta}$ and Lemma 8, we have

$$\min_{\pi \in \Pi} \sum_{i: z^{(0)}(i) \neq \pi(z(i))} \theta(i)^2 \leq \sum_{i \in S_I} \theta(i)^2 + 4 \sum_{i \in S} \theta(i)^2, \quad (37) \quad 1828$$

where 1829

$$S_0 = \{i : \|\hat{\mathbf{X}}_i\| = 0\}, S = \{i \in S_0^c : \|\hat{\mathbf{x}}_{z^{(0)}(i)} - \mathbf{X}_i^s\| \geq c_0 \Delta_{\min}/2\}. \quad 1830$$

1831 On one hand, note that for any set $P \in [p]$,

$$\begin{aligned} 1832 \quad \sum_{i \in P} \|\mathbf{X}_{i:}\|^2 &= \sum_{i \in P} \|\theta(i) \mathbf{S}_{z(i)} : (\Theta \mathbf{M})^{T, \otimes(K-1)}\|^2 \\ 1833 \quad &\geq \sum_{i \in P} \theta(i)^2 \min_{a \in [r]} \|\mathbf{S}_{a:}\|^2 \lambda_r^{2(K-1)}(\Theta \mathbf{M}) \\ 1834 \quad &\gtrsim \sum_{i \in P} \theta(i)^2 p^{K-1} r^{-(K-1)}, \end{aligned}$$

1835 where the last inequality follows Lemma 6, the assumption that
1836 $\min_{i \in [p]} \theta(i) \geq c$, and the constraint $\min_{a \in [r]} \|\mathbf{S}_{a:}\| \geq c_3$ in
1837 the parameter space (2). Thus, we have

$$1838 \quad \sum_{i \in P} \theta(i)^2 \lesssim \sum_{i \in P} \|\mathbf{X}_{i:}\|^2 p^{-(K-1)} r^{K-1}. \quad (38)$$

1839 On the other hand, note that

$$\begin{aligned} 1840 \quad &\sum_{i \in S} \|\mathbf{X}_{i:}\|^2 \\ 1841 \quad &\leq 2 \sum_{i \in S} \|\hat{\mathbf{X}}_{i:}\|^2 + 2 \sum_{i \in S} \|\hat{\mathbf{X}}_{i:} - \mathbf{X}_{i:}\|^2 \\ 1842 \quad &\leq \frac{8}{c_0^2 \Delta_{\min}^2} \sum_{i \in S} \|\hat{\mathbf{X}}_{i:}\|^2 \|\hat{\mathbf{x}}_{z^{(0)}(i)} - \mathbf{X}_{i:}^s\|^2 + 2 \|\hat{\mathcal{X}} - \mathcal{X}\|_F^2 \\ 1843 \quad &\leq \frac{16}{c_0^2 \Delta_{\min}^2} \sum_{i \in S} \|\hat{\mathbf{X}}_{i:}\|^2 \left[\|\hat{\mathbf{x}}_{z^{(0)}(i)} - \hat{\mathbf{X}}_{i:}^s\|^2 + \|\hat{\mathbf{X}}_{i:}^s - \mathbf{X}_{i:}^s\|^2 \right] \\ 1844 \quad &\quad + 2 \|\hat{\mathcal{X}} - \mathcal{X}\|_F^2 \quad (41) \end{aligned}$$

$$1845 \quad \leq \frac{16(1+\eta)}{c_0^2 \Delta_{\min}^2} \sum_{i \in S} \|\hat{\mathbf{X}}_{i:}\|^2 \|\hat{\mathbf{X}}_{i:}^s - \mathbf{X}_{i:}^s\|^2 + 2 \|\hat{\mathcal{X}} - \mathcal{X}\|_F^2 \quad (42)$$

$$1846 \quad \leq \left(\frac{16(1+\eta)}{c_0^2 \Delta_{\min}^2} + 2 \right) \|\hat{\mathcal{X}} - \mathcal{X}\|_F^2 \quad (43)$$

$$1847 \quad \lesssim \left(\frac{16(1+\eta)}{c_0^2 \Delta_{\min}^2} + 2 \right) (p^{K/2} r + pr^2 + r^K) \sigma^2, \quad (44)$$

1849 where inequalities (39) and (41) follow from the triangle
1850 inequality, (40) follows from the definition of S , (42) follows
1851 from the update rule of k -means in Step 6 of Sub-algorithm 1,
1852 (43) follows from Lemma 4, and the last inequality (44)
1853 follows from Lemma 7. Also, note that

$$\begin{aligned} 1854 \quad \sum_{i \in S_0} \|\mathbf{X}_{i:}\|^2 &= \sum_{i \in S_0} \|\hat{\mathbf{X}}_{i:} - \mathbf{X}_{i:}\|^2 \\ 1855 \quad &\leq \|\hat{\mathcal{X}} - \mathcal{X}\|_F^2 \\ 1856 \quad &\lesssim (p^{K/2} r + pr^2 + r^K) \sigma^2, \quad (45) \end{aligned}$$

1857 where the equation follows from the definition of S_0 . Therefore,
1858 combining the inequalities (37), (38), (44), and (45),
1859 we have

$$\begin{aligned} 1860 \quad &\min_{\pi \in \Pi} \sum_{i: z^{(0)}(i) \neq \pi(z(i))} \theta(i)^2 \\ 1861 \quad &\lesssim \left(\sum_{i \in S} \|\mathbf{X}_{i:}\|^2 + \sum_{i \in S_0} \|\mathbf{X}_{i:}\|^2 \right) p^{-(K-1)} r^{K-1} \\ 1862 \quad &\lesssim \frac{\sigma^2 r^{K-1}}{\Delta_{\min}^2 p^{K-1}} (p^{K/2} r + pr^2 + r^K). \quad (46) \end{aligned}$$

With the assumption that $\min_{i \in [p]} \theta(i) \geq c$, we finally obtain
the result

$$\ell(z^{(0)}, z) \lesssim \frac{1}{p} \min_{\pi \in \Pi} \sum_{i: z^{(0)}(i) \neq \pi(z(i))} \theta(i)^2 \lesssim \frac{r^K p^{-K/2}}{\text{SNR}}, \quad (47)$$

where the last inequality follows from the definition $\text{SNR} = \Delta_{\min}^2 / \sigma^2$.

Without the balanced θ , we have $\min_{z(i) \neq z(j)} \|\mathbf{X}_{i:}^s - \mathbf{X}_{j:}^s\| \geq c_0 \Delta_{\mathbf{X}}$. Replacing the definition of S with $\Delta_{\mathbf{X}}$, we obtain the desired result.

2) Next, we Show the Bound for $L(z^{(0)}, z)$: Note that $\mathbf{X}_{i:}^s$ have only r different values. We let $\mathbf{X}_a^s = \mathbf{X}_{i:}^s$ for all i such that $z(i) = a, a \in [r]$.

Notice that

$$\|\mathbf{X}_{i:}\|^2 \gtrsim p^{K-1} r^{-(K-1)} \quad (48)$$

and

$$\|\mathbf{X}_{i:} - \hat{\mathbf{X}}_{i:}\|^2 \leq \|\hat{\mathcal{X}} - \mathcal{X}\|_F^2 \lesssim p^{K/2} r + pr^2 + r^K. \quad (49)$$

Therefore, when p is large enough, we have

$$\begin{aligned} 1870 \quad &\sum_{i \in [p]} \|\mathbf{X}_{i:}\|^2 \|\hat{\mathbf{X}}_i^s - \hat{\mathbf{x}}_{z^{(0)}(i)}\|^2 \\ 1871 \quad &\lesssim \sum_{i \in [p]} (\|\mathbf{X}_{i:}\|^2 - \|\mathbf{X}_{i:} - \hat{\mathbf{X}}_{i:}\|^2) \|\hat{\mathbf{X}}_i^s - \hat{\mathbf{x}}_{z^{(0)}(i)}\|^2 \\ 1872 \quad &\lesssim \sum_{i \in [p]} \|\hat{\mathbf{X}}_{i:}\|^2 \|\hat{\mathbf{X}}_i^s - \hat{\mathbf{x}}_{z^{(0)}(i)}\|^2 \\ 1873 \quad &\lesssim \eta \sum_{i \in [p]} \|\hat{\mathbf{X}}_{i:}\|^2 \|\hat{\mathbf{X}}_i^s - \mathbf{X}_{i:}^s\|^2 \\ 1874 \quad &\lesssim \|\hat{\mathcal{X}} - \mathcal{X}\|_F^2 \\ 1875 \quad &\lesssim p^{K/2} r + pr^2 + r^K. \end{aligned} \quad (47)$$

Hence, we have

$$\begin{aligned} 1876 \quad \sum_{i \in [p]} \|\hat{\mathbf{X}}_i^s - \hat{\mathbf{x}}_{z^{(0)}(i)}\|^2 &\lesssim \sum_{i \in [p]} \theta(i)^2 \|\hat{\mathbf{X}}_i^s - \hat{\mathbf{x}}_{z^{(0)}(i)}\|^2 \\ 1877 \quad &\lesssim \frac{r^{K-1}}{p^{K-1}} \sum_{i \in [p]} \|\mathbf{X}_{i:}\|^2 \|\hat{\mathbf{X}}_i^s - \hat{\mathbf{x}}_{z^{(0)}(i)}\|^2 \\ 1878 \quad &\lesssim \frac{r^{K-1}}{p^{K-1}} (p^{K/2} r + pr^2 + r^K), \end{aligned} \quad (48)$$

where the first inequality follows from the assumption $\min_{i \in [p]} \theta(i) \geq c > 0$, the second inequality follows from the inequality (38), and the last inequality comes from the inequality (47).

Next, we consider the following quantity,

$$\begin{aligned} 1885 \quad &\sum_{i \in [p]} \theta(i) \|\mathbf{X}_{i:}^s - \hat{\mathbf{x}}_{z^{(0)}(i)}\|^2 \\ 1886 \quad &\lesssim \sum_{i \in [p]} \theta(i)^2 \|\mathbf{X}_{i:}^s - \hat{\mathbf{X}}_{i:}^s\|^2 + \sum_{i \in [p]} \theta(i)^2 \|\hat{\mathbf{X}}_{i:}^s - \hat{\mathbf{x}}_{z^{(0)}(i)}\|^2 \\ 1887 \quad &\lesssim \sum_{i \in [p]} \frac{\theta(i)^2}{\|\mathbf{X}_{i:}\|^2} \|\mathbf{X}_{i:} - \hat{\mathbf{X}}_{i:}\|^2 + \sum_{i \in [p]} \theta(i)^2 \|\hat{\mathbf{X}}_{i:}^s - \hat{\mathbf{x}}_{z^{(0)}(i)}\|^2 \\ 1888 \quad &\lesssim \frac{r^{K-1}}{p^{K-1}} (p^{K/2} r + pr^2 + r^K), \end{aligned} \quad (49)$$

where the first inequality follows from the assumption of $\theta(i)$ and triangle inequality, the second inequality follows from Lemma 4, and the last inequality follows from (48). In addition, with Theorem 4 and the condition $\text{SNR} \gtrsim p^{-K/2} \log p$, for all $a \in [r]$, we have

$$|z^{-1}(a) \cap (z^{(0)})^{-1}(a)| \geq |z^{-1}(a)| - p\ell(z^{(0)}, z) \gtrsim \frac{p}{r} - \frac{p}{\log p} \gtrsim \frac{p}{r},$$

when p is large enough. Therefore, for all $a \in [r]$, we have

$$\begin{aligned} \|\hat{\mathbf{x}}_a - \mathbf{X}_a^s\|^2 &= \frac{\sum_{i \in z^{-1}(a) \cap (z^{(0)})^{-1}(a)} \left\| \mathbf{X}_{i:}^s - \hat{\mathbf{x}}_{z^{(0)}(i)} \right\|^2}{|z^{-1}(a) \cap (z^{(0)})^{-1}(a)|} \\ &\lesssim \frac{r}{p} \left(\sum_{i \in [p]} \|\mathbf{X}_{i:}^s - \hat{\mathbf{X}}_{i:}^s\|^2 + \sum_{i \in [p]} \|\hat{\mathbf{X}}_{i:}^s - \hat{\mathbf{x}}_{z^{(0)}(i)}\|^2 \right) \\ &\lesssim \frac{r^K}{p^K} \left(p^{K/2} r + pr^2 + r^K \right), \end{aligned} \quad (50)$$

where the last inequality follows from the inequality (48).

Finally, we obtain

$$\begin{aligned} L^{(0)} &= \frac{1}{p} \sum_{i \in [p]} \theta(i) \sum_{b \in [r]} \mathbb{1} \left\{ z^{(0)}(i) = b \right\} \|[\mathbf{S}_{z(i):}]^s - [\mathbf{S}_{b:}]^s\|^2 \\ &\lesssim \frac{1}{p} \sum_{i \in [p], z^{(0)}(i) \neq z(i)} \theta(i) \|\mathbf{X}_{i:}^s - \mathbf{X}_{z^{(0)}(i)}^s\|^2 \\ &\lesssim \frac{1}{p} \sum_{i \in [p], z^{(0)}(i) \neq z(i)} \theta(i) \left(\|\mathbf{X}_{i:}^s - \hat{\mathbf{x}}_{z^{(0)}(i)}\|^2 \right. \\ &\quad \left. + \|\hat{\mathbf{x}}_{z^{(0)}(i)} - \mathbf{X}_{z^{(0)}(i)}^s\|^2 \right) \\ &\leq \bar{C} \frac{r^K}{p^K} \left(p^{K/2} r + pr^2 + r^K \right), \\ &\leq \bar{C} \Delta_{\min}^2 \end{aligned}$$

where the first inequality follows from Lemma 1, the third inequality follows from inequalities (49) and (50), and the last inequality follows from the assumption that $\text{SNR} \geq \tilde{C} p^{-K/2} \log p$. \square

Proof of Proposition 1: Sub-algorithm 3 shares the same algorithm strategy as Sub-algorithm 1 but with a different estimation of the mean tensor, $\hat{\mathcal{X}}'$. Hence, the proof of Proposition 1 follows the same proof idea with the proof of Theorem 4. Replacing the estimation $\hat{\mathcal{X}}$ by $\hat{\mathcal{X}}'$ in the proof of Theorem 4, we have

$$\begin{aligned} \min_{\pi \in \Pi} \sum_{i: z^{(0)}(i) \neq \pi(z(i))} \theta(i)^2 \\ \lesssim \left(\sum_{i \in S} \|\mathbf{X}_{i:}\|^2 + \sum_{i \in S_0} \|\mathbf{X}_{i:}\|^2 \right) p^{-(K-1)} r^{K-1}. \end{aligned} \quad (51)$$

By inequalities (43) and (45), we have

$$\sum_{i \in S} \|\mathbf{X}_{i:}\|^2 \leq \left(\frac{16(1+\eta)}{c_0^2 \Delta_{\min}^2} + 2 \right) \|\hat{\mathcal{X}}' - \mathcal{X}\|_F^2, \quad (52)$$

$$\sum_{i \in S_0} \|\mathbf{X}_{i:}\|^2 \leq \|\hat{\mathcal{X}}' - \mathcal{X}\|_F^2. \quad (53)$$

Hence, it suffices to find the upper bound of the estimation error $\|\hat{\mathcal{X}}' - \mathcal{X}\|_F^2$ to complete our proof. Note that the matricization $\text{Mat}_{sq}(\mathcal{X}) \in \mathbb{R}^{p^{\lceil K/2 \rceil} \times p^{\lceil K/2 \rceil}}$ has $\text{rank}(\text{Mat}_{sq}(\mathcal{X})) \leq r^{\lceil K/2 \rceil}$, and Bernoulli random variables follow the sub-Gaussian distribution with bounded variance $\sigma^2 = 1/4$. Apply Lemma 9 to $\mathbf{Y} = \text{Mat}_{sq}(\mathcal{Y})$, $\mathbf{X} = \text{Mat}_{sq}(\mathcal{X})$, and $\hat{\mathbf{X}} = \text{Mat}_{sq}(\hat{\mathcal{X}}')$. Then, with probability tending to 1 as $p \rightarrow \infty$, we have

$$\|\hat{\mathcal{X}}' - \mathcal{X}\|_F^2 = \|\text{Mat}_{sq}(\hat{\mathcal{X}}') - \text{Mat}_{sq}(\mathcal{X})\|_F^2 \lesssim p^{\lceil K/2 \rceil}. \quad (54)$$

Combining the estimation error (54) with inequalities (52), (53), and (51), we obtain

$$\min_{\pi \in \Pi} \sum_{i: z^{(0)}(i) \neq \pi(z(i))} \theta(i)^2 \lesssim \frac{\sigma^2 r^{K-1}}{\Delta_{\min}^2 p^{K-1}} p^{\lceil K/2 \rceil}. \quad (55)$$

Replace the inequality (46) in the proof of Theorem 4 by inequality (55). With the the same procedures to obtain $\ell(\hat{z}^{(0)}, z)$ and $L(\hat{z}^{(0)}, z)$ for Theorem 4, we finish the proof of Proposition 1. \square

3) Useful Definitions and Lemmas for the Proof of Theorem 4:

Lemma 4 (Basic Inequality): For any two nonzero vectors $\mathbf{v}_1, \mathbf{v}_2$ of same dimension, we have

$$\sin(\mathbf{v}_1, \mathbf{v}_2) \leq \|\mathbf{v}_1^s - \mathbf{v}_2^s\| \leq \frac{2 \|\mathbf{v}_1 - \mathbf{v}_2\|}{\max(\|\mathbf{v}_1\|, \|\mathbf{v}_2\|)}. \quad (56)$$

Proof of Lemma 4: For the first inequality, let $\alpha \in [0, \pi]$ denote the angle between \mathbf{v}_1 and \mathbf{v}_2 . We have

$$\|\mathbf{v}_1^s - \mathbf{v}_2^s\| = \sqrt{2(1 - \cos \alpha)} = 2 \sin \frac{\alpha}{2} \geq \sin \alpha, \quad (57)$$

where the equations follow from the properties of trigonometric function and the inequality follows from the fact the $\cos \frac{\alpha}{2} \leq 1$ and $\sin \alpha = 2 \sin \frac{\alpha}{2} \cos \frac{\alpha}{2} > 0$ for $\alpha \in [0, \pi]$.

For the second inequality, without loss of generality, we assume $\|\mathbf{v}_1\| \geq \|\mathbf{v}_2\|$. Then

$$\begin{aligned} \|\mathbf{v}_1^s - \mathbf{v}_2^s\| &= \left\| \frac{\mathbf{v}_1}{\|\mathbf{v}_1\|} - \frac{\mathbf{v}_2}{\|\mathbf{v}_1\|} + \frac{\mathbf{v}_2}{\|\mathbf{v}_1\|} - \frac{\mathbf{v}_2}{\|\mathbf{v}_2\|} \right\| \\ &\leq \frac{\|\mathbf{v}_1 - \mathbf{v}_2\|}{\|\mathbf{v}_1\|} + \frac{\|\mathbf{v}_2\| \|\mathbf{v}_1\| - \|\mathbf{v}_2\|}{\|\mathbf{v}_1\| \|\mathbf{v}_2\|} \\ &\leq \frac{2 \|\mathbf{v}_1 - \mathbf{v}_2\|}{\|\mathbf{v}_2\|}. \end{aligned} \quad (58)$$

Therefore, Lemma 4 is proved. \square

Definition 3 (Weighted Padding Vectors): For a vector $\mathbf{a} = [\mathbf{a}_i] \in \mathbb{R}^d$, we define the padding vector of \mathbf{a} with the weight collection $\mathbf{w} = \{\mathbf{w}_i : \mathbf{w}_i = [\mathbf{w}_{ik}] \in \mathbb{R}^{p_i}\}_{i=1}^d$ as

$$\text{Pad}_{\mathbf{w}}(\mathbf{a}) = [a_1 \circ \mathbf{w}_1, \dots, a_d \circ \mathbf{w}_d]^T, \quad (59)$$

where $a_i \circ \mathbf{w}_i = [a_i w_{i1}, \dots, a_i w_{ip_i}]^T$, for all $i \in [d]$. Here we also view $\text{Pad}_{\mathbf{w}}(\cdot) : \mathbb{R}^d \mapsto \mathbb{R}^{\sum_{i \in [d]} p_i}$ as an operator. We have the bounds of the weighted padding vector

$$\min_{i \in [d]} \|\mathbf{w}_i\|^2 \|\mathbf{a}\|^2 \leq \|\text{Pad}_{\mathbf{w}}(\mathbf{a})\|^2 \leq \max_{i \in [d]} \|\mathbf{w}_i\|^2 \|\mathbf{a}\|^2. \quad (60)$$

Further, we define the inverse weighted padding operator $\text{Pad}_{\mathbf{w}}^{-1} : \mathbb{R}^{\sum_{i \in [d]} p_i} \mapsto \mathbb{R}^d$ which satisfies

$$\text{Pad}_{\mathbf{w}}^{-1}(\text{Pad}_{\mathbf{w}}(\mathbf{a})) = \mathbf{a}. \quad (61)$$

Lemma 5 (Angle for Weighted Padding Vectors): Suppose that we have two non-zero vectors $\mathbf{a}, \mathbf{b} \in \mathbb{R}^d$. Given the weight collection \mathbf{w} , we have

$$\begin{aligned} \frac{\min_{i \in [d]} \|\mathbf{w}_i\|}{\max_{i \in [d]} \|\mathbf{w}_i\|} \sin(\mathbf{a}, \mathbf{b}) &\stackrel{*}{\leq} \sin(\text{Pad}_{\mathbf{w}}(\mathbf{a}), \text{Pad}_{\mathbf{w}}(\mathbf{b})) \\ &\stackrel{**}{\leq} \frac{\max_{i \in [d]} \|\mathbf{w}_i\|}{\min_{i \in [d]} \|\mathbf{w}_i\|} \sin(\mathbf{a}, \mathbf{b}). \quad (58) \end{aligned}$$

Proof of Lemma 5: We prove the two inequalities separately with similar ideas.

First, we prove the inequality $**$ in (58). Decomposing \mathbf{b} yields

$$\mathbf{b} = \cos(\mathbf{a}, \mathbf{b}) \frac{\|\mathbf{b}\|}{\|\mathbf{a}\|} \mathbf{a} + \sin(\mathbf{a}, \mathbf{b}) \frac{\|\mathbf{b}\|}{\|\mathbf{a}^\perp\|} \mathbf{a}^\perp,$$

where $\mathbf{a}^\perp \in \mathbb{R}^d$ is in the orthogonal complement space of \mathbf{a} . By the Definition 3, we have

$$\text{Pad}_{\mathbf{w}}(\mathbf{b}) = \cos(\mathbf{a}, \mathbf{b}) \frac{\|\mathbf{b}\|}{\|\mathbf{a}\|} \text{Pad}_{\mathbf{w}}(\mathbf{a}) + \sin(\mathbf{a}, \mathbf{b}) \frac{\|\mathbf{b}\|}{\|\mathbf{a}^\perp\|} \text{Pad}_{\mathbf{w}}(\mathbf{a}^\perp).$$

Note that $\text{Pad}_{\mathbf{w}}(\mathbf{a}^\perp)$ is not necessary equal to the orthogonal vector of $\text{Pad}_{\mathbf{w}}(\mathbf{a})$; i.e., $\text{Pad}_{\mathbf{w}}(\mathbf{a}^\perp) \neq (\text{Pad}_{\mathbf{w}}(\mathbf{a}))^\perp$. By the geometry property of trigonometric functions, we obtain

$$\begin{aligned} \sin(\text{Pad}_{\mathbf{w}}(\mathbf{a}), \text{Pad}_{\mathbf{w}}(\mathbf{b})) &\leq \frac{\|\mathbf{b}\| \|\text{Pad}_{\mathbf{w}}(\mathbf{a}^\perp)\|}{\|\mathbf{a}^\perp\| \|\text{Pad}_{\mathbf{w}}(\mathbf{b})\|} \sin(\mathbf{a}, \mathbf{b}) \\ &\leq \frac{\max_{i \in [d]} \|\mathbf{w}_i\|}{\min_{i \in [d]} \|\mathbf{w}_i\|} \sin(\mathbf{a}, \mathbf{b}), \end{aligned}$$

where the second inequality follows by applying the property (57) to vectors \mathbf{b} and \mathbf{a}^\perp .

Next, we prove inequality $*$ in (58). With the decomposition of $\text{Pad}_{\mathbf{w}}(\mathbf{b})$ and the inverse weighted padding operator, we have

$$\begin{aligned} \mathbf{b} &= \cos(\text{Pad}_{\mathbf{w}}(\mathbf{a}), \text{Pad}_{\mathbf{w}}(\mathbf{b})) \frac{\|\text{Pad}_{\mathbf{w}}(\mathbf{b})\|}{\|\text{Pad}_{\mathbf{w}}(\mathbf{a})\|} \mathbf{a} \\ &\quad + \sin(\text{Pad}_{\mathbf{w}}(\mathbf{a}), \text{Pad}_{\mathbf{w}}(\mathbf{b})) \frac{\|\text{Pad}_{\mathbf{w}}(\mathbf{b})\|}{\|(\text{Pad}_{\mathbf{w}}(\mathbf{a}))^\perp\|} \text{Pad}_{\mathbf{w}}^{-1}((\text{Pad}_{\mathbf{w}}(\mathbf{a}))^\perp). \end{aligned}$$

Therefore, we obtain

$$\begin{aligned} \sin(\mathbf{a}, \mathbf{b}) &\leq \frac{\|\text{Pad}_{\mathbf{w}}(\mathbf{b})\| \|\text{Pad}_{\mathbf{w}}^{-1}((\text{Pad}_{\mathbf{w}}(\mathbf{a}))^\perp)\|}{\|(\text{Pad}_{\mathbf{w}}(\mathbf{a}))^\perp\| \|\mathbf{b}\|} \sin(\text{Pad}_{\mathbf{w}}(\mathbf{a}), \text{Pad}_{\mathbf{w}}(\mathbf{b})) \\ &\leq \frac{\max_{i \in [d]} \|\mathbf{w}_i\|}{\min_{i \in [d]} \|\mathbf{w}_i\|} \sin(\text{Pad}_{\mathbf{w}}(\mathbf{a}), \text{Pad}_{\mathbf{w}}(\mathbf{b})), \end{aligned}$$

where the second inequality follows by applying the property (57) to vectors \mathbf{b} and $\text{Pad}_{\mathbf{w}}^{-1}((\text{Pad}_{\mathbf{w}}(\mathbf{a}))^\perp)$. \square

Lemma 6 (Singular Value of Weighted Membership Matrix): Under the parameter space (2) and assumption that $\min_{i \in [p]} \theta(i) \geq c$ for some constant $c > 0$, the singular values of ΘM are bounded as

$$\begin{aligned} \sqrt{p/r} &\lesssim \sqrt{\min_{a \in [r]} \|\theta_{z^{-1}(a)}\|^2} \leq \lambda_r(\Theta M) \\ &\leq \|\Theta M\|_\sigma \leq \sqrt{\max_{a \in [r]} \|\theta_{z^{-1}(a)}\|^2} \lesssim p/r. \end{aligned}$$

Proof of Lemma 6: Note that

$$(\Theta M)^T \Theta M = D,$$

with $D = \text{diag}(D_1, \dots, D_r)$ where $D_a = \|\theta_{z^{-1}(a)}\|^2, a \in [r]$. By the definition of singular values, we have

$$\sqrt{\min_{a \in [r]} \|\theta_{z^{-1}(a)}\|^2} \leq \lambda_r(\Theta M) \leq \|\Theta M\|_\sigma \leq \sqrt{\max_{a \in [r]} \|\theta_{z^{-1}(a)}\|^2}.$$

Since that $\min_{i \in [p]} \theta(i) \geq c$ by the constraints in parameter space, we have

$$\min_{a \in [r]} \|\theta_{z^{-1}(a)}\|^2 \geq c^2 \min_{a \in [r]} |z^{-1}(a)| \gtrsim \frac{p}{r},$$

where the last inequality follows from the constraint in parameter space (2). Finally, notice that

$$\sqrt{\max_{a \in [r]} \|\theta_{z^{-1}(a)}\|^2} \leq \max_{a \in [r]} \sqrt{\|\theta_{z^{-1}(a)}\|_1^2} \lesssim \frac{p}{r}.$$

Therefore, we complete the proof of Lemma 6. \square

Lemma 7 (Singular-Value Gap-Free Tensor Estimation Error Bound): Consider an order- K tensor $\mathcal{A} = \mathcal{X} + \mathcal{Z} \in \mathbb{R}^{p \times \dots \times p}$, where \mathcal{X} has Tucker rank (r, \dots, r) and \mathcal{Z} has independent sub-Gaussian entries with parameter σ^2 . Let $\hat{\mathcal{X}}$ denote the double projection estimated tensor in Step 2 of Sub-algorithm 1 in the main paper. Then with probability at least $1 - C \exp(-cp)$, we have

$$\|\hat{\mathcal{X}} - \mathcal{X}\|_F^2 \leq C \sigma^2 (p^{K/2} r + pr^2 + r^K),$$

where C, c are some positive constants.

Proof of Lemma 7: See [13, Proposition 1]. \square

Lemma 8 (Upper Bound of Misclustering Error): Let $z : [p] \mapsto [r]$ be a cluster assignment such that $|z^{-1}(a)| \asymp p/r$ for all $a \in [r]$ with $r \geq 2$. Let node i correspond to a vector $\mathbf{x}_i = \theta(i) \mathbf{v}_{z(i)} \in \mathbb{R}^d$, where $\{\mathbf{v}_a\}_{a=1}^r$ are the cluster centers and $\boldsymbol{\theta} = [\theta(i)] \in \mathbb{R}_+^p$ is the positive degree heterogeneity. Assume that $\boldsymbol{\theta}$ satisfies the balanced assumption (6) such that $\frac{\max_{a \in [r]} \|\theta_{z^{-1}(a)}\|^2}{\min_{a \in [r]} \|\theta_{z^{-1}(a)}\|^2} = 1 + o(1)$. Consider an arbitrary estimate \hat{z} with $\hat{\mathbf{x}}_i = \hat{\mathbf{v}}_{\hat{z}(i)}$ for all $i \in S$. Then, if

$$\min_{a \neq b \in [r]} \|\mathbf{v}_a - \mathbf{v}_b\| \geq 2c, \quad (59)$$

for some constant $c > 0$, we have

$$\min_{\pi \in \Pi} \sum_{i: \hat{z}(i) \neq \pi(z(i))} \theta(i)^2 \leq \sum_{i \in S_0} \theta(i)^2 + 4 \sum_{i \in S} \theta(i)^2,$$

where S_0 is defined in Step 4 of Sub-algorithm 1 and

$$S = \{i \in S_0^c : \|\hat{\mathbf{x}}_i - \mathbf{v}_{z(i)}\| \geq c\}.$$

Proof of Lemma 8: For each cluster $u \in [r]$, we use C_u to collect the subset of points for which the estimated and true positions $\hat{\mathbf{x}}_i, \mathbf{x}_i$ are within distance c . Specifically, define

$$C_u = \{i \in z^{-1}(u) \cap S_0^c : \|\hat{\mathbf{x}}_i - \mathbf{v}_{z(i)}\| < c\},$$

and divide $[r]$ into three groups based on C_u as

$$R_1 = \{u \in [r] : C_u = \emptyset\},$$

$$R_2 = \{u \in [r] : C_u \neq \emptyset, \text{ for all } i, j \in C_u, \hat{z}(i) = \hat{z}(j)\},$$

$$R_3 = \{u \in [r] : C_u \neq \emptyset, \text{ there exist } i, j \in C_u, \hat{z}(i) \neq \hat{z}(j)\}.$$

2056 Note that $\cup_{u \in [r]} C_u = S_0^c / S^c$ and $C_u \cap C_v = \emptyset$ for any $u \neq v$.
2057 Suppose there exist $i \in C_u$ and $j \in C_v$ with $u \neq v \in [r]$ and
2058 $\hat{z}(i) = \hat{z}(j)$. Then we have

2059 $\|\mathbf{v}_{z(i)} - \mathbf{v}_{z(j)}\| \leq \|\mathbf{v}_{z(i)} - \hat{\mathbf{x}}_i\| + \|\mathbf{v}_{z(j)} - \hat{\mathbf{x}}_j\| < 2c,$

2060 which contradicts to the assumption (59). Hence, the estimates
2061 $\hat{z}(i) \neq \hat{z}(j)$ for the nodes $i \in C_u$ and $j \in C_v$ with $u \neq v$.
2062 By the definition of R_2 , the nodes in $\cup_{u \in R_2} C_u$ have the same
2063 assignment with z and \hat{z} . Then, we have

2064 $\min_{\pi \in \Pi} \sum_{i: \hat{z}(i) \neq \pi(z(i))} \theta(i)^2 \leq \sum_{i \in S_0} \theta(i)^2 + \sum_{i \in S} \theta(i)^2 + \sum_{i \in \cup_{u \in R_2} C_u} \theta(i)^2.$

2065 We only need to bound $\sum_{i \in \cup_{u \in R_3} C_u} \theta(i)^2$ to finish the proof.
2066 Note that every C_u with $u \in R_3$ contains at least two
2067 nodes assigned to different clusters by \hat{z} . Then, we have
2068 $|R_2| + 2|R_3| \leq r$. Since $|R_1| + |R_2| + |R_3| = r$, we have
2069 $|R_3| \leq |R_1|$. Hence, we obtain

2070
$$\begin{aligned} \sum_{i \in \cup_{u \in R_3} C_u} \theta(i)^2 &\leq |R_3| \max_{a \in [r]} \|\boldsymbol{\theta}_{z^{-1}(a)}\|^2 \\ 2071 &\leq |R_1| \max_{a \in [r]} \|\boldsymbol{\theta}_{z^{-1}(a)}\|^2 \\ 2072 &\leq \frac{\max_{a \in [r]} \|\boldsymbol{\theta}_{z^{-1}(a)}\|^2}{\min_{a \in [r]} \|\boldsymbol{\theta}_{z^{-1}(a)}\|^2} \sum_{i \in \cup_{u \in R_1} z^{-1}(u)} \theta(i)^2 \\ 2073 &\leq 2 \sum_{i \in S} \theta(i)^2, \end{aligned}$$

2074 where the last inequality holds by the balanced assumption on
2075 $\boldsymbol{\theta}$ when p is large enough, and the fact that $\cup_{u \in R_1} z^{-1}(u) \subset S$.
2076 \square

2077 *Lemma 9 (Low-Rank Matrix Estimation):* Let $\mathbf{Y} = \mathbf{X} +$
2078 $\mathbf{E} \in \mathbb{R}^{m \times n}$, where $n > m$ and \mathbf{E} contains independent mean-
2079 zero sub-Gaussian entries with bounded variance σ^2 . Suppose
2080 $\text{rank}(\mathbf{X}) = r$. Consider the least square estimator

2081
$$\hat{\mathbf{X}} = \arg \min_{\mathbf{X}' \in \mathbb{R}^{m \times n}, \text{rank}(\mathbf{X}') \leq r} \|\mathbf{X}' - \mathbf{Y}\|_F^2.$$

2082 There exist positive constants C_1, C_2 such that

2083
$$\|\hat{\mathbf{X}} - \mathbf{X}\|_F^2 \leq C_1 \sigma^2 nr,$$

2084 with probability at least $1 - \exp(-C_2 nr)$.

2085 *Proof of Lemma 9:* Note that $\|\hat{\mathbf{X}} - \mathbf{Y}\|_F^2 \leq \|\mathbf{X} - \mathbf{Y}\|_F^2$ by
2086 the definition of least square estimator.

2087 We have

2088
$$\begin{aligned} \|\hat{\mathbf{X}} - \mathbf{X}\|_F^2 \\ 2089 &\leq 2 \langle \hat{\mathbf{X}} - \mathbf{X}, \mathbf{Y} - \mathbf{X} \rangle \\ 2090 &\leq 2 \|\hat{\mathbf{X}} - \mathbf{X}\|_F \sup_{\mathbf{T} \in \mathbb{R}^{m \times n}, \text{rank}(\mathbf{T}) \leq 2r, \|\mathbf{T}\|_F=1} \langle \mathbf{T}, \mathbf{Y} - \mathbf{X} \rangle \quad (60) \end{aligned}$$

2091 with probability at least $1 - \exp(-C_2 nr)$, where the second
2092 inequality follows by re-arrangement.

2093 Consider the SVD for matrix $\mathbf{T} = \mathbf{U} \Sigma \mathbf{V}^T$ with orthogonal
2094 matrices $\mathbf{U} \in \mathbb{R}^{m \times 2r}, \mathbf{V} \in \mathbb{R}^{n \times 2r}$ and diagonal matrix $\Sigma \in$

$\mathbb{R}^{2r \times 2r}$. We have

2095
$$\begin{aligned} &\sup_{\mathbf{T} \in \mathbb{R}^{m \times n}, \text{rank}(\mathbf{T}) \leq 2r, \|\mathbf{T}\|_F=1} \langle \mathbf{T}, \mathbf{Y} - \mathbf{X} \rangle \\ 2096 &= \sup_{\mathbf{T} \in \mathbb{R}^{m \times n}, \text{rank}(\mathbf{T}) \leq 2r, \|\mathbf{T}\|_F=1} \langle \mathbf{U} \Sigma, \mathbf{EV} \rangle \\ 2097 &= \sup_{\mathbf{v} \in \mathbb{R}^{2nr}} \mathbf{v}^T \mathbf{e} \leq C \sigma \sqrt{nr}, \quad (61) \end{aligned}$$

2098 with probability $1 - \exp(-C_2 nr)$, where C, C_2 are two
2099 positive constants, the vectorization $\mathbf{e} = \text{Vec}(\mathbf{EV}) \in \mathbb{R}^{2nr}$
2100 has independent mean-zero sub-Gaussian entries with bounded
2101 variance σ^2 due to the orthogonality of \mathbf{V} , and the last
2102 inequality follows from [36, Theorem 1.19].
2103

2104 Combining inequalities (60) and (61), we obtain the desired
2105 conclusion. \square

G. Proofs of Theorem 2 (Achievability) and Theorem 5

2106 *Proof of Theorem 2 (Achievability) and Theorem 5:* The
2107 proofs of Theorem 2 (Achievability) and Theorem 5 share the
2108 same idea. We prove the contraction step by step. In each
2109 step, we show the specific procedures for the algorithm loss
2110 and address the MLE loss by stating the difference.
2111

2112 We consider dTBM (1) with symmetric mean tensor, param-
2113 eters $(z, \mathcal{S}, \boldsymbol{\theta})$, fixed $r \geq 1, K \geq 2$, and i.i.d. noise. Let
2114 $(\hat{z}, \hat{\mathcal{S}}, \hat{\boldsymbol{\theta}})$ denote the MLE in (9), and $(z_k^{(0)}, \mathcal{S}^{(0)}, \boldsymbol{\theta}_k^{(0)})$ denote
2115 parameters related to the initialization. For the case $r = 1$,
2116 $\ell(z_k^{(t)}, z) = 0$ trivially for all $t \geq 0, k \in [k]$. Hence, we focus
2117 on the proof of the first mode clustering $z_1^{(t+1)}$ with $r \geq 2$; the
2118 extension for other modes can be obtained similarly. We drop
2119 the subscript k in the matricizations $\boldsymbol{\Theta}, \mathbf{M}_k, \mathbf{S}_k, \mathbf{X}_k$ and in
2120 estimates $z_k^{(0)}, z_k^{(t+1)}, z_k^{(t)}$ for ease of the notation. Without
2121 loss of generality, we assume that the variance $\sigma = 1$, and that
2122 the identity permutation minimizes the initial misclustering
2123 error; i.e., $\pi^{(0)} = \arg \min_{\pi \in \Pi} \sum_{i \in [p]} \mathbb{1} \{z^{(0)}(i) \neq \pi \circ z(i)\}$
2124 and $\pi^{(0)}(a) = a$ for all $a \in [r]$, and so for \hat{z} .
2125

2126 *Step 1 (Notation and Conditions):* We first introduce addi-
2127 tional notations and the necessary conditions used in the proof.
2128 We will verify that the conditions hold in our context under
2129 high probability in the last step of the proof.
2130

2131 *1) Notation:* 1) Projection. We use \mathbf{I}_d to denote the identity
2132 matrix of dimension d . For a vector $\mathbf{v} \in \mathbb{R}^d$, let $\text{Proj}(\mathbf{v}) \in$
2133 $\mathbb{R}^{d \times d}$ denote the projection matrix to \mathbf{v} . Then, $\mathbf{I}_d - \text{Proj}(\mathbf{v})$
2134 is the projection matrix to the orthogonal complement \mathbf{v}^\perp .
2135

2136 2) We define normalized membership matrices

2137
$$\mathbf{W} = \mathbf{M} \left(\text{diag}(\mathbf{1}_p^T \mathbf{M}) \right)^{-1}, \mathbf{W}^{(t)} = \mathbf{M}^{(t)} \left(\text{diag}(\mathbf{1}_p^T \mathbf{M}^{(t)}) \right)^{-1},$$

2138 weighted normalized membership matrices

2139
$$\mathbf{P} = \boldsymbol{\Theta} \mathbf{M} (\text{diag}(\|\boldsymbol{\theta}_{z^{-1}(1)}\|^2, \dots, \|\boldsymbol{\theta}_{z^{-1}(r)}\|^2))^{-1},$$

2140
$$\hat{\mathbf{P}} = \hat{\boldsymbol{\Theta}} \hat{\mathbf{M}} (\text{diag}(\|\hat{\boldsymbol{\theta}}_{z^{-1}(1)}\|^2, \dots, \|\hat{\boldsymbol{\theta}}_{z^{-1}(r)}\|^2))^{-1},$$

2141 and the dual normalized and dual weighted normalized mem-
2142 bership matrices

2143
$$\mathbf{V} = \mathbf{W}^{\otimes(K-1)}, \quad \mathbf{V}^{(t)} = \left(\mathbf{W}^{(t)} \right)^{\otimes(K-1)},$$

2144
$$\mathbf{Q} = \mathbf{P}^{\otimes K-1}, \quad \hat{\mathbf{Q}} = \hat{\mathbf{P}}^{\otimes K-1}.$$

2145 Also, let $\mathbf{B} = (\boldsymbol{\Theta} \mathbf{M})^{\otimes(K-1)}, \hat{\mathbf{B}} = (\hat{\boldsymbol{\Theta}} \hat{\mathbf{M}})^{\otimes(K-1)}$. By the
2146 definition, we have $\mathbf{B}^T \mathbf{Q} = \hat{\mathbf{B}}^T \hat{\mathbf{Q}} = \mathbf{I}_{r^{K-1}}$.
2147

3) We use $\mathcal{S}^{(t)}$ to denote the estimator of \mathcal{S} in the t -th iteration, $\hat{\mathcal{S}}$ for MLE, $\tilde{\mathcal{S}}$ to denote the oracle estimator of \mathcal{S} given true assignment z , and $\bar{\mathcal{S}}$ for weighted oracle estimator; i.e.,

$$\begin{aligned}\mathcal{S}^{(t)} &= \mathcal{Y} \times_1 (\mathbf{W}^{(t)})^T \times_2 \cdots \times_K (\mathbf{W}^{(t)})^T, \\ \tilde{\mathcal{S}} &= \mathcal{Y} \times_1 \mathbf{W}^T \times_2 \cdots \times_K \mathbf{W}^T, \\ \hat{\mathcal{S}} &= \mathcal{Y} \times_1 \hat{\mathbf{P}}^T \times_2 \cdots \times_K \hat{\mathbf{P}}^T, \\ \bar{\mathcal{S}} &= \mathcal{Y} \times_1 \mathbf{P}^T \times_2 \cdots \times_K \mathbf{P}^T.\end{aligned}$$

4) We define the matricizations of tensors

$$\begin{aligned}\mathbf{S} &= \text{Mat}(\mathcal{S}), \quad \mathbf{Y} = \text{Mat}(\mathcal{Y}), \quad \mathbf{X} = \text{Mat}(\mathcal{X}), \quad \mathbf{E} = \text{Mat}(\mathcal{E}), \\ \mathbf{S}^{(t)} &= \text{Mat}(\mathcal{S}^{(t)}), \quad \hat{\mathcal{S}} = \text{Mat}(\hat{\mathcal{S}}), \quad \tilde{\mathcal{S}} = \text{Mat}(\tilde{\mathcal{S}}), \quad \bar{\mathcal{S}} = \text{Mat}(\bar{\mathcal{S}}).\end{aligned}$$

5) We define the extended core tensor on $K - 1$ modes

$$\mathbf{A} = \mathbf{S}\mathbf{B}^T, \quad \bar{\mathbf{A}} = \bar{\mathbf{S}}\mathbf{B}^T, \quad \hat{\mathbf{A}} = \hat{\mathbf{S}}\hat{\mathbf{B}}^T.$$

By the assumption in parameter space (2), we have $\mathbf{A} = \mathbf{P}\mathbf{X} = \mathbf{W}\mathbf{X}$, $\hat{\mathbf{A}} = \hat{\mathbf{P}}\hat{\mathbf{X}} = \hat{\mathbf{W}}\hat{\mathbf{X}}$.

6) We define the angle-based misclustering loss in the t -th iteration and loss for MLE

$$\begin{aligned}L^{(t)} &= \frac{1}{p} \sum_{i \in [p]} \theta(i) \sum_{b \in [r]} \mathbb{1}\{z^{(t)}(i) = b\} \|[\mathbf{S}_{z(i)}]_s - [\mathbf{S}_b]_s\|^2, \\ L(\hat{z}) &= \frac{1}{p} \sum_{i \in [p]} \theta(i)^2 \sum_{b \in [r]} \mathbb{1}\{\hat{z}(i) = b\} \|[\mathbf{A}_{z(i)}]_s - [\mathbf{A}_b]_s\|^2.\end{aligned}$$

We also define the loss for oracle and weighted oracle estimators

$$\begin{aligned}\xi &= \frac{1}{p} \sum_{i \in [p]} \theta(i) \sum_{b \in [r]} \mathbb{1}\left\{ \langle \mathbf{E}_{i:} \mathbf{V}, [\tilde{\mathcal{S}}_{z(i)}]_s - [\tilde{\mathcal{S}}_b]_s \rangle \right. \\ &\quad \left. \leq -\frac{\theta(i)m}{4} \|[\mathbf{S}_{z(i)}]_s - [\mathbf{S}_b]_s\|^2 \right\} \\ &\quad \cdot \|[\mathbf{S}_{z(i)}]_s - [\mathbf{S}_b]_s\|^2, \\ \xi' &= \frac{1}{p} \sum_{i \in [p]} \theta(i)^2 \sum_{b \in [r]} \mathbb{1}\left\{ \langle \mathbf{E}_{i:} [\bar{\mathbf{A}}_{z(i)}]_s - [\bar{\mathbf{A}}_b]_s \rangle \right. \\ &\quad \left. \leq -\frac{m'}{4} \sqrt{\frac{p^{K-1}}{r^{K-1}}} \|[\mathbf{A}_{z(i)}]_s - [\mathbf{A}_b]_s\|_F^2 \right\} \\ &\quad \cdot \|[\mathbf{A}_{z(i)}]_s - [\mathbf{A}_b]_s\|^2.\end{aligned}$$

where m and m' are some positive universal constants.

Then we introduce the necessary conditions in Condition 1.

Step 2 (Misclustering Loss Decomposition): Next, we derive the upper bound of $L^{(t+1)}$ for $t = 0, 1, \dots, T - 1$. By Sub-algorithm 2, we update the assignment in t -th iteration via

$$z^{(t+1)}(i) = \arg \min_{a \in [r]} \|[\mathbf{Y}_{i:} \mathbf{V}^{(t)}]_s - [\mathbf{S}_a]_s\|^2,$$

following the facts that $\|\mathbf{a}^s - \mathbf{b}^s\|^2 = 1 - \cos(\mathbf{a}, \mathbf{b})$ for vectors \mathbf{a}, \mathbf{b} of same dimension and $\text{Mat}(\mathcal{Y}^d) = \mathbf{Y}\mathbf{V}^{(t)}$ where \mathcal{Y}^d is the reduced tensor defined in Step 8 of Sub-algorithm 2. Then the event $z^{(t+1)}(i) = b$ implies

$$\|[\mathbf{Y}_{i:} \mathbf{V}^{(t)}]_s - [\mathbf{S}_b]_s\|^2 \leq \|[\mathbf{Y}_{i:} \mathbf{V}^{(t)}]_s - [\mathbf{S}_{z(i)}]_s\|^2. \quad (67)$$

Note that the event (67) also holds for the degenerate entity i with $\|\mathbf{Y}_{i:} \mathbf{V}^{(t)}\| = 0$ due to the convention that $\mathbf{a}^s = \mathbf{0}$ if $\mathbf{a} = \mathbf{0}$. Arranging the terms in (67) yields the decomposition

$$\begin{aligned}2 \langle \mathbf{E}_{i:} \mathbf{V}, [\tilde{\mathcal{S}}_{z(i)}]_s - [\tilde{\mathcal{S}}_b]_s \rangle \\ \leq \|\mathbf{X}_{i:} \mathbf{V}^{(t)}\| \left(-\|[\mathbf{S}_{z(i)}]_s - [\mathbf{S}_b]_s\|^2 + G_{ib}^{(t)} + H_{ib}^{(t)} \right) + F_{ib}^{(t)},\end{aligned}$$

where

$$\begin{aligned}F_{ib}^{(t)} &= 2 \langle \mathbf{E}_{i:} \mathbf{V}^{(t)}, ([\tilde{\mathcal{S}}_{z(i)}]_s - [\mathbf{S}_{z(i)}]_s) - ([\tilde{\mathcal{S}}_b]_s - [\mathbf{S}_b]_s) \rangle \\ &\quad + 2 \langle \mathbf{E}_{i:} (\mathbf{V} - \mathbf{V}^{(t)}), [\tilde{\mathcal{S}}_{z(i)}]_s - [\tilde{\mathcal{S}}_b]_s \rangle,\end{aligned} \quad (68)$$

$$\begin{aligned}G_{ib}^{(t)} &= \left(\|[\mathbf{X}_{i:} \mathbf{V}^{(t)}]_s - [\mathbf{S}_{z(i)}]_s\|^2 \right. \\ &\quad \left. - \|[\mathbf{X}_{i:} \mathbf{V}^{(t)}]_s - [\mathbf{W}_{:z(i)}^T \mathbf{Y} \mathbf{V}^{(t)}]_s\|^2 \right) \\ &\quad - \left(\|[\mathbf{X}_{i:} \mathbf{V}^{(t)}]_s - [\mathbf{S}_b]_s\|^2 \right. \\ &\quad \left. - \|[\mathbf{X}_{i:} \mathbf{V}^{(t)}]_s - [\mathbf{W}_{:b}^T \mathbf{Y} \mathbf{V}^{(t)}]_s\|^2 \right),\end{aligned} \quad (69)$$

$$\begin{aligned}H_{ib}^{(t)} &= \|[\mathbf{X}_{i:} \mathbf{V}^{(t)}]_s - [\mathbf{W}_{:z(i)}^T \mathbf{Y} \mathbf{V}^{(t)}]_s\|^2 - \|[\mathbf{X}_{i:} \mathbf{V}^{(t)}]_s \\ &\quad - [\mathbf{W}_{:b}^T \mathbf{Y} \mathbf{V}^{(t)}]_s\|^2 + \|[\mathbf{S}_{z(i)}]_s - [\mathbf{S}_b]_s\|^2.\end{aligned} \quad (70)$$

Therefore, the event $\mathbb{1}\{z^{(t+1)}(i) = b\}$ can be upper bounded as

$$\begin{aligned}\mathbb{1}\{z^{(t+1)}(i) = b\} \\ \leq \mathbb{1}\left\{ z^{(t+1)}(i) = b, \langle \mathbf{E}_{j:} \mathbf{V}, [\tilde{\mathcal{S}}_{z(i)}]_s - [\tilde{\mathcal{S}}_b]_s \rangle \right. \\ \left. \leq -\frac{1}{4} \|\mathbf{X}_{i:} \mathbf{V}^{(t)}\| \|[\mathbf{S}_{z(i)}]_s - [\mathbf{S}_b]_s\|^2 \right\} \\ + \mathbb{1}\left\{ z^{(t+1)}(i) = b, \frac{1}{2} \|[\mathbf{S}_{z(i)}]_s - [\mathbf{S}_b]_s\|^2 \right. \\ \left. \leq \|\mathbf{X}_{i:} \mathbf{V}^{(t)}\|^{-1} F_{ib}^{(t)} + G_{ib}^{(t)} + H_{ib}^{(t)} \right\}.\end{aligned} \quad (71)$$

Note that

$$\begin{aligned}\|\mathbf{X}_{i:} \mathbf{V}^{(t)}\| &= \theta(i) \|\mathbf{S}_{i:} (\Theta \mathbf{M})^{\otimes(K-1), T} \mathbf{W}^{(t), \otimes K-1}\| \\ &\geq \theta(i) \|\mathbf{S}_{z(i)}\| \lambda_r^{K-1} (\Theta \mathbf{M}) \lambda_r^{K-1} (\mathbf{W}^{(t)}) \\ &\geq \theta(i)m,\end{aligned} \quad (72)$$

where the first inequality follows from the property of eigenvalues; the last inequality follows from Lemma 6, Lemma 10, and assumption that $\min_{a \in [r]} \|\mathbf{S}_{z(a)}\| \geq c_3 > 0$; and $m > 0$ is a positive constant related to c_3 . Plugging the lower bound of $\|\mathbf{X}_{i:} \mathbf{V}^{(t)}\|$ (72) into the inequality (71) gives

$$\mathbb{1}\{z^{(t+1)}(i) = b\} \leq A_{ib} + B_{ib}, \quad (73)$$

where

$$\begin{aligned} A_{ib} &= \mathbb{1} \left\{ z^{(t+1)}(i) = b, \langle \mathbf{E}_{i:} \mathbf{V}, [\tilde{\mathbf{S}}_{z(i):}]^s - [\tilde{\mathbf{S}}_{b:}]^s \rangle \right. \\ &\quad \left. \leq -\frac{\theta(i)m}{4} \|[\mathbf{S}_{z(i):}]^s - [\mathbf{S}_{b:}]^s\|^2 \right\}, \end{aligned}$$

$$\begin{aligned} B_{ib} &= \mathbb{1} \left\{ z^{(t+1)}(i) = b, \frac{1}{2} \|[\mathbf{S}_{z(i):}]^s - [\mathbf{S}_{b:}]^s\|^2 \right. \\ &\quad \left. \leq (\theta(i)m)^{-1} F_{ib}^{(t)} + G_{ib}^{(t)} + H_{ib}^{(t)} \right\}. \end{aligned}$$

Taking the weighted summation of (73) over $i \in [p]$ yields

$$L^{(t+1)} \leq \xi + \frac{1}{p} \sum_{i \in [p]} \sum_{b \in [r]/z(i)} \zeta_{ib}^{(t)},$$

where ξ is the oracle loss such that

$$\xi = \frac{1}{p} \sum_{i \in [p]} \theta(i) \sum_{b \in [r]/z(i)} A_{ib} \|[\mathbf{S}_{z(i):}]^s - [\mathbf{S}_{b:}]^s\|^2. \quad (74)$$

Similarly to ξ in (74), we define

$$\zeta_{ib}^{(t)} = \theta(i) B_{ib} \|[\mathbf{S}_{z(i):}]^s - [\mathbf{S}_{b:}]^s\|^2.$$

2) Now, we Show the Decomposition for MLE Loss: By the definition of Gaussian MLE, the estimator $\hat{\theta}$ satisfies $\hat{\theta}(i) = \langle \mathbf{Y}_{i:}, \hat{\mathbf{A}}_{\hat{z}(i):} \rangle / \|\hat{\mathbf{A}}_{\hat{z}(i):}\|_F^2$ for all $i \in [p]$. Hence, we have

$$\hat{z}(i) = \arg \min_{a \in [r_1]} \|[\mathbf{Y}_{i:}]^s - [\hat{\mathbf{A}}_{a:}]^s\|_F^2,$$

and the decomposition

$$L(\hat{z}) \leq \xi' + \frac{1}{p} \sum_{i \in [p]} \sum_{b \in [r]/z(i)} \zeta_{ib}',$$

Condition 1: (Intermediate Results) Let $\mathbb{O}_{p,r}$ denote the collection of all the p -by- r matrices with orthonormal columns. We have

$$\|\mathbf{EV}\|_\sigma \lesssim \sqrt{\frac{r^{K-1}}{p^{K-1}}} \left(p^{1/2} + r^{(K-1)/2} \right), \quad \|\mathbf{EV}\|_F \lesssim \sqrt{\frac{r^{2(K-1)}}{p^{K-2}}}, \quad \|\mathbf{W}_a^T \mathbf{EV}\| \lesssim \frac{r^K}{p^{K/2}}, \text{ for all } a \in [r], \quad (62)$$

$$\sup_{\mathbf{U}_k \in \mathbb{O}_{p,r}, k=2,\dots,K} \|\mathbf{E}(\mathbf{U}_2 \otimes \cdots \otimes \mathbf{U}_K)\|_\sigma \lesssim \left(\sqrt{r^{K-1}} + K\sqrt{pr} \right), \quad (63)$$

$$\sup_{\mathbf{U}_k \in \mathbb{O}_{p,r}, k=2,\dots,K} \|\mathbf{E}(\mathbf{U}_2 \otimes \cdots \otimes \mathbf{U}_K)\|_F \lesssim \left(\sqrt{pr^{K-1}} + K\sqrt{pr} \right), \quad (64)$$

$$\xi \leq \exp \left(-M \frac{\Delta_{\min}^2 p^{K-1}}{r^{K-1}} \right), \quad \xi' \lesssim \exp \left(-\frac{\Delta_{\min}^2 p^{K-1}}{r^{K-1}} \right), \quad (65)$$

$$L^{(t)} \leq \frac{\bar{C}}{\tilde{C}} \frac{\Delta_{\min}^2}{r \log p}, \quad \text{for } t = 0, 1, \dots, T, \quad L(\hat{z}) \leq \frac{\bar{C}}{\tilde{C}} \frac{\Delta_{\min}^2}{r \log p}, \quad (66)$$

where M is a positive universal constant in inequality (84), \bar{C}, \tilde{C} are positive universal constants in the proof of Theorem 4 and assumption $\text{SNR} \geq \tilde{C} p^{-K/2} \log p$, respectively. Further, inequality (62) holds by replacing \mathbf{V} to $\mathbf{V}^{(t)}, \mathbf{Q}, \hat{\mathbf{Q}}$ and $\mathbf{W}_{:a}$ to $\mathbf{W}_{:a}^{(t),T}, \mathbf{P}_{:a}^T, \hat{\mathbf{P}}_{:a}^T$ when initialization condition (66) holds.

where $\zeta_{ib}' = \theta(i)^2 B_{ib}' \|[\mathbf{A}_{z(i):}]^s - [\mathbf{A}_{b:}]^s\|^2$ and

$$A_{ib}' = \mathbb{1} \left\{ \hat{z}(i) = b, \langle \mathbf{E}_{i:}, [\tilde{\mathbf{A}}_{z(i):}]^s - [\tilde{\mathbf{A}}_{b:}]^s \rangle \right. \quad (2231) \\ \left. \leq -\frac{m'}{4} \sqrt{\frac{p^{K-1}}{r^{K-1}}} \|[\mathbf{A}_{z(i):}]^s - [\mathbf{A}_{b:}]^s\|_F^2 \right\}, \quad (2232)$$

$$\begin{aligned} B_{ib}' &= \mathbb{1} \left\{ \hat{z}(i) = b, -\frac{1}{2} \|[\mathbf{A}_{z(i):}]^s - [\mathbf{A}_{b:}]^s\|_F^2 \right. \quad (2233) \\ &\quad \left. \leq \sqrt{\frac{r^{K-1}}{(m')^2 p^{K-1}}} \hat{F}_{ib} + \hat{G}_{ib} + \hat{H}_{ib} \right\} \quad (2234) \end{aligned}$$

with terms

$$\hat{F}_{ib} = 2 \left\langle \mathbf{E}_{i:}, ([\tilde{\mathbf{A}}_{z(i):}]^s - [\hat{\mathbf{A}}_{a:}]^s) - ([\tilde{\mathbf{A}}_{b:}]^s - [\hat{\mathbf{A}}_{b:}]^s) \right\rangle, \quad (2236)$$

$$\hat{G}_{ib} = \left(\|\mathbf{X}_{i:}^s - [\hat{\mathbf{A}}_{z(i):}]^s\|_F^2 - \|\mathbf{X}_{i:}^s - [\mathbf{P}_{:z(i)}^T \mathbf{Y} \hat{\mathbf{Q}} \hat{\mathbf{B}}^T]^s\|_F^2 \right) \quad (2237)$$

$$- \left(\|\mathbf{X}_{i:}^s - [\hat{\mathbf{A}}_{b:}]^s\|_F^2 - \|\mathbf{X}_{i:}^s - [\mathbf{P}_{:b}^T \mathbf{Y} \hat{\mathbf{Q}} \hat{\mathbf{B}}^T]^s\|_F^2 \right), \quad (2238)$$

$$\begin{aligned} \hat{H}_{ib} &= \|\mathbf{X}_{i:}^s - [\mathbf{P}_{:z(i)}^T \mathbf{Y} \hat{\mathbf{Q}} \hat{\mathbf{B}}^T]^s\|_F^2 - \|\mathbf{X}_{i:}^s - [\mathbf{P}_{:b}^T \mathbf{Y} \hat{\mathbf{Q}} \hat{\mathbf{B}}^T]^s\|_F^2 \quad (2239) \\ &\quad + \|\mathbf{A}_{z(i):}^s - \mathbf{A}_{b:}^s\|_F^2. \quad (2240) \end{aligned}$$

Step 3 (Derivation of Contraction Inequality): In this step we derive the upper bound of ζ_{ib} and obtain the contraction inequality (24). We show the analysis in the following one-column box for a better presentation.

Step 4 (Verification of Condition 1): Last, we verify the Condition 1 under high probability to finish the proof. Note that the inequalities (62), (63), and (64) describe the property of the sub-Gaussian noise tensor \mathcal{E} , and the readers can find the proof directly in [13, Step 5, Proof of Theorem 2]. The initial condition (66) for MLE is satisfied by Lemma 13. Here, we include only the verification of inequalities (65) and (66) for algorithm estimators.

Now, we verify the oracle loss condition (65). Recall the definition of ξ ,

$$\xi = \frac{1}{p} \sum_{i \in [p]} \theta(i) \sum_{b \in [r]} \mathbb{1} \left\{ \langle \mathbf{E}_{i:} \mathbf{V}, [\tilde{\mathbf{S}}_{z(i):}]^s - [\tilde{\mathbf{S}}_{b:}]^s \rangle \right. \quad (2255) \\ \left. \leq -M \frac{\Delta_{\min}^2 p^{K-1}}{r^{K-1}} \right\}$$

$$\begin{aligned} &\leq -\frac{\theta(i)m}{4} \left\| [\mathbf{S}_{z(i)}]_s^s - [\mathbf{S}_b]_s^s \right\|^2 \\ &\cdot \left\| [\mathbf{S}_{z(i)}]_s^s - [\mathbf{S}_b]_s^s \right\|^2. \end{aligned} \quad \leq P_1 + P_2 + P_3, \quad 2265$$

2258 Let $e_i = \mathbf{E}_i \mathbf{V}$ denote the aggregated noise vector for all $i \in [p]$, and e_i 's are independent zero-mean sub-Gaussian vector in $\mathbb{R}^{r^{K-1}}$. The entries in e_i are independent zero-mean sub-Gaussian variables with sub-Gaussian norm upper bounded by $m_1 \sqrt{r^{K-1}/p^{K-1}}$ with some positive constant m_1 . We have the probability inequality

$$\mathbb{P} \left(\left\langle e_i, [\tilde{\mathbf{S}}_{z(i)}]_s^s - [\tilde{\mathbf{S}}_b]_s^s \right\rangle \leq -\frac{\theta(i)m}{4} \left\| [\mathbf{S}_{z(i)}]_s^s - [\mathbf{S}_b]_s^s \right\|^2 \right)$$

where

$$P_1 = \mathbb{P} \left(\left\langle e_i, [\mathbf{S}_{z(i)}]_s^s - [\mathbf{S}_b]_s^s \right\rangle \leq -\frac{\theta(i)m}{8} \left\| [\mathbf{S}_{z(i)}]_s^s - [\mathbf{S}_b]_s^s \right\|^2 \right), \quad 2266$$

$$P_2 = \mathbb{P} \left(\left\langle e_i, [\tilde{\mathbf{S}}_{z(i)}]_s^s - [\mathbf{S}_{z(i)}]_s^s \right\rangle \leq -\frac{\theta(i)m}{16} \left\| [\mathbf{S}_{z(i)}]_s^s - [\mathbf{S}_b]_s^s \right\|^2 \right), \quad 2267$$

$$P_3 = \mathbb{P} \left(\left\langle e_i, [\mathbf{S}_b]_s^s - [\tilde{\mathbf{S}}_b]_s^s \right\rangle \leq -\frac{\theta(i)m}{16} \left\| [\mathbf{S}_{z(i)}]_s^s - [\mathbf{S}_b]_s^s \right\|^2 \right). \quad 2268$$

For P_1 , notice that the inner product $\left\langle e_j, \mathbf{S}_{z(j)}^s - \mathbf{S}_b^s \right\rangle$ is a sub-Gaussian variable with sub-Gaussian norm bounded by

Step 3: Choose the constant \tilde{C} in the condition $\text{SNR} \geq \tilde{C} p^{-K/2} \log p$ that satisfies the condition of Lemma 11, inequalities (98), and (102). Note that

$$\begin{aligned} \zeta_{ib}^{(t)} &= \theta(i) \left\| [\mathbf{S}_{z(i)}]_s^s - [\mathbf{S}_b]_s^s \right\|^2 \mathbb{1} \left\{ z^{(t+1)}(i) = b, \frac{1}{2} \left\| [\mathbf{S}_{z(i)}]_s^s - [\mathbf{S}_b]_s^s \right\|^2 \leq (\theta(i)m)^{-1} F_{ib}^{(t)} + G_{ib}^{(t)} + H_{ib}^{(t)} \right\} \\ &\leq \theta(i) \left\| [\mathbf{S}_{z(i)}]_s^s - [\mathbf{S}_b]_s^s \right\|^2 \mathbb{1} \left\{ z^{(t+1)}(i) = b, \frac{1}{4} \left\| [\mathbf{S}_{z(i)}]_s^s - [\mathbf{S}_b]_s^s \right\|^2 \leq (\theta(i)m)^{-1} F_{ib}^{(t)} + G_{ib}^{(t)} \right\} \\ &\leq 64 \mathbb{1} \left\{ z^{(t+1)}(i) = b \right\} \left(\frac{(F_{ib}^{(t)})^2}{cm^2 \left\| [\mathbf{S}_{z(i)}]_s^s - [\mathbf{S}_b]_s^s \right\|^2} + \frac{\theta(i)(G_{ib}^{(t)})^2}{\left\| [\mathbf{S}_{z(i)}]_s^s - [\mathbf{S}_b]_s^s \right\|^2} \right) \end{aligned} \quad 2270$$

where the first inequality follows from the inequality (89) in Lemma 11, and the last inequality follows from the assumption that $\min_{i \in [p]} \theta(i) \geq c > 0$. Following [13, Step 4, Proof of Theorem 2] and Lemma 11, we have

$$\frac{1}{p} \sum_{i \in [p]} \sum_{b \in [r]/z(i)} \mathbb{1} \left\{ z^{(t+1)}(i) = b \right\} \frac{(F_{ib}^{(t)})^2}{cm^2 \left\| [\mathbf{S}_{z(i)}]_s^s - [\mathbf{S}_b]_s^s \right\|^2} \leq \frac{C_0 \bar{C}}{cm^2 \tilde{C}^2} L^{(t)},$$

for a positive universal constant C and

$$\begin{aligned} \frac{1}{p} \sum_{i \in [p]} \sum_{b \in [r]/z(i)} \mathbb{1} \left\{ z^{(t+1)}(i) = b \right\} \frac{\theta(i)(G_{ib}^{(t)})^2}{\left\| [\mathbf{S}_{z(i)}]_s^s - [\mathbf{S}_b]_s^s \right\|^2} &\leq \frac{1}{512} \frac{1}{p} \sum_{i \in [p]} \theta(i) \sum_{b \in [r]/z(i)} \mathbb{1} \left\{ z^{(t+1)}(i) = b \right\} (\Delta_{\min}^2 + L^{(t)}) \\ &\leq \frac{1}{512} (L^{(t+1)} + L^{(t)}), \end{aligned}$$

where the last inequality follows from the definition of $L^{(t)}$ and the constraint of θ in parameter space (2). For \tilde{C} also satisfies

$$\frac{C_0 \bar{C}}{cm^2 \tilde{C}^2} \leq \frac{1}{512}, \quad 75$$

we have

$$\frac{1}{p} \sum_{i \in [p]} \sum_{b \in [r]/z(i)} \zeta_{ib}^{(t)} \leq \frac{1}{8} L^{(t+1)} + \frac{1}{4} L^{(t)}. \quad 76$$

Plugging the inequality (76) into the decomposition (74), we obtain the contraction inequality

$$L^{(t+1)} \leq \frac{3}{2} \xi + \frac{1}{2} L^{(t)}, \quad 77$$

where $\frac{1}{2}$ is the contraction parameter.

Therefore, with \tilde{C} satisfying inequalities (75), (98) and (102), we obtain the conclusion in Theorem 5 via inequality (77) combining the inequality (65) in Condition 1 and Lemma 2.

We also have the contraction inequality for MLE.

Following the same derivation of (77) with the upper bound of $\hat{F}_{ib}, \hat{G}_{ib}, \hat{H}_{ib}$ in Lemma 12, we also have

$$L(\hat{z}) \leq \frac{3}{2} \xi' + \frac{1}{2} L(\hat{z}),$$

which indicates the conclusion $\ell(\hat{z}, z) \lesssim \Delta_{\min}^2 \exp \left(-\frac{p^{K-1}}{r^{K-1}} \Delta_{\min}^2 \right)$.

2272 $m_2 \sqrt{r^{K-1}/p^{K-1}} \|S_{z(i)}^s - S_{b:}^s\|$ with some positive constant
2273 m_2 . Then, by Chernoff bound, we have

$$2274 P_1 \lesssim \exp \left(-\frac{p^{K-1}}{r^{K-1}} \|S_{z(j)}^s - [S_{b:}]^s\|^2 \right). \quad (78)$$

2275 For P_2 and P_3 , we only need to derive the upper bound
2276 of P_2 due to the symmetry. By the law of total probability,
2277 we have

$$2278 P_2 \leq P_{21} + P_{22}, \quad (79)$$

2279 where with some positive constant $t > 0$,

$$\begin{aligned} 2280 P_{21} &= \mathbb{P} \left(t \leq \|[\tilde{S}_{z(i)}]^s - [S_{z(i)}]^s\| \right), \\ 2281 P_{22} &= \mathbb{P} \left(\left\langle e_i, [\tilde{S}_{z(i)}]^s - [S_{z(i)}]^s \right\rangle \leq -\frac{\theta(i)m}{16} \right. \\ 2282 &\quad \cdot \|S_{z(i)}^s - [S_{b:}]^s\|^2 \left| \|[\tilde{S}_{z(i)}]^s - [S_{z(i)}]^s\| < t \right. \right). \end{aligned}$$

2283 For P_{21} , note that the term $\mathbf{W}_{z(i)}^T \mathbf{EV} =$
2284 $\frac{\sum_{j \neq i, j \in [p]} \mathbf{1}\{z(j)=z(i)\} e_j}{\sum_{j \in [p]} \mathbf{1}\{z(j)=z(i)\}}$ is a sub-Gaussian vector with
2285 sub-Gaussian norm bounded by $m_3 \sqrt{r^K/p^K}$ with some
2286 positive constant m_3 . This implies

$$\begin{aligned} 2287 P_{21} &\leq \mathbb{P} \left(t \|S_{z(i)}\| \leq \|\tilde{S}_{z(i)} - S_{z(i)}\| \right) \\ 2288 &\leq \mathbb{P} \left(c_3 t \leq \|\mathbf{W}_{z(i)}^T \mathbf{EV}\| \right) \\ 2289 &\lesssim \exp \left(-\frac{p^K t^2}{r^K} \right), \end{aligned} \quad (80)$$

2290 where the first inequality follows from the basic inequality in
2291 Lemma 4, the second inequality follows from the assumption
2292 that $\min_{a \in [r]} \|S_{z(i)}\| \geq c_3 > 0$ in (2), and the last inequality
2293 follows from the Bernstein inequality.

2294 For P_{22} , the inner product $\left\langle e_i, [\tilde{S}_{z(i)}]^s - [S_{z(i)}]^s \right\rangle$ is
2295 also a sub-Gaussian variable with sub-Gaussian norm
2296 $m_4 \sqrt{r^{K-1}/p^{K-1}} t$, conditioned on $\|[\tilde{S}_{z(i)}]^s - [S_{z(i)}]^s\| < t$
2297 with some positive constant m_4 . Then, by Chernoff bound,
2298 we have

$$2299 P_{22} \lesssim \exp \left(-\frac{p^{K-1}}{r^{K-1} t^2} \|S_{z(j)}^s - [S_{b:}]^s\|^4 \right). \quad (81)$$

2300 We take $t = \|S_{z(i)}^s - [S_{b:}]^s\|$ in P_{21} and P_{22} , and plug
2301 the inequalities (80) and (81) into to the upper bound for
2302 P_2 in (79). We obtain that

$$2303 P_2 \lesssim \exp \left(-\frac{p^{K-1}}{r^{K-1}} \|S_{z(i)}^s - [S_{b:}]^s\|^2 \right). \quad (82)$$

2304 Combining the upper bounds (78) and (82) gives

$$\begin{aligned} 2305 \mathbb{P} \left(\left\langle e_i, [\tilde{S}_{z(i)}]^s - [S_{b:}]^s \right\rangle \leq -\frac{\theta(i)m}{4} \|S_{z(i)}^s - [S_{b:}]^s\|^2 \right) \\ 2306 \lesssim \exp \left(-\frac{p^{K-1}}{r^{K-1}} \|S_{z(i)}^s - [S_{b:}]^s\|^2 \right). \end{aligned} \quad (83)$$

Hence, we have

$$\begin{aligned} 2308 \mathbb{E} \xi &= \frac{1}{p} \sum_{i \in [p]} \theta(i) \sum_{b \in [r]} \mathbb{P} \left\{ \left\langle \mathbf{E}_i \mathbf{V}, [\tilde{S}_{z(i)}]^s - [S_{b:}]^s \right\rangle \right. \\ 2309 &\quad \left. \leq -\frac{\theta(i)m}{4} \|S_{z(i)}^s - [S_{b:}]^s\|^2 \right\} \|S_{z(i)}^s - [S_{b:}]^s\|^2 \\ 2310 &\lesssim \frac{1}{p} \sum_{i \in [p]} \theta(i) \max_{i \in [p], b \in [r]} \|S_{z(i)}^s - [S_{b:}]^s\|^2 \\ 2311 &\quad \cdot \exp \left(-\frac{p^{K-1}}{r^{K-1}} \|S_{z(i)}^s - [S_{b:}]^s\|^2 \right) \\ 2312 &\leq \exp \left(-M \frac{p^{K-1}}{r^{K-1}} \Delta_{\min}^2 \right), \end{aligned} \quad (84)$$

2313 where M is a positive constant, the first inequality follows
2314 from the constraint that $\sum_{i \in [p]} \theta(i) = p$, and the last inequality
2315 follows from (83).

2316 By Markov's inequality, we have

$$\begin{aligned} 2317 \mathbb{P} \left(\xi \lesssim \mathbb{E} \xi + \exp \left(-\frac{Mp^{K-1}}{2r^{K-1}} \Delta_{\min}^2 \right) \right) \\ 2318 \geq 1 - C \exp \left(-\frac{Mp^{K-1}}{2r^{K-1}} \Delta_{\min}^2 \right), \end{aligned}$$

2319 and thus the condition (65) holds with probability at least $1 - C \exp \left(-\frac{Mp^{K-1}}{2r^{K-1}} \Delta_{\min}^2 \right)$ for some constant $C > 0$.

2320 3) *The Initialization Condition for MLE Also Holds:* For
2321 ξ' , notice that $\langle \mathbf{E}_i \mathbf{A}_{a:}^s - \mathbf{A}_{b:}^s \rangle$ is a sub-Gaussian vector with
2322 variance bounded by $\|\mathbf{A}_{a:}^s - \mathbf{A}_{b:}^s\|^2$ and

$$\begin{aligned} 2324 \mathbb{P} \left(t \leq \|[\bar{\mathbf{A}}_{a:}]^s - \mathbf{A}_{a:}^s\| \right) &\leq (t \leq \|[\mathbf{P}_{a:}^T \mathbf{YQ}]^s - [\mathbf{P}_{a:}^T \mathbf{XQ}]^s\|) \\ 2325 &\leq \mathbb{P} \left(t \min_{a \in [r]} \|\mathbf{S}_{a:}\| \leq \|\mathbf{P}_{a:}^T \mathbf{EQ}\| \right) \\ 2326 &\lesssim \exp \left(-\frac{p^K t^2}{r^K} \right), \end{aligned}$$

2327 where the first inequality follows from the property in later
2328 inequality (105). We also have

$$\xi' \lesssim \left(-\frac{p^{K-1}}{r^{K-1}} \Delta_{\min}^2 \right). \quad (85)$$

2329 Finally, we verify the bounded loss condition (66) for algorithm
2330 estimator by induction. With output $z^{(0)}$ from Sub-
2331 algorithm 2 and the assumption $\text{SNR} \geq \tilde{C} p^{-K/2} \log p$, by Theorem
2332 4, we have

$$2333 L^{(0)} \leq \frac{\tilde{C} \Delta_{\min}^2}{\tilde{C} r \log p}, \quad \text{when } p \text{ is large enough.}$$

2334 Therefore, the condition (66) holds for $t = 0$. Assume that
2335 the condition (66) also holds for all $t \leq t_0$. Then, by the
2336 decomposition (77), we have

$$\begin{aligned} 2338 L^{(t_0+1)} &\leq \frac{3}{2} \xi + \frac{1}{2} L^{(t_0)} \\ 2339 &\leq \exp \left(-M \frac{p^{K-1}}{r^{K-1}} \Delta_{\min}^2 \right) + \frac{\Delta_{\min}^2}{r \log p} \\ 2340 &\leq \frac{\tilde{C}}{\tilde{C} r \log p} \Delta_{\min}^2, \end{aligned}$$

where the second inequality follows from the condition (65) and the last inequality follows from the assumption that $\Delta_{\min}^2 \gtrsim p^{-K/2} \log p$. Thus, the condition (66) holds for t_0+1 , and the condition (66) is proved by induction. \square

4) Useful Lemmas for the Proof of Theorem 5:

Lemma 10 (Singular-Value Property of Membership Matrices): Under the setup of Theorem 5, suppose that the condition (66) holds. Then, for all $a \in [r]$, we have $|(\mathbf{z}^{(t)})^{-1}(a)| \asymp p/r$. Moreover, we have

$$\lambda_r(\mathbf{M}) \asymp \|\mathbf{M}\|_\sigma \asymp \sqrt{p/r}, \quad \lambda_r(\mathbf{W}) \asymp \|\mathbf{W}\|_\sigma \asymp \sqrt{r/p}, \\ \lambda_r(\mathbf{P}) \asymp \|\mathbf{P}\|_\sigma \asymp \min_{a \in [r]} \|\boldsymbol{\theta}_{\mathbf{z}^{-1}(a)}\|^{-1} \lesssim \sqrt{r/p}. \quad (85)$$

The inequalities (85) also hold by replacing \mathbf{M} and \mathbf{W} to $\mathbf{M}^{(t)}$ and $\mathbf{W}^{(t)}$ respectively. Further, we have

$$\lambda_r(\mathbf{W}\mathbf{W}^T) \asymp \|\mathbf{W}\mathbf{W}^T\|_\sigma \asymp r/p, \quad (86)$$

which is also true for $\mathbf{W}^{(t)}\mathbf{W}^{(t),T}$.

Proof of Lemma 10: The proof for the inequality (85) for \mathbf{M}, \mathbf{W} can be found in [13, Proof of Lemma 4]. The inequalities for \mathbf{P} follows the same derivation with balance assumption on $\boldsymbol{\theta}$ and $\min_{i \in [p]} \theta(i) \geq c$.

For inequality (86), note that for all $k \in [r]$,

$$\begin{aligned} \lambda_k(\mathbf{W}\mathbf{W}^T) &= \sqrt{\text{eigen}_k(\mathbf{W}\mathbf{W}^T\mathbf{W}\mathbf{W}^T)} \\ &\asymp \sqrt{\frac{r}{p} \text{eigen}_k(\mathbf{W}\mathbf{W}^T)} \\ &= \sqrt{\frac{r}{p} \lambda_k^2(\mathbf{W})} \asymp \frac{r}{p}, \end{aligned}$$

where $\text{eigen}_k(\mathbf{A})$ denotes the k -th largest eigenvalue of the square matrix \mathbf{A} , the first inequality follows the fact that $\mathbf{W}^T\mathbf{W}$ is a diagonal matrix with elements of order r/p , and the second equation follows from the definition of singular value. \square

Lemma 11 (Upper Bound for $F_{ib}^{(t)}, G_{ib}^{(t)}$ and $H_{ib}^{(t)}$): Under the Condition 1 and the setup of Theorem 5 with fixed $r \geq 2$, assume the constant \tilde{C} in the condition $\text{SNR} \geq \tilde{C}p^{-K/2} \log p$ is large enough to satisfy the inequalities (98) and (102). As $p \rightarrow \infty$, we have

$$\begin{aligned} \max_{i \in [p]} \max_{b \neq z(i)} \frac{(F_{ib}^{(t)})^2}{\|[\mathbf{S}_{z(i)}]_s - [\mathbf{S}_b]_s\|^2} \\ \lesssim \frac{rL^{(t)}}{\Delta_{\min}^2} \|\mathbf{E}_{i:}\mathbf{V}\|^2 + \left(1 + \frac{rL^{(t)}}{\Delta_{\min}^2}\right) \|\mathbf{E}_{i:}(\mathbf{V} - \mathbf{V}^{(t)})\|^2, \quad (87) \end{aligned}$$

$$\max_{i \in [p]} \max_{b \neq z(i)} \frac{(G_{ib}^{(t)})^2}{\|[\mathbf{S}_{z(i)}]_s - [\mathbf{S}_b]_s\|^2} \leq \frac{1}{512} (\Delta_{\min}^2 + L^{(t)}), \quad (88)$$

$$\max_{i \in [p]} \max_{b \neq z(i)} \frac{|H_{ib}^{(t)}|}{\|[\mathbf{S}_{z(i)}]_s - [\mathbf{S}_b]_s\|^2} \leq \frac{1}{4}. \quad (89)$$

Similarly, when the SNR $\geq \tilde{C}p^{-(K-1)} \log p$ with a large constant \tilde{C} , we have

$$\max_{i \in [p]} \max_{b \neq z(i)} \frac{(\hat{F}_{ib})^2}{\|[\mathbf{A}_{z(i)}]_s - [\mathbf{A}_b]_s\|^2} \lesssim p^{K-1} \frac{rL(\hat{z})}{\Delta_{\min}^2} \quad (2380)$$

$$\max_{i \in [p]} \max_{b \neq z(i)} \frac{(\hat{G}_{ib})^2}{\|[\mathbf{A}_{z(i)}]_s - [\mathbf{A}_b]_s\|^2} \leq \frac{1}{512} (\Delta_{\min}^2 + L(\hat{z})), \quad (2381)$$

$$\max_{i \in [p]} \max_{b \neq z(i)} \frac{|\hat{H}_{ib}|}{\|[\mathbf{A}_{z(i)}]_s - [\mathbf{A}_b]_s\|^2} \leq \frac{1}{4}. \quad (2382)$$

Proof of Lemma 11: We prove the the first three inequalities in Lemma 11 separately.

1) Upper bound for $F_{ib}^{(t)}$, i.e., inequality (87). Recall the definition of $F_{ib}^{(t)}$,

$$\begin{aligned} F_{ib}^{(t)} &= 2 \left\langle \mathbf{E}_{i:}\mathbf{V}^{(t)}, \left([\tilde{\mathbf{S}}_{z(i)}]_s - [\mathbf{S}_{z(i)}]_s\right) - \left([\tilde{\mathbf{S}}_b]_s - [\mathbf{S}_b]_s\right) \right\rangle \\ &\quad + 2 \left\langle \mathbf{E}_{i:}(\mathbf{V} - \mathbf{V}^{(t)}), [\tilde{\mathbf{S}}_{z(i)}]_s - [\tilde{\mathbf{S}}_b]_s \right\rangle. \end{aligned} \quad (2387)$$

By Cauchy-Schwartz inequality, we have

$$\begin{aligned} &\left(F_{ib}^{(t)}\right)^2 \\ &\leq 8 \left(\left\langle \mathbf{E}_{i:}\mathbf{V}^{(t)}, \left([\tilde{\mathbf{S}}_{z(i)}]_s - [\mathbf{S}_{z(i)}]_s\right) - \left([\tilde{\mathbf{S}}_b]_s - [\mathbf{S}_b]_s\right) \right\rangle \right)^2 \\ &\quad + 8 \left(\left\langle \mathbf{E}_{i:}(\mathbf{V} - \mathbf{V}^{(t)}), [\tilde{\mathbf{S}}_{z(i)}]_s - [\tilde{\mathbf{S}}_b]_s \right\rangle \right)^2 \\ &\leq 8 \left(\|\mathbf{E}_{i:}\mathbf{V}\|^2 + \|\mathbf{E}_{i:}(\mathbf{V} - \mathbf{V}^{(t)})\|^2 \right) \max_{a \in [r]} \|[\tilde{\mathbf{S}}_a]_s - [\mathbf{S}_a]_s\|^2 \\ &\quad + \|\mathbf{E}_{i:}(\mathbf{V} - \mathbf{V}^{(t)})\|^2 \|[\tilde{\mathbf{S}}_{z(i)}]_s - [\tilde{\mathbf{S}}_b]_s\|. \end{aligned} \quad (90)$$

Note that for all $a \in [r]$,

$$\begin{aligned} \|[\tilde{\mathbf{S}}_a]_s - [\mathbf{S}_a]_s\|^2 &= \|[\mathbf{W}_{:a}^T \mathbf{Y} \mathbf{V}]_s - [\mathbf{W}_{:a}^{(t),T} \mathbf{Y} \mathbf{V}^{(t)}]_s\|^2 \\ &\leq 2 \|[\mathbf{W}_{:a}^T \mathbf{Y} \mathbf{V}]_s - [\mathbf{W}_{:a}^{(t),T} \mathbf{Y} \mathbf{V}]_s\|^2 \\ &\quad + 2 \|[\mathbf{W}_{:a}^{(t),T} \mathbf{Y} \mathbf{V}]_s - [\mathbf{W}_{:a}^{(t),T} \mathbf{Y} \mathbf{V}^{(t)}]_s\|^2 \\ &\lesssim \frac{r^2(L^{(t)})^2}{\Delta_{\min}^2} + \frac{rr^{2K} + pr^{K+2}}{p^K} \frac{L^{(t)}}{\Delta_{\min}^2} \\ &\lesssim rL^{(t)} + \frac{rr^{2K} + pr^{K+2}}{p^K} \frac{L^{(t)}}{\Delta_{\min}^2} \\ &\lesssim rL^{(t)}, \end{aligned} \quad (91)$$

where the second inequality follows from the inequalities (108) and (109) in Lemma 12, the third inequality follows from the condition (66) in Condition 1, and the last inequality follows from the assumption that $\Delta_{\min}^2 \geq \tilde{C}p^{-K/2} \log p$.

Note that

$$\begin{aligned} &\|[\tilde{\mathbf{S}}_{z(i)}]_s - [\tilde{\mathbf{S}}_b]_s\|^2 \\ &= \|[\tilde{\mathbf{S}}_{z(i)}]_s - [\mathbf{S}_{z(i)}]_s + [\mathbf{S}_{z(i)}]_s - [\mathbf{S}_b]_s + [\mathbf{S}_b]_s - [\tilde{\mathbf{S}}_b]_s\|^2 \\ &\lesssim \|[\mathbf{S}_{z(i)}]_s - [\mathbf{S}_b]_s\|^2 + \max_{a \in [r]} \|[\mathbf{S}_a]_s - [\tilde{\mathbf{S}}_a]_s\|^2 \\ &\lesssim \|[\mathbf{S}_{z(i)}]_s - [\mathbf{S}_b]_s\|^2 + \max_{a \in [r]} \frac{1}{\|\mathbf{S}_a\|^2} \|\mathbf{W}_{:a}^T \mathbf{E} \mathbf{V}\|^2 \\ &\lesssim \|[\mathbf{S}_{z(i)}]_s - [\mathbf{S}_b]_s\|^2, \end{aligned} \quad (92)$$

where the second inequality follows from Lemma 4, and the last inequality follows from the assumptions on $\|\mathbf{S}_{a:}\|$ in the parameter space (2), the inequality (62) in Condition 1 and the assumption $\Delta_{\min}^2 \gtrsim p^{-K/2} \log p$.

Therefore, we finish the proof of inequality (87) by plugging the inequalities (91) and (92) into the upper bound (90).

2) Upper bound for $G_{ib}^{(t)}$, i.e., inequality (88). By definition of $G_{ib}^{(t)}$, we rearrange terms and obtain

$$\begin{aligned} G_{ib}^{(t)} &= \left(\|[\mathbf{X}_{i:} \mathbf{V}^{(t)}]^s - [\mathbf{S}_{z(i):}^{(t)}]^s\|^2 \right. \\ &\quad \left. - \|[\mathbf{X}_{i:} \mathbf{V}^{(t)}]^s - [\mathbf{W}_{:z(i)}^T \mathbf{Y} \mathbf{V}^{(t)}]^s\|^2 \right) \\ &\quad - \left(\|[\mathbf{X}_{i:} \mathbf{V}^{(t)}]^s - [\mathbf{S}_{b:}^{(t)}]^s\|^2 \right. \\ &\quad \left. - \|[\mathbf{X}_{i:} \mathbf{V}^{(t)}]^s - [\mathbf{W}_{:b}^T \mathbf{Y} \mathbf{V}^{(t)}]^s\|^2 \right) \\ &= 2 \left\langle [\mathbf{X}_{i:} \mathbf{V}^{(t)}]^s, \left([\mathbf{W}_{:z(i)}^T \mathbf{Y} \mathbf{V}^{(t)}]^s - [\mathbf{S}_{z(i):}^{(t)}]^s \right) \right. \\ &\quad \left. - \left([\mathbf{W}_{:b}^T \mathbf{Y} \mathbf{V}^{(t)}]^s - [\mathbf{S}_{b:}^{(t)}]^s \right) \right\rangle \\ &= G_1 + G_2 - G_3, \end{aligned} \quad (93)$$

where

$$\begin{aligned} G_1 &= \|[\mathbf{W}_{:z(i)}^T \mathbf{Y} \mathbf{V}^{(t)}]^s - [\mathbf{S}_{z(i):}^{(t)}]^s\|^2 - \|[\mathbf{W}_{:b}^T \mathbf{Y} \mathbf{V}^{(t)}]^s - [\mathbf{S}_{b:}^{(t)}]^s\|^2, \\ G_2 &= 2 \left\langle [\mathbf{X}_{i:} \mathbf{V}^{(t)}]^s - [\mathbf{W}_{:z(i)}^T \mathbf{Y} \mathbf{V}^{(t)}]^s, [\mathbf{W}_{:z(i)}^T \mathbf{Y} \mathbf{V}^{(t)}]^s - [\mathbf{S}_{z(i):}^{(t)}]^s \right\rangle, \\ G_3 &= 2 \left\langle [\mathbf{X}_{i:} \mathbf{V}^{(t)}]^s - [\mathbf{W}_{:b}^T \mathbf{Y} \mathbf{V}^{(t)}]^s, [\mathbf{W}_{:b}^T \mathbf{Y} \mathbf{V}^{(t)}]^s - [\mathbf{S}_{b:}^{(t)}]^s \right\rangle. \end{aligned}$$

For G_1 , we have

$$\begin{aligned} |G_1|^2 &\leq \left| \|[\mathbf{W}_{:z(i)}^T \mathbf{Y} \mathbf{V}^{(t)}]^s - [\mathbf{S}_{z(i):}^{(t)}]^s\|^2 \right. \\ &\quad \left. - \|[\mathbf{W}_{:b}^T \mathbf{Y} \mathbf{V}^{(t)}]^s - [\mathbf{S}_{b:}^{(t)}]^s\|^2 \right|^2 \\ &\leq \max_{a \in [r]} \|[\mathbf{W}_{:a}^T \mathbf{Y} \mathbf{V}^{(t)}]^s - [\mathbf{W}_{:a}^{(t),T} \mathbf{Y} \mathbf{V}^{(t)}]^s\|^4 \\ &\leq C^4 \frac{r^4}{\Delta_{\min}^4} (L^{(t)})^4 + \frac{r^2 r^{4K} + p^2 r^{2K+4}}{p^{2K}} \frac{(L^{(t)})^2}{\Delta_{\min}^4} \\ &\leq C^4 \frac{\bar{C}}{\tilde{C}^3} \left(\Delta_{\min}^4 + \Delta_{\min}^2 L^{(t)} \right), \end{aligned} \quad (94)$$

where the third inequality follows from the inequality (110) in Lemma 12 and the last inequality follows from the assumption that $\Delta_{\min}^2 \geq \tilde{C} p^{-K/2} \log p$ and inequality (66) in Condition 1.

For G_2 , noticing that $[\mathbf{X}_{i:} \mathbf{V}^{(t)}]^s = [\mathbf{W}_{:z(i)}^T \mathbf{X} \mathbf{V}^{(t)}]^s$, we have

$$\begin{aligned} |G_2|^2 &\leq 2 \|[\mathbf{X}_{i:} \mathbf{V}^{(t)}]^s - [\mathbf{W}_{:z(i)}^T \mathbf{Y} \mathbf{V}^{(t)}]^s\|^2 \\ &\quad \cdot \|[\mathbf{W}_{:z(i)}^T \mathbf{Y} \mathbf{V}^{(t)}]^s - [\mathbf{S}_{z(i):}^{(t)}]^s\|^2 \\ &\leq \frac{2}{\|\mathbf{W}_{:z(i)}^T \mathbf{X} \mathbf{V}^{(t)}\|^2} \max_{a \in [r]} \|\mathbf{W}_{:a}^T \mathbf{E} \mathbf{V}^{(t)}\|^2 \\ &\quad \cdot \max_{a \in [r]} \|[\mathbf{W}_{:a}^T \mathbf{Y} \mathbf{V}^{(t)}]^s - [\mathbf{W}_{:a}^{(t),T} \mathbf{Y} \mathbf{V}^{(t)}]^s\|^2 \end{aligned}$$

$$\leq C' \frac{r^{2K-1} + K p r^{K+1}}{p^K} \quad (2446)$$

$$\cdot \left(\frac{r^2}{\Delta_{\min}^2} (L^{(t)})^2 + \frac{r r^{2K} + p r^{K+2}}{p^K} \frac{L^{(t)}}{\Delta_{\min}^2} \right) \quad (2447)$$

$$\leq \frac{C'}{\tilde{C}^2} \Delta_{\min}^2 L^{(t)}, \quad (2448)$$

where C' is a positive universal constant, the second inequality follows from Lemma 4, the third inequality follows from the inequality (63) in Condition 1, the inequalities (110) and (129) in the proof of Lemma 12, and the last inequality follows from the assumption $\Delta_{\min}^2 \geq \tilde{C} p^{-K/2} \log p$ and inequality (66) in Condition 1.

For G_3 , note that by triangle inequality

$$\begin{aligned} &\|[\mathbf{X}_{i:} \mathbf{V}^{(t)}]^s - [\mathbf{W}_{:b}^T \mathbf{X} \mathbf{V}^{(t)}]^s\|^2 \\ &\leq \|\mathbf{S}_{z(i):}^s - \mathbf{S}_{b:}^s\|^2 + 2 \max_{a \in [r]} \|[\mathbf{W}_{:a}^T \mathbf{X} \mathbf{V}^{(t)}]^s - [\mathbf{W}_{:a}^T \mathbf{X} \mathbf{V}^{(t)}]^s\|^2 \\ &\leq \|\mathbf{S}_{z(i):}^s - \mathbf{S}_{b:}^s\|^2 + C \frac{r^2 (L^{(t)})^2}{\Delta_{\min}^2}, \end{aligned} \quad (96)$$

where the last inequality follows from the inequality (128) in the proof of Lemma 12 and C is a positive constant. Then we have

$$\begin{aligned} |G_3|^2 &\leq 2 \|[\mathbf{X}_{i:} \mathbf{V}^{(t)}]^s - [\mathbf{W}_{:b}^T \mathbf{Y} \mathbf{V}^{(t)}]^s\|^2 \\ &\quad \cdot \max_{a \in [r]} \|[\mathbf{W}_{:a}^T \mathbf{Y} \mathbf{V}^{(t)}]^s - [\mathbf{W}_{:a}^{(t),T} \mathbf{Y} \mathbf{V}^{(t)}]^s\|^2 \\ &\leq 2 \left(\|[\mathbf{X}_{i:} \mathbf{V}^{(t)}]^s - [\mathbf{W}_{:b}^T \mathbf{X} \mathbf{V}^{(t)}]^s\|^2 \right. \\ &\quad \left. + \|[\mathbf{W}_{:b}^T \mathbf{Y} \mathbf{V}^{(t)}]^s - [\mathbf{W}_{:b}^T \mathbf{X} \mathbf{V}^{(t)}]^s\|^2 \right) \\ &\quad \cdot \max_{a \in [r]} \|[\mathbf{W}_{:a}^T \mathbf{Y} \mathbf{V}^{(t)}]^s - [\mathbf{W}_{:a}^{(t),T} \mathbf{Y} \mathbf{V}^{(t)}]^s\|^2 \\ &\leq C^2 \left(\|\mathbf{S}_{z(i):}^s - \mathbf{S}_{b:}^s\|^2 + C \frac{r^2 (L^{(t)})^2}{\Delta_{\min}^2} \right) \\ &\quad \cdot \left(\frac{r^2 (L^{(t)})^2}{\Delta_{\min}^2} + \frac{r r^{2K} + p r^{K+2}}{p^K} \frac{L^{(t)}}{\Delta_{\min}^2} \right) + \frac{C'}{\tilde{C}^2} \Delta_{\min}^2 L^{(t)} \\ &\leq \frac{C^2 \bar{C}^2}{\tilde{C}} \|\mathbf{S}_{z(i):}^s - \mathbf{S}_{b:}^s\|^2 (\Delta_{\min}^2 + L^{(t)}) \\ &\quad + \frac{C^3 C' \bar{C}^2}{\tilde{C}^2} \left(\Delta_{\min}^4 + \Delta_{\min}^2 L^{(t)} \right), \end{aligned} \quad (97)$$

where the third inequality follows from the same procedure to derive (94) and (95), and the last inequality follows from the assumption $\Delta_{\min}^2 \geq \tilde{C} p^{-K/2} \log p$ and inequality (66) in Condition 1.

Choose the \tilde{C} such that

$$3 \left(C^4 \frac{\bar{C}}{\tilde{C}^3} + \frac{C'}{\tilde{C}^2} + \frac{C^2 \bar{C}^2}{\tilde{C}} + \frac{C^3 C' \bar{C}^2}{\tilde{C}^2} \right) \leq \frac{1}{512}. \quad (98)$$

Then, we finish the proof of inequality (88) by plugging the inequalities (94), (95), and (97) into the upper bound (93).

3) Upper bound for $H_{ib}^{(t)}$, i.e., the inequality (89). By definition of H_{ib} , we rearrange terms and obtain

$$\begin{aligned} H_{ib} &= \|[\mathbf{X}_{i:}\mathbf{V}^{(t)}]^s - [\mathbf{W}_{:z(i)}^T \mathbf{Y} \mathbf{V}^{(t)}]^s\|^2 \\ &\quad - \|[\mathbf{X}_{i:}\mathbf{V}^{(t)}]^s - [\mathbf{W}_{:b}^T \mathbf{Y} \mathbf{V}^{(t)}]^s\|^2 + \|[\mathbf{S}_{z(i):}]^s - [\mathbf{S}_{b:}]^s\|^2 \\ &= \|[\mathbf{X}_{i:}\mathbf{V}^{(t)}]^s - [\mathbf{W}_{:z(i)}^T \mathbf{Y} \mathbf{V}^{(t)}]^s\|^2 \\ &\quad + \left(\|[\mathbf{S}_{z(i):}]^s - [\mathbf{S}_{b:}]^s\|^2 - \|[\mathbf{X}_{i:}\mathbf{V}^{(t)}]^s - [\mathbf{W}_{:b}^T \mathbf{Y} \mathbf{V}^{(t)}]^s\|^2 \right) \\ &\quad - \left(\|[\mathbf{X}_{i:}\mathbf{V}^{(t)}]^s - [\mathbf{W}_{:b}^T \mathbf{Y} \mathbf{V}^{(t)}]^s\| \right. \\ &\quad \quad \left. - \|[\mathbf{X}_{i:}\mathbf{V}^{(t)}]^s - [\mathbf{W}_{:b}^T \mathbf{X} \mathbf{V}^{(t)}]^s\| \right) \\ &= H_1 + H_2 + H_3, \end{aligned}$$

where

$$\begin{aligned} H_1 &= \|[\mathbf{X}_{i:}\mathbf{V}^{(t)}]^s - [\mathbf{W}_{:z(i)}^T \mathbf{Y} \mathbf{V}^{(t)}]^s\|^2 \\ &\quad - \|[\mathbf{W}_{:b}^T \mathbf{X} \mathbf{V}^{(t)}]^s - [\mathbf{W}_{:b}^T \mathbf{Y} \mathbf{V}^{(t)}]^s\|^2, \\ H_2 &= \|[\mathbf{S}_{z(i):}]^s - [\mathbf{S}_{b:}]^s\|^2 - \|[\mathbf{X}_{i:}\mathbf{V}^{(t)}]^s - [\mathbf{W}_{:b}^T \mathbf{X} \mathbf{V}^{(t)}]^s\|^2, \\ H_3 &= 2 \left\langle [\mathbf{X}_{i:}\mathbf{V}^{(t)}]^s - [\mathbf{W}_{:b}^T \mathbf{X} \mathbf{V}^{(t)}]^s, \right. \\ &\quad \quad \left. [\mathbf{W}_{:b}^T \mathbf{Y} \mathbf{V}^{(t)}]^s - [\mathbf{W}_{:b}^T \mathbf{X} \mathbf{V}^{(t)}]^s \right\rangle. \end{aligned}$$

For H_1 , we have

$$\begin{aligned} |H_1| &\leq \frac{4 \max_{a \in [r]} \|\mathbf{W}_{:a}^T \mathbf{E} \mathbf{V}^{(t)}\|^2}{\|\mathbf{W}_{:z(i)}^T \mathbf{X} \mathbf{V}^{(t)}\|^2} \\ &\leq \frac{r^{2K-1} + K p r^{K+1}}{p^K} \\ &\leq \tilde{C}^{-2} \|[\mathbf{S}_{z(i):}]^s - [\mathbf{S}_{b:}]^s\|^2, \end{aligned} \quad (99)$$

following the derivation of G_2 in inequality (95) and the assumption that $\Delta_{\min}^2 \geq \tilde{C} p^{-K/2} \log p$.

For H_2 , by the inequality (96), we have

$$\begin{aligned} |H_2| &\lesssim 2 \max_{a \in [r]} \|[\mathbf{W}_{:a}^T \mathbf{X} \mathbf{V}^{(t)}]^s - [\mathbf{W}_{:a}^T \mathbf{X} \mathbf{V}^{(t)}]^s\|^2 \\ &\lesssim \frac{r^2 (L^{(t)})^2}{\Delta_{\min}^2} \\ &\leq C \frac{\bar{C}^2}{\tilde{C}^2} \|[\mathbf{S}_{z(i):}]^s - [\mathbf{S}_{a:}]^s\|^2, \end{aligned} \quad (100)$$

where the last inequality follows from the condition (66) in Condition 1.

For H_3 , by Cauchy-Schwartz inequality, we have

$$\begin{aligned} |H_3| &\lesssim \|[\mathbf{X}_{i:}\mathbf{V}^{(t)}]^s - [\mathbf{W}_{:b}^T \mathbf{X} \mathbf{V}^{(t)}]^s\| |H_1|^{1/2} \\ &\leq 2 \tilde{C}^{-1} \|[\mathbf{S}_{z(i):}]^s - [\mathbf{S}_{a:}]^s\|^2, \end{aligned} \quad (101)$$

following the inequalities (96) and (99).

Choose \tilde{C} such that

$$\tilde{C}^{-2} + C \frac{\bar{C}^2}{\tilde{C}^2} + \tilde{C}^{-1} \leq \frac{1}{4}. \quad (102)$$

Therefore, we finish the proof of inequality (89) combining inequalities (99), (100), and (101).

5) Next, we Show the Upper Bounds for \hat{F}_{ib} , \hat{G}_{ib} and \hat{H}_{ib} :
By Lemma 1, we have

$$\|\mathbf{S}_{a:}^s - \mathbf{S}_{b:}^s\| = (1 + o(1)) \|\mathbf{A}_{a:}^s - \mathbf{A}_{b:}^s\|. \quad (2516)$$

Also, notice that the matrix product of \mathbf{B}^T corresponds to the padding operation in Lemma 5, and the padding weights are balanced such that $\|\mathbf{v} \mathbf{B}\| = (1 + o(1)) \max_a \|\theta_{z^{-1}(a)}\|^{(K-1)/2} \|\mathbf{v}\|$ for all $\mathbf{v} \in \mathbb{R}^{r(K-1)}$. For two vectors $\mathbf{v}_1, \mathbf{v}_2 \in \mathbb{R}^{r^{K-1}}$, we have

$$\|\mathbf{v}_1^s - \mathbf{v}_2^s\| = (1 + o(1)) \|[\mathbf{v}_1 \mathbf{B}^T]^s - [\mathbf{v}_2 \mathbf{B}^T]^s\|. \quad (103) \quad (2522)$$

The equation (103) also holds for $\hat{\mathbf{B}}^T$.

Note that for all $i \in [p]$ we have

$$\begin{aligned} \|\mathbf{A}_{i:} \hat{\mathbf{Q}}\| &= \|\mathbf{S}_{z(i):} \mathbf{B}^T \hat{\mathbf{Q}}\| \\ &= \|\mathbf{S}_{z(i):} \hat{\mathbf{D}}^{\otimes(K-1)}\| \\ &= (1 + o(1)) \|\mathbf{S}_{z(i):}\| \\ &= (1 + o(1)) \max_a \|\theta_{z^{-1}(a)}\|^{-(K-1)/2} \|\mathbf{A}_{i:}\|, \end{aligned} \quad (104) \quad (2525-2528)$$

where the third inequality follows from the singular property of MLE confusion matrix (135) and the last inequality follows from the fact that $\mathbf{A}_{i:} = \mathbf{S}_{z(i):} \mathbf{B}^T$ and Lemma 10. Above equation indicates that $\mathbf{A}_{i:}$ is the span space of the singular values as $p \rightarrow \infty$. Also, notice that the row space of $\mathbf{P}_{:a}^T \mathbf{Y} \hat{\mathbf{Q}} \hat{\mathbf{B}}^T$ is equal to the column space of $\hat{\mathbf{Q}}$, and $\mathbf{A}_{i:} \neq \mathbf{P}_{:a}^T \mathbf{Y} \hat{\mathbf{Q}} \hat{\mathbf{B}}^T$ in noisy case.

Hence, for all $a \in [r]$, we have

$$\begin{aligned} &\|[\mathbf{X}_i \hat{\mathbf{Q}}]^s - [\mathbf{P}_{:a}^T \mathbf{Y} \hat{\mathbf{Q}}]^s\| \\ &= \left\| \frac{\mathbf{A}_{z(i):} \hat{\mathbf{Q}}}{\|\mathbf{A}_{z(i):} \hat{\mathbf{Q}}\|} - \frac{\mathbf{P}_{:a}^T \mathbf{Y} \hat{\mathbf{Q}}}{\|\mathbf{P}_{:a}^T \mathbf{Y} \hat{\mathbf{Q}}\|} \right\| \\ &= (1 + o(1)) \left\| \frac{\mathbf{A}_{z(i):}}{\|\mathbf{A}_{z(i):}\|} - \frac{\mathbf{P}_{:a}^T \mathbf{Y} \hat{\mathbf{Q}} \hat{\mathbf{B}}^T}{\|\mathbf{P}_{:a}^T \mathbf{Y} \hat{\mathbf{Q}} \hat{\mathbf{B}}^T\|} \right\| \\ &= (1 + o(1)) \|[\mathbf{X}_i]^s - [\mathbf{P}_{:a}^T \mathbf{Y} \hat{\mathbf{Q}} \hat{\mathbf{B}}^T]^s\| \end{aligned} \quad (105) \quad (2537-2540)$$

where the second equation follows from (104), $\|\mathbf{P}_{:a}^T \mathbf{Y} \hat{\mathbf{Q}} \hat{\mathbf{B}}^T\| = (1 + o(1)) \max_a \|\theta_{z^{-1}(a)}\|^{(K-1)/2} \|\mathbf{P}_{:a}^T \mathbf{Y} \hat{\mathbf{Q}}\|$, and singular property of $\hat{\mathbf{B}}^T$. Similar result holds after replacing $\mathbf{P}_{:a}^T \mathbf{Y} \hat{\mathbf{Q}}$ by $\mathbf{P}_{:a}^T \mathbf{Y} \mathbf{Q}$ or $\mathbf{P}_{:a}^T \mathbf{Y} \hat{\mathbf{Q}}$.

We are now ready to show the upper bounds for \hat{F}_{ib} , \hat{G}_{ib} and \hat{H}_{ib} .

For \hat{F}_{ib} , we have

$$\begin{aligned} (\hat{F}_{ib})^2 &\leq \|\mathbf{E}_{i:}\|^2 \|[\bar{\mathbf{A}}_{a:}]^s - [\hat{\mathbf{A}}_{a:}]^s\|^2 \\ &\leq \|\mathbf{E}_{i:}\|^2 \left[\|[\bar{\mathbf{S}}_{a:} \mathbf{B}^T]^s - [\bar{\mathbf{S}}_{a:} \hat{\mathbf{B}}^T]^s\| \right. \\ &\quad \quad \left. + \|[\bar{\mathbf{S}}_{a:} \hat{\mathbf{B}}^T]^s - [\hat{\mathbf{S}}_{a:} \hat{\mathbf{B}}^T]^s\| \right]^2 \\ &\lesssim \|\mathbf{E}_{i:}\|^2 \left[\|[\bar{\mathbf{S}}_{a:} \mathbf{B}^T \hat{\mathbf{Q}}]^s - [\bar{\mathbf{S}}_{a:}]^s\| + \|[\bar{\mathbf{S}}_{a:}]^s - [\hat{\mathbf{S}}_{a:}]^s\| \right]^2. \end{aligned} \quad (2549-2552)$$

Following similar derivations in inequalities (91), (92), and the upper bound for J_1 in the proof of Lemma 12, respectively,

we have

$$\|[\bar{S}_{a:}]^s - [\hat{S}_{a:}]^s\| \lesssim rL(\hat{z}), \quad \|[\bar{S}_{a:}]^s - [\bar{S}_{b:}]^s\| \lesssim \|S_{a:}^s - S_{b:}^s\|^2,$$

and

$$\|[\bar{S}_{a:}\mathbf{B}^T\hat{\mathbf{Q}}]^s - [\bar{S}_{a:}]^s\| \lesssim L(\hat{z}).$$

We then obtain the upper bound for \hat{F}_{ib} by noticing that $\|\mathbf{E}_i\|^2 \lesssim p^{K-1}$.

For \hat{G}_{ib} and \hat{H}_{ib} , by the property (105), we have

$$(1 + o(1))\hat{G}_{ib}$$

$$= \left(\|[\mathbf{X}_{i:}\hat{\mathbf{Q}}]^s - [\hat{S}_{a:}]^s\|_F^2 - \|[\mathbf{X}_{i:}\hat{\mathbf{Q}}]^s - [\mathbf{P}_{:a}^T\mathbf{Y}\hat{\mathbf{Q}}]^s\|_F^2 \right) \\ - \left(\|[\mathbf{X}_{i:}\hat{\mathbf{Q}}]^s - [\hat{S}_{b:}]^s\|_F^2 - \|[\mathbf{X}_{i:}\hat{\mathbf{Q}}]^s - [\mathbf{P}_{:b}^T\mathbf{Y}\hat{\mathbf{Q}}]^s\|_F^2 \right),$$

$$(1 + o(1))\hat{H}_{ib}$$

$$= \|[\mathbf{X}_{i:}\hat{\mathbf{Q}}]^s - [\mathbf{P}_{:a}^T\mathbf{Y}\hat{\mathbf{Q}}]^s\|_F^2 - \|[\mathbf{X}_{i:}\hat{\mathbf{Q}}]^s - [\mathbf{P}_{:b}^T\mathbf{Y}\hat{\mathbf{Q}}]^s\|_F^2 \\ + \|A_{a:}^s - A_{b:}^s\|_F^2.$$

We obtain the upper bounds following the proof for inequalities (88) and (89). \square

Lemma 12 (Relationship Between Misclustering Loss and Intermediate Parameters): Under the Condition 1 and the setup of Theorem 5 with fixed $r \geq 2$, as $p \rightarrow \infty$, we have

$$\|\mathbf{V} - \mathbf{V}^{(t)}\|_\sigma \lesssim \sqrt{\frac{r^{K-1}}{p^{K-1}} \frac{r}{\Delta_{\min}^2} L^{(t)}}, \quad (106)$$

$$\|\mathbf{E}(\mathbf{V} - \mathbf{V}^{(t)})\|_\sigma \lesssim \sqrt{\frac{r^{K-1}(pr^{K-1} + pr)}{p^{K-1}} \frac{r}{\Delta_{\min}^2} L^{(t)}}, \quad (107)$$

$$\max_{b \in [r]} \|[\mathbf{W}_{:b}^T\mathbf{Y}\mathbf{V}]^s - [\mathbf{W}_{:b}^{(t),T}\mathbf{Y}\mathbf{V}]^s\| \\ \leq C \left(\frac{rL^{(t)}}{\Delta_{\min}} + \sqrt{\frac{r^{2K} + pr^{K+1}}{p^K} \frac{\sqrt{L^{(t)}}}{\Delta_{\min}}} \right), \quad (108)$$

$$\max_{b \in [r]} \|[\mathbf{W}_{:b}^{(t),T}\mathbf{Y}\mathbf{V}]^s - [\mathbf{W}_{:b}^{(t),T}\mathbf{Y}\mathbf{V}^{(t)}]^s\| \\ \leq C \left(\sqrt{\frac{rr^{2K} + pr^{K+2}}{p^K} \frac{\sqrt{L^{(t)}}}{\Delta_{\min}}} + \frac{rL^{(t)}}{\Delta_{\min}} \right), \quad (109)$$

$$\max_{b \in [r]} \|[\mathbf{W}_{:b}^T\mathbf{Y}\mathbf{V}^{(t)}]^s - [\mathbf{W}_{:b}^{(t),T}\mathbf{Y}\mathbf{V}^{(t)}]^s\| \\ \leq C \left(\frac{rL^{(t)}}{\Delta_{\min}} + \sqrt{\frac{rr^{2K} + pr^{K+2}}{p^K} \frac{\sqrt{L^{(t)}}}{\Delta_{\min}}} \right), \quad (110)$$

for some positive universal constant C . In addition, the inequality (109) also holds by replacing $\mathbf{W}_{:b}^{(t)}$ to $\mathbf{W}_{:b}$. Further, the above inequalities holds after replacing \mathbf{W} to \mathbf{P} , \mathbf{V} to \mathbf{Q} , and $L^{(t)}$ to $L(\hat{z})$.

Proof of Lemma 12: We follow and use several intermediate conclusions in [13, Proof of Lemma 5]. We prove each inequality separately.

1) Inequality (106). By [13, Proof of Lemma 5], we have

$$\|\mathbf{V} - \mathbf{V}^{(t)}\|_\sigma \lesssim \sqrt{\frac{r^{K-1}}{p^{K-1}} r \ell^{(t)}}.$$

Then, we complete the proof of inequality (106) by applying Lemma 2 to the above inequality.

2) Inequality (107). By [13, Proof of Lemma 5], we have

$$\|\mathbf{E}(\mathbf{V} - \mathbf{V}^{(t)})\|_\sigma \lesssim \sqrt{\frac{r^{K-1}(pr^{K-1} + pr)}{p^{K-1}} r \ell^{(t)}}. \quad (107)$$

Also, we complete the proof of inequality (106) by applying Lemma 2 to the above inequality.

3) Inequality (108). We upper bound the desired quantity by triangle inequality,

$$\|[\mathbf{W}_{:b}^T\mathbf{Y}\mathbf{V}]^s - [\mathbf{W}_{:b}^{(t),T}\mathbf{Y}\mathbf{V}]^s\| \leq I_1 + I_2 + I_3, \quad (108)$$

where

$$I_1 = \left\| \frac{\mathbf{W}_{:b}^T\mathbf{Y}\mathbf{V}}{\|\mathbf{W}_{:b}^T\mathbf{X}\mathbf{V}\|} - \frac{\mathbf{W}_{:b}^{(t),T}\mathbf{Y}\mathbf{V}}{\|\mathbf{W}_{:b}^{(t),T}\mathbf{X}\mathbf{V}\|} \right\|, \quad (109)$$

$$I_2 = \left\| \left(\frac{1}{\|\mathbf{W}_{:b}^T\mathbf{Y}\mathbf{V}\|} - \frac{1}{\|\mathbf{W}_{:b}^{(t),T}\mathbf{X}\mathbf{V}\|} \right) \mathbf{W}_{:b}^T\mathbf{Y}\mathbf{V} \right\|, \quad (110)$$

$$I_3 = \left\| \left(\frac{1}{\|\mathbf{W}_{:b}^{(t),T}\mathbf{Y}\mathbf{V}\|} - \frac{1}{\|\mathbf{W}_{:b}^{(t),T}\mathbf{X}\mathbf{V}\|} \right) \mathbf{W}_{:b}^{(t),T}\mathbf{Y}\mathbf{V} \right\|. \quad (111)$$

Next, we upper bound the quantities I_1, I_2, I_3 separately.

For I_1 , we further bound I_1 by triangle inequality,

$$I_1 \leq I_{11} + I_{12}, \quad (112)$$

where

$$I_{11} = \left\| \frac{\mathbf{W}_{:b}^T\mathbf{X}\mathbf{V}}{\|\mathbf{W}_{:b}^T\mathbf{X}\mathbf{V}\|} - \frac{\mathbf{W}_{:b}^{(t),T}\mathbf{X}\mathbf{V}}{\|\mathbf{W}_{:b}^{(t),T}\mathbf{X}\mathbf{V}\|} \right\|, \quad (113)$$

and

$$I_{12} = \left\| \frac{\mathbf{W}_{:b}^T\mathbf{E}\mathbf{V}}{\|\mathbf{W}_{:b}^T\mathbf{X}\mathbf{V}\|} - \frac{\mathbf{W}_{:b}^{(t),T}\mathbf{E}\mathbf{V}}{\|\mathbf{W}_{:b}^{(t),T}\mathbf{X}\mathbf{V}\|} \right\|. \quad (114)$$

We first consider I_{11} . Define the confusion matrix $\mathbf{D} = \mathbf{M}^T \Theta^T \mathbf{W}^{(t)} = [D_{ab}] \in \mathbb{R}^{r \times r}$ where

$$D_{ab} = \frac{\sum_{i \in [p]} \theta(i) \mathbb{1}\{z(i) = a, z^{(t)}(i) = b\}}{\sum_{i \in [p]} \mathbb{1}\{z^{(t)}(i) = b\}}, \text{ for all } a, b \in [r]. \quad (115)$$

By Lemma 10, we have $\sum_{i \in [p]} \mathbb{1}\{z^{(t)}(i) = b\} \gtrsim p/r$. Then, we have

$$\sum_{a \neq b, a, b \in [r]} D_{ab} \lesssim \frac{r}{p} \sum_{i: z^{(t)}(i) \neq z(i)} \theta(i) \lesssim \frac{L^{(t)}}{\Delta_{\min}^2} \lesssim \frac{1}{\log p}, \quad (116)$$

and for all $b \in [r]$,

$$D_{bb} = \frac{\sum_{i \in [p]} \theta(i) \mathbb{1}\{z(i) = z^{(t)}(i) = b\}}{\sum_{i \in [p]} \mathbb{1}\{z^{(t)}(i) = b\}} \quad (117)$$

$$\geq \frac{c(\sum_{i \in [p]} \mathbb{1}\{z^{(t)}(i) = b\} - p\ell^{(t)})}{\sum_{i \in [p]} \mathbb{1}\{z^{(t)}(i) = b\}} \quad (118)$$

$$\gtrsim 1 - \frac{1}{\log p}, \quad (119)$$

under the inequality (66) in Condition 1. By the definition of $\mathbf{W}, \mathbf{W}^{(t)}, \mathbf{V}$, we have

$$\frac{\mathbf{W}_{:b}^T \mathbf{X} \mathbf{V}}{\|\mathbf{W}_{:b}^T \mathbf{X} \mathbf{V}\|} = [\mathbf{S}_{b:}]^s,$$

and

$$\frac{\mathbf{W}_{:b}^{(t),T} \mathbf{X} \mathbf{V}}{\|\mathbf{W}_{:b}^{(t),T} \mathbf{X} \mathbf{V}\|} = [D_{bb} \mathbf{S}_{b:} + \sum_{a \neq b, a \in [r]} D_{ab} \mathbf{S}_{a:}]^s.$$

Let α denote the angle between $\mathbf{S}_{b:}$ and $D_{bb} \mathbf{S}_{b:} + \sum_{a \neq b, a \in [r]} D_{ab} \mathbf{S}_{a:}$. To roughly estimate the range of α , we consider the inner product

$$\begin{aligned} & \left\langle \mathbf{S}_{b:}, D_{bb} \mathbf{S}_{b:} + \sum_{a \neq b, a \in [r]} D_{ab} \mathbf{S}_{a:} \right\rangle \\ &= D_{bb} \|\mathbf{S}_{b:}\|^2 + \sum_{a \neq b} D_{ab} \langle \mathbf{S}_{b:}, \mathbf{S}_{a:} \rangle \\ &\geq D_{bb} \|\mathbf{S}_{b:}\|^2 - \sum_{a \neq b, a \in [r]} D_{ab} \|\mathbf{S}_{b:}\| \max_{a \in [r]} \|\mathbf{S}_{a:}\| \\ &\geq C, \end{aligned}$$

where C is a positive constant, and the last inequality holds when p is large enough following the constraint of $\|\mathbf{S}_{b:}\|$ in parameter space (2) and the bounds of \mathbf{D} in (111) and (112).

The positive inner product between $\mathbf{S}_{b:}$ and $D_{bb} \mathbf{S}_{b:} + \sum_{a \neq b, a \in [r]} D_{ab} \mathbf{S}_{a:}$ indicates $\alpha \in [0, \pi/2]$, and thus $2 \sin \frac{\alpha}{2} \leq \sqrt{2} \sin \alpha$. Then, by the geometry property of trigonometric function, we have

$$\begin{aligned} & \| [D_{bb} \mathbf{S}_{b:} + \sum_{a \neq b, a \in [r]} D_{ab} \mathbf{S}_{a:}] \sin \alpha \| \\ &= \| (\mathbf{I}_d - \text{Proj}(\mathbf{S}_{b:})) \sum_{a \neq b, a \in [r]} D_{ab} \mathbf{S}_{a:} \| \\ &\leq \sum_{a \neq b, a \in [r]} D_{ab} \| (\mathbf{I}_d - \text{Proj}(\mathbf{S}_{b:})) \mathbf{S}_{a:} \| \\ &= \sum_{a \neq b, a \in [r]} D_{ab} \| \mathbf{S}_{a:} \sin(\mathbf{S}_{b:}, \mathbf{S}_{a:}) \| \\ &\leq \sum_{a \neq b, a \in [r]} D_{ab} \|\mathbf{S}_{a:}\| \|\mathbf{S}_{b:}^s - \mathbf{S}_{a:}^s\|, \end{aligned} \quad (113)$$

where the first inequality follows from the triangle inequality, and the last inequality follows from Lemma 4. Note that with bounds (111) and (112), when p is large enough, we have

$$\begin{aligned} \|\mathbf{W}_{:b}^{(t),T} \mathbf{X} \mathbf{V}\| &= \|D_{bb} \mathbf{S}_{b:} + \sum_{a \neq b, a \in [r]} D_{ab} \mathbf{S}_{a:}\| \\ &\geq D_{bb} \|\mathbf{S}_{b:}\| - \sum_{a \neq b, a \in [r]} D_{ab} \|\mathbf{S}_{a:}\| \\ &\geq C_1, \end{aligned} \quad (114)$$

for some positive constant C_1 . Notice that $I_{11} = \sqrt{1 - \cos \alpha} = 2 \sin \frac{\alpha}{2}$. Therefore, we obtain

$$\begin{aligned} I_{11} &\leq \sqrt{2} \sin \alpha \\ &= \frac{\| [D_{bb} \mathbf{S}_{b:} + \sum_{a \neq b, a \in [r]} D_{ab} \mathbf{S}_{a:}] \sin \alpha \|}{\| D_{bb} \mathbf{S}_{b:} + \sum_{a \neq b, a \in [r]} D_{ab} \mathbf{S}_{a:} \|} \\ &\leq \frac{1}{C_1} \sum_{a \neq b, a \in [r]} D_{ab} \|\mathbf{S}_{a:}\| \|\mathbf{S}_{b:}^s - \mathbf{S}_{a:}^s\| \\ &\lesssim \frac{r}{p} \sum_{i \in [p]} \theta(i) \sum_{b \in [r]} \mathbb{1} \{ z^{(t)}(i) = b \} \|\mathbf{S}_{b:}^s - \mathbf{S}_{a:}^s\| \\ &\leq \frac{r L^{(t)}}{\Delta_{\min}}, \end{aligned} \quad (115)$$

where the second inequality follows from (113) and (114), and the last two inequalities follow by the definition of D_a and $L^{(t)}$, and the constraint of $\|\mathbf{S}_{b:}\|$ in parameter space (2).

We now consider I_{12} . By triangle inequality, we have

$$\begin{aligned} I_{12} &\leq \frac{1}{\|\mathbf{W}_{:b}^T \mathbf{X} \mathbf{V}\|} \| (\mathbf{W}_{:b}^T - \mathbf{W}_{:b}^{(t),T}) \mathbf{E} \mathbf{V} \| \\ &\quad + \frac{\| (\mathbf{W}_{:b}^T - \mathbf{W}_{:b}^{(t),T}) \mathbf{X} \mathbf{V} \|}{\|\mathbf{W}_{:b}^T \mathbf{X} \mathbf{V}\| \|\mathbf{W}_{:b}^{(t),T} \mathbf{X} \mathbf{V}\|} \|\mathbf{W}_{:b}^{(t),T} \mathbf{E} \mathbf{V}\|. \end{aligned} \quad (116)$$

By [13, Proof of Lemma 5], we have

$$\begin{aligned} \| (\mathbf{W}_{:b}^T - \mathbf{W}_{:b}^{(t),T}) \mathbf{E} \mathbf{V} \| &\lesssim \sqrt{\frac{r^{2K} + pr^{K+1}}{p^K} \frac{\sqrt{L^{(t)}}}{\Delta_{\min}}}. \quad (116) \\ \text{Notice that} \quad & \\ \| (\mathbf{W}_{:b}^T - \mathbf{W}_{:b}^{(t),T}) \mathbf{X} \mathbf{V} \| &\leq \|\mathbf{W}_{:b}^T - \mathbf{W}_{:b}^{(t),T}\| \|\mathbf{X} \mathbf{V}\|_F \quad (117) \\ &\lesssim \frac{r^{3/2} L^{(t)}}{\sqrt{p} \Delta_{\min}^2} \|S\| \|\Theta M\|_\sigma \\ &\lesssim \frac{\sqrt{r L^{(t)}}}{\Delta_{\min}}, \end{aligned}$$

where the second inequality follows from [13, Inequality (121), Proof of Lemma 5] and the last inequality follows from Lemma 6 and (66) in Condition 1. Note that $\|\mathbf{W}_{:b}^T \mathbf{X} \mathbf{V}\| = \|\mathbf{S}_{b:}\| \geq c_3$ and $\|\mathbf{W}_{:b}^{(t),T} \mathbf{X} \mathbf{V}\| \geq C_1$ by inequality (114). Therefore, we have

$$\begin{aligned} I_{12} &\lesssim \| (\mathbf{W}_{:b}^T - \mathbf{W}_{:b}^{(t),T}) \mathbf{E} \mathbf{V} \| \\ &\quad + \| (\mathbf{W}_{:b}^T - \mathbf{W}_{:b}^{(t),T}) \mathbf{X} \mathbf{V} \| \|\mathbf{W}_{:b}^{(t),T} \mathbf{E} \mathbf{V}\| \\ &\lesssim \sqrt{\frac{r^{2K} + pr^{K+1}}{p^K} \frac{\sqrt{L^{(t)}}}{\Delta_{\min}}} + \frac{\sqrt{r L^{(t)}}}{\Delta_{\min}} \sqrt{\frac{r^{2K}}{p^K}} \\ &\lesssim \sqrt{\frac{r^{2K} + pr^{K+1}}{p^K} \frac{\sqrt{L^{(t)}}}{\Delta_{\min}}}, \end{aligned} \quad (118)$$

where second inequality follows from the inequalities (116), (117), and (62) in Condition 1.

Hence, combining inequalities (115) and (118) yields

$$I_1 \lesssim \frac{r L^{(t)}}{\Delta_{\min}} + \sqrt{\frac{r^{2K} + pr^{K+1}}{p^K} \frac{\sqrt{L^{(t)}}}{\Delta_{\min}}}. \quad (119)$$

For I_2 and I_3 , recall that $\|\mathbf{W}_{:b}^T \mathbf{X} \mathbf{V}\| = \|\mathbf{S}_{b:}\| \geq c_3$ and $\|\mathbf{W}_{:b}^{(t),T} \mathbf{X} \mathbf{V}\| \geq C_1$ by inequality (114). By triangle inequality and (62) in Condition 1, we have

$$I_2 \leq \frac{\|\mathbf{W}_{:b}^T \mathbf{E} \mathbf{V}\|}{\|\mathbf{W}_{:b}^T \mathbf{X} \mathbf{V}\|} \lesssim \|\mathbf{W}_{:b}^T \mathbf{E} \mathbf{V}\| \lesssim \frac{r^K}{p^{K/2}}, \quad (120)$$

and

$$I_3 \leq \frac{\|\mathbf{W}_{:b}^{(t),T} \mathbf{E} \mathbf{V}\|}{\|\mathbf{W}_{:b}^{(t),T} \mathbf{X} \mathbf{V}\|} \lesssim \|\mathbf{W}_{:b}^{(t),T} \mathbf{E} \mathbf{V}\| \lesssim \frac{r^K}{p^{K/2}}. \quad (121)$$

Therefore, combining the inequalities (119), (120), and (121), we finish the proof of inequality (108).

4) Inequality (109). Here we only show the proof of inequality (109) with $\mathbf{W}_{:b}^{(t)}$. The proof also holds by replacing $\mathbf{W}_{:b}^{(t)}$ to $\mathbf{W}_{:b}$, and we omit the repeated procedures.

We upper bound the desired quantity by triangle inequality

$$\|[\mathbf{W}_{:b}^{(t),T} \mathbf{Y} \mathbf{V}]^s - [\mathbf{W}_{:b}^{(t),T} \mathbf{Y} \mathbf{V}^{(t)}]^s\| \leq J_1 + J_2 + J_3,$$

where

$$J_1 = \left\| \frac{\mathbf{W}_{:b}^{(t),T} \mathbf{Y} \mathbf{V}}{\|\mathbf{W}_{:b}^{(t),T} \mathbf{X} \mathbf{V}\|} - \frac{\mathbf{W}_{:b}^{(t),T} \mathbf{Y} \mathbf{V}^{(t)}}{\|\mathbf{W}_{:b}^{(t),T} \mathbf{X} \mathbf{V}^{(t)}\|} \right\|,$$

$$J_2 = \left\| \left(\frac{1}{\|\mathbf{W}_{:b}^{(t),T} \mathbf{Y} \mathbf{V}\|} - \frac{1}{\|\mathbf{W}_{:b}^{(t),T} \mathbf{X} \mathbf{V}\|} \right) \mathbf{W}_{:b}^{(t),T} \mathbf{Y} \mathbf{V} \right\|,$$

$$J_3 = \left\| \left(\frac{1}{\|\mathbf{W}_{:b}^{(t),T} \mathbf{Y} \mathbf{V}^{(t)}\|} - \frac{1}{\|\mathbf{W}_{:b}^{(t),T} \mathbf{X} \mathbf{V}^{(t)}\|} \right) \mathbf{W}_{:b}^{(t),T} \mathbf{Y} \mathbf{V}^{(t)} \right\|.$$

Next, we upper bound the quantities J_1, J_2, J_3 separately.

For J_1 , by triangle inequality, we have

$$J_1 \leq J_{11} + J_{12},$$

where

$$J_{11} = \left\| \frac{\mathbf{W}_{:b}^{(t),T} \mathbf{X} \mathbf{V}}{\|\mathbf{W}_{:b}^{(t),T} \mathbf{X} \mathbf{V}\|} - \frac{\mathbf{W}_{:b}^{(t),T} \mathbf{X} \mathbf{V}^{(t)}}{\|\mathbf{W}_{:b}^{(t),T} \mathbf{X} \mathbf{V}^{(t)}\|} \right\|$$

and

$$J_{12} = \left\| \frac{\mathbf{W}_{:b}^{(t),T} \mathbf{E} \mathbf{V}}{\|\mathbf{W}_{:b}^{(t),T} \mathbf{X} \mathbf{V}\|} - \frac{\mathbf{W}_{:b}^{(t),T} \mathbf{E} \mathbf{V}^{(t)}}{\|\mathbf{W}_{:b}^{(t),T} \mathbf{X} \mathbf{V}^{(t)}\|} \right\|.$$

We first consider J_{11} . Define the matrix $\mathbf{V}^k := \mathbf{W}^{\otimes(k-1)} \otimes \mathbf{W}^{(t), \otimes(K-k)}$ for $k = 2, \dots, K-1$, and denote $\mathbf{V}^1 = \mathbf{V}^{(t)}, \mathbf{V}^K = \mathbf{V}$. Also, define the quantity

$$J_{11}^k = \|[\mathbf{W}_{:b}^{(t),T} \mathbf{X} \mathbf{V}^k]^s - [\mathbf{W}_{:b}^{(t),T} \mathbf{X} \mathbf{V}^{k+1}]^s\|,$$

for $k = 1, \dots, K-1$. Let β_k denote the angle between $\mathbf{W}_{:b}^{(t),T} \mathbf{X} \mathbf{V}^k$ and $\mathbf{W}_{:b}^{(t),T} \mathbf{X} \mathbf{V}^{k+1}$. With the same idea to prove I_{11} in inequality (115), we bound J_{11}^k by the trigonometric function of β_k .

To roughly estimate the range of β_k , we consider the inner product between $\mathbf{W}_{:b}^{(t),T} \mathbf{X} \mathbf{V}^k$ and $\mathbf{W}_{:b}^{(t),T} \mathbf{X} \mathbf{V}^{k+1}$. Before the specific derivation of the inner product, note that

$$\mathbf{W}_{:b}^{(t),T} \mathbf{X} \mathbf{V}^k = \text{Mat}_1(\mathcal{T}_k), \quad \mathbf{W}_{:b}^{(t),T} \mathbf{X} \mathbf{V}^{k+1} = \text{Mat}_1(\mathcal{T}_{k+1}),$$

where

$$\mathcal{T}_k = \mathcal{X} \times_1 \mathbf{W}_{:b}^{(t),T} \times_2 \mathbf{W}^T \times_3 \cdots \times_k \mathbf{W}^T$$

$$\times_{k+1} \mathbf{W}^{(t),T} \times_{k+2} \cdots \times_K \mathbf{W}^{(t),T}$$

$$\mathcal{T}_{k+1} = \mathcal{X} \times_1 \mathbf{W}_{:b}^{(t),T} \times_2 \mathbf{W}^T \times_3 \cdots \times_k \mathbf{W}^T$$

$$\times_{k+1} \mathbf{W}^T \times_{k+2} \cdots \times_K \mathbf{W}^{(t),T}.$$

Recall the definition of confusion matrix $\mathbf{D} = \mathbf{M}^T \Theta^T \mathbf{W}^{(t)} = [\mathbf{D}_{ab}] \in \mathbb{R}^{r \times r}$. We have

$$\langle \mathbf{W}_{:b}^{(t),T} \mathbf{X} \mathbf{V}^k, \mathbf{W}_{:b}^{(t),T} \mathbf{X} \mathbf{V}^{k+1} \rangle$$

$$= \langle \text{Mat}_{k+1}(\mathcal{T}_k), \text{Mat}_{k+1}(\mathcal{T}_{k+1}) \rangle$$

$$= \langle \mathbf{D}^T \mathbf{S} \mathbf{Z}^k, \mathbf{S} \mathbf{Z}^k \rangle$$

$$= \sum_{b \in [r]} \left(D_{bb} \|\mathbf{S}_{b:} \mathbf{Z}^k\|^2 + \sum_{a \neq b, a \in [r]} D_{ab} \langle \mathbf{S}_{a:} \mathbf{Z}^k, \mathbf{S}_{b:} \mathbf{Z}^k \rangle \right)$$

$$\gtrsim (1 - \log p^{-1}) \min_{a \in [r]} \|\mathbf{S}_{a:} \mathbf{Z}^k\|^2 - \log p^{-1} \max_{a \in [r]} \|\mathbf{S}_{a:} \mathbf{Z}^k\|^2, \quad (122)$$

where $\mathbf{Z}^k = \mathbf{D}_{:b} \otimes \mathbf{I}_r^{\otimes(k-1)} \otimes \mathbf{D}^{\otimes(K-k-1)}$, the equations follow by the tensor algebra and definitions, and the last inequality follows from the bounds of \mathbf{D} in (111) and (112).

Note that

$$\|\mathbf{D}\|_\sigma \leq \|\mathbf{D}\|_F$$

$$\leq \sqrt{\sum_{b \in [r]} D_{bb}^2 + (\sum_{a \neq b, a \in [r]} D_{ab})^2}$$

$$\lesssim \sqrt{r + \log^2 p^{-1}} \lesssim 1, \quad (123)$$

where the second inequality follows from inequality (111), and the fact that for all $b \in [r]$,

$$D_{bb} \lesssim \frac{r}{p} \sum_{i: z(i)=b} \theta(i) \lesssim 1.$$

Also, we have

$$\lambda_r(\mathbf{D}) \geq \lambda_r(\mathbf{W}^{(t)}) \lambda_r(\Theta \mathbf{M}) \gtrsim 1, \quad (124)$$

following the Lemma 6 and Lemma 10. Then, for all $k \in [K]$, we have

$$1 \lesssim \|\mathbf{D}_{:b}\| \lambda_r(\mathbf{D})^{K-k-1} \leq \lambda_{r^{K-2}}(\mathbf{Z}^k)$$

$$\leq \|\mathbf{Z}^k\|_\sigma \leq \|\mathbf{D}_{:b}\| \|\mathbf{D}\|_\sigma^{K-k-1} \lesssim 1. \quad (125)$$

Thus, we have bounds

$$\max_{a \in [r]} \|\mathbf{S}_{a:} \mathbf{Z}^k\| \leq \max_{a \in [r]} \|\mathbf{S}_{a:}\| \|\mathbf{Z}^k\|_\sigma \lesssim 1,$$

$$\min_{a \in [r]} \|\mathbf{S}_{a:} \mathbf{Z}^k\| \geq \min_{a \in [r]} \|\mathbf{S}_{a:}\| \lambda_{r^{K-2}}(\mathbf{Z}^k) \gtrsim 1.$$

Hence, when p is large enough, the inner product (122) is positive, which implies $\beta_k \in [0, \pi/2]$ and thus $2 \sin \frac{\beta_k}{2} \leq \sqrt{2} \sin \beta_k$.

2755 Next, we upper bound the trigonometric function $\sin \beta_k$.
 2756 Note that

$$\begin{aligned} 2757 \sin \beta_k &= \sin(\mathbf{D}_{:b}^T \mathbf{S} \mathbf{I}_r^{\otimes k-1} \otimes \mathbf{D}^{\otimes K-k}, \mathbf{D}_{:b}^T \mathbf{S} \mathbf{I}_r^{\otimes k} \otimes \mathbf{D}^{\otimes K-k-1}) \\ 2758 &\leq \sin \beta_{k1} + \sin \beta_{k2}, \end{aligned}$$

2759 where

$$\begin{aligned} 2760 \sin \beta_{k1} &= \sin(\mathbf{D}_{:b}^T \mathbf{S} \mathbf{I}_r^{\otimes k-1} \otimes \mathbf{D}^{\otimes K-k}, \\ 2761 &\quad \mathbf{D}_{:b}^T \mathbf{S} \mathbf{I}_r^{\otimes k-1} \otimes \tilde{\mathbf{D}} \otimes \mathbf{D}^{\otimes K-k-1}), \\ 2762 \sin \beta_{k2} &= \sin(\mathbf{D}_{:b}^T \mathbf{S} \mathbf{I}_r^{\otimes k-1} \otimes \tilde{\mathbf{D}} \otimes \mathbf{D}^{\otimes K-k-1}, \\ 2763 &\quad \mathbf{D}_{:b}^T \mathbf{S} \mathbf{I}_r^{\otimes k} \otimes \mathbf{D}^{\otimes K-k-1}), \end{aligned}$$

2764 and $\tilde{\mathbf{D}}$ is the normalized confusion matrix with entries $\tilde{\mathbf{D}}_{ab} = \frac{\sum_{i \in [p]} \theta(i) \mathbf{1}\{z^{(t)}=b, z(i)=a\}}{\sum_{i \in [p]} \theta(i) \mathbf{1}\{z^{(t)}=b\}}$.

2765 To bound $\sin \beta_{k1}$, recall Definition 2 that for any cluster
 2766 assignment \bar{z} in the ε -neighborhood of true z ,

$$\begin{aligned} 2768 \mathbf{p}(\bar{z}) &= (|\bar{z}^{-1}(1)|, \dots, |\bar{z}^{-1}(r)|)^T, \\ 2769 \mathbf{p}_{\theta}(\bar{z}) &= (\|\theta_{\bar{z}^{-1}(1)}\|_1, \dots, \|\theta_{\bar{z}^{-1}(r)}\|_1)^T. \end{aligned}$$

2770 Note that we have $\ell^{(t)} \leq \frac{L^{(t)}}{\Delta_{\min}^2} \leq \frac{\bar{C}}{C} r \log^{-1}(p)$ by Condition 1 and Lemma 2. Then, with the locally linear stability
 2771 assumption, the θ is $\ell^{(t)}$ -locally linearly stable; i.e.,

$$2773 \sin(\mathbf{p}(z^{(t)}), \mathbf{p}_{\theta}(z^{(t)})) \lesssim \frac{L^{(t)}}{\Delta_{\min}}.$$

2774 Note that $\text{diag}(\mathbf{p}(z^{(t)}))\mathbf{D} = \text{diag}(\mathbf{p}_{\theta}(z^{(t)}))\tilde{\mathbf{D}}$, and
 2775 $\sin(\mathbf{a}, \mathbf{b}) = \min_{c \in \mathbb{R}} \frac{\|\mathbf{a}-c\mathbf{b}\|}{\|\mathbf{a}\|}$ for vectors \mathbf{a}, \mathbf{b} of same
 2776 dimension. Let $c_0 = \arg \min_{c \in \mathbb{R}} \frac{\|\mathbf{p}(z^{(t)}) - c\mathbf{p}_{\theta}(z^{(t)})\|}{\|\mathbf{p}(z^{(t)})\|}$. Then,
 2777 we have

$$\begin{aligned} 2778 \min_{c \in \mathbb{R}} \|\mathbf{D} - c\tilde{\mathbf{D}}\|_F \\ 2779 &\leq \|\mathbf{I}_r - c_0 \text{diag}(\mathbf{p}(z^{(t)})) \text{diag}^{-1}(\mathbf{p}_{\theta}(z^{(t)}))\|_F \|\mathbf{D}\|_F \\ 2780 &\lesssim \frac{\|\mathbf{p}(z^{(t)}) - c_0 \mathbf{p}_{\theta}(z^{(t)})\|}{\min_{a \in [r]} \|\theta_{z^{(t)}, -1(a)}\|_1} \\ 2781 &= \frac{\|\mathbf{p}(z^{(t)})\|}{\min_{a \in [r]} \|\theta_{z^{(t)}, -1(a)}\|_1} \sin(\mathbf{p}(z^{(t)}), \mathbf{p}_{\theta}(z^{(t)})) \\ 2782 &\lesssim \frac{L^{(t)}}{\Delta_{\min}}, \end{aligned}$$

2783 where the last inequality follows from Lemma 10, the
 2784 constraint $\min_{i \in [p]} \theta(i) \geq c > 0$, $\|\mathbf{p}(z^{(t)})\| \lesssim p$ and
 2785 $\min_{a \in [r]} \|\theta_{z^{(t)}, -1(a)}\|_1 \gtrsim p$.

2786 By the geometry property of trigonometric function,
 2787 we have

$$\begin{aligned} 2788 \sin \beta_{k1} &= \min_{c \in \mathbb{R}} \frac{\|\mathbf{D}_{:b}^T \mathbf{S} \mathbf{I}_r^{\otimes k-1} \otimes (\mathbf{D} - c\tilde{\mathbf{D}}) \otimes \mathbf{D}^{\otimes K-k-1}\|}{\|\mathbf{D}_{:b}^T \mathbf{S} \mathbf{I}_r^{\otimes k-1} \otimes \mathbf{D}^{\otimes K-k}\|} \\ 2789 &\leq \frac{\|\mathbf{D}_{:b}^T \mathbf{S}\| \|\mathbf{D} - c_0 \tilde{\mathbf{D}}\|_{\sigma} \|\mathbf{D}\|_{\sigma}^{K-k-1}}{\|\mathbf{D}_{:b}^T \mathbf{S}\| \lambda_r^{K-k}(\mathbf{D})} \\ 2790 &\lesssim \|\mathbf{D} - c_0 \tilde{\mathbf{D}}\|_F \\ 2791 &\lesssim \frac{L^{(t)}}{\Delta_{\min}}, \end{aligned} \tag{126}$$

2792 where the second inequality follows from the singular property
 2793 of \mathbf{D} in (123), (124) and the constraint of \mathbf{S} in (2).

2794 To bound $\sin \beta_{k2}$, let $\mathbf{C} = \text{diag}(\{\|\mathbf{S}_{a:}\|\}_{a \in [r]})$. We have

$$\begin{aligned} 2795 \sin \beta_{k2} &\lesssim \frac{\|\mathbf{D}_{:b}^T \mathbf{S} \mathbf{I}_r^{\otimes k-1} \otimes (\mathbf{I}_r - \tilde{\mathbf{D}}) \otimes \mathbf{D}^{\otimes K-k-1}\|}{\|\mathbf{D}_{:b}^T \mathbf{S} \mathbf{I}_r^{\otimes k} \otimes \mathbf{D}^{\otimes K-k-1}\|} \\ 2796 &\lesssim \frac{\|(\mathbf{I}_r - \tilde{\mathbf{D}}^T) \mathbf{S} \mathbf{Z}^k\|_F}{\|\mathbf{D}_{:b}^T \mathbf{S}\| \lambda_r^{K-k-1}(\mathbf{D})} \\ 2797 &\lesssim \|(\mathbf{I}_r - \tilde{\mathbf{D}}^T) \mathbf{S} \mathbf{C}^{-1}\|_F \|\mathbf{C} \mathbf{Z}^k\|_{\sigma} \\ 2798 &\lesssim \frac{r}{p} \sum_{i \in [p]} \theta(i) \sum_{b \in [r]} \mathbf{1}\{z^{(t)}(i) = b\} \|\mathbf{S}_{b:}^s - \mathbf{S}_{z(i)}^s\| \\ 2799 &\lesssim \frac{L^{(t)}}{\Delta_{\min}}, \end{aligned} \tag{127}$$

2800 where the third inequality follows from the singular property
 2801 of \mathbf{D} and the boundedness of \mathbf{S} , and the fourth inequality
 2802 follows from the definition of $\tilde{\mathbf{D}}$, boundedness of \mathbf{S} , the
 2803 lower bound of θ , and the singular property of \mathbf{Z}^k in inequality
 2804 (125), and the last line follows from the definition of $L^{(t)}$.
 2805 Combining (126) and (127) yields

$$\sin \beta_k \leq \sin \beta_{k1} + \sin \beta_{k2} \lesssim \frac{L^{(t)}}{\Delta_{\min}}.$$

2806 Finally, by triangle inequality, we obtain

$$2807 J_{11} \leq \sum_{k=1}^{K-1} J_{11}^k \lesssim \sum_{k=1}^{K-1} \sin \beta_k \lesssim (K-1) \frac{r L^{(t)}}{\Delta_{\min}}. \tag{128}$$

2808 We now consider J_{12} . By triangle inequality, we have

$$\begin{aligned} 2809 J_{12} &\leq \frac{1}{\|\mathbf{W}_{:b}^{(t),T} \mathbf{X} \mathbf{V}\|} \|\mathbf{W}_{:b}^{(t),T} \mathbf{E}(\mathbf{V} - \mathbf{V}^{(t)})\| \\ 2810 &\quad + \frac{\|\mathbf{W}_{:b}^{(t),T} \mathbf{X}(\mathbf{V} - \mathbf{V}^{(t)})\|}{\|\mathbf{W}_{:b}^{(t),T} \mathbf{X} \mathbf{V}\| \|\mathbf{W}_{:b}^{(t),T} \mathbf{X} \mathbf{V}^{(t)}\|} \|\mathbf{W}_{:b}^{(t),T} \mathbf{E} \mathbf{V}^{(t)}\|. \end{aligned} \tag{129}$$

2812 Note that

$$\begin{aligned} 2813 \|\mathbf{W}_{:b}^{(t),T} \mathbf{X} \mathbf{V}^{(t)}\| &= \|\mathbf{D}^T \mathbf{S} \mathbf{Z}^1\| \\ 2814 &\geq \lambda_r(\mathbf{D}) \|\mathbf{S}\| \lambda_{r^{K-2}}(\mathbf{Z}^1) \gtrsim 1, \\ 2815 \end{aligned} \tag{129}$$

2816 where the inequality follows from the bounds (124) and (125).
 2817 By [13, Proof of Lemma 5], we have

$$\begin{aligned} 2818 \|\mathbf{W}_{:b}^{(t),T} \mathbf{E}(\mathbf{V} - \mathbf{V}^{(t)})\| \\ 2819 &\lesssim \sqrt{\frac{r^{2K+1} + pr^{2+K}}{p^K}} \frac{(K-1)\sqrt{L^{(t)}}}{\Delta_{\min}}. \end{aligned} \tag{130}$$

2820 Notice that

$$\begin{aligned} 2821 \|\mathbf{X}(\mathbf{V}^k - \mathbf{V}^{k+1})\|_F \\ 2822 &\leq \|(\mathbf{I} - \mathbf{D}^T) \mathbf{S}(\mathbf{I}_r^{\otimes(k-1)} \otimes \mathbf{D}^{\otimes(K-k-1)})\|_F \\ 2823 &\leq \|(\mathbf{W}^T - \mathbf{W}^{(t),T}) \Theta \mathbf{M}\|_F \|\mathbf{S}\|_F \|\mathbf{D}\|_{\sigma}^{K-k-1} \\ 2824 &\lesssim \|\mathbf{W}^T - \mathbf{W}^{(t),T}\| \|\Theta \mathbf{M}\|_{\sigma} \\ 2825 &\lesssim \frac{\sqrt{r L^{(t)}}}{\Delta_{\min}}, \end{aligned} \tag{131}$$

where the first inequality follows from the tensor algebra in inequality (122), the second inequality follows from the fact that $\mathbf{I} = \mathbf{W}^T \Theta \mathbf{M}$, and the last inequality follows from [13, Proof of Lemma 5]. It follows from (131) and Lemma 10 that

$$\begin{aligned} \|\mathbf{W}_{:b}^{(t),T} \mathbf{X}(\mathbf{V} - \mathbf{V}^{(t)})\| &\leq \|\mathbf{W}_{:b}^{(t),T}\| \sum_{k=1}^{K-1} \|\mathbf{X}(\mathbf{V}^k - \mathbf{V}^{k+1})\|_F \\ &\lesssim \frac{\sqrt{rL^{(t)}}}{\sqrt{p}\Delta_{\min}}. \end{aligned} \quad (132)$$

Note that $\|\mathbf{W}_{:b}^{(t),T} \mathbf{X} \mathbf{V}\|$ and $\|\mathbf{W}_{:b}^{(t),T} \mathbf{X} \mathbf{V}^{(t)}\|$ are lower bounded by inequalities (114) and (129), respectively. We have

$$\begin{aligned} J_{12} &\lesssim \|\mathbf{W}_{:b}^{(t),T} \mathbf{E}(\mathbf{V} - \mathbf{V}^{(t)})\| \\ &\quad + \|\mathbf{W}_{:b}^{(t),T} \mathbf{X}(\mathbf{V} - \mathbf{V}^{(t)})\| \|\mathbf{W}_{:b}^{(t),T} \mathbf{E} \mathbf{V}^{(t)}\| \\ &\lesssim \sqrt{\frac{r^{2K+1} + pr^{2+K}}{p^K} \frac{\sqrt{L^{(t)}}}{\Delta_{\min}}} + \frac{\sqrt{rL^{(t)}}}{\sqrt{p}\Delta_{\min}} \sqrt{\frac{r^{2K}}{p^K}} \\ &\lesssim \sqrt{\frac{r^{2K+1} + pr^{2+K}}{p^K} \frac{\sqrt{L^{(t)}}}{\Delta_{\min}}}, \end{aligned}$$

where the second inequality follows from inequalities (130), (132), and the inequality (62) in Condition 1.

For J_2 and J_3 , recall that $\|\mathbf{W}_{:b}^{(t),T} \mathbf{X} \mathbf{V}\|$ and $\|\mathbf{W}_{:b}^{(t),T} \mathbf{X} \mathbf{V}^{(t)}\|$ are lower bounded by inequalities (114) and (129), respectively. By triangle inequality and inequality (62) in Condition 1, we have

$$J_2 \leq \frac{\|\mathbf{W}_{:b}^{(t),T} \mathbf{E} \mathbf{V}\|}{\|\mathbf{W}_{:b}^{(t),T} \mathbf{X} \mathbf{V}\|} \lesssim \|\mathbf{W}_{:b}^{(t),T} \mathbf{E} \mathbf{V}\| \lesssim \frac{r^K}{p^{K/2}}, \quad (133)$$

and

$$J_3 \leq \frac{\|\mathbf{W}_{:b}^{(t),T} \mathbf{E} \mathbf{V}^{(t)}\|}{\|\mathbf{W}_{:b}^{(t),T} \mathbf{X} \mathbf{V}^{(t)}\|} \lesssim \|\mathbf{W}_{:b}^{(t),T} \mathbf{E} \mathbf{V}\| \lesssim \frac{r^K}{p^{K/2}}. \quad (134)$$

Therefore, combining the inequalities (128), (133), and (134), we finish the proof of inequality (109).

5) Inequality (110). By triangle inequality, we upper bound the desired quantity

$$\begin{aligned} &\|[\mathbf{W}_{:b}^T \mathbf{Y} \mathbf{V}^{(t)}]^s - [\mathbf{W}_{:b}^{(t),T} \mathbf{Y} \mathbf{V}^{(t)}]^s\| \\ &\leq \|[\mathbf{W}_{:b}^T \mathbf{Y} \mathbf{V}^{(t)}]^s - [\mathbf{W}_{:b}^T \mathbf{Y} \mathbf{V}]^s\| \\ &\quad + \|[\mathbf{W}_{:b}^T \mathbf{Y} \mathbf{V}]^s - [\mathbf{W}_{:b}^{(t),T} \mathbf{Y} \mathbf{V}]^s\| \\ &\quad + \|[\mathbf{W}_{:b}^{(t),T} \mathbf{Y} \mathbf{V}]^s - [\mathbf{W}_{:b}^{(t),T} \mathbf{Y} \mathbf{V}^{(t)}]^s\| \\ &\lesssim \frac{rL^{(t)}}{\Delta_{\min}} + \sqrt{\frac{r^{2K} + pr^{K+2}}{p^K} \frac{\sqrt{L^{(t)}}}{\Delta_{\min}}}, \end{aligned}$$

following the inequalities (108) and (109). Therefore, we finish the proof of inequality (110).

6) Next, we Show the Intermediate Inequalities Holds With \mathbf{P}, \mathbf{Q} and $L(\hat{z})$: Consider the MLE confusion matrix $\hat{\mathbf{D}} = \mathbf{M}^T \Theta^T \hat{\mathbf{P}} = \llbracket \hat{D}_{ab} \rrbracket \in \mathbb{R}^{r \times r}$ with entries

$$\begin{aligned} \hat{D}_{ab} &= \frac{\sum_{i \in [p]} \theta(i)\hat{\theta}(i)\mathbf{1}\{z(i) = a, \hat{z}(i) = b\}}{\|\hat{\theta}_{\hat{z}^{-1}(b)}\|^2} \\ &= \frac{\sum_{i \in [p]} (1 + o(p^{K-2}))(\hat{\theta}(i))^2 \mathbf{1}\{z(i) = a, \hat{z}(i) = b\}}{\|\hat{\theta}_{\hat{z}^{-1}(b)}\|^2}, \end{aligned} \quad (135)$$

where the second equation follows from Lemma 13, and thus $\sum_{a \in [r]} \hat{D}_{ab} = 1 + o(1)$. By the derivation of (111), (112), (124), and (123), we have

$$\begin{aligned} \sum_{a \neq b \in [r]} \hat{D}_{ab} &\lesssim \frac{1}{p} \sum_{i \in [p]} \mathbf{1}\{\hat{z}(i) \neq z(i)\}(\hat{\theta}(i))^2 \lesssim \frac{1}{\log p}, \\ \hat{D}_{bb} &\gtrsim 1 - \frac{1}{\log p}, \quad \lambda_{\min}(\hat{\mathbf{D}}) \asymp \|\hat{\mathbf{D}}\|_\sigma = (1 + o(1)). \end{aligned}$$

for all $a \neq b \in [r]$.

Now, we are ready to show the intermediate inequalities. First, by Lemma 1 and $\min_{i \in [p]} \theta(i) \geq c$, we have

$$\|\mathbf{S}_{a:}^s - \mathbf{S}_{b:}^s\| \asymp \|\mathbf{A}_{a:}^s - \mathbf{A}_{b:}^s\|.$$

Then we can replace the $L^{(t)}$ by $L(\hat{z})$ in the proof of Lemma 12. The analogies of inequalities (106), (107), (108), (109), and (110) hold by using the MLE confusion matrix and the definition of $L(\hat{z})$.

Particularly, for the analogy of (109), the usage of MLE confusion matrix avoids the stability condition on θ . Let $\bar{\mathbf{D}}$ be the normalized version of $\hat{\mathbf{D}}$. The angle in inequality (126) decays to 0 at speed $p^{-(K-2)} \lesssim \Delta_{\min}$ when $K \geq 3$, and the inequality (127) holds by the fact that

$$\begin{aligned} \|(\mathbf{I}_r - \bar{\mathbf{D}})\mathbf{S}\mathbf{C}^{-1}\|_F &\lesssim \frac{r}{p} \sum_{i \in [p]} (\theta(i))^2 \sum_{b \in [r]} \|\mathbf{S}_{b:}^s - \mathbf{S}_{z(i):}^s\| \\ &\lesssim \frac{r}{p} \sum_{i \in [p]} (\theta(i))^2 \sum_{b \in [r]} \|\mathbf{A}_{b:}^s - \mathbf{A}_{z(i):}^s\|. \end{aligned}$$

□

Lemma 13 (Polynomial Estimation Error of MLE): Let $(\hat{z}, \hat{\mathcal{S}}, \hat{\theta})$ denote the MLE in (9) with fixed $K \geq 2$ and symmetric mean tensor, and $\hat{\mathcal{X}}$ denote the mean tensor consisting of parameter $(\hat{z}, \hat{\mathcal{S}}, \hat{\theta})$. With high probability going to 1 as $p \rightarrow \infty$, we have

$$\|\mathcal{X} - \hat{\mathcal{X}}\|_F^2 \lesssim \sigma^2 (r^K + Kpr),$$

with probability going to 1. When SNR $\gtrsim p^{-(K-1)} \log p$, θ is balanced, and $\min_{i \in [p]} \theta(i) \geq c$ for some positive constant c , the MLE satisfies

$$\frac{1}{p} \sum_{i \in [p]} \mathbf{1}\{\hat{z}(i) \neq z(i)\}(\theta(i))^2 \lesssim \frac{1}{r \log p},$$

$$\frac{1}{p} \sum_{i \in [p]} \mathbf{1}\{\hat{z}(i) \neq z(i)\}(\hat{\theta}(i))^2 \lesssim \frac{1}{r \log p},$$

$$\text{and } L(\hat{z}) \lesssim \frac{\Delta_{\min}^2}{r \log p},$$

Further, we have

$$\theta(i)^2 = (1 + o(p^{-(K-2)}))\hat{\theta}(i)^2.$$

Proof of Lemma 13: Without loss of generality, we assume $\sigma^2 = 1$ and identity mapping minimizes the misclustering error for MLE. For arbitrary two sets of parameters $(z, \mathcal{S}, \boldsymbol{\theta}), (z', \mathcal{S}', \boldsymbol{\theta}') \in \mathcal{P}(\gamma)$ and corresponding mean tensors $\mathcal{X}, \mathcal{X}'$, we have

$$\begin{aligned} & \text{rank}(\text{Mat}_k(\mathcal{X}) - \text{Mat}_k(\mathcal{X}')) \\ & \leq \text{rank}(\text{Mat}_k(\mathcal{X})) + \text{rank}(\text{Mat}_k(\mathcal{X}')) \\ & \leq 2r, \quad k \in [K]. \end{aligned}$$

Hence, we have

$$\mathcal{X} - \mathcal{X}' \in \mathcal{Q}(2r, \dots, 2r), \quad (136)$$

where $\mathcal{Q}(r, \dots, r) := \{\text{Tucker tensor with rank } (r, \dots, r)\}$. Then, we obtain that

$$\begin{aligned} & \mathbb{P}(\|\mathcal{X} - \hat{\mathcal{X}}_{ML}\|_F \geq t) \\ & \leq 2\mathbb{P}\left(\sup_{\mathcal{X}, \mathcal{X}' \in \mathcal{Q}(r, \dots, r)} \left\langle \frac{\mathcal{X} - \mathcal{X}'}{\|\mathcal{X} - \mathcal{X}'\|_F}, \mathcal{E} \right\rangle \geq t\right) \\ & \leq 2\mathbb{P}\left(\sup_{\mathcal{T} \in \mathcal{Q}(2r, \dots, 2r) \cap \{\|\mathcal{T}\|_F=1\}} \langle \mathcal{T}, \mathcal{E} \rangle \geq t\right) \\ & \lesssim \exp(-Kpr), \end{aligned}$$

with the choice $t \asymp \sigma\sqrt{(Kpr + r^K)}$. Here the first inequality follows from [10, Lemma 1], the second inequality follows from (136), and the last inequality follows from [37, Lemma E5].

When $\Delta_{\min}^2 \gtrsim p^{-(K-1)} \log p$, we replace the vector $\hat{x}_{\hat{z}(i)}$ and $\hat{\mathbf{X}}$ by our MLE estimator in the proof of Theorem 4. With estimation error $\|\mathcal{X} - \hat{\mathcal{X}}\|_F^2 \lesssim (r^K + Kpr)$ and $\Delta_{\min}^2 \gtrsim p^{-(K-1)} \log p$, we have

$$\begin{aligned} \frac{1}{p} \sum_{i \in [p]} \mathbb{1}\{\hat{z}(i) \neq z(i)\} (\theta(i))^2 & \lesssim \frac{r^{K-1}}{\Delta_{\min}^2 p^K} \|\mathcal{X} - \hat{\mathcal{X}}\|_F^2 \\ & \lesssim \frac{r^{K-2}}{p^{K-1} \Delta_{\min}^2} \\ & \lesssim \frac{1}{r \log p}, \end{aligned}$$

and

$$L(\hat{z}) \lesssim \frac{\Delta_{\min}^2}{r \log p}.$$

Above result holds for $\hat{\theta}(i)$ after switching the parameters \mathbf{X} with $\hat{\mathbf{X}}$ and switch $\boldsymbol{\theta}$ with $\hat{\boldsymbol{\theta}}$ in the proof.

Last, notice that for all $a \in [r]$

$$\begin{aligned} & (1 - O(1)) \frac{p^2}{r^2} \|\mathbf{W}_{:a}^T \mathbf{X} - \hat{\mathbf{W}}_{:a}^T \hat{\mathbf{X}}\|_F^2 \\ & \leq \sum_{\hat{z}(i)=z(i)=a} (\theta(i) \mathbf{W}_{:a}^T \mathbf{X} - \hat{\theta}(i) \hat{\mathbf{W}}_{:a}^T \hat{\mathbf{X}})^2 \\ & \leq \|\mathcal{X} - \hat{\mathcal{X}}\|_F^2 \leq pr, \end{aligned}$$

where the first inequality follows from the facts that $\ell(\hat{z}, z) \lesssim \frac{1}{\log p}, |z^{-1}(a)| \asymp p/r$,

$$\begin{aligned} |z^{-1}(a)| - C \frac{p}{r} \ell(\hat{z}, z) & \leq |\hat{z}^{-1}(a)| \leq |z^{-1}(a)| + C \frac{p}{r} \ell(\hat{z}, z), \\ |z^{-1}(a)| - C \frac{p}{r} \ell(\hat{z}, z) & \leq \sum_{z(i)=\hat{z}(i)=a} \theta(i) \leq |z^{-1}(a)|, \end{aligned}$$

and

$$|\hat{z}^{-1}(a)| - C \frac{p}{r} \ell(\hat{z}, z) \leq \sum_{\hat{z}(i)=z(i)=a} \hat{\theta}(i) \leq |\hat{z}^{-1}(a)|.$$

Hence, for all $i \in [p]$

$$\begin{aligned} & (\theta(i) - \hat{\theta}(i))^2 \|\mathbf{W}_{:a}^T \mathbf{X}\|_F^2 - O(p) \\ & \leq \|(\theta(i) - \hat{\theta}(i)) \mathbf{W}_{:a}^T \mathbf{X}\|_F^2 - \|\hat{\theta}(i)(\mathbf{W}_{:a}^T \mathbf{X} - \hat{\mathbf{W}}_{:a}^T \hat{\mathbf{X}})\|_F^2 \\ & \leq \|\mathcal{X} - \hat{\mathcal{X}}\|_F^2 \leq pr, \end{aligned}$$

where the first inequality follows from $\|\mathbf{W}_{:a}^T \mathbf{X} - \hat{\mathbf{W}}_{:a}^T \hat{\mathbf{X}}\|_F^2 \lesssim 1/p$ and $\hat{\theta}(i) \lesssim \frac{p}{r}$. Notice that for all $a \in [r]$

$$\|\mathbf{W}_{:a}^T \mathbf{X}\|_F^2 \geq \|\mathbf{S}_a\|_F^2 \lambda_{\min}^{2(K-1)} (\Theta \mathbf{M}) \gtrsim p^{K-1}.$$

The inequality indicates that $\theta(i)^2 = (1 + o(p^{-(K-2)}))\hat{\theta}(i)^2$. \square

ACKNOWLEDGMENT

The authors would like to thank Zheng Tracy Ke, Anru Zhang, Rungang Han, and Yuetian Luo for helpful discussions and for sharing software packages.

REFERENCES

- [1] A. Anandkumar, R. Ge, D. J. Hsu, S. M. Kakade, and M. Telgarsky, “Tensor decompositions for learning latent variable models,” *J. Mach. Learn. Res.*, vol. 15, pp. 2773–2832, Aug. 2014.
- [2] L. Wang, D. Durante, R. E. Jung, and D. B. Dunson, “Bayesian network-response regression,” *Bioinformatics*, vol. 33, no. 12, pp. 1859–1866, 2017.
- [3] P. Koniusz and A. Cherian, “Sparse coding for third-order supersymmetric tensor descriptors with application to texture recognition,” in *Proc. IEEE Conf. Comput. Vis. Pattern Recognit. (CVPR)*, Jun. 2016, pp. 5395–5403.
- [4] M. Wang, J. Fischer, and Y. S. Song, “Three-way clustering of multi-tissue multi-individual gene expression data using semi-nonnegative tensor decomposition,” *Ann. Appl. Statist.*, vol. 13, no. 2, pp. 1103–1127, Jun. 2019.
- [5] V. Hore et al., “Tensor decomposition for multiple-tissue gene expression experiments,” *Nature Genet.*, vol. 48, no. 9, p. 1094, 2016.
- [6] D. Ghoshdastidar and A. Dukkipati, “Uniform hypergraph partitioning: Provable tensor methods and sampling techniques,” *J. Mach. Learn. Res.*, vol. 18, no. 50, pp. 1–41, 2017.
- [7] D. Ghoshdastidar and A. Dukkipati, “Consistency of spectral hypergraph partitioning under planted partition model,” *Ann. Statist.*, vol. 45, no. 1, pp. 289–315, 2017.
- [8] K. Ahn, K. Lee, and C. Suh, “Community recovery in hypergraphs,” *IEEE Trans. Inf. Theory*, vol. 65, no. 10, pp. 6561–6579, Oct. 2019.
- [9] Z. T. Ke, F. Shi, and D. Xia, “Community detection for hypergraph networks via regularized tensor power iteration,” 2019, *arXiv:1909.06503*.
- [10] M. Wang and Y. Zeng, “Multiway clustering via tensor block models,” in *Proc. Adv. Neural Inf. Process. Syst.*, vol. 32, 2019, pp. 715–725.
- [11] E. Abbe, “Community detection and stochastic block models: Recent developments,” *J. Mach. Learn. Res.*, vol. 18, pp. 1–86, Jan. 2018.
- [12] E. C. Chi, B. J. Gaines, W. W. Sun, H. Zhou, and J. Yang, “Provable convex co-clustering of tensors,” *J. Mach. Learn. Res.*, vol. 21, no. 214, pp. 1–58, 2020.
- [13] R. Han, Y. Luo, M. Wang, and A. R. Zhang, “Exact clustering in tensor block model: Statistical optimality and computational limit,” *J. Roy. Stat. Soc., Ser. B, Stat. Methodol.*, vol. 84, no. 5, pp. 1666–1698, Nov. 2022.

- | | | |
|------|---|------|
| 2990 | [14] P. J. Bickel and A. Chen, "A nonparametric view of network models and | 3035 |
| 2991 | Newman–Girvan and other modularities," <i>Proc. Nat. Acad. Sci. USA</i> , | 3036 |
| 2992 | vol. 106, no. 50, pp. 21068–21073, 2009. | 3037 |
| 2993 | [15] C. Gao, Z. Ma, A. Y. Zhang, and H. H. Zhou, "Community detection in degree-corrected block models," <i>Ann. Statist.</i> , vol. 46, no. 5, | 3038 |
| 2994 | pp. 2153–2185, Oct. 2018. | 3039 |
| 2995 | [16] K. Ahn, K. Lee, and C. Suh, "Hypergraph spectral clustering in the | 3040 |
| 2996 | weighted stochastic block model," <i>IEEE J. Sel. Topics Signal Process.</i> , | 3041 |
| 2997 | vol. 12, no. 5, pp. 959–974, Oct. 2018. | 3042 |
| 2998 | [17] M. Yuan, R. Liu, Y. Feng, and Z. Shang, "Testing community structure | 3043 |
| 2999 | for hypergraphs," <i>Ann. Statist.</i> , vol. 50, no. 1, pp. 147–169, Feb. 2022. | 3044 |
| 3000 | [18] Y. Chi, Y. M. Lu, and Y. Chen, "Nonconvex optimization meets low- | 3045 |
| 3001 | rank matrix factorization: An overview," <i>IEEE Trans. Signal Process.</i> , | 3046 |
| 3002 | vol. 67, no. 20, pp. 5239–5269, Oct. 2019. | 3047 |
| 3003 | [19] S.-Y. Yun and A. Proutiere, "Optimal cluster recovery in the labeled | 3048 |
| 3004 | stochastic block model," in <i>Proc. Adv. Neural Inf. Process. Syst.</i> , vol. 29, | 3049 |
| 3005 | 2016, pp. 973–981. | 3050 |
| 3006 | [20] C. Kim, A. S. Bandeira, and M. X. Goemans, "Stochastic block | 3051 |
| 3007 | model for hypergraphs: Statistical limits and a semidefinite programming | 3052 |
| 3008 | approach," 2018, <i>arXiv:1807.02884</i> . | 3053 |
| 3009 | [21] L. De Lathauwer, B. De Moor, and J. Vandewalle, "A multilinear | 3054 |
| 3010 | singular value decomposition," <i>SIAM J. Matrix Anal. Appl.</i> , vol. 21, | 3055 |
| 3011 | no. 14, pp. 1253–1278, 2006. | 3056 |
| 3012 | [22] Z. Zhang, G. I. Allen, H. Zhu, and D. Dunson, "Tensor network | 3057 |
| 3013 | factorizations: Relationships between brain structural connectomes and | |
| 3014 | traits," <i>NeuroImage</i> , vol. 197, pp. 330–343, Aug. 2019. | |
| 3015 | [23] A. Zhang and D. Xia, "Tensor SVD: Statistical and computational | |
| 3016 | limits," <i>IEEE Trans. Inf. Theory</i> , vol. 64, no. 11, pp. 7311–7338, | |
| 3017 | Nov. 2018. | |
| 3018 | [24] M. Brennan and G. Bresler, "Reducibility and statistical-computational | |
| 3019 | gaps from secret leakage," in <i>Proc. 33rd Conf. Learn. Theory</i> , vol. 125, | |
| 3020 | 2020, pp. 648–847. | |
| 3021 | [25] Y. Lu and H. H. Zhou, "Statistical and computational guarantees of | |
| 3022 | Lloyd's algorithm and its variants," 2016, <i>arXiv:1612.02099</i> . | |
| 3023 | [26] E. Abbe, J. Fan, K. Wang, and Y. Zhong, "Entrywise eigenvector analysis | |
| 3024 | of random matrices with low expected rank," <i>Ann. Statist.</i> , vol. 48, no. 3, | |
| 3025 | pp. 1452–1474, Jun. 2020. | |
| 3026 | [27] C. Mu, B. Huang, J. Wright, and D. Goldfarb, "Square deal: Lower | |
| 3027 | bounds and improved relaxations for tensor recovery," in <i>Proc. 31th Int.</i> | |
| 3028 | <i>Conf. Mach. Learn. (ICML)</i> , vol. 32, 2014, pp. 73–81. | |
| 3029 | [28] L. Florescu and W. Perkins, "Spectral thresholds in the bipartite stochastic | |
| 3030 | block model," in <i>Proc. 29th Conf. Learn. Theory</i> , vol. 49, 2016, | |
| 3031 | pp. 943–959. | |
| 3032 | [29] C. Gao and A. Y. Zhang, "Iterative algorithm for discrete structure | |
| 3033 | recovery," <i>Ann. Statist.</i> , vol. 50, no. 2, pp. 1066–1094, Apr. 2022. | |
| 3034 | | |
| | [30] I. E. Chien, C.-Y. Lin, and I.-H. Wang, "On the minimax misclassification | |
| | ratio of hypergraph community detection," <i>IEEE Trans. Inf. Theory</i> , | |
| | vol. 65, no. 12, pp. 8095–8118, Dec. 2019. | |
| | [31] M. Meilă, "Local equivalences of distances between clusterings—A | |
| | geometric perspective," <i>Mach. Learn.</i> , vol. 86, no. 3, pp. 369–389, | |
| | Mar. 2012. | |
| | [32] D. C. Van Essen et al., "The WU-minn human connectome project: | |
| | An overview," <i>NeuroImage</i> , vol. 80, pp. 62–79, Oct. 2013. | |
| | [33] R. S. Desikan et al., "An automated labeling system for subdividing | |
| | the human cerebral cortex on MRI scans into gyral based regions of | |
| | interest," <i>NeuroImage</i> , vol. 31, no. 3, pp. 968–980, Jul. 2006. | |
| | [34] J. Hu, C. Lee, and M. Wang, "Generalized tensor decomposition with | |
| | features on multiple modes," <i>J. Comput. Graph. Statist.</i> , vol. 31, no. 1, | |
| | pp. 204–218, Jan. 2022. | |
| | [35] S. H. Lee, J. M. Magallanes, and M. A. Porter, "Time-dependent com- | |
| | munity structure in legislation cosponsorship networks in the congress | |
| | of the republic of Peru," <i>J. Complex Netw.</i> , vol. 5, no. 1, pp. 127–144, | |
| | 2017. | |
| | [36] P. Rigollet and J.-C. Hütter, "High dimensional statistics," <i>Lect. Notes</i> | |
| | <i>Course 18S997</i> , vol. 813, no. 814, p. 46, 2015. | |
| | [37] R. Han, R. Willett, and A. R. Zhang, "An optimal statistical and com- | |
| | putational framework for generalized tensor estimation," <i>Ann. Statist.</i> , | |
| | vol. 50, no. 1, pp. 1–29, Feb. 2022. | |

Jiaxin Hu received the B.S. degree from Wuhan University in 2019 and the master's degree in statistics from the University of Wisconsin–Madison in 2020, where she is currently pursuing the Ph.D. degree with the Department of Statistics. Her research interests include tensor methods, network analysis, and applications in genetics and social science.

Miaoyan Wang received the B.S. degree in mathematics from Fudan University in 2010 and the Ph.D. degree in statistics from the University of Chicago in 2015. She is currently an Assistant Professor of statistics at the University of Wisconsin–Madison. She is also a Faculty Affiliate with the Mathematical Foundations of Machine Learning and the Institute for Foundations of Data Science. Her research interests include the intersection of statistics, machine learning, and genetics. She was a recipient of NSF CAREER Award in 2022, Best Student Paper Awards (with her as an Advisor) from American Statistical Association (three times in 2021, 2022, and 2023), and New England Statistical Society in 2022.